BioMed Research International

Chronic Pain: New Insights in Molecular and Cellular Mechanisms

Guest Editors: Livio Luongo, Marzia Malcangio, Daniela Salvemini, and Katarzyna Starowicz

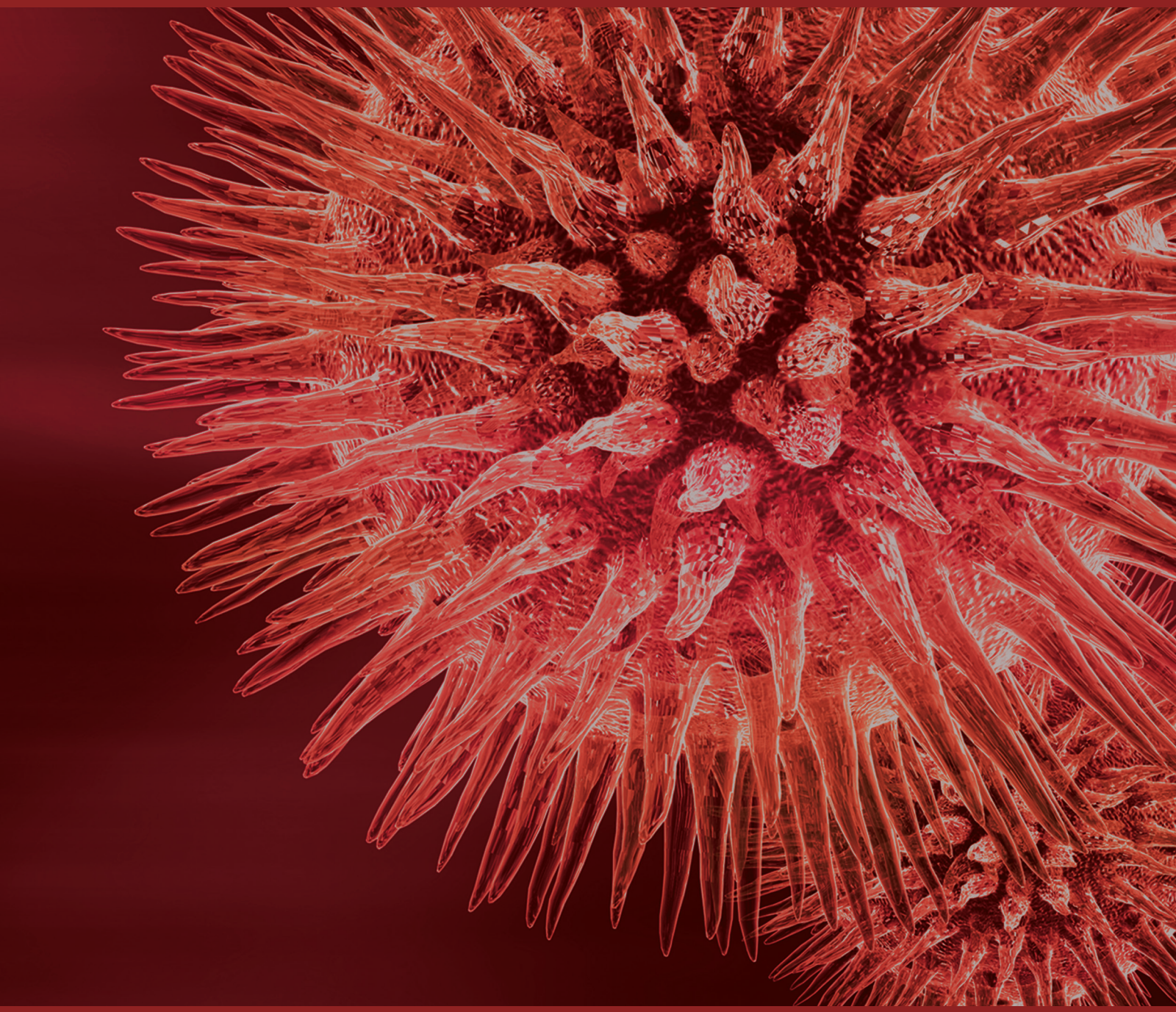

Chronic Pain: New Insights in Molecular and Cellular Mechanisms

BioMed Research International

Chronic Pain: New Insights in Molecular and Cellular Mechanisms

Guest Editors: Livio Luongo, Marzia Malcangio, Daniela Salvemini, and Katarzyna Starowicz

Contents

Hindawi Publishing Corporation
BioMed Research International
Volume 2015, Article ID 676725, 2 pages
http://dx.doi.org/10.1155/2015/676725

Editorial

Chronic Pain: New Insights in Molecular and Cellular Mechanisms

Livio Luongo,[1] Marzia Malcangio,[2] Daniela Salvemini,[3] and Katarzyna Starowicz[4]

[1]*Department of Experimental Medicine, Division of Pharmacology, Second University of Naples, 80138 Naples, Italy*
[2]*Wolfson Centre for Age Related Diseases, King's College London, Guy's Campus, London SE1 1UL, UK*
[3]*Saint Louis University School of Medicine, Saint Louis, MO 63104, USA*
[4]*Laboratory of Pain Pathophysiology, Department of Pain Pharmacology, Institute of Pharmacology, Polish Academy of Sciences, UL Smetna 12, Krakow, Poland*

Correspondence should be addressed to Livio Luongo; livio.luongo@gmail.com

Received 25 November 2014; Accepted 25 November 2014

Chronic pain such as neuropathic pain, osteoarthritic pain, or abnormal pain associated with neurological diseases represents a debilitating condition which strongly affects the quality of life of patients. The mechanisms at the basis of the induction and maintenance of chronic pain are still poorly understood. Thus, an appropriate therapy for chronic pain is not yet available and there are many failures in treatments.

Recent evidence suggests a role for central and peripheral immune cells (microglia, macrophages, astrocytes, mast cells, and T-cells) in the initiation of peripheral and central sensitization. They mediate the plastic changes occurring within pain pathways that result in sensory dysfunctions and behavioural correlates, such as thermal/mechanical hyperalgesia and tactile allodynia. Because of the complex molecular and cellular mechanisms involved in the neuropathic pain induction and maintenance, several mediators have been demonstrated to be crucial in its induction and maintenance in the last years.

Historically the NMDA receptor for glutamate has been deeply investigated for the spinal wind-up occurring in the establishment of tactile allodynia. The role of the NMDA NR2B subunit as well as a possible pharmacological activity of its natural agonist, the D-aspartic acid, has been further clarified in this issue. More recent data suggest a role for lipid-mediated pathways such as sphingosine-1-phosphate or endocannabinoid systems in the modulation of spinal and supraspinal events associated with peripheral neuropathy [1, 2]. Besides the endocannabinoids also the "so-called" endocannabinoid-like molecules such as palmitoylethanolamide and oleoylethanolamide (PEA and OEA) have been demonstrated to be potentially useful to treat neuropathic pain-associated allodynia and hyperalgesia [3–5].

In this issue further investigations on the possible alterations in the anandamide metabolism in the development of neuropathic pain have been addressed. Moreover, the possible use of the palmitoylethanolamide in the delay of morphine tolerance has also been suggested. In this special issue, focused on further understanding of the molecular and cellular mechanisms at the basis of the chronic neuropathic pain, several other neuromodulatory systems have been analyzed. A possible role of a new class of chemokines, the prokineticins, of the somatostatin receptor activation, of the nociceptin/orphanin, and of the mTOR pathway in neuropathic pain mechanisms has been further elucidated. Moreover, the possible use of a still far stem cells therapy has been reviewed in the issue.

Nowadays a pivotal role of microglia in the establishment of tactile allodynia is confirmed. The microglia activation and recruitment seem to be highly regulated by purinergic system. Indeed, it has been highlighted that the abnormal ATP release in the dorsal horn of the spinal cord is responsible for the BDNF release from microglia through a mechanism mediated by P_2X_4 which, in turn, causes the shift in neuronal anion gradient [6]. Moreover, also a role for the P_2X_7 in the

microglial release of IL-1β and other proinflammatory molecules such as cathepsin S has been demonstrated [7]. The role of the purinergic system in the regulation of glial and microglial cells has been extensively reviewed in the paper by G. Magni and S. Ceruti.

In conclusion, we hope that the readers will find in this special issue a discreet panoramic view of the puzzling mechanisms involved in chronic pain development.

Livio Luongo
Marzia Malcangio
Daniela Salvemini
Katarzyna Starowicz

References

[1] D. Salvemini, T. Doyle, M. Kress, and G. Nicol, "Therapeutic targeting of the ceramide-to-sphingosine 1-phosphate pathway in pain," *Trends in Pharmacological Sciences*, vol. 34, no. 2, pp. 110–118, 2013.

[2] L. Luongo, S. Maione, and V. di Marzo, "Endocannabinoids and neuropathic pain: focus on neuron-glia and endocannabinoid-neurotrophin interactions," *European Journal of Neuroscience*, vol. 39, no. 3, pp. 401–408, 2014.

[3] S. D. Skaper, L. Facci, M. Fusco et al., "Palmitoylethanolamide, a naturally occurring disease-modifying agent in neuropathic pain," *Inflammopharmacology*, vol. 22, no. 2, pp. 79–94, 2014.

[4] L. Luongo, F. Guida, S. Boccella et al., "Palmitoylethanolamide reduces formalin-induced neuropathic-like behaviour through spinal glial/microglial phenotypical changes in mice," *CNS and Neurological Disorders—Drug Targets*, vol. 12, no. 1, pp. 45–54, 2013.

[5] K. Starowicz, W. Makuch, M. Korostynski et al., "Full inhibition of spinal FAAH leads to TRPV1-mediated analgesic effects in neuropathic rats and possible lipoxygenase-mediated remodeling of anandamide metabolism," *PLoS ONE*, vol. 8, no. 4, Article ID e60040, 2013.

[6] J. A. Coull, S. Beggs, D. Boudreau et al., "BDNF from microglia causes the shift in neuronal anion gradient underlying neuropathic pain," *Nature*, vol. 438, no. 7070, pp. 1017–1021, 2005.

[7] A. K. Clark, R. Wodarski, F. Guida, O. Sasso, and M. Malcangio, "Cathepsin S release from primary cultured microglia is regulated by the P2X7 receptor," *GLIA*, vol. 58, no. 14, pp. 1710–1726, 2010.

Hindawi Publishing Corporation
BioMed Research International
Volume 2015, Article ID 894732, 12 pages
http://dx.doi.org/10.1155/2015/894732

Research Article

Delay of Morphine Tolerance by Palmitoylethanolamide

Lorenzo Di Cesare Mannelli, Francesca Corti, Laura Micheli, Matteo Zanardelli, and Carla Ghelardini

Dipartimento di Neuroscienze, Psicologia, Area del Farmaco e Salute del Bambino-Neurofarba-Sezione di Farmacologia e Tossicologia, Università di Firenze, Viale Pieraccini 6, 50139 Florence, Italy

Correspondence should be addressed to Lorenzo Di Cesare Mannelli; lorenzo.mannelli@unifi.it

Received 28 May 2014; Accepted 18 July 2014

Academic Editor: Livio Luongo

In spite of the potency and efficacy of morphine, its clinical application for chronic persistent pain is limited by the development of tolerance to the antinociceptive effect. The cellular and molecular mechanisms underlying morphine tolerance are complex and still unclear. Recently, the activation of glial cells and the release of glia-derived proinflammatory mediators have been suggested to play a role in the phenomenon. *N*-Palmitoylethanolamine (PEA) is an endogenous compound with antinociceptive effects able to reduce the glial activation. On this basis, 30 mg kg^{-1} PEA was subcutaneously daily administered in morphine treated rats (10 mg kg^{-1} intraperitoneally, daily). PEA treatment significantly attenuated the development of tolerance doubling the number of days of morphine antinociceptive efficacy in comparison to the vehicle + morphine group. PEA prevented both microglia and astrocyte cell number increase induced by morphine in the dorsal horn; on the contrary, the morphine-dependent increase of spinal TNF-α levels was not modified by PEA. Nevertheless, the immunohistochemical analysis revealed significantly higher TNF-α immunoreactivity in astrocytes of PEA-protected rats suggesting a PEA-mediated decrease of cytokine release from astrocyte. PEA intervenes in the nervous alterations that lead to the lack of morphine antinociceptive effects; a possible application of this endogenous compound in opioid-based therapies is suggested.

1. Introduction

Opioids remain an integral part of clinical pain management [1]. Although often successful in acute settings, long-term use of opioids may be accompanied by waning levels of analgesic response not readily attributable to advancing underlying disease, necessitating dose escalation to manage pain. Analgesic tolerance has been invoked to explain such declines in opioid effectiveness over time. This undesirable manifestation, along with other adverse effects caused by escalating doses (e.g., oversedation, respiratory depression, and constipation), significantly decreases quality of life in patients with chronic pain [2].

Lines of evidence have demonstrated that multiple factors are known to be involved in morphine tolerance [3], mainly involving neuronal mechanisms of adaptation and sensitization. On the other hand, chronic morphine treatment activates spinal and cortical glial cells [4–7] which contribute the development of antinociceptive tolerance [6, 8]. Direct and indirect morphine-evoked signals [7] produce microglia and astrocyte changes [9] ultimately resulting in increased production of many substances such as free radicals, nitric oxide, proinflammatory cytokines and chemokines, prostaglandins, complement proteins, neurotoxins, neurotrophic factors, and excitatory amino acids which actively opposes the analgesic effects of morphine and contributes to the development of tolerance [10, 11]. Moreover, pharmacological glial inhibition decreases morphine-induced cytokine release and attenuates tolerance [7]. Administration of the glial metabolic inhibitor fluorocitrate has been found to attenuate the development of morphine tolerance [6]. Minocycline, propentofylline, and pentoxifylline reduced glial cell activation and significantly blocked the development of morphine tolerance in naive mice, as well as in a model of neuropathic pain [5, 12, 13]. Lu et al. [14] showed that patients receiving pentoxifylline exhibited longer patient-controlled analgesia trigger times in the presence of attenuated perioperative cytokine response and required less morphine consumption. However the side

effects of these compounds limit their prolonged use in persistent pain conditions [15].

N-Palmitoylethanolamine (PEA), the endogenous amide between palmitic acid and ethanolamine, belongs to the family of fatty acid ethanolamides (FAEs), a class of lipid mediators. PEA exerts antinociceptive effects in several animal models [16, 17]. Its safety and efficacy were shown in a variety of clinical trials focused on pain state treatment: diabetic neuropathy, carpal tunnel syndrome, dental and temporomandibular joint pain, and arthritic, postherpetic, and chemotherapy-induced neuropathic pain [18, 19]. Moreover, PEA protects nervous tissue in neuropathic conditions [20], prevents neurotoxicity and neurodegeneration [21, 22], and inhibits peripheral inflammation and mast cell degranulation [23]. Further, PEA reduced the activation of microglia and astrocytes [24]. PEA normalized spinal microglia and astrocyte activation in the rat model of inflammatory pain induced by formalin [25] as well as after spinal cord trauma in mice [26]. Treatment with PEA reduced microglial activation and the number of astrocytes in the model of Parkinson's disease induced by 1-methyl-4-phenyl-1,2,3,6-tetrahydropyridine (MPTP) [27] and counteracts reactive gliosis after β-amyloid peptide injection in rat brain [28].

Based on the hypothesis that the glial cell modulator PEA may influence the development of morphine tolerance, the antinociceptive effect of repeated treatment with the alkaloid was evaluated overtime during PEA administration.

2. Material and Methods

2.1. Animals. Male Sprague-Dawley rats (Harlan, Varese, Italy), weighing 200–250 g at the beginning of the experimental procedure, were used for all the experiments. Animals were housed in CeSAL (Centro Stabulazione Animali da Laboratorio, University of Florence) and used no earlier than one week after their arrival. Four rats were housed per cage (size 26 × 41 cm); animals were fed with standard laboratory diet and tap water *ad libitum* and kept at 23 ± 1°C with a 12 h light/dark cycle, light at 7 a.m. All animal manipulations were carried out according to the European Community guidelines for animal care (DL 116/92, application of the European Communities Council Directive of 24 November 1986; 86/609/EEC). The ethical policy of the University of Florence complies with the Guide for the Care and Use of Laboratory Animals of the US National Institutes of Health (NIH Publication number 85-23, revised 1996; University of Florence assurance number: A5278-01). Formal approval to conduct the described experiments was obtained from the Animal Subjects Review Board of the University of Florence and the research was authorized by the Italian Ministry of Health (Decree 54/2014-B). All efforts were made to minimize animal suffering and to reduce the number of animals used.

2.2. Pharmacological Treatments. Micronized PEA (Epitech, Padova, Italy) was dissolved in PEG and Tween 80 2 : 1 (Sigma-Aldrich, Milan, Italy) and kept overnight under gentle agitation with a microstirring bar. Before injection, sterile saline was added so that the final concentrations of PEG and Tween 80 were 20 and 10% v/v, respectively. Drug was injected daily (9 a.m., from day 1 to day 11) subcutaneously (s.c.) in a dose of 30 mg kg^{-1}. Morphine (S.A.L.A.R.S., Como, Italy) was dissolved in sterile saline and injected daily (2 p.m., from day 1 to day 11) intraperitoneally (i.p.) in a dose of 10 mg kg^{-1}. Behavioral measurements were performed immediately before and 30 min after morphine administration. Dosages were chosen on the basis of previous studies [20, 29, 30]. The described dosages were administered with respect to the body weight and all injections were given in a mean volume of 0.3 mL. Control animals were treated with vehicle.

2.3. Paw Pressure Test. The nociceptive threshold in the rat was determined with an analgesiometer (Ugo Basile, Varese, Italy), according to the method described by [31]. Briefly, constantly increasing pressure was applied to a small area of the dorsal surface of the hind paw using a blunt conical mechanical probe. Mechanical pressure was increased until vocalization or a withdrawal reflex occurred while rats were lightly restrained. Vocalization or withdrawal reflex thresholds were expressed in grams. Rats scoring below 40 g or over 75 g during the test before drug administration were rejected (25%). For analgesia measures, mechanical pressure application was stopped at 120 g [32].

2.4. Plantar Test. Pain thermal sensitivity was measured using a plantar test apparatus (Ugo Basile, Varese, Italy), wherein the paw withdrawal latency to a thermal stimulus was measured, as described previously [33]. The apparatus used a test unit containing a heat source that radiated a light beam. An adjustable angled mirror on the test unit was used to locate the correct targeting area on the paw. The beam source was set with an active intensity of 40%, an idle intensity of 10%, and a cut-off time of 25 s. The paw withdrawal latency comprised the time from the start of the beam light until the animal withdrew the paw from the heat stimulus (reaction time was measured to 0.01 s). An acrylic six-chamber container was used to separate the rats that were placed on the glass base. The baseline paw withdrawal latency values were close to 10 s when the current parameters were used. Measurements were taken in duplicate at least 1 min apart, and the average was used for statistical analysis. Behavioural responses of both left and right paws were measured.

2.5. Immunofluorescence Staining. On days 6 and 11, rats were sacrificed; the L4/L5 segments of the spinal cord were exposed from the lumbovertebral column via laminectomy and identified by tracing the dorsal roots from their respective DRG. According to [34–36], formalin-fixed cryostat sections (7 μm) were washed 3× with phosphate-buffered saline (PBS) and 0.3% Triton X-100 for 5 min and then were incubated, at room temperature, for 1 h in blocking solution (PBS, 0.3% Triton X-100, and 5% albumin bovine serum; PBST). Slices were incubated overnight at 4°C in PBST containing rabbit primary antisera. The primary antibody

used was directed against ionized calcium binding adapter molecule 1 (Iba1; rabbit, 1 : 1000; Wako, Richmond, VA, USA) for microglial staining or against glial fibrillary acidic protein (GFAP; rabbit, 1 : 1000; DAKO, Carpinteria, CA, USA) for astrocyte staining. The following day slides were washed 3× with PBS and 0.3% Triton X-100 for 5 min and then sections were incubated in goat anti-rabbit IgG secondary antibody labeled with Alexa Fluor 568 (1 : 500; Invitrogen, Carlsbad, USA) and DAPI (4′,6-diamidin-2-phenylindole; 1 : 2000; Life Technologies-Thermo scientific, Rockford, IL, USA), a nuclei marker, in PBST at room temperature for 2 h, in the dark. After 3× PBS and 0.3% Triton X-100 wash for 10 min, slices were mounted using ProLong Gold (Life Technologies-Thermo scientific, Rockford, IL, USA) as a mounting medium.

Negative control sections (no exposure to the primary antisera) were processed concurrently with the other sections for all immunohistochemical studies, in order to exclude the presence of nonspecific immunofluorescent staining or cross immunostaining.

Images were acquired by using an Olympus BX63 microscope equipped with an Olympus XM10 camera and coupled to *CellSens Dimension* Software (Olympus, Milan, Italy).

Quantitative analysis of GFAP and Iba1-positive cells was performed by collecting three independent fields through a 20x 0.40NA objective in the dorsal horn of each rat spinal cord. GFAP and Iba1-positive cells were counted using the "cell counter" plugin of ImageJ (NIH, Bethesda, Maryland, USA).

2.6. Double Immunofluorescence Staining. To evaluate the tumor necrosis factor-α (TNF-α) expression in the dorsal horn of rat spinal cord, double immunofluorescent labeling of TNF-α and GFAP for astrocytes or OX42 for microglia was performed. Formalin-fixed cryostat sections (7 μm) were washed 3× with PBS and 0.3% Triton X-100 for 5 min and then were incubated, at room temperature, for 1 h in PBST. To visualize TNF-α and microglia the primary antibodies used were directed against TNF-α (rabbit, 1 : 1000; Thermo scientific, Rockford, IL, USA) and OX42, a microglia marker (mouse, 1 : 150; BD Bioscience, Becton&Dickinson, New Jersey, USA). Antibodies were incubated overnight at 4°C in PBST. The following day, slides were washed 3× PBS and 0.3% Triton X-100 for 5 min and then sections were incubated in goat anti-rabbit IgG secondary antibody labeled with Alexa Fluor 568 (1 : 500, Invitrogen, Carlsbad, USA), to visualize TNF-α, and in goat anti-mouse IgG secondary antibody labeled with Alexa Fluor 488 (1 : 500; Invitrogen, Carlsbad, USA), to visualize microglia, and DAPI (1 : 2000, Life Technologies-Thermo scientific, Rockford, IL, USA), a nuclei marker, in PBST at room temperature for 2 h in the dark. After 3× PBS and 0.3% Triton X-100 wash for 10 min, slices were mounted using ProLong Gold (Life Technologies-Thermo scientific, Rockford, IL, USA) as a mounting medium. The same procedure was repeated to visualize TNF-α and astrocytes using the described antibody directed against TNF-α and a mouse GFAP Alexa Fluor 488 conjugated (1 : 200; Millipore, Temecula, CA, USA). Negative control sections (no exposure to the primary antisera) were processed concurrently with the other sections for all immunohistochemical studies, in order to exclude the presence of nonspecific immunofluorescent staining or cross immunostaining. Images were acquired as above. Quantitative analysis of TNF-α and GFAP expression or TNF-α and OX42 expression was performed by collecting three independent fields through a 20x 0.40NA objective in the dorsal horn of each rat spinal cord. Colocalization that can be described as the spatial overlap of two or more dyes in a multichannel image of TNF-α and GFAP or of TNF-α and OX42 was evaluated using the "JACoP" (just another colocalization plugin) plugin of ImageJ (NIH, Bethesda, Maryland, USA). Colocalization can be estimated by calculating a number of values representing the proportion of colocalized pixels. These values are called colocalization coefficients [37]. In this work we evaluated the overlap coefficient: it indicates an actual overlap of the signals and is considered to represent the true degree of colocalization [38].

2.7. Enzyme-Linked Immunosorbent Assay (ELISA) TNF-α. The dorsal horns of the spinal cord were homogenized in lysis buffer containing 50 mM Tris-HCl pH 8.0, 150 mM NaCl, 1 mM EDTA, 0.5% Triton X-100, Complete Protease Inhibitor (Roche, Milan, Italy), in ice, and centrifuged at 13,000 ×g for 15 minutes at 4°C. The protein concentration of the supernatant was quantified by BCA assay kit (Sigma-Aldrich, St. Louis, MO, USA). TNF-α was measured using commercially available enzyme immunoassays (rat TNF-α ELISA set, eBiosciences, San Diego, CA, USA) according to the manufacturer's instructions. The protein expression was normalized to the total protein amount per spinal cord and reported as pg/mg.

2.8. Statistical Analysis. Behavioral measurements were performed on 12 rats for each treatment carried out in 2 different experimental sets. Measurements were taken in duplicate at least 1 min apart; the responses of both left and right paws were measured. For behavioral experiments one-way analysis of variance (ANOVA) followed by Fisher's protected least significant difference procedure was used. ELISA and immunohistochemical analyses were performed on 6 rats per group. Six sections of spinal cord for each animal were evaluated. For statistical analysis, data were analyzed by one-way ANOVA followed by multiple comparisons with the Bonferroni post hoc test.

All behavioral assessments were made by researchers blinded to rat treatment. Slides from control and experimental groups were labeled with numbers so that the person performing the image analysis was blinded as to the experimental group. In addition, all images were captured and analyzed by an investigator other than the one who performed measurements to avoid possible bias. Since behavioral measurements were performed 30 min after morphine injection, different animal groups were used for paw pressure and plantar tests. ELISA and immunohistochemical analysis were performed on tissues from the same animals used for behavioral analysis. Data about the control group vehicle + vehicle are the mean of values obtained on days 6 and 11. For all the immunochemical analyses no differences were

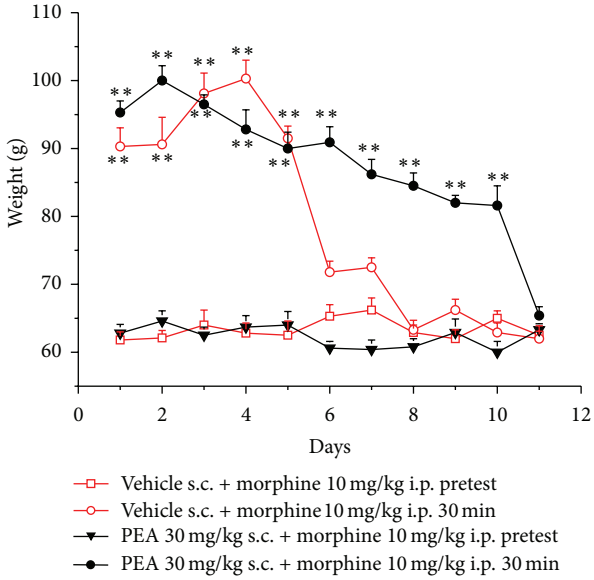

Figure 1: Analgesia measurement, paw pressure test. Animals were treated daily with 30 mg kg^{-1} PEA s.c. or with vehicle. The pain threshold was evaluated every day immediately before and 30 min after the injection i.p. of 10 mg kg^{-1} morphine. Each value represents the mean ± SEM of 12 rats per group, performed in 2 different experimental sets. $^{**}P < 0.01$ versus pretest values.

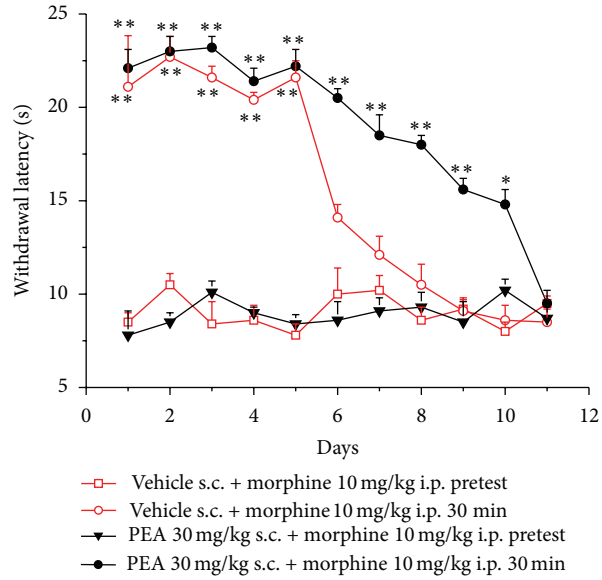

Figure 2: Analgesia measurement, plantar test. Animals were treated daily with 30 mg kg^{-1} PEA s.c. or with vehicle. The pain threshold was evaluated every day immediately before and 30 min after the injection i.p. of 10 mg kg^{-1} morphine. Each value represents the mean ± SEM of 12 rats per group, performed in 2 different experimental sets. $^{**}P < 0.01$ versus pretest values.

highlighted in the vehicle + vehicle group on days 6 and 11. Data were analyzed using the "Origin 7.5" software (OriginLab, Northampton, MA, USA). Differences were considered significant at $P < 0.05$.

3. Results

Ten mg kg^{-1} morphine administered i.p. (30 min after injection) increased the weight tolerated on the posterior paw up to 90.3 ± 2.7 g in comparison to the threshold before treatment (pretest) of 61.8 ± 1.2 g (Figure 1). A similar effect was maintained when morphine was newly injected in the following days till day 5. The same dose was unable to significantly increase pain threshold from day 6. In the group treated with 30 mg kg^{-1} PEA s.c. (daily) the antinociceptive effect of morphine reached 95.3 ± 1.7 g (Figure 1). The efficacy of morphine was significant up to day 10 (81.6 ± 2.9 g). PEA per se did not alter the response to the paw pressure as shown by the values of pretest (before morphine injection) of the group PEA + morphine. Figure 2 shows the results obtained with the plantar test. The withdrawal latency to a painful thermal stimulus was increased by morphine to 21.1 ± 2.7 s in comparison to the pretest value of 8.5 ± 0.5 s (vehicle + morphine group). In the presence of PEA treatment the significance of morphine-induced analgesia lasted till day 10 (14.8 ± 0.8 s).

The spinal cord was analyzed on days 6 and 11 when tolerance to the antinociceptive effect of morphine was developed in the vehicle + morphine and in the PEA + morphine group, respectively.

Alkaloid treatment progressively increased the number of Iba1-positive cells in the dorsal horn (Figure 3). On day 6, microglia density was significantly higher in the group vehicle + morphine in comparison to vehicle + vehicle group. PEA fully prevented the morphine-induced microglia activation on day 6 and on day 11 the effect was still significant in comparison to vehicle + morphine (Figure 3). Similar results were obtained when microglia was analyzed by OX42 immunoreactivity (Supplemental information, Figure S1 available online at http://dx.doi.org/10.1155/2014/894732). The expression of GFAP in the dorsal horn is shown in Figure 4. The analysis of GFAP-positive cells reveals a morphine-induced increase in astrocyte cell density on day 6 as well as on day 11 (vehicle + morphine). PEA reduced astrocyte cell number at both time points (Figure 4; PEA + morphine).

In dorsal horn homogenate TNF-α levels were measured (Table 1). Vehicle + morphine treated rats showed a 112% and 168% increase of the cytokine on days 6 and 11, respectively. PEA did not alter this increment. As shown in Figures 5 and 6, TNF-α localization was studied by immunohistochemistry.

Table 1: TNF-α levels in the spinal cord.

	TNF-α levels (pg/mg proteins)		
	vehicle + vehicle	vehicle + morphine	PEA + morphine
	12.2 ± 3.2		
Day 6		25.9 ± 3.8*	30.7 ± 5.0*
Day 11		32.7 ± 6.4*	28.4 ± 3.0*

In the dorsal horn of the spinal cord, TNF-α levels were measured by ELISA on days 6 and 11. Rats were treated daily i.p. with 10 mg kg^{-1} morphine and 30 mg kg^{-1} PEA and compared with vehicle treatment. Each value represents the mean ± SEM of 6 rats per group, performed in 2 different experimental sets. $^{*}P < 0.05$ versus vehicle + vehicle.

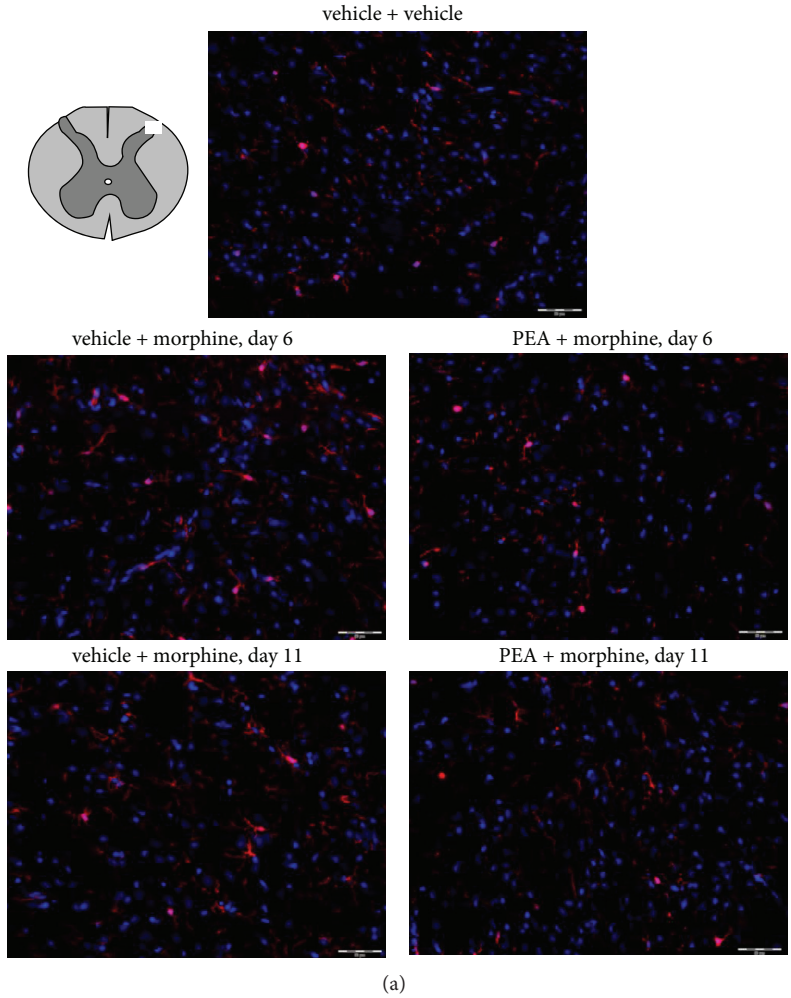

(a)

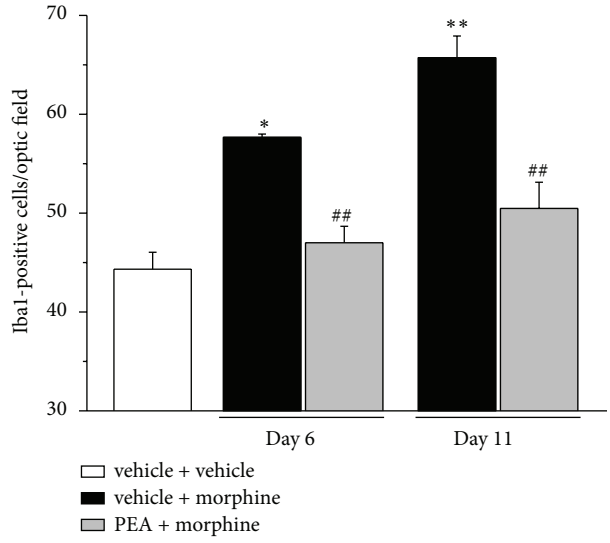

(b)

Figure 3: Iba1-positive cell density in the dorsal horn of the spinal cord. 30 mg kg^{-1} PEA s.c. and 10 mg kg^{-1} morphine i.p. were administered daily and immunohistochemical analysis was performed on days 6 and 11; (a) representative images of merged Iba1-labeled microglia cells (red), plus DAPI-labeled cell nuclei (blue); scale bar: 50 μm. (b) Quantitative analysis of cellular density was performed evaluating 6 animals for each group. Each value represents the mean ± SEM of 6 rats per group, performed in 2 different experimental sets. $^{*}P < 0.05$ and $^{**}P < 0.01$ versus vehicle + vehicle; $^{\#\#}P < 0.01$ versus vehicle + morphine.

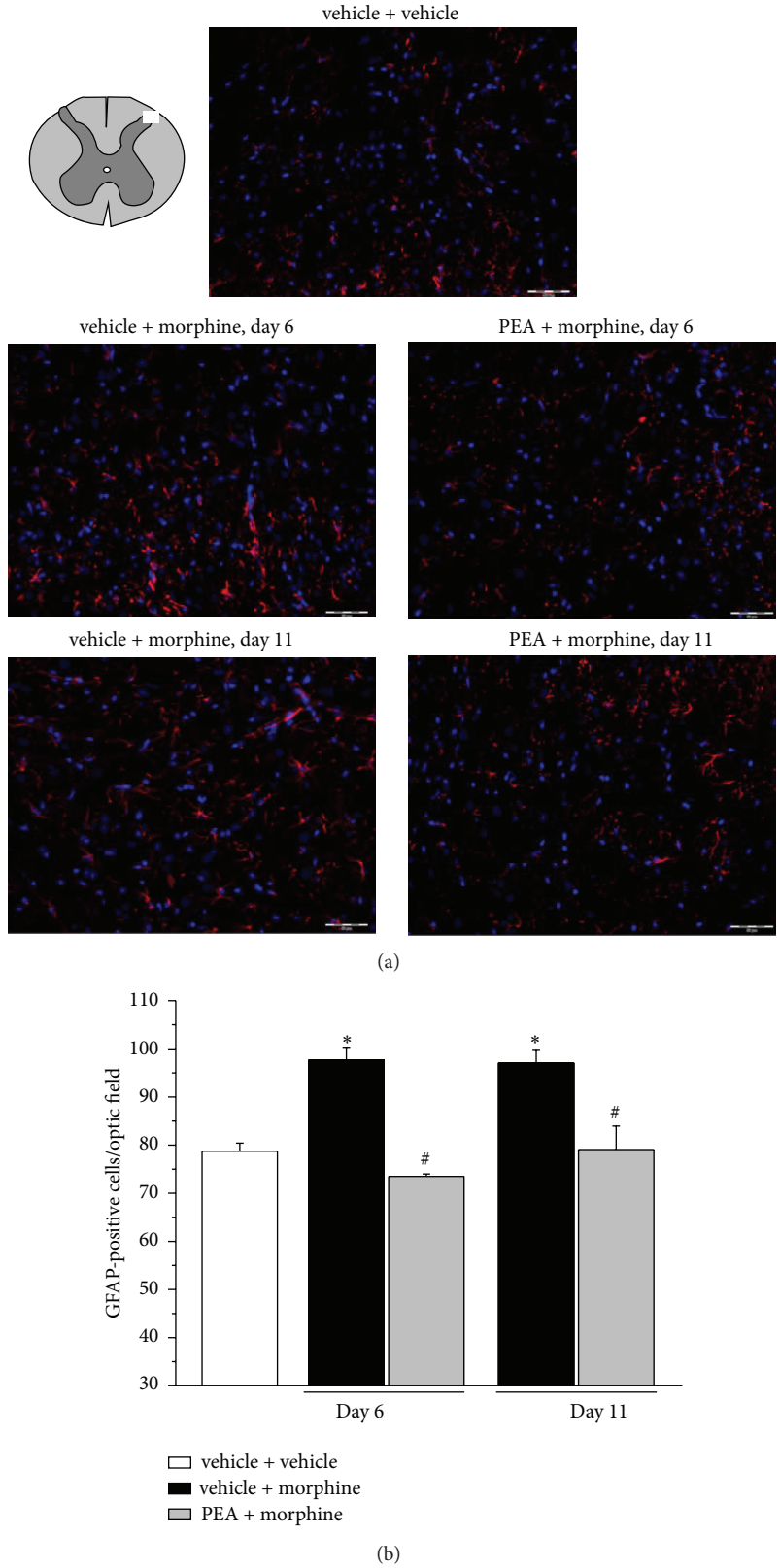

FIGURE 4: GFAP-positive cell density in the dorsal horn of the spinal cord. 30 mg kg^{-1} PEA s.c. and 10 mg kg^{-1} morphine i.p. were administered daily and immunohistochemical analysis was performed on days 6 and 11; (a) representative images of merged GFAP-labeled astrocyte cells (red), plus DAPI-labeled cell nuclei (blue); scale bar: 50 μm. (b) Quantitative analysis of cellular density was performed evaluating 6 animals for each group. Each value represents the mean ± SEM of 6 rats per group, performed in 2 different experimental sets. $^{*}P < 0.05$ versus vehicle + vehicle; $^{\#}P < 0.05$ versus vehicle + morphine.

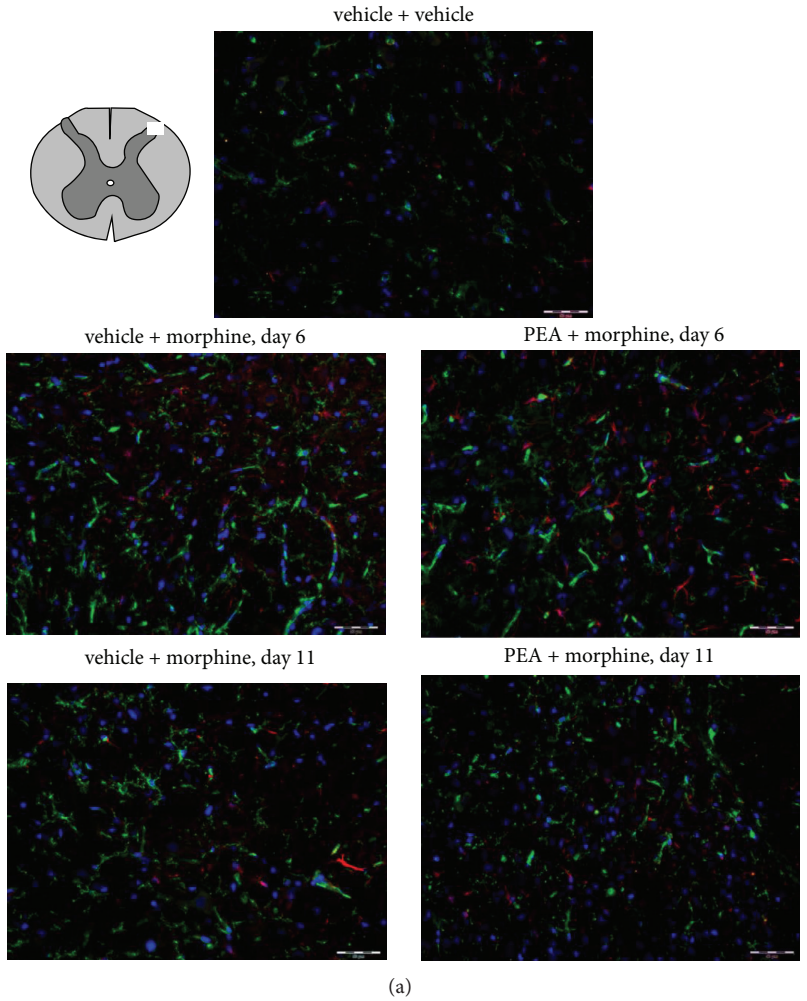

(a)

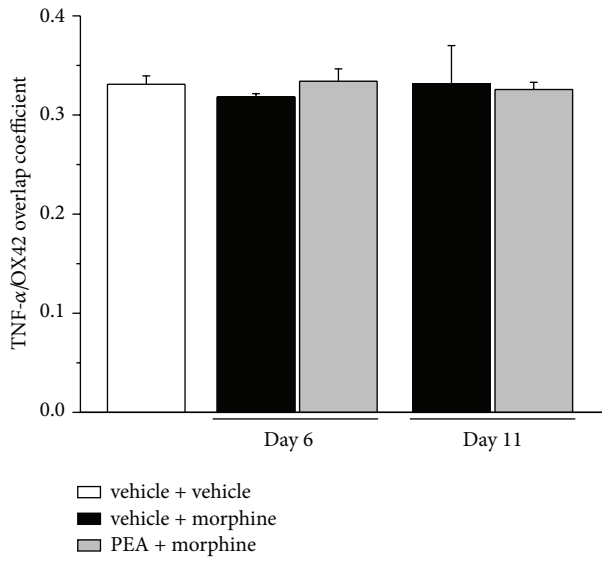

(b)

Figure 5: Colocalization of TNF-α and OX42 in the dorsal horn of the spinal cord. 30 mg kg^{-1} PEA s.c. and 10 mg kg^{-1} morphine i.p. were administered daily and immunohistochemical analysis was performed on days 6 and 11; (a) representative images of merged TNF-α (red), OX42 (green), and DAPI (blue) labeling; scale bar: 50 μm. (b) Quantitative analysis of the overlap coefficient for TNF-α and OX42 expression performed evaluating 6 animals for each group. Each value represents the mean ± SEM of 6 rats per group, performed in 2 different experimental sets.

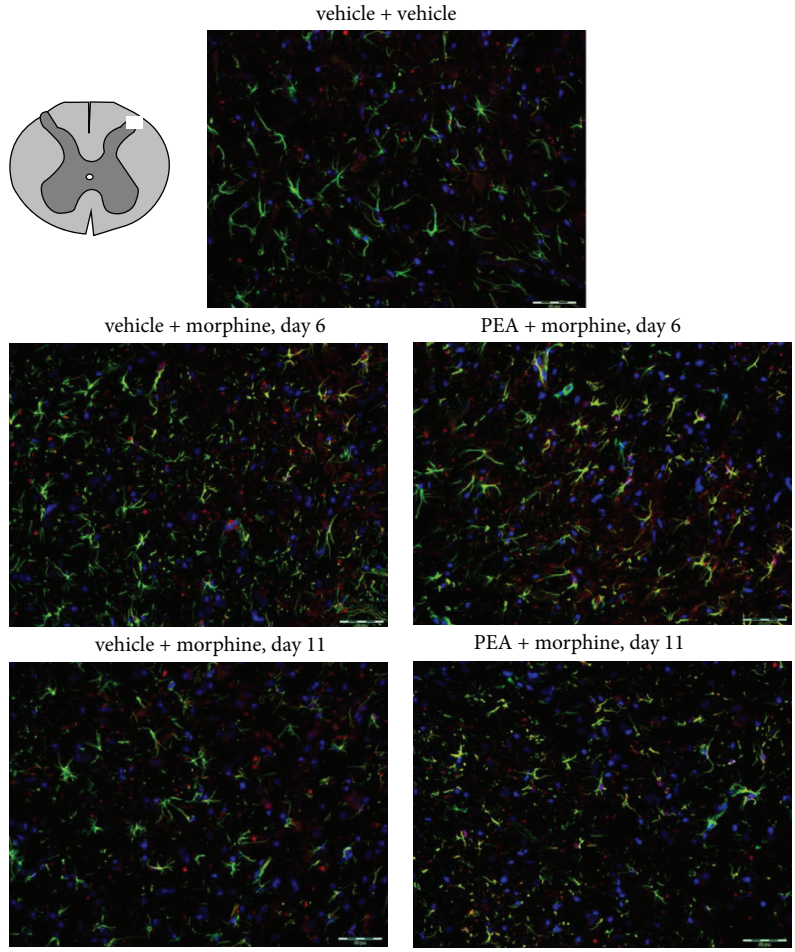

(a)

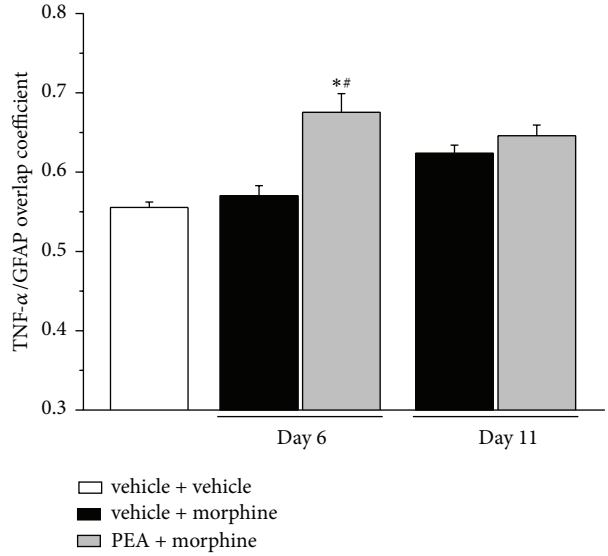

(b)

Figure 6: Colocalization of TNF-α and GFAP in the dorsal horn of the spinal cord. 30 mg kg^{-1} PEA s.c. and 10 mg kg^{-1} morphine i.p. were administered daily and immunohistochemical analysis was performed on days 6 and 11; (a) representative images of merged TNF-α (red), GFAP (green), and DAPI (blue) labeling; scale bar: 50 μm. (b) Quantitative analysis of the overlap coefficient for TNF-α and GFAP expression performed evaluating 6 animals for each group. Each value represents the mean ± SEM of 6 rats per group, performed in 2 different experimental sets. $^{*}P < 0.05$ versus vehicle + vehicle; $^{\#}P < 0.05$ versus vehicle + morphine.

In the spinal dorsal horn of vehicle + vehicle treated rats, TNF-α immunoreactivity was scarcely colocalized with the microglial marker OX42 and the overlap coefficient was not modified by treatments (Figure 5). The colocalization of TNF-α with GFAP was more evident even though morphine repeated treatment did not alter the value. On the contrary, after 6 days of treatment, PEA (PEA + morphine) significantly increased the overlap between TNF-α and GFAP (Figure 6). On day 11, after the development of tolerance also in the PEA group, the cytokine presence in astrocytes decreased to the level of vehicle + morphine group (Figure 6). For all the immunochemical analyses no differences were highlighted in the vehicle + vehicle group on days 6 and 11.

4. Discussion

The present data show the property of PEA to double the number of days of morphine treatment efficacy. The pain threshold evaluated by both mechanical and thermal stimuli is still significantly increased by the alkaloid after 10 days of treatment in animals receiving PEA. This result is not influenced by *per se* antinociceptive effects of PEA as shown by pretest values recorded before morphine treatment. This piece is added to the intriguing mosaic of the pain reliever effects of PEA.

Both opioid tolerance and neuropathic pain conditions share features of diminished morphine analgesia, leading to suggestions of a common mechanism [39]. Among complex signaling networks, glial cell modulation emerges in neuropathic pain [40–42] and in antinociceptive tolerance [6] as well as in PEA effects [24].

To the best of our knowledge, this is the first evidence of morphine-induced glial activation characterized by an increase in cell density without consistent morphological alteration of both microglia and astrocytes. This glial profile is evident on day 6 when morphine lacks its antinociceptive properties. PEA prevents the glial cell number increase and prolongs morphine efficacy up to day 10 suggesting a relationship between glial inhibition and attenuation of tolerance. Nevertheless, the preventative effect on the glial density increase is maintained also on day 11 after the onset of tolerance in the group PEA + morphine suggesting a further mechanism based on glia functions. Glial cells activated by morphine secrete large amounts of proinflammatory cytokines including interleukin-1β (IL-1β), IL-6, and TNF-α, ATP, and nitric oxide (NO), accelerating the development of the antinociceptive tolerance [43]. Moreover, IL-1β, IL-6, and TNF-α have also been shown to oppose acute and chronic opioid analgesia [44]. Glia-derived proinflammatory cytokines inhibit the antinociceptive effect of morphine by sensitizing pain-transmission neurons in animals with morphine tolerance and neuropathic pain [45]. Both central and peripheral administration of the proinflammatory cytokines TNF-α, IL-1β, and IL-6 facilitate pain transmission [46, 47] and the reduction of the antinociceptive effect of morphine can be reversed by inhibition of glial metabolism, antagonism of IL-1 receptors, and induction of anti-inflammatory cytokine IL-10 expression [6, 48]. In the present study, the expression levels of TNF-α in spinal cord tissue homogenate are increased after 6 and 11 days of morphine treatment but PEA does not modify this alteration. The double immunofluorescence analysis of dorsal horn revealed a preferential localization of TNF-α astrocyte in comparison to microglia cells and, interestingly, significantly higher TNF-α immunoreactivity in astrocytes of PEA-protected rats (day 6) is shown. Since the presence of TNF-α in GFAP-positive cells decreases on day 11, PEA seems to be able to delay the cytokine release from astrocyte paralleling with tolerance attenuation. The relevance of astrocyte-released TNF-α in tolerance mechanisms was highlighted by Wang et al. [49] which demonstrated, after a 7-day treatment with morphine, the cytokine upregulation in astrocytes by a calcitonin gene-related peptide- (CGRP-) mediated increase of phosphorylated ERK [49]. Furthermore Shen and coworkers [50] confirmed the role of TNF-α since etanercept, a recombinant soluble p75 TNF receptor:Fc fusion protein [51], preserved a significant antinociceptive effect of morphine in morphine-tolerant rats suppressing proinflammatory cytokine expression and neuroinflammation in microglia [50]. On the contrary, the glial modulation profile and cytokine levels during the period of morphine efficacy remain to be assessed. Even though some relevant upstream signals, including ceramide and nitroxidative stress [52], were shown further research is necessary to clearly highlight the neuron-glia network in the development of morphine tolerance.

PEA is a naturally occurring amide between palmitic acid and ethanolamine; it is a lipid messenger known to mimic several endocannabinoid-driven actions even though PEA does not bind CB1, CB2, and abn-CBD receptors [53]. So far, numerous actions of PEA on immune cells such as modulation of cytokine release from macrophages, attenuation of leukocyte extravasation, and inhibition of mast cell degranulation have been described [54, 55]. Anti-inflammatory effects of PEA have been associated with peroxisome proliferator-activated receptor- (PPAR-) α activation [56]. PPAR-α, well known for its role in lipid metabolism, controls transcriptional programs involved in the development of inflammation through mechanisms that include direct interactions with the proinflammatory transcription factors NF-kB and AP1 and modulation of IkB function [57]. The pivotal role of PPAR-α in the PEA pharmacodynamic mechanisms has been demonstrated for pain relief [17] as well as for the PEA neurorestorative properties after peripheral nerve injury [20]. PPAR-α participates also in the PEA modulation of microglial cells [58]. The involvement of PPAR-α in morphine tolerance development is not actually established; on the contrary, the PPAR-γ agonist pioglitazone reduced the tolerance to the analgesic effect of morphine [59]. An "entourage effect hypothesis" has also been put forward to account for the pharmacological actions of PEA. Based on an activity enhancement of other endogenous compounds (e.g., the endocannabinoid anandamide [16]), by potentiating their affinity for a receptor or by inhibiting their metabolic degradation [60], PEA may indirectly stimulate the transient receptor potential vanilloid type 1 (TRPV1) and the cannabinoid receptors [24]. Interestingly, morphine is able to modulate endocannabinoid levels. Viganò et al. [61] showed

modified brain levels of arachidonoylethanolamide (anandamide, AEA) and 2-arachidonoylglycerol (2-AG) after morphine treatment, and differences were highlighted between compounds depending on the duration of morphine exposure and brain area. In particular, a single morphine injection increased AEA whereas it returned to the basal level after 3 days of treatment [61]. CB1 and opioid receptors are colocalized in brain regions important for the expression of morphine dependence [62] and, finally, compounds that modulate the CB1 receptor systems can modulate the development of morphine tolerance and dependence [63]. Repeated administration of the naturally occurring cannabinoid agonist Δ9-tetrahydrocannabinol or the CB1 receptor agonist CP-55940 attenuates morphine antinociceptive tolerance [63–65]. Cannabinoids act on glia and neurons to inhibit the release of proinflammatory molecules, including IL-1β, TNF-α, and NO [66, 67], and enhance the release of the anti-inflammatory cytokines IL-4 and IL-10 [68]. In particular, anandamide reduces the release of TNF-α from astrocytes [66] and the CB2 receptor stimulation attenuated morphine-induced microglial proinflammatory mediator increases, interfering with morphine effect by acting on the Akt-ERK1/2 signalling pathway [69]. On the other hand, PEA reduces activation of microglia and astrocytes expressing cannabinoid CB2 receptors in mice underwent compressive trauma of spinal cord [26].

5. Conclusion

Multiple properties of PEA converge to an interaction with signals evoked by morphine. The evidence of a delayed development of tolerance to the antinociceptive effects of morphine in the presence of PEA suggests a possible application of this endogenous compound in opioid-based therapies.

Conflict of Interests

Carla Ghelardini received a grant from Epitech (Padova, Italy). All other authors declare that there is no conflict of interests regarding the publication of this paper.

Acknowledgment

This work was supported by the Italian Ministry of Instruction, University and Research.

References

[1] A. Trescot, S. E. Glaser, H. Hansen, R. Benyamin, S. Patel, and L. Manchikanti, "Effectiveness of opioids in the treatment of chronic non-cancer pain," *Pain Physician*, vol. 11, no. 2, pp. S181–S200, 2008.

[2] J.-T. Xu, J.-Y. Zhao, X. Zhao et al., "Opioid receptor-triggered spinal mTORC1 activation contributes to morphine tolerance and hyperalgesia," *Journal of Clinical Investigation*, vol. 124, no. 2, pp. 592–603, 2014.

[3] D. Zhou, M.-L. Chen, Y.-Q. Zhang, and Z.-Q. Zhao, "Involvement of spinal microglial P2X7 receptor in generation of tolerance to morphine analgesia in rats," *Journal of Neuroscience*, vol. 30, no. 23, pp. 8042–8047, 2010.

[4] Y. Cui, Y. Chen, J. L. Zhi, R. X. Guo, J. Q. Feng, and P. X. Chen, "Activation of p38 mitogen-activated protein kinase in spinal microglia mediates morphine antinociceptive tolerance," *Brain Research*, vol. 1069, no. 1, pp. 235–243, 2006.

[5] Y. Cui, X.-X. Liao, W. Liu et al., "A novel role of minocycline: attenuating morphine antinociceptive tolerance by inhibition of p38 MAPK in the activated spinal microglia," *Brain, Behavior, and Immunity*, vol. 22, no. 1, pp. 114–123, 2008.

[6] P. Song and Z.-Q. Zhao, "The involvement of glial cells in the development of morphine tolerance," *Neuroscience Research*, vol. 39, no. 3, pp. 281–286, 2001.

[7] J. Mika, "Modulation of microglia can attenuate neuropathic pain symptoms and enhance morphine effectiveness," *Pharmacological Reports*, vol. 60, no. 3, pp. 297–307, 2008.

[8] L. R. Watkins, M. R. Hutchinson, I. N. Johnston, and S. F. Maier, "Glia: novel counter-regulators of opioid analgesia," *Trends in Neurosciences*, vol. 28, no. 12, pp. 661–669, 2005.

[9] R. J. Horvath, R. P. Landry, E. A. Romero-Sandoval, and J. A. DeLeo, "Morphine tolerance attenuates the resolution of postoperative pain and enhances spinal microglial p38 and extracellular receptor kinase phosphorylation," *Neuroscience*, vol. 169, no. 2, pp. 843–854, 2010.

[10] H. Hameed, M. Hameed, and P. J. Christo, "The effect of morphine on glial cells as a potential therapeutic target for pharmacological development of analgesic drugs," *Current Pain and Headache Reports*, vol. 14, no. 2, pp. 96–104, 2010.

[11] L. N. Eidson and A. Z. Murphy, "Blockade of toll-like receptor 4 attenuates morphine tolerance and facilitates the pain relieving properties of morphine," *The Journal of Neuroscience*, vol. 33, no. 40, pp. 15952–15963, 2013.

[12] V. Raghavendra, F. Y. Tanga, and J. A. DeLeo, "Attenuation of morphine tolerance, withdrawal-induced hyperalgesia , and associated spinal inflammatory immune responses by propentofylline in rats," *Neuropsychopharmacology*, vol. 29, no. 2, pp. 327–334, 2004.

[13] J. Mika, M. Osikowicz, W. Makuch, and B. Przewlocka, "Minocycline and pentoxifylline attenuate allodynia and hyperalgesia and potentiate the effects of morphine in rat and mouse models of neuropathic pain," *European Journal of Pharmacology*, vol. 560, no. 2-3, pp. 142–149, 2007.

[14] C.-H. Lu, P.-C. Chao, C. O. Borel et al., "Preincisional intravenous pentoxifylline attenuating perioperative cytokine response, reducing morphine consumption, and improving recovery of bowel function in patients undergoing colorectal cancer surgery," *Anesthesia and Analgesia*, vol. 99, no. 5, pp. 1465–1471, 2004.

[15] Y. Han, C. Jiang, J. Tang et al., "Resveratrol reduces morphine tolerance by inhibiting microglial activation via AMPK signalling," *European Journal of Pain*, vol. 18, no. 10, pp. 1458–1470, 2014.

[16] A. Calignano, G. La Rana, A. Giuffrida, and D. Piomelli, "Control of pain initiation by endogenous cannabinoids," *Nature*, vol. 394, no. 6690, pp. 277–281, 1998.

[17] J. LoVerme, R. Russo, G. La Rana et al., "Rapid broad-spectrum analgesia through activation of peroxisome proliferator-activated receptor-alpha," *Journal of Pharmacology and Experimental Therapeutics*, vol. 319, no. 3, pp. 1051–1061, 2006.

[18] J. M. K. Hesselink, "New targets in pain, non-neuronal cells, and the role of palmitoylethanolamide," *Open Pain Journal*, vol. 5, no. 1, pp. 12–23, 2012.

[19] J. M. K. Hesselink, "Chronic idiopathic axonal neuropathy and pain, treated with the endogenous lipid mediator palmitoylethanolamide: a case collection," *International Medical Case Reports Journal*, vol. 6, no. 1, pp. 49–53, 2013.

[20] L. Di Cesare Mannelli, G. D'Agostino, A. Pacini et al., "Palmitoylethanolamide is a disease-modifying agent in peripheral neuropathy: pain relief and neuroprotection share a PPAR-alpha-mediated mechanism," *Mediators of Inflammation*, vol. 2013, Article ID 328797, 12 pages, 2013.

[21] D. M. Lambert, S. Vandevoorde, G. Diependaele, S. J. Govaerts, and A. R. Robert, "Anticonvulsant activity of N-palmitoylethanolamide, a putative endocannabinoid, in mice," *Epilepsia*, vol. 42, no. 3, pp. 321–327, 2001.

[22] G. D'Agostino, R. Russo, C. Avagliano, C. Cristiano, R. Meli, and A. Calignano, "Palmitoylethanolamide protects against the amyloid-β25-35-induced learning and memory impairment in mice, an experimental model of alzheimer disease," *Neuropsychopharmacology*, vol. 37, no. 7, pp. 1784–1792, 2012.

[23] S. Mazzari, R. Canella, L. Petrelli, G. Marcolongo, and A. Leon, "N-(2-Hydroxyethyl) hexadecanamide is orally active in reducing edema formation and inflammatory hyperalgesia by down-modulating mast cell activation," *European Journal of Pharmacology*, vol. 300, no. 3, pp. 227–236, 1996.

[24] S. D. Skaper, L. Facci, and P. Giusti, "Glia and mast cells as targets for palmitoylethanolamide, an anti-inflammatory and neuroprotective lipid mediator," *Molecular Neurobiology*, vol. 48, no. 2, pp. 340–352, 2013.

[25] L. Luongo, F. Guida, S. Boccella et al., "Palmitoylethanolamide reduces formalin-induced neuropathic-like behaviour through spinal glial/microglial phenotypical changes in mice," *CNS and Neurological Disorders: Drug Targets*, vol. 12, no. 1, pp. 45–54, 2013.

[26] E. Esposito, I. Paterniti, E. Mazzon et al., "Effects of palmitoylethanolamide on release of mast cell peptidases and neurotrophic factors after spinal cordinjury," *Brain, Behavior, and Immunity*, vol. 25, pp. 1099–1112, 2011.

[27] E. Esposito, D. Impellizzeri, E. Mazzon, I. Paterniti, and S. Cuzzocrea, "Neuroprotective activities of palmitoylethanolamide in an animal model of Parkinson's disease," *PLoS ONE*, vol. 7, no. 8, Article ID e41880, 2012.

[28] C. Scuderi, G. Esposito, A. Blasio et al., "Palmitoylethanolamide counteracts reactive astrogliosis induced by β-amyloid peptide," *Journal of Cellular and Molecular Medicine*, vol. 15, no. 12, pp. 2664–2674, 2011.

[29] B. Habibi-Asl, K. Hassanzadeh, and M. Charkhpour, "Central administration of minocycline and riluzole prevents morphine-induced tolerance in rats," *Anesthesia & Analgesia*, vol. 109, no. 3, pp. 936–942, 2009.

[30] J. X. Li, D. A. Thorn, Y. Qiu, B. W. Peng, and Y. Zhang, "Antihyperalgesic effects of imidazoline I(2) receptor ligands in rat models of inflammatory and neuropathic pain," *British Journal of Pharmacology*, vol. 171, no. 6, pp. 1580–1590, 2014.

[31] L. Di Cesare Mannelli, D. Bani, A. Bencini et al., "Therapeutic effects of the superoxide dismutase mimetic compound $MnIIMe_2DO2A$ on experimental articular pain in rats," *Mediators of Inflammation*, vol. 2013, Article ID 905360, 11 pages, 2013.

[32] G. E. Leighton, R. E. Rodriguez, R. G. Hill, and J. Hughes, "κ-Opioid agonists produce antinociception after i.v. and i.c.v. but not intrathecal administration in the rat," *British Journal of Pharmacology*, vol. 93, no. 3, pp. 553–560, 1988.

[33] K. Hargreaves, R. Dubner, F. Brown, C. Flores, and J. Joris, "A new and sensitive method for measuring thermal nociception in cutaneous hyperalgesia," *Pain*, vol. 32, no. 1, pp. 77–88, 1988.

[34] L. Di Cesare Mannelli, A. Pacini, L. Bonaccini, M. Zanardelli, T. Mello, and C. Ghelardini, "Morphologic features and glial activation in rat oxaliplatin-dependent neuropathic pain," *The Journal of Pain*, vol. 14, no. 12, pp. 1585–1600, 2013.

[35] L. Di Cesare Mannelli, A. Pacini, C. Matera et al., "Involvement of α7 nAChR subtype in rat oxaliplatin-induced neuropathy: effects of selective activation," *Neuropharmacology*, vol. 79, pp. 37–48, 2014.

[36] D. Tomassoni, F. Amenta, C. Amantini et al., "Brain activity of Thioctic acid enantiomers: *In vitro* and *in vivo* studies in an animal model of cerebrovascular injury," *International Journal of Molecular Sciences*, vol. 14, no. 3, pp. 4580–4595, 2013.

[37] V. Zinchuk, O. Zinchuk, and T. Okada, "Quantitative colocalization analysis of multicolor confocal immunofluorescence microscopy images: pushing pixels to explore biological phenomena," *Acta Histochemica et Cytochemica*, vol. 40, no. 4, pp. 101–111, 2007.

[38] V. Zinchuk and O. Grossenbacher-Zinchuk, "Recent advances in quantitative colocalization analysis: focus on neuroscience," *Progress in Histochemistry and Cytochemistry*, vol. 44, no. 3, pp. 125–172, 2009.

[39] D. J. Mayer, J. Mao, J. Holt, and D. D. Price, "Cellular mechanisms of neuropathic pain, morphine tolerance, and their interactions," *Proceedings of the National Academy of Sciences of the United States of America*, vol. 96, no. 14, pp. 7731–7736, 1999.

[40] J. Scholz and C. J. Woolf, "The neuropathic pain triad: neurons, immune cells and glia," *Nature Neuroscience*, vol. 10, no. 11, pp. 1361–1368, 2007.

[41] C. Nativi, R. Gualdani, E. Dragoni et al., "A TRPA1 antagonist reverts oxaliplatin-induced neuropathic pain," *Scientific Reports*, vol. 3, article 2005, 2013.

[42] L. Di Cesare Mannelli, A. Pacini, L. Micheli, A. Tani, M. Zanardelli, and C. Ghelardini, "Glial role in oxaliplatin-induced neuropathic pain," *Experimental Neurology*, vol. 261, pp. 22–33, 2014.

[43] I. Berrios, C. Castro, and D. P. Kuffler, "Morphine: axon regeneration, neuroprotection, neurotoxicity, tolerance, and neuropathic pain," *Puerto Rico Health Sciences Journal*, vol. 27, no. 2, pp. 119–128, 2008.

[44] M. R. Hutchinson, B. D. Coats, S. S. Lewis et al., "Proinflammatory cytokines oppose opioid-induced acute and chronic analgesia," *Brain, Behavior, and Immunity*, vol. 22, no. 8, pp. 1178–1189, 2008.

[45] G. B. Stefano, "Autoimmunovascular regulation: morphine and ancondamide and ancondamide stimulated nitric oxide release," *Journal of Neuroimmunology*, vol. 83, no. 1-2, pp. 70–76, 1998.

[46] A. J. Reeve, S. Patel, A. Fox, K. Walker, and L. Urban, "Intrathecally administered endotoxin or cytokines produce allodynia, hyperalgesia and changes in spinal cord neuronal responses to nociceptive stimuli in the rat," *European Journal of Pain*, vol. 4, no. 3, pp. 247–257, 2000.

[47] J. A. DeLeo, R. W. Colburn, M. Nichols, and A. Malhotra, "Interleukin-6-mediated hyperalgesia/allodynia and increased spinal IL-6 expression in a rat mononeuropathy model," *Journal of Interferon & Cytokine Research*, vol. 16, no. 9, pp. 695–700, 1996.

[48] I. N. Johnston, E. D. Milligan, J. Wieseler-Frank et al., "A role for proinflammatory cytokines and fractalkine in analgesia, tolerance, and subsequent pain facilitation induced by chronic intrathecal morphine," *Journal of Neuroscience*, vol. 24, no. 33, pp. 7353–7365, 2004.

[49] Z. Wang, W. Ma, J.-G. Chabot, and R. Quirion, "Cell-type specific activation of p38 and ERK mediates calcitonin gene-related peptide involvement in tolerance to morphine-induced analgesia," *The FASEB Journal*, vol. 23, no. 8, pp. 2576–2586, 2009.

[50] C.-H. Shen, R.-Y. Tsai, M.-S. Shih et al., "Etanercept restores the antinociceptive effect of morphine and suppresses spinal neuroinflammation in morphine-tolerant rats," *Anesthesia and Analgesia*, vol. 112, no. 2, pp. 454–459, 2011.

[51] D. L. Scott and G. H. Kingsley, "Tumor necrosis factor inhibitors for rheumatoid arthritis," *The New England Journal of Medicine*, vol. 355, no. 7, pp. 704–712, 2006.

[52] M. M. Ndengele, S. Cuzzocrea, E. Masini et al., "Spinal ceramide modulates the development of morphine antinociceptive tolerance via peroxynitrite-mediated nitroxidative stress and neuroimmune activation," *Journal of Pharmacology and Experimental Therapeutics*, vol. 329, no. 1, pp. 64–75, 2009.

[53] K. Mackie and N. Stella, "Cannabinoid receptors and endocannabinoids: evidence for new players," *AAPS Journal*, vol. 8, no. 2, article 34, pp. E298–E306, 2006.

[54] R. A. Ross, H. C. Brockie, and R. G. Pertwee, "Inhibition of nitric oxide production in RAW264.7 macrophages by cannabinoids and palmitoylethanolamide," *European Journal of Pharmacology*, vol. 401, no. 2, pp. 121–130, 2000.

[55] E. V. Berdyshev, "Cannabinoid receptors and the regulation of immune response," *Chemistry and Physics of Lipids*, vol. 108, no. 1-2, pp. 169–190, 2000.

[56] J. Lo Verme, J. Fu, G. Astarita et al., "The nuclear receptor peroxisome proliferator-activated receptor-α mediates the anti-inflammatory actions of palmitoylethanolamide," *Molecular Pharmacology*, vol. 67, no. 1, pp. 15–19, 2005.

[57] C. K. Glass and S. Ogawa, "Combinatorial roles of nuclear receptors in inflammation and immunity," *Nature Reviews Immunology*, vol. 6, no. 1, pp. 44–55, 2006.

[58] A. Franklin, S. Parmentier-Batteur, L. Walter, D. A. Greenberg, and N. Stella, "Palmitoylethanolamide increases after focal cerebral ischemia and potentiates microglial cell motility," *Journal of Neuroscience*, vol. 23, no. 21, pp. 7767–7775, 2003.

[59] G. de Guglielmo, G. Scuppa, M. Kallupi, S. Stopponi, and R. Ciccocioppo, "Modulation of PPARγ receptors regulates tolerance to morphine analgesia," in *Proceedings of the 36th Congresso della Società Italiana di Farmacologia*, Torino, Italy, October 2013.

[60] D. Smart, K.-O. Jonsson, S. Vandevoorde, D. M. Lambert, and C. J. Fowler, "'Entourage' effects of N-acyl ethanolamines at human vanilloid receptors. Comparison of effects upon anandamide-induced vanilloid receptor activation and upon anandamide metabolism," *British Journal of Pharmacology*, vol. 136, no. 3, pp. 452–458, 2002.

[61] D. Viganò, M. Valenti, M. G. Cascio, V. Di Marzo, D. Parolaro, and T. Rubino, "Changes in endocannabinoid levels in a rat model of behavioural sensitization to morphine," *European Journal of Neuroscience*, vol. 20, no. 7, pp. 1849–1857, 2004.

[62] M. Navarro, J. Chowen, M. R. A. Carrera et al., "CB1 cannabinoid receptor antagonist-induced opiate withdrawal in morphine-dependent rats," *NeuroReport*, vol. 9, no. 15, pp. 3397–3402, 1998.

[63] B. D. Fischer, S. J. Ward, F. E. Henry, and L. A. Dykstra, "Attenuation of morphine antinociceptive tolerance by a CB1 receptor agonist and an NMDA receptor antagonist: interactive effects," *Neuropharmacology*, vol. 58, no. 2, pp. 544–550, 2010.

[64] D. L. Cichewicz and S. P. Welch, "Modulation of oral morphine antinociceptive tolerance and naloxone-precipitated withdrawal signs by oral δ9-tetrahydrocannabinol," *Journal of Pharmacology and Experimental Therapeutics*, vol. 305, no. 3, pp. 812–817, 2003.

[65] P. A. Smith, D. E. Selley, L. J. Sim-Selley, and S. P. Welch, "Low dose combination of morphine and Δ9-tetrahydrocannabinol circumvents antinociceptive tolerance and apparent desensitization of receptors," *European Journal of Pharmacology*, vol. 571, no. 2-3, pp. 129–137, 2007.

[66] F. Molina-Holgado, A. Lledó, and C. Guaza, "Anandamide suppresses nitric oxide and TNF-α responses to Theiler's virus or endotoxin in astrocytes," *NeuroReport*, vol. 8, no. 8, pp. 1929–1933, 1997.

[67] G. A. Cabral, K. N. Harmon, and S. J. Carlisle, "Cannabinoid-mediated inhibition of inducible nitric oxide production by rat microglial cells: evidence for CB1 receptor participation," *Advances in Experimental Medicine and Biology*, vol. 493, pp. 207–214, 2001.

[68] T. W. Klein, B. Lane, C. A. Newton, and H. Friedman, "The cannabinoid system and cytokine network," *Proceedings of the Society for Experimental Biology and Medicine*, vol. 225, no. 1, pp. 1–8, 2000.

[69] S. Merighi, S. Gessi, K. Varani, D. Fazzi, P. Mirandola, and P. A. Borea, "Cannabinoid CB2 receptor attenuates morphine-induced inflammatory responses in activated microglial cells," *British Journal of Pharmacology*, vol. 166, no. 8, pp. 2371–2385, 2012.

Hindawi Publishing Corporation
BioMed Research International
Volume 2015, Article ID 905906, 10 pages
http://dx.doi.org/10.1155/2015/905906

Research Article

D-Aspartate Modulates Nociceptive-Specific Neuron Activity and Pain Threshold in Inflammatory and Neuropathic Pain Condition in Mice

Serena Boccella,[1] Valentina Vacca,[2,3] Francesco Errico,[4,5] Sara Marinelli,[2,3] Marta Squillace,[4] Francesca Guida,[1] Anna Di Maio,[4] Daniela Vitucci,[4] Enza Palazzo,[6] Vito De Novellis,[1] Sabatino Maione,[1] Flaminia Pavone,[2,3] and Alessandro Usiello[4,7]

[1] *Pharmacology Division, Department of Experimental Medicine, The Second University of Naples, Via Costantinopoli 16, 80138 Naples, Italy*
[2] *CNR, National Research Council, Cell Biology and Neurobiology Institute, Roma, Italy*
[3] *IRCCS, Santa Lucia Foundation, Rome, Italy*
[4] *Laboratory of Behavioural Neuroscience, Ceinge Biotecnologie Avanzate, Via G. Salvatore 486, 80145 Naples, Italy*
[5] *Department of Molecular Medicine and Medical Biotechnology, University of Naples "Federico II", Naples, Italy*
[6] *Department of Anaesthesiology, Surgery and Emergency, The Second University of Naples, Naples, Italy*
[7] *Department of Environmental, Biological and Pharmaceutical Sciences and Technologies, The Second University of Naples, Naples, Italy*

Correspondence should be addressed to Sabatino Maione; sabatino.maione@unina2.it and Alessandro Usiello; usiello@ceinge.unina.it

Received 12 June 2014; Accepted 24 July 2014

Academic Editor: Livio Luongo

D-Aspartate (D-Asp) is a free D-amino acid found in the mammalian brain with a temporal-dependent concentration based on the postnatal expression of its metabolizing enzyme D-aspartate oxidase (DDO). D-Asp acts as an agonist on NMDA receptors (NMDARs). Accordingly, high levels of D-Asp in knockout mice for *Ddo* gene ($Ddo^{-/-}$) or in mice treated with D-Asp increase NMDAR-dependent processes. We have here evaluated in $Ddo^{-/-}$ mice the effect of high levels of free D-Asp on the long-term plastic changes along the nociceptive pathway occurring in chronic and acute pain condition. We found that $Ddo^{-/-}$ mice show an increased evoked activity of the nociceptive specific (NS) neurons of the dorsal horn of the spinal cord (L4–L6) and a significant decrease of mechanical and thermal thresholds, as compared to control mice. Moreover, *Ddo* gene deletion exacerbated the nocifensive responses in the formalin test and slightly reduced pain thresholds in neuropathic mice up to 7 days after chronic constriction injury. These findings suggest that the NMDAR agonist, D-Asp, may play a role in the regulation of NS neuron electrophysiological activity and behavioral responses in physiological and pathological pain conditions.

1. Introduction

D-Aspartate (D-Asp) is abundantly found in the brain during embryonic and perinatal periods, while it strongly decreases during adulthood [1–3]. D-Asp is selectively metabolized by D-aspartate oxidase (DDO), the only enzyme that degrades bicarboxylic D-amino acids, including N-methyl-D-aspartate (NMDA) [4]. DDO is widely expressed in the adult brain, since its activity strongly increases from postnatal phase until 6 weeks of life [5]. In mammals, D-Asp plays a role in glutamatergic neurotransmission acting as an agonist on NMDA receptors (NMDARs) through the binding to each of the GluN2 subunits [6–9]. Accordingly, *in vitro* electrophysiological studies have demonstrated that D-Asp is able to induce inward currents in CA1 pyramidal neurons in an NMDAR-dependent manner [8]. Genetically engineered animal models with a deletion of the *Ddo* gene ($Ddo^{-/-}$), showing nonphysiological high levels of D-Asp, have been

generated to gain insight into the physiological role of this D-amino acid and of its catabolic enzyme [10]. The levels of D-Asp were up to 10–20-fold higher in the brain of $Ddo^{-/-}$ mice, as compared to the wild type littermates [11]. In line with its pharmacological features, we have demonstrated that excessive levels of D-Asp in the brain, in both $Ddo^{-/-}$ mice and mice chronically treated with D-Asp, are associated with an enhanced NMDAR-dependent long term potentiation (LTP) in the hippocampus and a loss of the long term depression (LTD) in the striatum [6–9, 12]. Windup is the LTP analogous mechanism at spinal cord dorsal horn level, leading to central sensitization at the base of chronic pain development and establishment [13, 14]. Similar to LTP, windup relies on NMDAR activation-dependent mechanism. Indeed, intrathecal injection of NMDA yields exaggerated behavioral responses to thermal and low intensity mechanical stimuli [15] while the peripheral administration of MK801, a noncompetitive NMDAR antagonist, reduces the excitability of spinal cord neurons under chronic pain conditions and inhibits formalin-induced inflammatory pain [16].

In the present study, $Ddo^{-/-}$ mice were used to investigate the consequences of high D-Asp levels on pain responses and nociceptive specific (NS) neuron activity in chronic pain by analyzing (i) thermal and mechanical thresholds in naïve mice, (ii) the evoked activity of the nociceptive specific (NS) neurons of the dorsal horn of the spinal cord (L4–L6), (iii) mechanical allodynia in a model of neuropathic pain induced by the chronic constriction injury (CCI) of the sciatic nerve, and, finally, (iv) the nocifensive responses in the formalin test.

2. Methods

2.1. Animals. Knockout mice for the *Ddo* gene were generated as described previously [10]. Adult male and female wild type ($Ddo^{+/+}$) and knockout ($Ddo^{-/-}$) 90-day-old mice, derived from mating of heterozygous ($Ddo^{+/-}$) mice and back-crossed to the F5 generation to C57BL/6J strain, were used. Animals were housed in standard transparent plastic cages, in groups of 4, lined with sawdust under a standard 12/12-h light/dark cycle (07:00 AM/07:00 PM), with food and water available *ad libitum*. Testing was performed blind to treatment group to which each subject belonged. All procedures were in strict accordance with the Italian National law (DL116/92, application of the European Communities Council Directive 86/609/EEC) on care and handling of the animals and with the guidelines of the Committee for Research and Ethical Issues of IASP.

2.2. Surgery. $Ddo^{-/-}$ and wild type mice underwent the chronic constriction injury (CCI) of the sciatic nerve according to Bennett and Xie [17] for inducing neuropathic pain (day 0). Briefly, animals were anaesthetized with sodium pentobarbital (50 mg/kg, i.p.), the right sciatic nerve was exposed through a 1 cm longitudinal skin incision, and three ligatures were loosely tied around the nerve just proximal to the trifurcation. The wound was then closed with 4-0 silk suture. In the following, the injured right hind paw will be named as ipsilateral paw and the uninjured left hind paw will be named as contralateral paw. Control $Ddo^{-/-}$ and wild type mice underwent a sham surgery with exposure of the sciatic nerve without ligature.

2.3. Extracellular Recordings of Nociceptive Neurons. For *in vivo* single unit extracellular recording, experimental groups consisted of 6–8 mice which included at least 3/4 male and 3/4 female subjects with more than one neuron recorded in each mouse. The single extracellular recordings were performed 7 days after surgery in $Ddo^{-/-}$ and $Ddo^{+/+}$ female or male mice.

On the day of electrophysiological recording experiments (day 7), mice were initially anesthetized with sodium pentobarbital (50 mg/kg i.p.). After tracheal cannulation, a catheter was placed into the right external jugular vein to allow continuous infusion of propofol (5–10 mg/kg/h, i.v.). Spinal cord segments L4–L6 were exposed medially by laminectomy, near the dorsal root entry zone, up to a depth of 1 mm [18]. An elliptical rubber ring (about 3×5 mm) was tightly sealed with silicone gel onto the surface of the cord. This ring formed a trough with about 50 μL capacity over the spinal segments used for topical spinal drug application. It also provided access to the spinal neurons that receive input from the ipsilateral paw, where the mechanical stimulation was applied. Animals were then secured in a stereotaxic apparatus (David Kopf Instruments, Tujunga, CA, USA) supported by clamps attached to the vertebral processes on either side of the exposure site. The exposed area of the spinal cord was initially framed by agar and then filled with mineral oil. Body temperature was maintained at 37°C with a temperature-controlled heating pad [19, 20]. A glass-insulated tungsten filament electrode (3–5 MΩ; FHC Frederick Haer & Co., ME, USA) was used to record single unit extracellular activity of dorsal horn NS neurons. NS neurons were defined as those neurons that respond only to high-intensity (noxious) stimulation [19]. To confirm NS response patterns, each neuron was characterized while applying a mechanical stimulation to the ipsilateral hind paw using a von Frey filament with 97.8 mN bending force (noxious stimulation) for 2 s until it buckled slightly [21]. Only neurons that responded specifically to the noxious hind paw stimulation, without responding to stimulation of the surrounding tissue, were included in sham and neuropathic mice recordings. The recorded signals were amplified and displayed on a digital storage oscilloscope to ensure that the unit under study was unambiguously discriminated throughout the experiment. Signals were also fed into a window discriminator, whose output was processed by an interface CED 1401 (Cambridge Electronic Design Ltd., UK) connected to a Pentium III PC. Spike2 software (CED, version 4) was used to create peristimulus rate histograms online and to store and analyze digital records of single unit activity offline. Configuration, shape, and height of the recorded action potentials were monitored and recorded continuously using a window discriminator and Spike2 software for online and offline analysis. This study only included neurons whose spike configuration remained constant and could be clearly discriminated from activity in the background throughout the experiment, indicating that the activity from one neuron only and from the same neuron was measured. The neuronal

activity was expressed as spikes/sec (Hz). At the end of the experiment, each animal was killed with a lethal dose of urethane.

2.4. Behavioral Testing. Mechanical withdrawal threshold was tested by using a Dynamic Plantar Aesthesiometer (Ugo Basile, Model 37400), an apparatus that generates a mechanical force linearly increasing with time. The force is applied to the plantar surface of the mice hind paw, and the nociceptive threshold is defined as the force, in grams, at which the mouse withdraws its paw [22]. Neuropathic wild type and $Ddo^{-/-}$ mice were tested for the sensitivity of both ipsilateral and contralateral hind paws to normally nonnoxious punctuate mechanical stimuli, at different time intervals from postoperative day 3 to day 31 and reported in Figure 4. At each testing day, the ipsi- and contralateral withdrawal forces were taken as mean of three consecutive measurements per paw with 10 s interval between each measurement. Experimental data are expressed as mean ± S.E.M.

Thermal withdrawal threshold was measured by exposing the plantar surface of both hind paws to an infrared heat stimulus delivered through an automatic device (Plantar test, Ugo Basile, Comerio, Italy). This apparatus basically consists of a movable infrared generator placed below a glass pane upon which animal is placed. After an acclimation period, the infrared source placed under the glass floor was positioned directly beneath the hind paw and trial began. When the animal felt pain and withdrew its paw, the infrared source switched off and the reaction time counter stopped [23]. The withdrawal latency to the nearest 0.1 s was automatically determined. To avoid damage of hind paw skin tissue, a cut-off time of 15 s was imposed. Thermal withdrawal latency of both hind paws was recorded as the mean of the three trials (s) for three consecutive trials with at least 10 seconds between each trial and was plotted.

Formalin test was used to evaluate the response to inflammatory pain [24]. Formalin solution (20 μL of 5% in saline) was subcutaneously (s.c.) injected into the dorsal surface of the right hind paw of mice using a microsyringe equipped with a 26-gauge needle. Mice were then put back into the chamber and the observation period started. The nocifensive responses, that is, the total amount of time the animal spent licking the injected paw, were taken as index of pain and measured in sec. Nocifensive responses were recorded continuously for 40 minutes and calculated in blocks of consecutive 5 min periods.

2.5. Data Analysis. For electrophysiology experiments 2-way ANOVA for repeated measures followed by Bonferroni post hoc test for multiple comparisons has been used to analyse statistical differences between the different groups of mice. Data derived from male and female mice were analyzed separately.

Concerning behavioral experiments data were expressed as mean ± standard error of the mean (S.E.M). Statistical analysis was carried out by using Student's t-test to analyse mechanical and thermal nociceptive threshold or two-way ANOVA for repeated measures and one-way ANOVA to evaluate mechanical allodynia and formalin-induced inflammatory pain. Data derived from male and female mice were analyzed separately as well as the two phases of formalin test considered.

3. Results

3.1. Effect of the Ddo Gene Ablation on NS Neuron Activity of Female Mice in Control and Neuropathic Pain Conditions. The results are based on NS neurons (two cells recorded from each animal) at a depth of 0.7–1 mm from the surface of the spinal cord. This cell population was characterized by a mean rate of spontaneous firing of 0.015 ± 0.002 Hz. Thus, only cells showing this pattern of basal firing were chosen for the recordings. The electrophysiological studies have measured the onset of excitation (the time from the application of the stimulus artefact to the first evoked spike exceeding the average baseline value + 2 standard deviations), the frequency of the evoked excitatory responses, and the duration of excitation (the period in ms of the increased firing activity which exceeds the average baseline value + 2 standard deviations). The effect of *Ddo* gene deletion on NS neuron activity was firstly considered in female $Ddo^{+/+}$ and $Ddo^{-/-}$ mice. No change in the spontaneous firing activity of NS neurons has been found in the sham wild type mice (0.08 ± 0.001 spikes/s) (Figure 1) with respect to the naïve (not shown). In contrast, the deletion of the *Ddo* gene caused a significant decrease in the onset of the evoked activity and an increase in the duration and the frequency of the evoked activity (237 ± 18 ms, $F_{(3,10)} = 21.02$; 12 ± 0.66 s, $F_{(3,10)} = 56.56$; and 24.18 ± 2.11 Hz, $F_{(3,10)} = 31$, resp.; $P < 0.05$, $n = 6$) in sham $Ddo^{-/-}$ mice as compared to the sham wild type ones (Figure 1).

We observed an overall NS neuron hyperexcitability in CCI as compared with sham in wild type mice. In particular, we found a significant reduction in the onset and an increase in the frequency and in the duration of the evoked activity 7 days after CCI (202 ± 25.36 ms, $F_{(3,10)} = 24.83$; 27.8 ± 2.39 Hz, $F_{(3,10)} = 42.10$; and 38.5 ± 6.6 s, $F_{(3,10)} = 25.69$, resp.; $P < 0.05$, $n = 6$), as compared to the sham (410 ± 33.16 ms, 11 ± 1 Hz, 4.8 ± 0.8 s, resp.; $n = 8$) in wild type mice. Surprisingly, the CCI caused a significant increase in the onset and a reduction in the frequency and duration of the evoked activity (350 ± 20 ms, $F_{(3,10)} = 17.64$; 14.0 ± 1.28 Hz, $F_{(3,10)} = 25.95$; and 8.3 ± 1 s, $F_{(3,10)} = 20.47$, resp.; $P < 0.05$, $n = 7$) of NS neurons with respect to the shams in $Ddo^{-/-}$ mice (Figures 1(e), 1(f), and 1(g)). Representative ratemeter records show the activity of a single NS neuron in sham (Figures 1(a) and 1(b)) and in CCI (Figures 1(c) and 1(d)) wild type and $Ddo^{-/-}$ mice.

3.2. Effect of the Ddo Gene Ablation on NS Neuron Activity of Male Mice in Control and Neuropathic Pain Conditions. No change in the spontaneous firing activity of NS neurons has been found in sham wild type male mice (368 ± 28.2 ms, 10.7 ± 0.44 Hz, 3.7 ± 0.48 s, resp.; $n = 7$) (Figure 2) with respect to the naïve (not shown). Instead, we found a significant

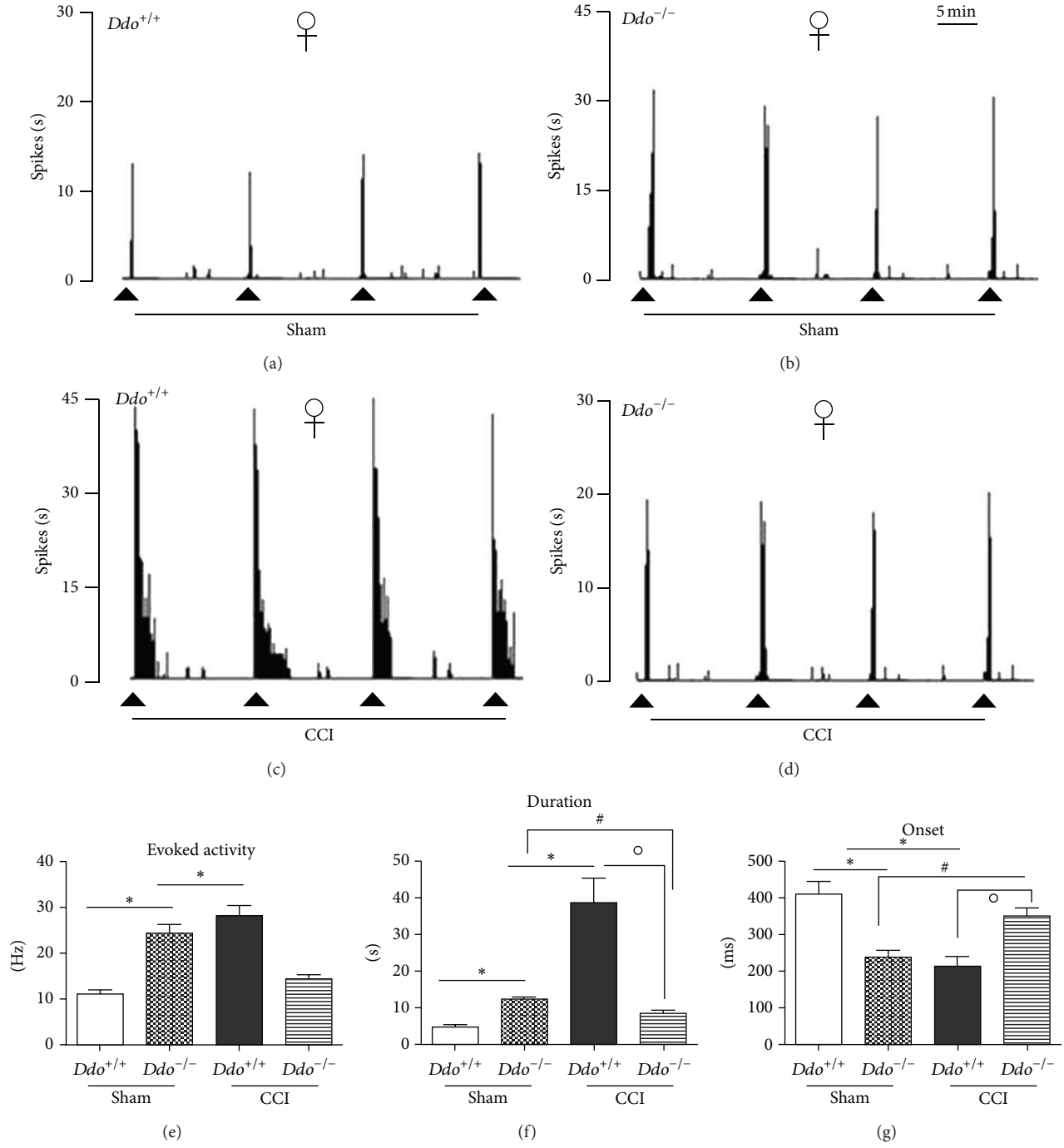

Figure 1: Representative ratemeters showing the responses of a single spinal NS neuron to a mechanical noxious stimulation (von Frey filaments 97.8 mN/2 sec) in $Ddo^{+/+}$ (a and c) and $Ddo^{-/-}$ (b and d) female mice 7 days after sham (a and b) or CCI (c and d) surgery. The lower panels show the evoked activity (e), the duration (f), and the onset (g) of the evoked activity induced by the noxious stimulation in NS neurons in sham and CCI $Ddo^{+/+}$ or $Ddo^{-/-}$ female mice. Small black arrows (a–d) indicate the noxious stimulation on mouse hind paw and grey scale bar indicates 5 min interval in ratemeter. Each point represents the mean ± S.E.M of 6–8 neurons of different groups of mice. P values < 0.05 were considered statistically significant (two-way ANOVA followed by Bonferroni posttest, for comparisons between groups). *indicates significant differences versus sham/$Ddo^{+/+}$, $^{\#}$significant differences versus sham/$Ddo^{-/-}$, and $^{\circ}$significant differences versus CCI/$Ddo^{+/+}$.

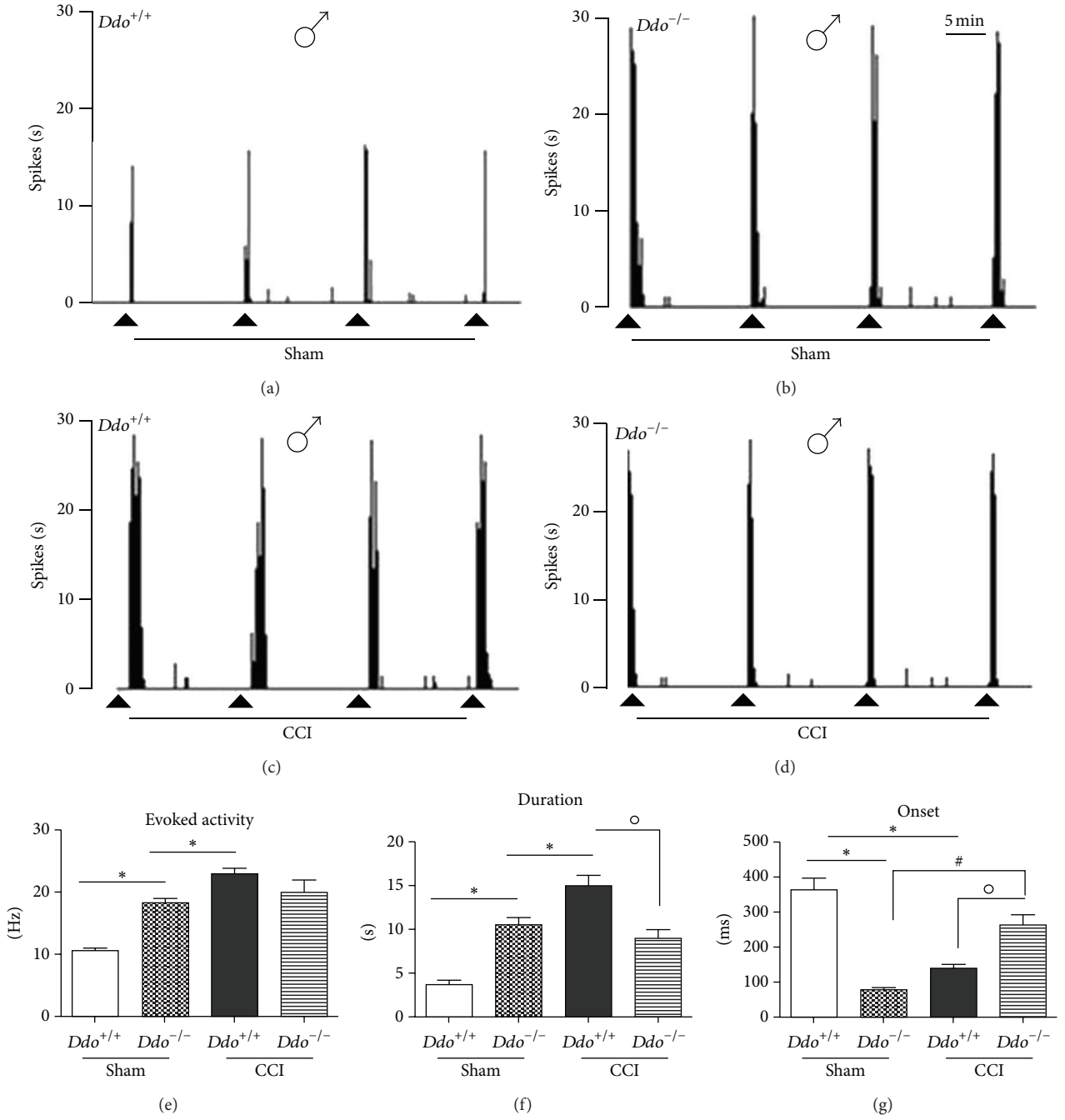

Figure 2: Representative ratemeters showing the responses of a single spinal NS neuron to a mechanical noxious stimulation (von Frey filaments 97.8 mN/2 sec) in $Ddo^{+/+}$ (a and c) and $Ddo^{-/-}$ (b and d) male mice 7 days after sham (a and b) or CCI (c and d) surgery. The lower panels show the evoked activity (e), the duration (f), and the onset (g) of the evoked activity induced by the noxious stimulation in NS neurons in sham and CCI $Ddo^{+/+}$ or $Ddo^{-/-}$ male mice. Small black arrows indicate the noxious stimulation on mouse hind paw and grey scale bar indicates 5 min intervals for ratemeter. Each point represents the mean ± S.E.M of 6–8 neurons of different groups of mice. P values < 0.05 were considered statistically significant (two-way ANOVA followed by Bonferroni posttest, for comparisons between groups). *indicates significant differences versus Sham/$Ddo^{+/+}$, #significant differences versus sham/$Ddo^{-/-}$, and °significant differences versus CCI/$Ddo^{+/+}$.

decrease in the onset and an increase in the duration and the frequency of the evoked activity of NS neurons in sham $Ddo^{-/-}$ mice (76 ± 8.3 ms, $F_{(3,10)} = 98.33$; 10.6 ± 0.84 s, $F_{(3,10)} = 91.5$; and 18.4 ± 0.63 Hz, $F_{(3,10)} = 50.87$, resp.; $P < 0.05$, $n = 6$) (Figure 2).

The CCI caused a significant reduction in the onset and an increase in the frequency and in the duration of the evoked activity in wild type mice (264 ± 28 ms, $F_{(3,10)} = 150.99$; 23 ± 0.9 Hz; $F_{(3,10)} = 150$ and 15.06 ± 1.23 s, $F_{(3,10)} = 73.25$, resp.; $P < 0.05$, $n = 8$) as compared to the sham group (368 ± 28.2 ms,

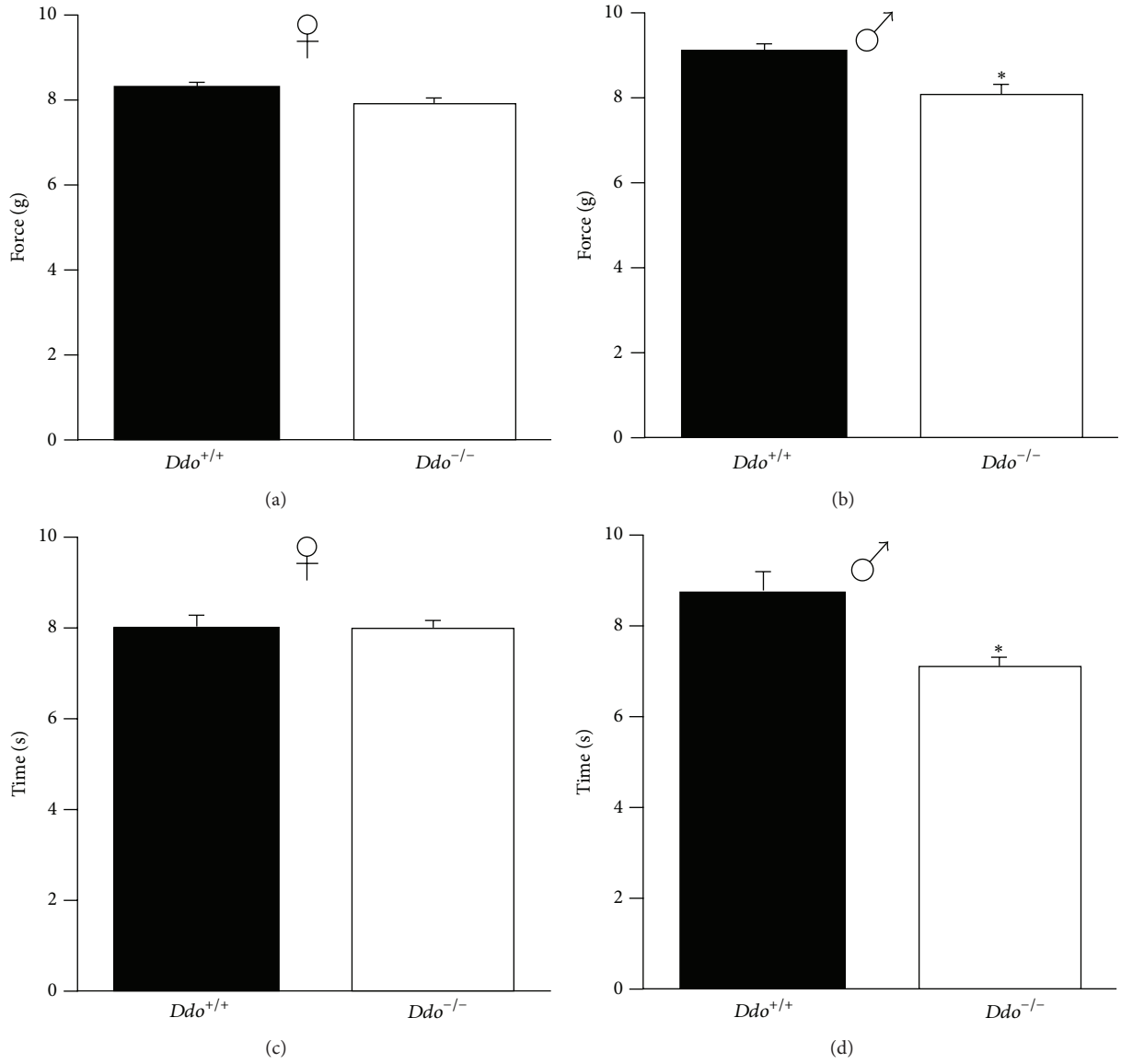

FIGURE 3: Mechanical (a and b) and thermal (c and d) nociceptive thresholds in female (♀, a and c) and male (♂, b and d) $Ddo^{+/+}$ and $Ddo^{-/-}$ naive mice. Number of mice for experimental groups: $n = 21$ (♀$Ddo^{+/+}$), $n = 18$ (♂$Ddo^{+/+}$), $n = 23$ (♀$Ddo^{-/-}$), and $n = 15$ (♂$Ddo^{-/-}$). $^{*}P < 0.05$.

10.7 ± 0.44 Hz, 3.7 ± 0.48 s, resp., $n = 6$). Male $Ddo^{-/-}$ mice, 7 days after CCI, showed a significant increase in the onset of the evoked activity of NS neurons (264 ± 28 ms, $F_{(3,10)} = 44.7$, $P < 0.05, n = 6$) as compared to sham. A significant reduction in the duration of the evoked activity (9 ± 1 s, $F_{(3,10)} = 14.33$, $P < 0.05$, $n = 6$) was also observed 7 days after CCI in $Ddo^{-/-}$ male mice. No significant changes were instead observed in the frequency of the evoked activity in $Ddo^{-/-}$ male mice 7 days after the CCI (Figure 2). Representative ratemeter records show the activity of single NS neuron in wild type and $Ddo^{-/-}$ male mice 7 days after the sham or CCI surgery (Figures 2(a), 2(b), 2(c), and 2(d)).

3.3. Effect of the Ddo Gene Ablation on Mechanical Withdrawal Threshold and Thermal Withdrawal Latency. First, we have investigated whether wild type mice differ in the nociceptive mechanical and thermal threshold depending on sex. A significant difference was observed for the behavioral response to mechanical stimulus in the aesthesiometer test, with females having a lower threshold in comparison with males (t value: −3.542; $P < 0.01$), while no differences were detected for the thermal stimulus (t value: −1.161; $P = 0.253$). With regard to the deletion of the *Ddo* gene, we observed a higher sensitivity to both mechanical and thermal stimuli in male $Ddo^{-/-}$ naive mice (t value: −2.982; $P < 0.05$ and t value: −2.728; $P < 0.01$, resp.) in comparison with male wild type naive animals (Figures 3(b) and 3(d)). On the contrary, the mechanical and thermal thresholds in female $Ddo^{-/-}$ naive mice did not differ (t value: −1.560; $P = 0.126$ and t value: −0.297; $P = 0.767$, resp.) from those observed in female

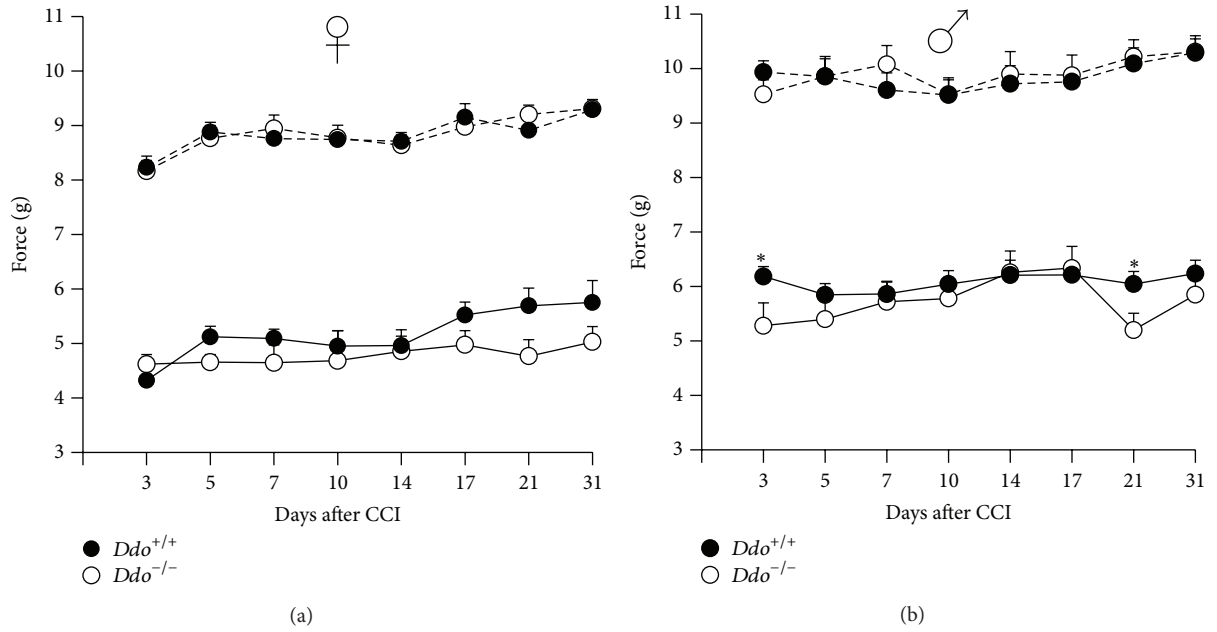

Figure 4: Time course of mechanical withdrawal thresholds (expressed as applied force in grams) of the ipsilateral hind paws after the chronic constriction injury (CCI) of the sciatic nerve in female (a) and male (b) $Ddo^{+/+}$ and $Ddo^{-/-}$ mice. Number of mice for experimental groups: $n = 10$ (♀$Ddo^{+/+}$), $n = 11$ (♀$Ddo^{-/-}$), $n = 13$ (♂$Ddo^{+/+}$), and $n = 10$ (♂$Ddo^{-/-}$). $^{*}P < 0.05$.

control naive mice (Figures 3(a) and 2(c)), suggesting that high D-Asp-mediated nociceptive response may be linked to sex-related factors.

3.4. Neuropathic Pain. The unilateral ligature of the sciatic nerve, performed in CCI model of neuropathic pain, induces mechanical allodynia in the hind paw ipsilaterally to the ligature. The time course of the mechanical withdrawal thresholds of both ipsilateral and contralateral hind paws, in $Ddo^{+/+}$ and $Ddo^{-/-}$ mice, has been measured for 31 days and reported in Figure 4. In all experimental groups the mechanical withdrawal thresholds decreased after CCI by about 50% in the ipsilateral, compared to contralateral hind paw. Animals withdrew their ipsilateral paw after very low stimuli (4-5 g and 5-6 g for females and males, resp.), which did not evoke reaction in contralateral paw; for this reason we considered only the response of the ipsilateral hind paw to measure mechanical allodynia. In mutant animals we observed a slight decrease in mechanical withdrawal threshold, even if two-way ANOVA for repeated measures showed a significant main effect for time ($F_{(7,133)} = 4{,}735$; $P < 0.01$ and $F_{(7,147)} = 2{,}491$; $P < 0.01$ for females and males, resp.) but not for genotype ($F_{(1,133)} = 1{,}644$; $P = 0.215$ and $F_{(1,147)} = 1{,}362$; $P = 0.256$ for females and males, resp.) or for time x genotype interaction ($F_{(7,133)} = 1{,}932$; $P = 0.06$ and $F_{(7,147)} = 1{,}332$; $P = 0.238$ for females and males, resp.). When a comparison between $Ddo^{-/-}$ and $Ddo^{+/+}$ mice was carried out day by day, a significant difference ($P < 0.05$) was found at day 3 and at day 21 after CCI in male mice. Indeed, $Ddo^{-/-}$ animals showed a further decrease in mechanical allodynia induced by the sciatic nerve ligation, in comparison with wild type animals.

3.5. Inflammatory Pain. To study behavioral response to inflammatory pain, we carried out the formalin test. Subcutaneous injection of formalin into the dorsal surface of the hind paw elicits a well-known biphasic behavioral response, as previously reported [25]. Figure 5 shows the cumulative licking time induced by formalin test during phase 1 (0–10 min) and phase 2 (10–40 min) induced by formalin. Our data indicate that, in both genders, the nocifensive responses observed during the second phase were significantly higher in $Ddo^{-/-}$ mice, when compared to wild type littermates ($F_{(1,18)} = 6{,}590$; $P < 0.01$ and $F_{(1,18)} = 5{,}985$; $P < 0.05$ for females and males, resp.). Conversely, no differences between genotypes were observed in the nocifensive responses recorded during the first phase, independently of the sex ($F_{(1,18)} = 0{,}006$; $P = 0.938$ and $F_{(1,18)} = 0{,}010$; $P = 0.9206$ for females and males, resp.).

4. Discussion

In the present work, we found that higher D-Asp levels in $Ddo^{-/-}$ mice reduce nociceptive threshold in physiological and chronic pain conditions. In addition, we demonstrated, by *in vivo* single unit electrophysiological recordings, that *Ddo* gene ablation consistently affects the spinal NS neuron activity in both sham and neuropathic male and female animals. Furthermore, we reported that both $Ddo^{-/-}$ female and male mutants show increased evoked activity of spinal NS neurons, as compared to wild type animals, thus suggesting that increased D-Asp levels play a role in the transmission of noxious signals in the spinal cord in physiological condition. This hyperexcitability of NS neurons in the dorsal horn of the spinal cord was also associated with a significant reduction in

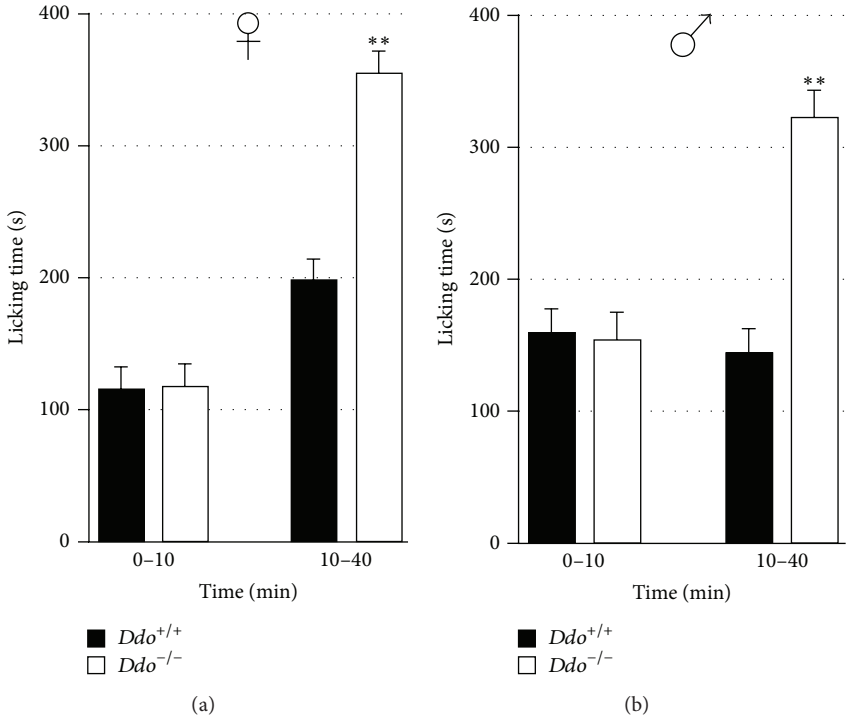

Figure 5: Cumulative time of the nocifensive response during phase 1 (0–10 min) and phase 2 (10–40 min) (b and d) in female (a and b) and male (c and d) $Ddo^{+/+}$ and $Ddo^{-/-}$ mice. Number of mice for experimental groups: $n = 10$ (♀$Ddo^{+/+}$), $n = 10$ (♀$Ddo^{-/-}$), $n = 10$ (♂$Ddo^{+/+}$), and $n = 10$ (♂$Ddo^{-/-}$). $^{**}P < 0.01$.

both mechanical and thermalnociceptive thresholds in male $Ddo^{-/-}$ mice, as compared to wild type. Interestingly, the hyperexcitability of NS neurons in the dorsal horn of the spinal cord was not associated with reduced thermal and mechanical thresholds in female $Ddo^{-/-}$ mice, highlighting a sex-dependent effect for this response. Overall, these findings indicate that high free D-Asp levels in mutant mice mediate an altered electrophysiological response and behavioral pain perception in basal conditions.

The molecular targets on which D-Asp could act are not fully known. However, NMDAR has been proposed to be involved in D-Asp-mediated central effects [26–28]. Accordingly, we have previously demonstrated that increased D-Asp levels enhance the NMDAR-dependent LTP in hippocampal slices [6–8]. Events comparable to LTP into the spinal cord have been proposed as cellular mechanisms leading to pain amplification in chronic pain conditions. Hyperalgesia and tactile allodynia are the main behavioral dysfunctions related to central sensitization associated with chronic pain [29, 30]. Consistently, NMDARs play a crucial role in the central sensitization at spinal cord dorsal horn level and NMDAR blockers have been suggested as pharmacological tools able to attenuate neuropathic pain [31, 32]. In particular, Pendersen and Gjerstad have previously shown that spinal administration of GluN2B antagonist is able to normalize the abnormal neuronal activity and attenuate the magnitude of spinal cord LTP, following peripheral nerve injury [33].

Here we have examined the effect of D-Asp on the spinal neuronal evoked activity in *Ddo* knockout mice in pathological pain condition induced by chronic constriction injury. Whilst neuropathy condition did not change or slightly reduced the nociceptive threshold in mutants, in comparison with wild type mice, paradoxically it strongly normalized the neuronal oversensitization found in naïve $Ddo^{-/-}$ mice. Indeed, in mutant mice the decrease in the onset and the increase in frequency and duration of the evoked activity to mechanical noxious stimuli of NS neurons found in sham were consistently reduced in CCI animals. Although this observation remains to be clarified at molecular level, we hypothesize the existence of NMDARs desensitization processes in mutant spinal cord under neuropathy state. In this respect, desensitization of macroscopic currents in the presence of saturating concentrations of glutamate and glycine agonists has been previously described [34] and defined as glycine-independent or glycine-insensitive. Therefore, we speculate that CCI could trigger a dramatic increase in spinal glutamate release that, combined with the high levels of D-Asp, may induce desensitization of NMDARs in $Ddo^{-/-}$ mice.

Desensitization of NMDARs in spinal cord of mutant mice could explain also behavioural data showing that neuropathic pain in $Ddo^{-/-}$ was almost unaltered compared to wild type mice except at day 3 and day 21.

Furthermore, in this study we have also examined the nocifensive behavior induced by peripheral formalin injection. The local injection of formalin into the hind paw of rodents represents a model for inducing persistent inflammatory pain, which generates a nociceptive biphasic

response, oedema, and inflammation [35]. While no difference was observed in the early formalin phase, which is caused by direct activation of nociceptive sensory afferents, we found a significant increase of the late phase, which is due to the release of inflammatory mediators and also associated with central sensitization [36, 37]. The important role of D-Asp in the inflammatory component of formalin pain was put in evidence by the worsening of nocifensive response in terms of time spent in licking the injected paw in $Ddo^{-/-}$ mice, as compared with wild type animals. In the formalin pain model, the nocifensive response appears to be associated with altered spinal neuronal activity [36, 38] and thus the exacerbation of the nocifensive responses in $Ddo^{-/-}$ mice, which express NS neurons hyperactivity, and appears consistent. The disparity observed between sexes may reflect hormonal and genetic factors together with a different modulatory influence of the immune system [39, 40]. However, further studies are needed to explain the differences in pain perception between males and females and thus investigate a possible relation between *Ddo* gene deletion and gender in pain mechanisms.

5. Conclusions

Our study using $Ddo^{-/-}$ mice provides evidence that high levels of D-Asp affect electrophysiological and behavioral responses in physiological, inflammatory, and neuropathic pain conditions. We found an increased evoked activity of the NS neurons and a significant decrease of mechanical and thermal thresholds in $Ddo^{-/-}$ mice, as compared to controls. *Ddo* gene deletion exacerbated the nocifensive responses in the formalin test and slightly reduced pain thresholds in neuropathic mice. However, the spinal neuronal hyperexcitability caused by the *Ddo* gene deletion was no more observed 7 days after the sciatic nerve lesion. In conclusion, based on the agonistic role of D-Asp on NMDARs, the $Ddo^{-/-}$ mice may offer a substantial tool to further investigate the NMDAR-mediated mechanisms involved in neuropathic pain.

Disclosure

Serena Boccella and Valentina Vacca share cofirst authorship.

Conflict of Interests

The authors declare that there is no conflict of interests regarding the publication of this paper.

References

[1] K. Sakai, H. Homma, J. Lee et al., "Emergence of D-aspartic acid in the differentiating neurons of the rat central nervous system," *Brain Research*, vol. 808, no. 1, pp. 65–71, 1998.

[2] M. J. Schell, O. B. Cooper, and S. H. Snyder, "D-aspartate localizations imply neuronal and neuroendocrine roles," *Proceedings of the National Academy of Sciences of the United States of America*, vol. 94, no. 5, pp. 2013–2018, 1997.

[3] H. Wolosker, A. D'Aniello, and S. H. Snyder, "D-aspartate disposition in neuronal and endocrine tissues: ontogeny, biosynthesis and release," *Neuroscience*, vol. 100, no. 1, pp. 183–189, 2000.

[4] A. D'Aniello, A. Vetere, and L. Petrucelli, "Further study on the specificity of d-amino acid oxidase and of d-aspartate oxidase and time course for complete oxidation of d-amino acids," *Comparative Biochemistry and Physiology B: Comparative Biochemistry*, vol. 105, no. 3-4, pp. 731–734, 1993.

[5] P. P. van Veldhoven, C. Brees, and G. P. Mannaerts, "D-aspartate oxidase, a peroxisomal enzyme in liver of rat and man," *Biochimica et Biophysica Acta*, vol. 1073, no. 1, pp. 203–208, 1991.

[6] F. Errico, R. Nisticò, F. Napolitano et al., "Increased D-aspartate brain content rescues hippocampal age-related synaptic plasticity deterioration of mice," *Neurobiology of Aging*, vol. 32, no. 12, pp. 2229–2243, 2011.

[7] F. Errico, R. Nisticò, F. Napolitano et al., "Persistent increase of d-aspartate in d-aspartate oxidase mutant mice induces a precocious hippocampal age-dependent synaptic plasticity and spatial memory decay," *Neurobiology of Aging*, vol. 32, no. 11, pp. 2061–2074, 2011.

[8] F. Errico, R. Nisticò, G. Palma et al., "Increased levels of d-aspartate in the hippocampus enhance LTP but do not facilitate cognitive flexibility," *Molecular and Cellular Neuroscience*, vol. 37, no. 2, pp. 236–246, 2008.

[9] F. Errico, S. Rossi, F. Napolitano et al., "D-aspartate prevents corticostriatal long-term depression and attenuates schizophrenia-like symptoms induced by amphetamine and MK-801," *Journal of Neuroscience*, vol. 28, no. 41, pp. 10404–10414, 2008.

[10] F. Errico, M. T. Pirro, A. Affuso et al., "A physiological mechanism to regulate d-aspartic acid and NMDA levels in mammals revealed by d-aspartate oxidase deficient mice," *Gene*, vol. 374, no. 1-2, pp. 50–57, 2006.

[11] F. Errico, F. Napolitano, R. Nisticò, and A. Usiello, "New insights on the role of free D-aspartate in the mammalian brain," *Amino Acids*, vol. 43, no. 5, pp. 1861–1871, 2012.

[12] F. Errico, A. Bonito-Oliva, V. Bagetta et al., "Higher free d-aspartate and N-methyl-d-aspartate levels prevent striatal depotentiation and anticipate l-DOPA-induced dyskinesia," *Experimental Neurology*, vol. 232, no. 2, pp. 240–250, 2011.

[13] S. Pockett, "Spinal cord synaptic plasticity and chronic pain," *Anesthesia and Analgesia*, vol. 80, no. 1, pp. 173–179, 1995.

[14] J. Sandkühler, "Learning and memory in pain pathways," *Pain*, vol. 88, no. 2, pp. 113–118, 2000.

[15] A. H. Dickenson, V. Chapman, and G. M. Green, "The pharmacology of excitatory and inhibitory amino acid-mediated events in the transmission and modulation of pain in the spinal cord," *General Pharmacology*, vol. 28, no. 5, pp. 633–638, 1997.

[16] T. Ushida, T. Tani, M. Kawasaki, O. Iwatsu, and H. Yamamoto, "Peripheral administration of an *N*-methyl-D-aspartate receptor antagonist (MK-801) changes dorsal horn neuronal responses in rats," *Neuroscience Letters*, vol. 260, no. 2, pp. 89–92, 1999.

[17] G. J. Bennett and Y. K. Xie, "A peripheral mononeuropathy in rat that produces disorders of pain sensation like those seen in man," *Pain*, vol. 33, no. 1, pp. 87–107, 1988.

[18] B. C. Hains and S. G. Waxman, "Activated microglia contribute to the maintenance of chronic pain after spinal cord injury," *Journal of Neuroscience*, vol. 26, no. 16, pp. 4308–4317, 2006.

[19] S. McGaraughty, K. L. Chu, R. J. Perner, S. DiDomenico, M. E. Kort, and P. R. Kym, "TRPA1 modulation of spontaneous and mechanically evoked firing of spinal neurons in uninjured, osteoarthritic, and inflamed rats," *Molecular Pain*, vol. 6, article 14, 2010.

[20] A. Telleria-Diaz, M. Schmidt, S. Kreusch et al., "Spinal antinociceptive effects of cyclooxygenase inhibition during inflammation: involvement of prostaglandins and endocannabinoids," *Pain*, vol. 148, no. 1, pp. 26–35, 2010.

[21] D. A. Simone, S. G. Khasabov, and D. T. Hamamoto, "Changes in response properties of nociceptive dorsal horn neurons in a murine model of cancer pain," *Sheng Li Xue Bao*, vol. 60, no. 5, pp. 635–644, 2008.

[22] S. Marinelli, V. Vacca, R. Ricordy et al., "The analgesic effect on neuropathic pain of retrogradely transported botulinum neurotoxin A involves Schwann cells and astrocytes," *PLoS ONE*, vol. 7, no. 10, Article ID e47977, 2012.

[23] V. Vacca, S. Marinelli, S. Luvisetto, and F. Pavone, "Botulinum toxin A increases analgesic effects of morphine, counters development of morphine tolerance and modulates glia activation and μ opioid receptor expression in neuropathic mice," *Brain, Behavior, and Immunity*, vol. 32, pp. 40–50, 2013.

[24] F. Pavone, S. Luvisetto, S. Marinelli et al., "The Rac GTPase-activating bacterial protein toxin CNF1 induces analgesia up-regulating μ-opioid receptors," *Pain*, vol. 145, no. 1-2, pp. 219–229, 2009.

[25] A. Tjølsen, O.-G. Berge, S. Hunskaar, J. H. Rosland, and K. Hole, "The formalin test: an evaluation of the method," *Pain*, vol. 51, no. 1, pp. 5–17, 1992.

[26] G. E. Fagg and A. Matus, "Selective association of N-methyl aspartate and quisqualate types of L-glutamate receptor with brain postsynaptic densities," *Proceedings of the National Academy of Sciences of the United States of America*, vol. 81, no. 21, pp. 6876–6880, 1984.

[27] J. B. Monahan and J. Michel, "Identification and characterization of an N-methyl-D-aspartate-specific L-[3H]glutamate recognition site in synaptic plasma membranes," *Journal of Neurochemistry*, vol. 48, no. 6, pp. 1699–1708, 1987.

[28] H. J. Olverman, A. W. Jones, K. N. Mewett, and J. C. Watkins, "Structure/activity relations of N-methyl-d-aspartate receptor ligands as studied by their inhibition of [3H]d2-amino-5-phosphonopentanoic acid binding in rat brain membranes," *Neuroscience*, vol. 26, no. 1, pp. 17–31, 1988.

[29] M. Costigan, J. Scholz, and C. J. Woolf, "Neuropathic pain: a maladaptive response of the nervous system to damage," *Annual Review of Neuroscience*, vol. 32, pp. 1–32, 2009.

[30] J. Sandkühler, "Models and mechanisms of hyperalgesia and allodynia," *Physiological Reviews*, vol. 89, no. 2, pp. 707–758, 2009.

[31] S. Collins, M. J. Sigtermans, A. Dahan, W. W. A. Zuurmond, and R. S. G. M. Perez, "NMDA receptor antagonists for the treatment of neuropathic pain," *Pain Medicine*, vol. 11, no. 11, pp. 1726–1742, 2010.

[32] D. J. Hewitt, "The use of NMDA-receptor antagonists in the treatment of chronic pain," *Clinical Journal of Pain*, vol. 16, no. 2 supplement, pp. S73–S79, 2000.

[33] L. M. Pedersen and J. Gjerstad, "Spinal cord long-term potentiation is attenuated by the NMDA-2B receptor antagonist Ro 25-6981," *Acta Physiologica*, vol. 192, no. 3, pp. 421–427, 2008.

[34] R. Nahum-Levy, D. Lipinski, S. Shavit, and M. Benveniste, "Desensitization of NMDA receptor channels is modulated by glutamate agonists," *Biophysical Journal*, vol. 80, no. 5, pp. 2152–2166, 2001.

[35] C. A. Porro and M. Cavazzuti, "Spatial and temporal aspects of spinal cord and brainstem activation in the formalin pain model," *Progress in Neurobiology*, vol. 41, no. 5, pp. 565–607, 1993.

[36] D. Dubuisson and S. G. Dennis, "The formalin test: a quantitative study of the analgesic effects of morphine, meperidine, and brain stem stimulation in rats and cats," *Pain*, vol. 4, no. 2, pp. 161–174, 1977.

[37] F. Guida, L. Luongo, G. Aviello et al., "Salvinorin A reduces mechanical allodynia and spinal neuronal hyperexcitability induced by peripheral formalin injection," *Molecular Pain*, vol. 8, article 60, 2012.

[38] R. Cadet, L. Aigouy, and A. Woda, "Enhanced nociceptive behaviour following conditioning injection of formalin in the perioral area of the rat," *Brain Research*, vol. 676, no. 1, pp. 189–195, 1995.

[39] A. M. Aloisi and G. Sorda, "Relationship of female sex hormones with pain perception: focus on estrogens," *Pain Management*, vol. 1, no. 3, pp. 229–38, 2011.

[40] V. Vacca, S. Marinelli, L. Pieroni, A. Urbani, S. Luvisetto, and F. Pavone, "Higher pain perception and lack of recovery from neuropathic pain in females: a behavioural, immunohistochemical, and proteomic investigation on sex-related differences in mice," *Pain*, vol. 155, no. 2, pp. 388–402, 2014.

Hindawi Publishing Corporation
BioMed Research International
Volume 2015, Article ID 301292, 15 pages
http://dx.doi.org/10.1155/2015/301292

Research Article

Prokineticin 2 Upregulation in the Peripheral Nervous System Has a Major Role in Triggering and Maintaining Neuropathic Pain in the Chronic Constriction Injury Model

Roberta Lattanzi,[1] Daniela Maftei,[1] Veronica Marconi,[1] Fulvio Florenzano,[2] Silvia Franchi,[3] Elisa Borsani,[4] Luigi Fabrizio Rodella,[4] Gianfranco Balboni,[5] Severo Salvadori,[6] Paola Sacerdote,[3] and Lucia Negri[1]

[1]*Department of Physiology and Pharmacology "Vittorio Erspamer", Sapienza University of Rome, 00185 Rome, Italy*
[2]*Confocal Microscopy Unit, European Brain Research Institute (EBRI) "Rita Levi-Montalcini", 00143 Rome, Italy*
[3]*Department of Pharmacological and Biomolecular Sciences, University of Milan, 20129 Milan, Italy*
[4]*Unit of Human Anatomy, Department of Biomedical Sciences and Biotechnologies, University of Brescia, 25123 Brescia, Italy*
[5]*Department of Life and Environment Sciences, University of Cagliari, 09124 Cagliari, Italy*
[6]*Department of Chemical and Pharmaceutical Sciences, University of Ferrara, 44-100 Ferrara, Italy*

Correspondence should be addressed to Lucia Negri; lucia.negri@uniroma1.it

Received 11 June 2014; Accepted 3 October 2014

Academic Editor: Livio Luongo

The new chemokine Prokineticin 2 (PROK2) and its receptors (PKR_1 and PKR_2) have a role in inflammatory pain and immunomodulation. Here we identified PROK2 as a critical mediator of neuropathic pain in the chronic constriction injury (CCI) of the sciatic nerve in mice and demonstrated that blocking the prokineticin receptors with two PKR_1-preferring antagonists (PC1 and PC7) reduces pain and nerve damage. PROK2 mRNA expression was upregulated in the injured nerve since day 3 post injury (dpi) and in the ipsilateral DRG since 6 dpi. PROK2 protein overexpression was evident in Schwann Cells, infiltrating macrophages and axons in the peripheral nerve and in the neuronal bodies and some satellite cells in the DRG. Therapeutic treatment of neuropathic mice with the PKR-antagonist, PC1, impaired the PROK2 upregulation and signalling. This fact, besides alleviating pain, brought down the burden of proinflammatory cytokines in the damaged nerve and prompted an anti-inflammatory repair program. Such a treatment also reduced intraneural oedema and axon degeneration as demonstrated by the physiological skin innervation and thickness conserved in CCI-PC1 mice. These findings suggest that PROK2 plays a crucial role in neuropathic pain and might represent a novel target of treatment for this disease.

1. Introduction

Identification of the neurobiological processes engaged in the pathological state that occurs during neuropathic pain may provide future therapeutic targets. Chemokines and their receptors are receiving growing interest as modulators of neuronal plasticity and for their ability to enhance nociceptive transmission under conditions of neuropathic pain [1]. In particular a new family of chemokines, Prokineticin 2 (PROK2) also known as Bv8 and its receptors, two G-protein coupled receptors, PKR_1 and PKR_2, emerged as key signals in immune system and inflammatory diseases [2].

In an animal model of CFA-induced paw inflammation, we brought evidence that Bv8/PROK2, upregulated in granulocyte invading the inflamed tissue is a major determinant in triggering and maintaining inflammatory pain [3]. Neutrophils and macrophages are the major sources of PROK2 which is strongly upregulated in inflammatory diseases and tumours, associated with infiltrating cells [4, 5]. *In vivo* and *in vitro* experiments from our and other groups demonstrated

potent chemotactic and immunomodulatory activities of the prokineticins, able to promote the production of proinflammatory cytokines from different immune cells and to modulate T cell function by reducing anti-inflammatory cytokines production and promoting Th1 responses [5–7].

The typical immune cell response to tissue injury is largely conserved in the lesioned peripheral nervous system: many neutrophils from the circulation invade the area immediately around the nerve injury site within 8–24 hours and haematogenous macrophages by 3-4 days post injury, whereas lymphocyte accumulation in the injured nerve is delayed by a week or more [8].

We can reasonably presume that PROK2 released by haematogenous neutrophils invading the damaged nerve triggers inflammation and contributes to pain.

Besides, in the immune system, PROK2 is also expressed in discrete nuclei into the brain and is constitutively expressed, at very low levels, in some DRG neurons also expressing the vanilloid receptor TRPV1 [9–11]. PROK2 binds PKR_1 and PKR_2, expressed in small and medium cells of rat dorsal root ganglia (DRG) and within the superficial laminae in the spinal dorsal horn [2, 12]. Peripheral administration of the mammalian PROK2 or its amphibian homologue Bv8 in rodents induced hyperalgesia and allodynia by activating the PKRs on peripheral nociceptors. *In vitro* analysis of functional PKRs on DRG neurons shows a remarkable overlap in neurons that respond both to Bv8 and capsaicin (~90%) and to Bv8 and mustard oil (~60%) indicating a high degree of colocalization of functional PKRs with TRPV1 and TRPA1 channels [13] supporting the possibility that these receptors contribute to nociceptive signalling. Moreover Bv8, increasing CGRP and SP expression, induced long-lasting sensitization of nociceptors resulting in enhanced responses to evoking stimuli, including Bv8 itself or capsaicin, so providing a basis for long-lasting hypersensitivity that may result in conditions of tissue injury [14].

We have recently demonstrated in an animal model of neuropathic pain, the chronic constriction injury of the sciatic nerve (CCI), that 10 days after nerve injury an important activation of the prokineticin system is evident at peripheral and central level and that pharmacological blocking of the prokineticin receptors with the antagonist PC1 abolishes pain and controls some pathophysiological processes underlying the neuropathy.

Here we analysed the time-course of PROK2 upregulation in the DRG and in the injured sciatic nerve of mice repeatedly treated with saline or with PC1 for 7 days and demonstrated that the antihyperalgesic effect of PC1 temporally correlates with its ability to reduce the neuropathy-induced increase of PROK2 expression. The recent availability of a new prokineticin receptor antagonist, PC7, endowed with higher affinity and selectivity for the PKR1 pushed us to evaluate its antihyperalgesic effect in comparison with that of PC1 [15, 16]. Finally, because CCI of sciatic nerve decreases the density of paw skin innervation and induces epidermal thinning we also compared the fibre-density in the dermis and the skin thickness of the injured paw of mice treated with PC1 or with saline in comparison with sham operated mice.

2. Methods

2.1. Animal Preparation. Experiments were carried out in male CD1 mice (25–30 g, Harlan Laboratories, Italy) according to protocols approved by the Animal Care and Use Committee of the Italian Ministry of Health and in compliance with the IASP and European Community (E.C.L358/118/12/86) guidelines. All efforts were made to minimize animal suffering and to reduce the number of animals used. Animals were housed individually in cages, under conditions of optimum light, temperature, and humidity (12 : 12 h light/dark cycles, 22± 2°C, 50–60%) with food and water ad libitum and acclimatized to the environment for 4-5 days before surgery or pharmacologic treatment.

2.2. Neuropathic Pain Model

2.2.1. Chronic Constriction Injury of the Sciatic Nerve (CCI). Mononeuropathy was induced by the CCI of the sciatic nerve [17] in CD1 mice anesthetized by intraperitoneal injection of ketamine-xylazine (60 mg kg^{-1} + 10 mg kg^{-1}). The sciatic nerve was exposed and three loose ligatures with 4–0 silk suture thread were made around the nerve with a 1.0–1.5 mm interval between each of them. In sham-operated mice, an identical dissection was performed on the same side, except that the sciatic nerve was not tied.

2.3. Nociceptive Behavioural Tests. Behavioural experiments were carried out by researchers blind to treatments, between 10 am and 2 pm, in a reserved quiet temperature-controlled room. Mice were habituated to the testing environment and were handled daily two times for at least three days before baseline testing.

For testing heat sensitivity, animals were put in plastic boxes and allowed 30 min for habituation before examination. Heat sensitivity was tested by radiant heat using Hargreaves apparatus (Ugo Basile, Italy) and expressed as paw withdrawal latency (PWL). The radiant heat intensity is adjusted so that basal PWL is between 10 and 12 s with a cutoff of 20 s to prevent tissue damage. For testing mechanical sensitivity, animals were put in boxes on an elevated metal mesh floor and allowed 30 min for habituation before examination. Mechanical allodynia was assessed using the Dynamic Plantar Aesthesiometer (Ugo Basile Italy). The filament was applied to the skin of the midplantar area of the hind paw, and it began to exert an increasing upward force, reaching a maximum of 30 g in 10 s, until the paw was withdrawn. The paw withdrawal threshold (PWT) was defined as the force, in grams, at which the mouse withdrew its paw. PWL and PWT of ipsilateral and contralateral paws were measured thrice, and the reported value is the mean of the three evaluations.

2.4. Experimental Design. The PKR antagonists PC1 [16] and PC7 were injected in mice subcutaneously (s.c., 50 μL for 10 g body weight) into the flank region of the mouse.

PC1 was administrated chronically at the dose of 150 μg kg^{-1}, s.c., twice a day for 7 days.

Increasing doses of PC7 (5, 15, and 45 μg kg^{-1}) were administrated s.c. as a single bolus in different groups of mice, on day 3 post injury (dpi). Then we chose the highest, more effective dose (45 μg kg^{-1} s.c.) for the repeated treatment, twice a day for 4 days.

PC7 (2-(5-(4-fluorobenzyl)-1-(4-methoxybenzyl)-1,4,5,6-tetrahydro-4,6-dioxo-1,3,5-triazin-2-ylamino)-ethyl)-guanidine) is a triazinic compound which displays higher affinity for the PKR_1 (IC_{50} = 56 ± 12 nM, in displacement of ^{125}I-MIT; IC_{50} = 66 ± 12 nM in BRET assay) than for PKR_2 (IC_{50} = 5230 ± 700 nM in displacement of ^{125}I-MIT; IC_{50} = 4135 ± 600 nM in BRET assay) and is able to antagonize the Bv8-induced hyperalgesia at doses ten times lower than PC1 [15].

Mice were divided as follows: (i) CCI mice treated with saline (CCI-saline, n = 8); (ii) CCI mice treated with PC1 150 μg kg^{-1} s.c., twice a day for 7 days or PC7 45 μg kg^{-1} s.c., twice a day for 4 days, starting from day 3 after CCI (CCI-PC1, CCI-PC7, n = 8/group); (iii) Sham-operated mice treated with saline (n = 5); (iv) Sham-operated mice treated with PC1 150 μg kg^{-1} s.c., twice a day for 7 days or PC7 45 μg kg^{-1} s.c., twice a day for 4 days, starting from day 3 after sham surgery (n = 5/group) (data not shown).

In sham, CCI-saline, and CCI-PC1 or CCI-PC7 animals, mechanical allodynia and thermal hyperalgesia were assessed before and from days 1 to 12 after CCI.

2.5. Biochemical and Histochemical Evaluation

2.5.1. RNA Extraction and Real-Time PCR. Total RNA was extracted from L4-L5 DRG and sciatic nerve, pooled from two mice, using the Trizol reagent (Invitrogen, Carlsbad, CA) according to the manufacturer's instruction. RNA yield and purity were determined by spectrophotometry absorption at 260 and 280 nm. To obtain cDNA, 1 μg of mRNA underwent to Reverse Transcription (Promega, Madison, WI). The resulting cDNA was stored at −20°C until used for the further analysis. Messenger RNA expression was quantitatively measured with quantitative (q) real time PCR using iCycler Bio-Rad. The reaction was performed in a 25 μL volume using SensiMix SYBR Green & Fluorescein kit (Bioline, London, UK). All the measures were performed in triplicate. The reaction conditions were as follows: 95°C for 10 min (Polymerase activation), followed by 40 cycles at 95°C for 15 min, 55–50°C (temp. depends on the Tm of primers) for 15 sec and 72°C for 15 sec. The reaction mixture without the cDNA was used as control. The primer sequences used in this study were as follows for PROK2: forward 5′-CTCGGAAAGTTCCATTTTGG-3′ and reverse 5′-TTCCGGGCCAAGCAAATAAACC-3′, Glyceralde-hydes-3-phosphate dehydrogenase (GAPDH): forward 5′-GCCAAGGCTGTGGGCAAGGT-3′ and reverse 5′-TCTCCAGGCGGCACGTCAGA-3′. The Ct value of the specific gene of interest was normalized to the Ct value of the endogenous control, GAPDH, and the comparative Ct method (2-ΔΔCt) was then applied using sham mice group as calibrator. Results are mean ± SEM of at least 3 experiments.

2.5.2. Cytokine Protein Measurement. Ten days after injury nerve samples were homogenized in ice-cold phosphate-buffered saline containing a protease inhibitor cocktail (Roche Diagnostics, Monza, Italy). IL-6, IL-1β, IL-10 TNFα, and IL-17 protein contents were determined by a multiplex enzyme-linked immunosorbent assay using ultrasensitive murine ELISA (Milliplex, Millipore, Vimodrone, Italy). A standard curve ranging on average from 0.15 pg/mL to 3700 pg/mL was prepared and then fitted by Bio-Plex Manager software.

2.5.3. Immunofluorescence. At 10 dpi DRG, sciatic nerve and plantar skin were dissected from transcardially perfused (PBS followed by 4% paraformaldehyde) mice embedded in cryostat medium and frozen. Serial sections (20 μm) were cut using a cryostat and thaw-mounted onto glass slides. Prior to immunofluorescence staining all sections were blocked with 3% normal donkey serum (serum source was the same as the secondary antibody producing species), containing 0.3% Triton X-100 for 1 h at room temperature. Then the sections were incubated at 4°C overnight with the following primary antibodies diluted in PBS-0.3% Triton X-100: 1/200 rabbit polyclonal anti-PROK2 (AbCam, Cambridge, UK), 1/400 mouse polyclonal anti-glial fibrillary acidic protein (GFAP) (Immunological Sciences, Italy), 1/100 rat monoclonal anti-CD11b (BD Pharmigen, Italy), 1/300 mouse monoclonal anti-S100β (Sigma-Aldrich, Milano, Italy), 1/200 mouse monoclonal [NF-200] to hypophosphorylated neurofilament H (AbCam, Cambridge, UK), and 1/300 goat polyclonal anti-CGRP (AbCam, Cambridge, UK). The sections were then incubated for 2 h at room temperature in 1 : 200 anti-species IgG antibodies coupled to Alexa Fluor-488 or 555 (Immunological Sciences, Italy). Nuclei were stained with DAPI 1/500. The stained sections were examined at confocal laser scanning microscope (Leica SP5, Leica Microsystems, Germany). Immunofluorescence intensity or immunoreactive area was measured in five fields (300 μm^2) for every section in at least 10 sections for every experimental group (http://imagej.nih.gov/ij/index.html free software).

The specificity of the anti-PROK2 antibody was tested preadsorbing it with the protein PROK2 (500 ng) overnight at 4°C before incubation with tissue.

2.5.4. Plantar Skin Histology. At 10 dpi the skin samples from plantar surface of sham, CCI-saline, and CCI-PC1 mice were embedded in paraffin in a correct orientation, so that they could be sectioned perpendicular to the skin surface.Plantar skin sections (5 μm) were deparaffinized, hydrated and stained by a brief immersion in Mayer's hematoxylin and eosin, followed by a brief dehydration in ethanol and xylene, and mounted with DPX mounting medium (Sigma, St. Louis, MO, USA). Sections were photographed at 20x magnification (Olympus U-CMAD3, Japan). Epidermal thickness, indicated as the distance between the dermoepidermal junction and the top of the outer most granular layer, was evaluated in three sections per tissue sample. On each image 4-5 measurements were made along the strip of epidermis to assess the average thickness. Data were expressed as mean ± SEM.

2.6. Evans Blue Assay. The permeability of blood nerve barrier (BNB) was determined by Evans Blue dye extravasation in sciatic nerve, 3 dpi. Evans Blue dye (4%, 5 mL/kg) was injected into the tail vein of anaesthetized mice. After 30 min animals were perfused with PBS. The sciatic nerves were removed and incubated in 1 mL formamide (Sigma-Aldrich) at 60°C for 24 h. Evan's Blue concentration was determined using a spectrophotometer (Shimadzu UV-160A) at a wavelength of 620 nm.

The data are expressed as μg of Evans Blue per g of tissue.

2.7. Statistic. Results are expressed as mean ± SEM. When appropriate, One-way ANOVA followed by Tukey's posttest for multiple comparisons or Two-way ANOVA followed by Bonferroni's posttest repeated measures were performed using GraphPad Prism 5 for Windows version 5.4. Differences were considered significant at $^{*\circ}P < 0.05$, $^{**\circ\circ}P < 0.01$, and $^{***\circ\circ\circ}P < 0.001$.

3. Results and Discussion

3.1. Nociceptive Behavioural Results. Figure 1 shows that, since day 3 after CCI, thermal and mechanical nociceptive thresholds decrease of 40%–50% in the ipsilateral compared to contralateral hind paw. Both allodynia and thermal hyperalgesia were observed at the following postlesion time points: 3, 6, 10, and 12 days.

Therapeutic treatment of CCI mice with PC1 from day 3 (when hyperalgesia peaks) to day 9 post injury (dpi) abolished thermal and also mechanical hyperalgesia so that from 6 up to 12 dpi PWL and PWT of injured paw did not differ from those of sham mice (Figure 1).

Availability of a new Bv8 antagonist, named PC7, able to antagonize the Bv8-induced hyperalgesia at doses ten times lower than PC1 and endowed with higher selectivity for the PKR_1 [15] pushed us to evaluate its efficacy in this neuropathic pain model. Single bolus s.c. injections of PC7 at 3 dpi, when thermal and mechanical hyperalgesia reached full development, dose-dependently reduced pain (Figures 2(a), and 2(b)) at doses (5, 15, and 45 μg kg^{-1}) about 3 times lower than the doses of PC1 which we have already demonstrated able to reduce/abolish the CCI-induced thermal and tactile hyperalgesia [16]. The antihyperalgesic effect of the highest dose (45 μg kg^{-1}, s.c.) peaked in 15 minutes and lasted for 3 h. Then we treated the mice with the highest dose (45 μg kg^{-1}, s.c) two times/day for only four days (3 to 6 dpi) and measured the nociceptive threshold every morning up to 12 dpi. Like PC1, PC7-treatment abolished the nerve-injury-induced thermal and mechanical hyperalgesia within 2 days and continued to confer protection over the observation period, up to 12 dpi (Figures 2(c), and 2(d)). Repeated administration of PC1 or PC7 did not change the thermal and mechanical nociceptive thresholds of sham mice (data not shown).

The prompt reversal of pain after acute administration depends on blocking the PKRs on peripheral sensory neurons. Indeed, as we have already demonstrated both receptors mediate the Bv8/PROK2-induced decrease of nociceptive threshold: PKR_1 in cooperation with TRPV1 is the receptor mainly responsible for thermal hyperalgesia and PKR_2 mainly contributes to mechanical allodynia [16].

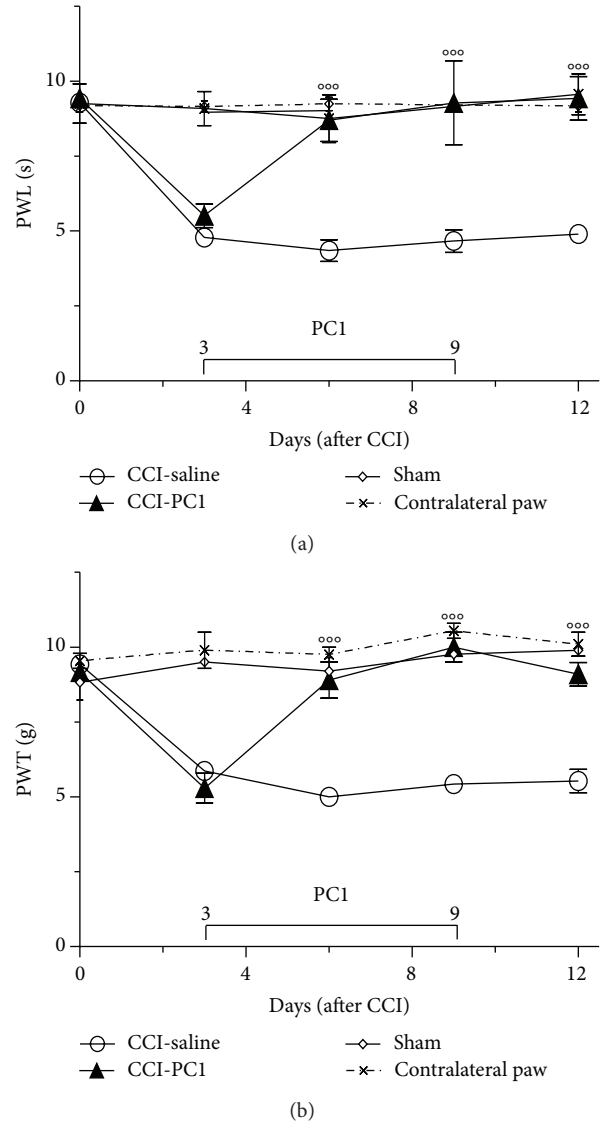

Figure 1: Repeated systemic injections of PC1 (150 μg kg^{-1}, twice a day) from 3 to 9 dpi reverted the CCI-induced thermal hyperalgesia (a) and mechanical allodynia (b) in two days. The antihyperalgesic effect lasted after treatment withdrawal, for all the observation period. Data represent means ± SEM of 6–9 mice. Two-way ANOVA was used for statistical evaluation, followed by Bonferroni's test. $^{\circ\circ\circ}P < 0.001$ CCI-PC1 versus CCI-saline mice.

3.2. PROK2 mRNA Time-Course in DRG and Sciatic Nerve. In a previous paper we have already demonstrated that at 10 dpi PROK2 was overexpressed in the periphery and in the spinal cord of neuropathic mice but was maintained close to physiological levels in neuropathic mice treated with PC1 for 7 days.

Here we studied in detail the time-course (from day 1 to 17) of injury-induced PROK2 mRNA overexpression in the

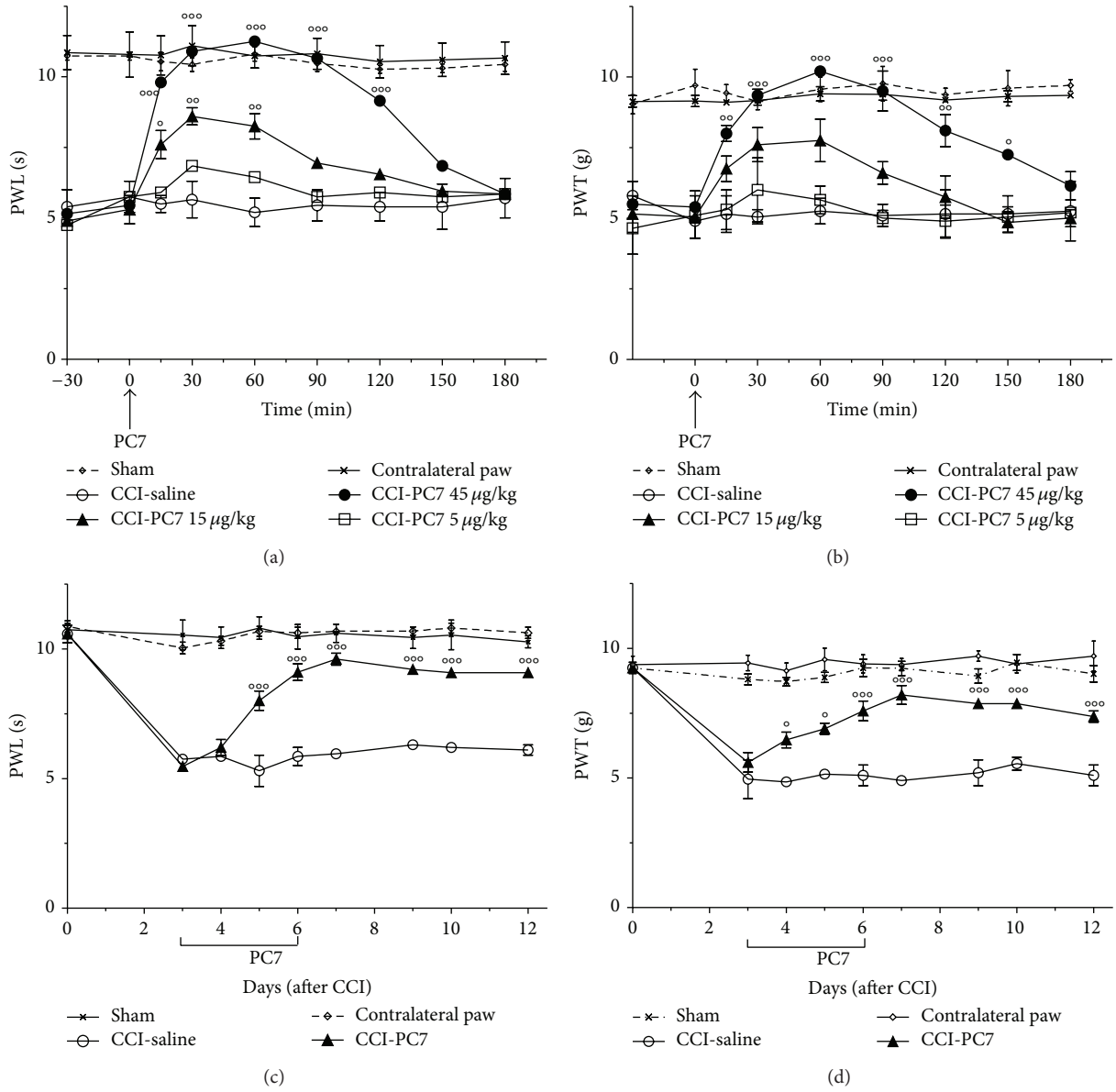

Figure 2: Antihyperalgesic effect of PC7. A single bolus s.c. injection of PC7 (5, 15, and 45 $\mu g\,kg^{-1}$) on day 3 after CCI dose-dependently reverted the established CCI-induced thermal hyperalgesia (a) and mechanical allodynia (b). The highest dose of PC7 (45 $\mu g\,kg^{-1}$) abolished hyperalgesia for about 3 h. Repeated systemic injections of PC7 (45 $\mu g\,kg^{-1}$, twice a day) from 3 to 7 dpi significantly reduced the CCI-induced thermal hyperalgesia (c) and mechanical allodynia (d) for all the observation period. Data represent means ± SEM of 5 mice. Two-way ANOVA was used for statistical evaluation, followed by Bonferroni's test. $^{\circ}P < 0.05$; $^{\circ\circ}P < 0.01$; $^{\circ\circ\circ}P < 0.001$ CCI-PC7 versus CCI-saline mice.

peripheral nervous system. PROK2 levels in the peripheral nervous system of healthy animals were negligible. RT-PCR gave 33.49 ± 0.09 Ct in the sciatic nerve and 33.97 ± 0.41 Ct in the DRG. However, as reported in Figure 3(a), in the sciatic nerve the PROK2 expression was significantly increased at 3 dpi (about 3-fold) when thermal and mechanical hyperalgesia were already evident, reached its maximal expression (8 fold) at 10 dpi, and then started to decrease up to 17 dpi. In the ipsilateral L4-6 DRG it started to increase later, at 6 dpi, and showed a constant tendency to increase up to 17 dpi (Figure 3(b)). The fact that PROK2 overexpression in DRG was delayed and lasted longer than in sciatic nerve indicates the presence of a flow of activation that, starting from the periphery, moves towards the centre. The early increase of PROK2 expression in the injured nerve is probably associated with neutrophils and Schwann Cells (SC) which express PROK2 (see afterwards) and which begin to dedifferentiate and to proliferate within 48 h of injury reaching the peak of proliferation around 4 dpi [8]. Given that PROK2 promotes survival and migration of granulocytic and monocytic lineages, the injury induced increase of PROK2 in the nerve might activate PKR_1 expressed on different immune cells thus promoting the further recruitment of new ones. Infiltration of macrophages rich in PROK2 together with the subsequent

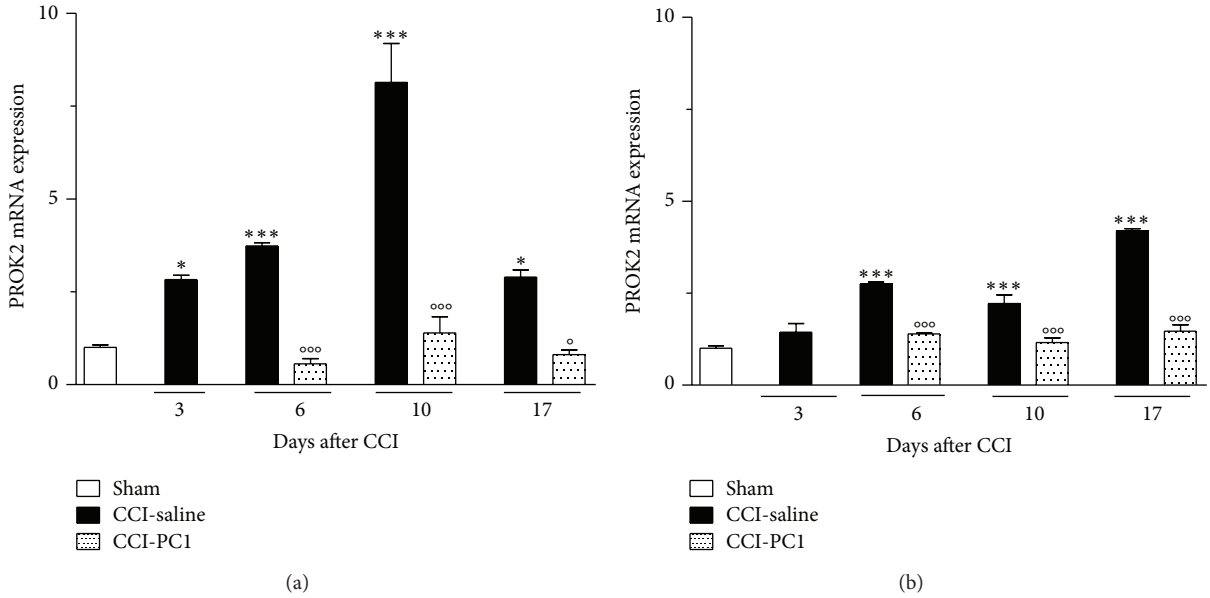

Figure 3: Time-course of PROK2 mRNA expression in injured sciatic nerve and ipsilateral DRG of CCI-saline mice and CCI-PC1 mice. PROK2 levels in the peripheral nervous system of healthy animals were negligible (33.49 ± 0.09 Ct in sciatic nerve, 33.97 ± 0.41 Ct in DRG). In the sciatic nerve (a) PROK2 expression was significantly increased at 3 dpi, reached its maximal expression at 10 dpi, and then started to decrease up to 17 dpi. In the ipsilateral L 4–6 DRGs (b) PROK2 mRNA was significantly increased at 6 dpi and showed a constant tendency to increase up to 17 dpi. Data are mean ± SEM of 5 animals. One-way ANOVA was used for statistical evaluation, followed by Tukey test for multiple comparisons. $^{*}P < 0.05$, $^{***}P < 0.001$ CCI-saline versus sham; $^{\circ}P < 0.05$ CCI-PC1 versus CCI-saline.

PROK2 upregulation in the nerve (see afterwards) answers for the further increase in PROK2 mRNA that gets to maximum level in the nerve at 10 dpi. The PROK2 mRNA levels in the sciatic nerve and DRG of PC1 treated mice did not differ from the PROK2 levels of sham animals at any time points.

Then we performed a detailed analysis of the cellular localization and modulation of PROK2 in the peripheral nervous system at 10 dpi, the time of its maximal expression.

3.3. PROK2 Localization in Dorsal Root Ganglia. At 10 dpi, immunohistochemical analysis demonstrated a strong increase of immunoreactive protein PROK2 in the ipsilateral DRG of neuropathic mice respect to DRG of sham-operated mice, where the PROK2 signal was very faint (Figures 4(a), and 4(b)). Moreover in the ipsilateral DRG, the number of PROK2 positive neurons was frankly increased respect to sham mice, with immunofluorescence distributed in the whole cell body. PROK2 showed a cytoplasmatic vesicular pattern, characteristic of proteins that are packaged and transported/released. PROK2 fluorescence was also increased in some GFAP positive cells around the neuronal bodies (Figure 4, arrows) indicating that PROK2 is expressed also by satellite cells. In PC1-treated mice PROK2 signal was significantly reduced mainly in neurons, compared to the saline-treated neuropathic mice (Figure 4(c)) as demonstrated by comparison of PROK2 immunofluorescence intensity in sham, CCI-saline, and CCI-PC1 mice (Figure 4(d)).

3.4. PROK2 Localization in Sciatic Nerve. In the sciatic nerve of sham-operated mice PROK2 immunoreactivity (green) was very faint and appeared colocalized in GFAP positive cells (yellow) (Figure 5(a)) whereas on 10 dpi a heavy infiltration of PROK2-positive cells (green colour, Figure 5(b)) was evident in the neuroma in the immediate proximity of the injury. The PROK2 positive cells are macrophages as demonstrated, in Figure 5(d), by double staining (yellow) with the macrophage marker CD11b (red). But they are also activated Schwann cells (SC) GFAP-positive (Figure 5(e)) and myelinating SC identified by S100β (Figure 5(f)). One week repeated treatment with the PKR-antagonist dramatically reduced the PROK2 immunofluorescence but not the number of infiltrating cells (Figure 5(c)). However, comparing the percent CD11b-, GFAP-, and S100β-positive area in injured nerve from saline-treated mice with respect to injured nerve from PC1-treated mice showed that the %GFAP-positive area was significantly reduced by PC1-treatment suggesting a lesser activation of SC whereas the pharmacological treatment had not affected macrophage recruitment nor myelinating SC (Figures 6(a)–6(i)). Lesser activation of SC may be a proof of lesser axonal degeneration in PC1-treated animals.

In longitudinal sections of the sciatic nerve (Figures 7, 8, and 9), immunofluorescence staining of nerve proximal and distal to the lesion demonstrated a dramatic increase of PROK2 signal (green) in the endoneurial space. The green signal was distributed in elongated structures, probably axons, and appeared more intense in the proximal than distal nerve suggesting that it is transported from DRG towards the peripheral terminals.

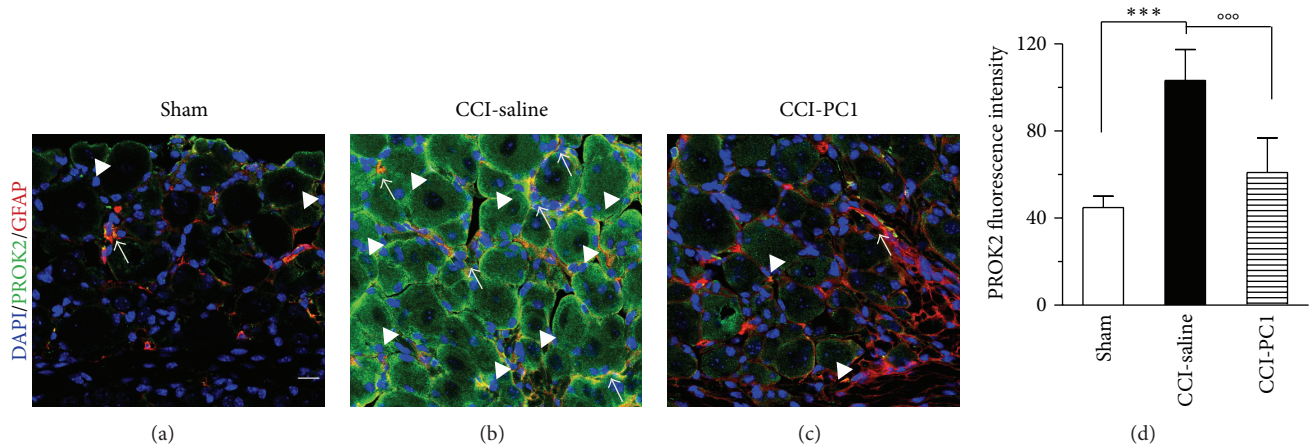

Figure 4: Representative sections of mouse L4-L5 ipsilateral DRG, at 10 dpi, from sham (a), CCI-saline (b), and CCI-PC1 (c) mice. Immunofluorescence double-staining of PROK2 (green) with GFAP (marker for satellite cells, red). Cell nuclei were counterstained with DAPI (blue fluorescence). In DRG of sham-operated mice the PROK2 signal was very faint, localized only along cell membrane of some neurons, mainly small sized (arrowheads), and in few GFAP+ satellite cells (arrow) (a). In neurons of CCI-saline mice, PROK2 immunofluorescence was significantly increased and showed a vesicular cytoplasmatic pattern which is dense in proximity of the neuronal membrane (arrowheads). The number of PROK2+ satellite cells is increased (arrows). PROK2 signal in CCI-PC1 mice was comparable with that of sham mice (c). Scale bar, 30 μm. (d) Evaluation of PROK2 fluorescence intensity. One-way ANOVA was used for statistical evaluation, followed by Tukey test for multiple comparisons $^{***}P < 0.001$ CCI-saline versus sham mice; $^{°°°}P < 0.001$ CCI-PC1 versus CCI-saline mice.

Double staining with GFAP demonstrated PROK2 in SC (yellow) scattered between fibres in the proximal nerve (Figure 7(a)) and mainly aligned to form a band in the distal nerve (Figure 7(c)), probably the bands of Büngner, which provide a supportive substrate and growth factors for regenerating axons [18]. In the injured sciatic nerve from PC1-treated mice the PROK2 immunofluorescence was dramatically reduced both in the fibres and in the SC (Figures 7(b) and 7(d)).

In the distal but not proximal injured nerve we found large CD11b+ cells many of which are also positive for PROK2 in neuropathic mice (Figure 7(e)), whereas the CD11b+ cells did not show any costaining with PROK2 in PC1-treated neuropathic mice (Figure 7(f)), confirming that PC1 treatment prevented the PROK2 upregulation also in macrophages.

In CCI-mice double-stained with NF200, which recognizes the heavy chain of neurofilaments in myelinated fibres [19], strong PROK2-green signal was localized between NF200 positive fibres. This staining was not found in the nerve of PC1-treated mice (Figures 8(a)–8(e)).

Double staining with CGRP, which recognizes peptidergic neurons, demonstrated the presence of PROK2 protein in CGRP-immunoreactive (IR) fibres in proximal and in distal injured nerve of saline treated mice. PROK2 signal was very low in injured nerve of PC1-treated mice (Figures 9(a)–9(e)).

These analyses clearly demonstrate that during nerve injury a large amount of PROK2 is expressed by almost all cell types present in the nerve, both resident and infiltrating, for a sustained period of time.

Bv8/PROK2-PKRs are therefore ligand/receptor pairs in the regulation of pain sensation [20, 21] and the transient receptor potential vanilloid 1 (TRPV1) is a critical molecular link between PKRs and primary sensory neuron activation [13]. TRPV1 is upregulated by nerve injury and TRPV1, as well as the PKRs, is also expressed in sensory nerve axons of peripheral nerves, not only at peripheral terminal [16, 22]. It is quite possible, therefore, that axonal TRPV1, just like peripheral terminal TRPV1, may also become sensitized by the persistent activation of the PKRs due to the presence of PROK2. PC1/PC7 reducing PROK2 availability and blocking the PKRs prevents nociceptor sensitization.

3.5. Cytokines in the Sciatic Nerve. Injury of the peripheral nervous system induces immune and nonimmune cells to produce cytokines at and distal to lesion sites. Proinflammatory cytokines contribute to axonal damage and they also stimulate spontaneous nociceptor activity [23].

We and others have analyzed the time-course of the production of pro- and anti-inflammatory cytokines in the nervous tissues after sciatic nerve injury [24, 25]. Schwann cells, resident activated macrophages, and fibroblast rapidly upregulate the expression and production of TNFα, IL-1β, and G-CSF which are detected between 5 and 10 h after injury. Inflammatory cytokines and chemokines advance the recruitment of blood-borne macrophages that begins 2 to 3 days after the injury concomitantly with production and secretion of IL-6 and IL-10 proteins. IL-17 positive cells have been demonstrated in the endoneurium of the injured sciatic nerve 7 days following CCI [26] and IL-17 has been demonstrated to have a role in later phases of the processes of the development of neuropathic pain [27]. As shown in Table 1, in our experimental setting, at 10 dpi, we found still high levels of IL-1β, IL-6, and IL-17 but they were reduced at levels nonsignificantly different from basal in animals treated with the PKR antagonist. Moreover the pharmacological treatment increased the levels of the anti-inflammatory cytokines

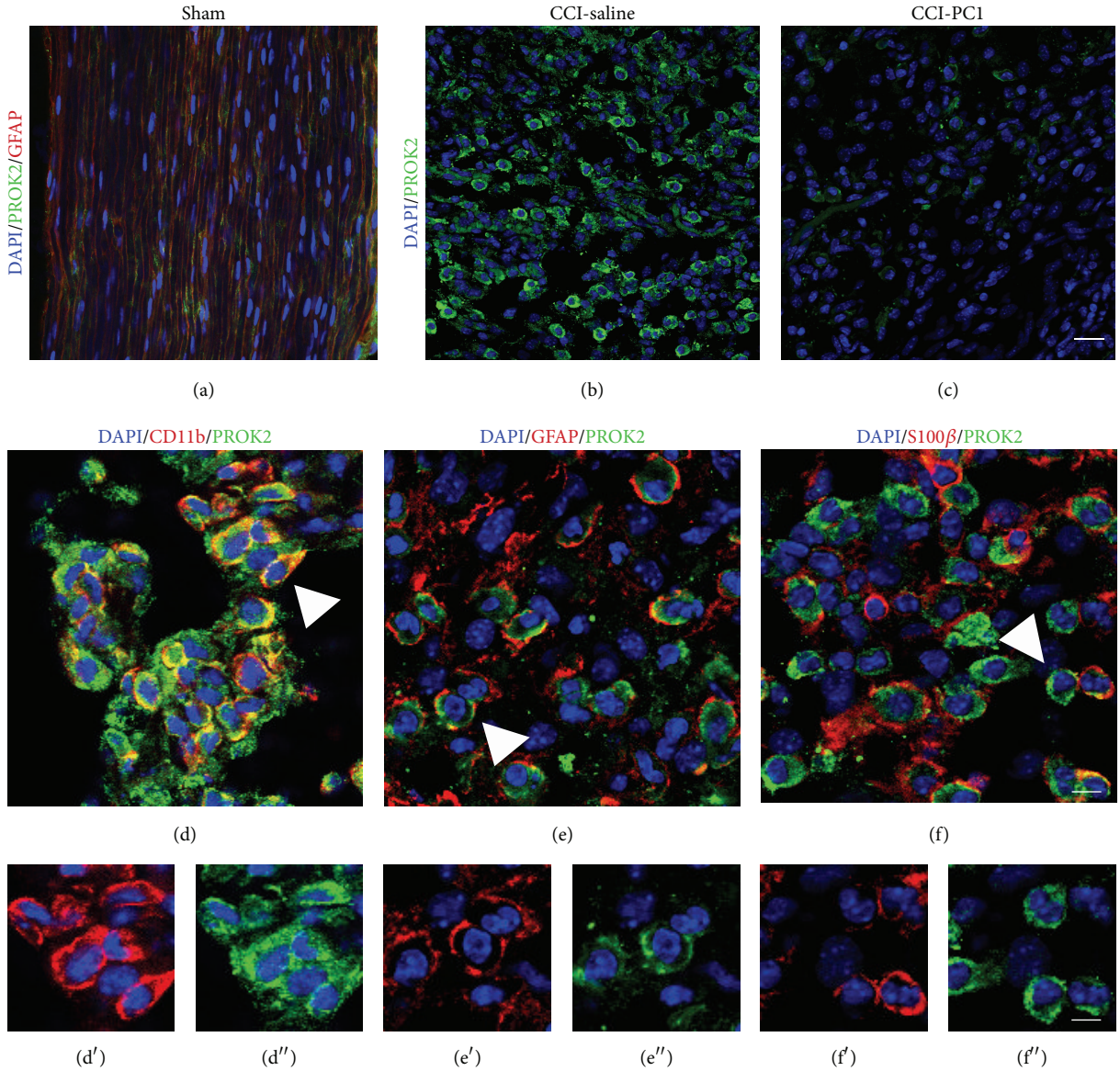

Figure 5: Representative images of sciatic nerve section in the immediate proximity of the injury, from sham (a), CCI-saline (b), and CCI-PC1 (c) mice at 10 dpi. (a) In the sciatic nerve of sham-operated mice PROK2 immunoreactivity (green) was very faint and colocalized with GFAP (red) in elongated SC. (b) A heavy infiltration of PROK2-positive cells (green) was evident in the nerve from CCI-saline mice. (c) PC1 treatment significantly reduced the PROK2 immunoreactivity in these cells. Scale bar, 30 μm. Immunofluorescence double-staining showing colocalization (yellow, arrowheads) of PROK2 (green) with CD11b (macrophage marker, red) (d), GFAP (Schwann cell marker, red) (e), and S100β (Schwann cell marker, red) (f) in the immediate proximity of the injury in the sciatic nerve of CCI-saline mice. (d′) CD11b (red), (e′) GFAP (red), (f′) S100β (red), and (d″, e″, f″) PROK2 (green) shown in single channels. Scale bar, 10 μm. Cell nuclei were counterstained with DAPI (blue fluorescence).

Table 1: Sciatic nerve cytokine levels ten days after CCI and after seven-day PC-1 treatment.

Cytokine pg/mg protein	Sham	CCI-Saline	CCI-PC1
TNFα	0	6.4 ± 3.1	0.97 ± 1.33°
IL-1β	64.26 ± 13.59	557.7 ± 121**	222.5 ± 110.31°
IL-6	4.92 ± 3.37	13.35 ± 6.15*	4.30 ± 2.88°
IL-17	0.97 ± 0.13	13.9 ± 1*	3.1 ± 1.8°
IL-10	556.8 ± 50.35	326.8 ± 8.99*	867.3 ± 95.2$^{\circ\circ\circ}$

Values are means ± SD of 5 nerves.
$^{*}P < 0.05$; $^{**}P < 0.01$ CCI-Saline versus Sham; $^{\circ}P < 0.05$, $^{\circ\circ\circ}P < 0.001$ CCI-PC1 versus CCI-Saline.

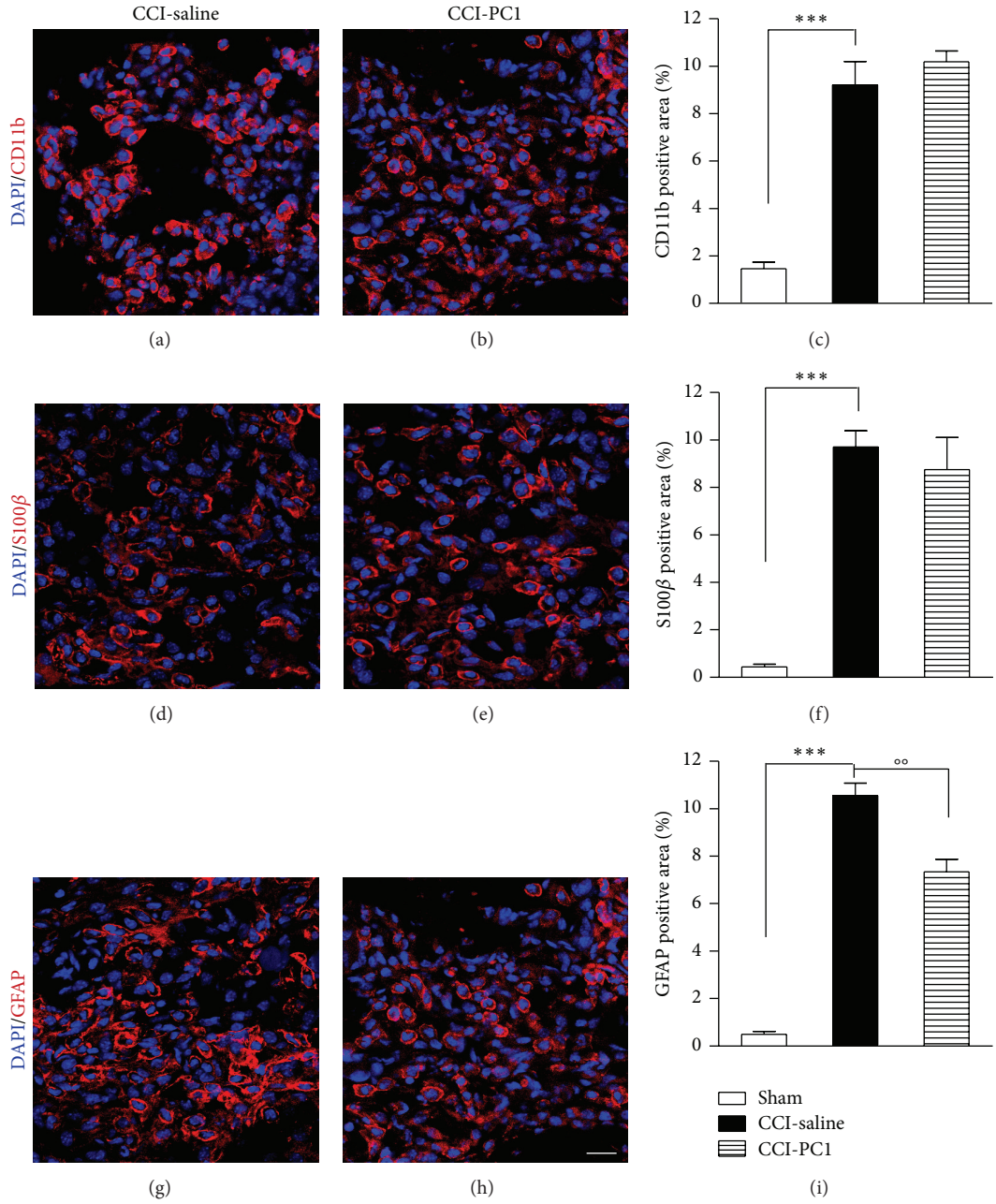

Figure 6: Immunostaining of activated macrophages (CD11b+, red), S100β+ SC (red), and GFAP+ SC (red) in the neuroma from CCI-saline and CCI-PC1 mice ((a)–(h)). Repeated treatment with the PKR-antagonist significantly reduced the GFAP+ activated SC (i) but did not affect S100β+ SC or macrophage infiltration ((c), (f)).

IL-10, reestablishing the physiological balance between pro- and anti-inflammatory cytokines and bringing the innate-immune response to conclusion far earlier than what happens during spontaneous course of Wallerian degeneration. These data suggest that PC1 is able to direct the polarization of recruited macrophages towards the M2 phenotype [28] which is involved in tissue repair.

3.6. Skin Innervation and Thickness. CCI of the sciatic nerve produces partial denervation of the paw skin and results in a significant reduction in epidermal thickness of the plantar surface of the injured paw [29]. Accordingly, in our setting, epidermis of the paw ipsilateral to the injured nerve was significantly thinner than that of contralateral paw ($32.1 \pm 2.1\,\mu$m versus $44.1 \pm 3.3\,\mu$m, $P < 0.05$) at 10 dpi. The overall organization of denervated epidermis preserved normal histological organization, but the vital layers showed reduction in thickness. PC1 treatment prevented the thinning of the plantar skin ($57.3 \pm 2.4\,\mu$m) (Figure 10).

According to data reported by Peleshok and Ribeiro-da-Silva [30] immunohistochemical staining for CGRP and

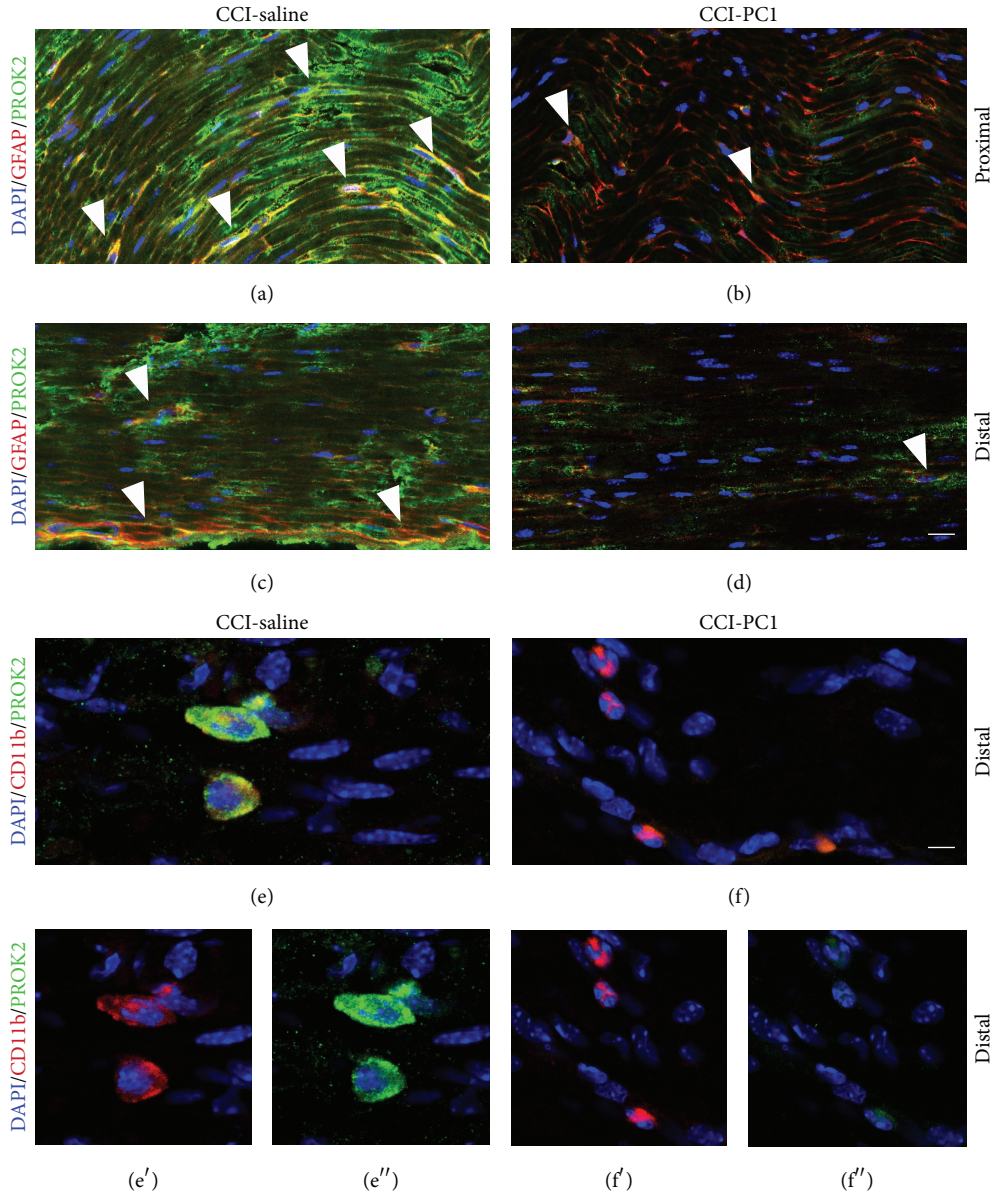

Figure 7: Representative images of CCI-induced upregulation of PROK2 in the longitudinally sliced sciatic nerve proximal and distal to the lesion. At 10 dpi a dramatic increase of PROK2 signal (green, a and c) in fibres and in GFAP+ structures (yellow) was evident both proximal and distal to the lesion. The PROK2 signal was dramatically reduced in the nerve from CCI-PC1 mice (green, b and d). Scale bar: 30 μm. High-magnification images showed macrophages that infiltrate the nerve distal to the lesion (scale bar: 10 μm). (e) Double immunofluorescence labelling for PROK2 (green) and CD11b (red) showing that in the CCI-saline mice the infiltrating macrophages contain PROK2 (yellow). (f) PROK2 signal was absent in macrophages infiltrating the nerve from CCI-PC1 mice. (e′, f′) CD11b (red), and (e″, f″) PROK2 (green) shown in single channels. Cell nuclei were counterstained with DAPI (blue fluorescence).

NF200 of plantar skin of neuropathic mice at 10 dpi demonstrated a virtual absence of CGRP-IR fibres and a dramatic reduction of NF100-IR fibres (Figures 11(b) and 11(e)) in comparison with sham-operated mice (Figures 11(a) and 11(d)). Conversely in PC1-treated neuropathic mice a thick network of CGRP-IR fibres of higher density than that of sham animals was seen and the NF200 innervation pattern resembled that seen in the sham-operated mice also if the signal appeared less intense (Figures 11(c) and 11(f)). These results indicate that repeated treatment with PKR_1-antagonist protected from axonal damage.

3.7. Intraneural Oedema and Blood Nerve Barrier Permeabilization. The constrictive ligatures around the sciatic nerve evoke intraneural edema that causes the nerve to strangulate beneath the ligatures and induce axotomy of mostly large-diameter myelinated axons, sparing mainly C-fibres. Peripheral nerve injury and C-fibres activation increase the blood-nerve barrier (BNB) permeabilization in 24–48 h [31]. The PKRs are expressed also on endothelial cells where they may regulate cell proliferation and vascular leakage [32]. Because we know that systemic injection of PC1 rapidly reduced oedema of the inflamed paw [3] here we decided to

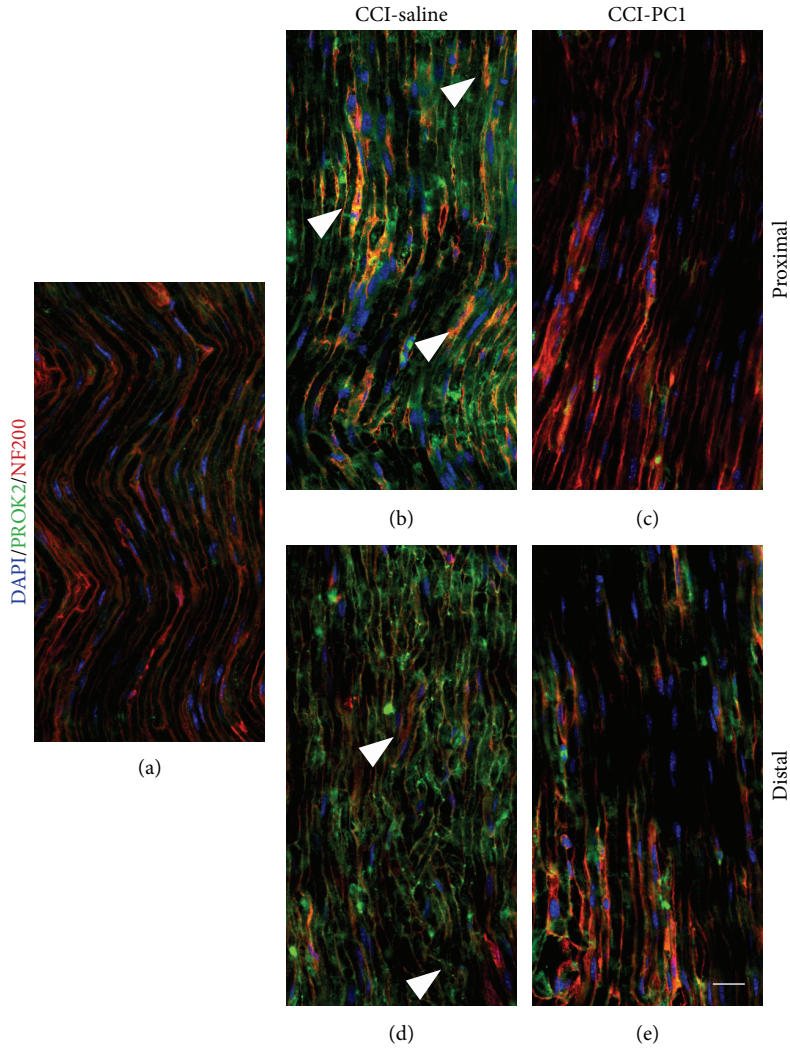

Figure 8: Confocal images of representative sections of longitudinally sliced sciatic nerve, proximal and distal to the lesion, immunostained for PROK2 (green) and NF200 (red) from sham-operated, CCI-saline and CCI-PC1 mice at 10 dpi. Scale bar: 30 μm. PROK2-green signal was localized between NF200 positive fibers in CCI-saline mice but was not found in the nerve from CCI-PC1 mice.

verify if the treatment with PKR-antagonist might reduce the blood-nerve barrier permealization consequent to peripheral nerve injury. As demonstrated by Figure 12, the Evans Blue dye extravasation in the sciatic nerve is dramatically reduced already after 2-day-treatment of neuropathic mice with 150 $\mu g\,kg^{-1}$ of PC1. Plasma extravasation depends on activation of endothelial PKR_2 [32]. PC1, at the doses here used in therapeutic schedule, may block also PKR_2 so exerting further beneficial effect in maintaining the blood-nerve barrier function and in reducing oedema.

Reduced intraneural oedema may result in sparing more axons from degeneration as demonstrated by the fact that skin innervation and skin thickness of neuropathic mice treated with the PKR-antagonist look like that of sham mice.

4. Conclusions

The results that we here present support an important role for PROK2 in the pathogenesis of neuroinflammation and neuropathic pain. In support of this hypothesis, we show that blocking the prokineticin receptors with two PKR_1-preferring antagonists reduced pain and nerve damage. The major finding of this study is that the nerve damage induces an important PROK2-increase in resident and infiltrating cells but also in the sensory neurons and that impairment of PROK2 production is linked to amelioration of pathology indicating PROK2 as precocious determinant in the process of neuroinflammation.

A few studies focused on the mechanisms involved in regulating the expression of PROK2 in myeloid cells demonstrated that PROK2-upregulation occurs through G-CSF-induced activation of STAT3 that binds the enhancer site of its promoter [33, 34], IL-6 cooperates with G-CSF to increase the expression of Bv8/PROK2 gene in neutrophils [35], and moreover Bv8 itself activates STAT3 [36]. Therefore, PROK2 is involved in a self-perpetuating cycle because it also increases its own production as a result of PKR_1 activation [3].

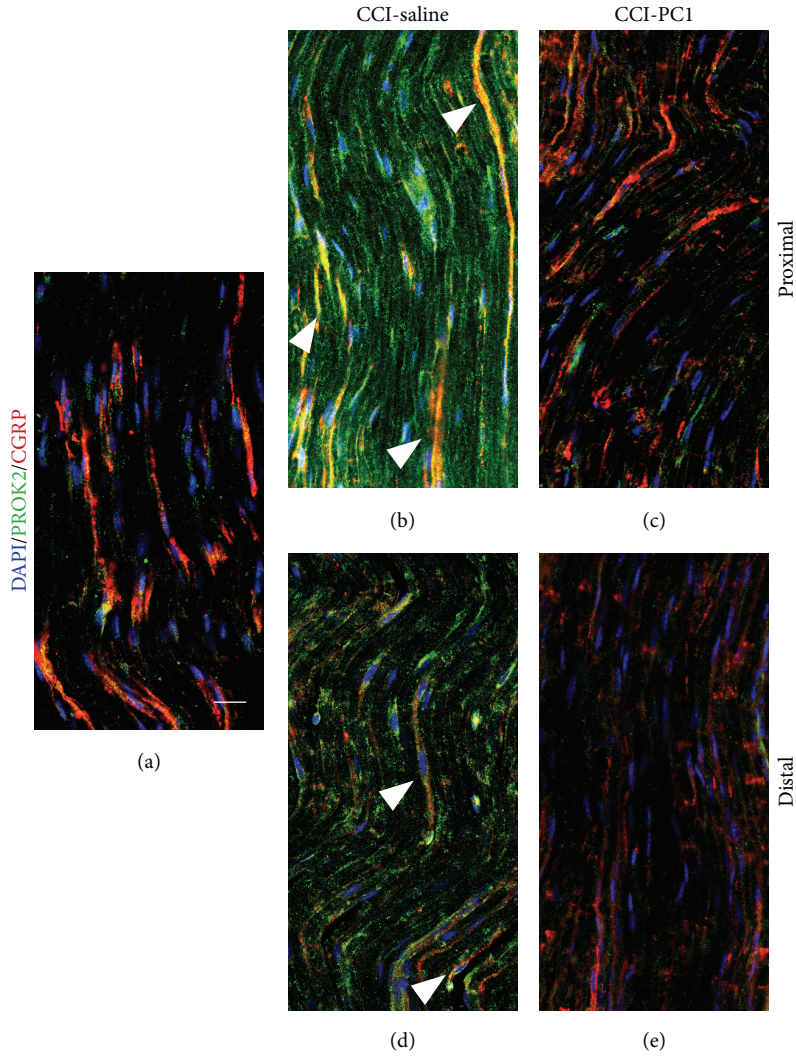

Figure 9: Confocal images of representative sections of longitudinally sliced sciatic nerve proximal and distal to the lesion, immunostained for PROK2 (green) and CGRP (red) from sham-operated, CCI-saline and CCI-PC1 mice at 10 dpi. Scale bar: 30 μm.

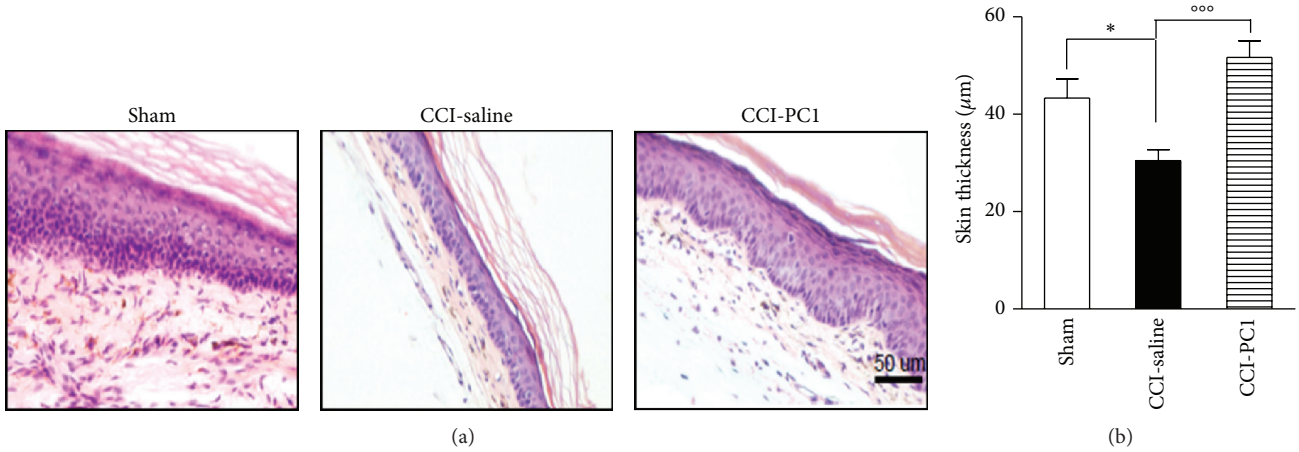

Figure 10: (a) Histological examination of the plantar skin from sham, CCI-saline, and CCI-PC1 mice stained with hematoxylin-eosin at 10 dpi. (b) Quantification of epidermal thickness of the sham, CCI/saline, and CCI/PC1 mice (3 section/animal). Data are expressed as mean ± SEM of 4-5 animals. One-way ANOVA was used for statistical evaluation, followed by Tukey test for multiple comparisons: $^{*}P < 0.05$; $^{°°°}P < 0.001$.

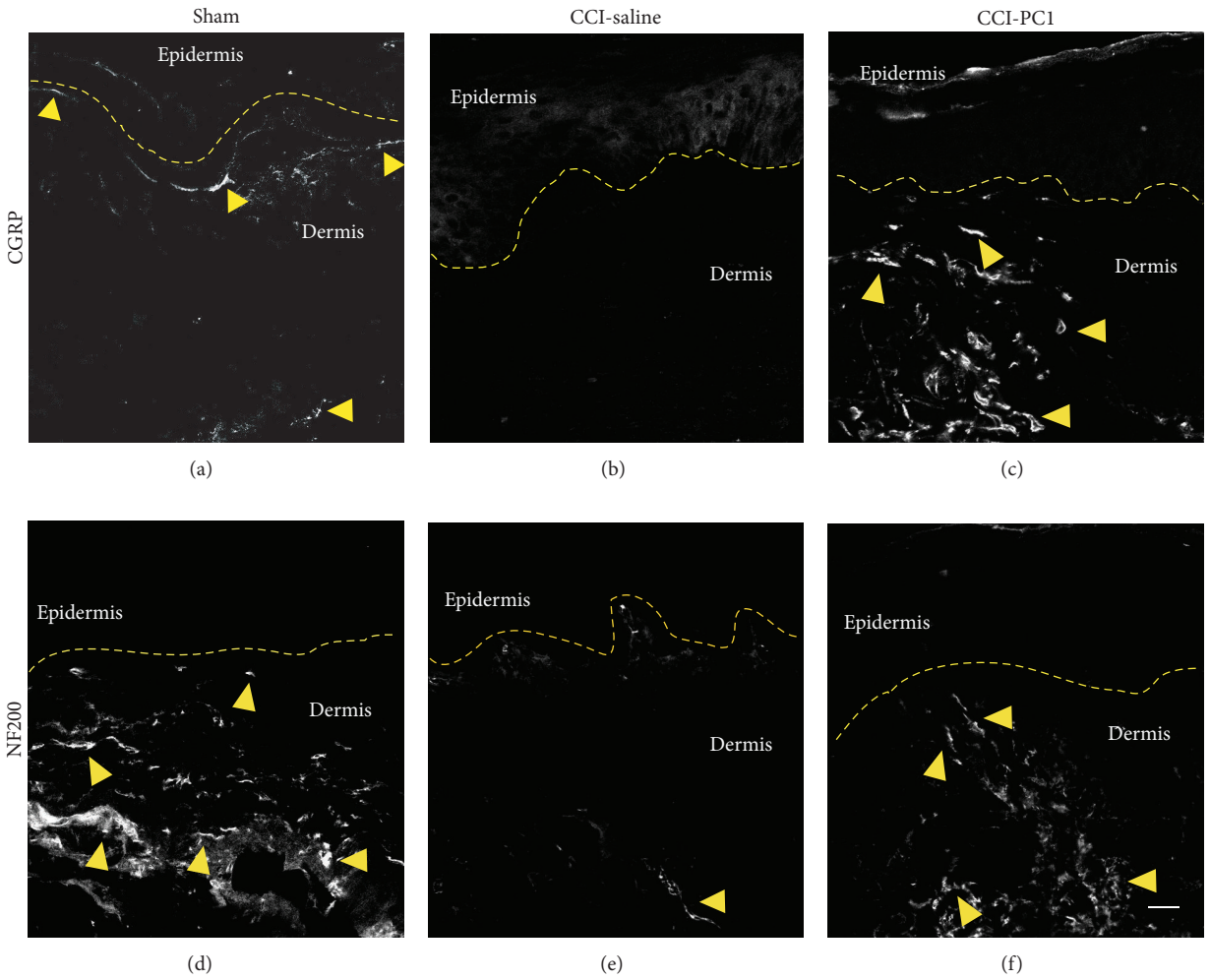

Figure 11: Confocal images of representative skin sections immunostained for CGRP and NF200 from sham-operated, CCI-saline, and CCI-PC1 mice at 10 dpi. (a) In sham-operated mice the CGRP positive fibers were distributed along the dermoepidermal junction. (b) In CCI-saline mice the CGRP positive fibers were absent. (c) In CCI-PC1 mice the CGRP positive fibers were present in dermis. (d) In sham-operated mice the NF200 positive fibers were distributed along the dermoepidermal junction and in dermis. (e) In CCI-saline mice very few NF200 positive fibers were observed. (f) In CCI-PC1 mice the NF200 positive fibers were present in dermis. Dashed line represents the dermoepidermal junction. Scale bar 20 μm.

Intracellular pathway regulating the expression of PROK2 in neurons has not yet been clarified but it may be well-funded to imagine a mechanism like that described in myeloid cells. Indeed, STAT3 activation by G-CSF, IL-6, and IL-1β signalling was recently demonstrated in DRG neurons [37, 38]. Receptors and signalling mediators of G-CSF are functionally expressed on sensory neurons also containing TRPV1 [37], some of which constitutively express PROK2 mRNA [11], and G-CSF rapidly produced phosphorylation of STAT3 in cultured DRG neurons [39]. Hence it is likely that the cytokines released early during the Wallerian-degeneration trigger synthesis of PROK2 in the sensitive neurons. STAT3 is required for T helper type 17 (Th17) generation [40] and Ferrara's group recently demonstrated that IL-17 indirectly contributes to recruitment of Bv8-positive granulocytes in tissues infiltrated by Th17 cells [41]. Interestingly, we also demonstrated that switching off the PROK2 production and signalling significantly decreases the burden of proinflammatory cytokines in the lesioned nerve and prompts an anti-inflammatory repair program.

Taken together, these considerations indicate that availability of molecules, like these PKR_1-preferring antagonists, which in addition to direct modulating nociceptor excitability also control the PROK2 synthesis and release, improves the efficacy in reducing neuroinflammation and neuropathic pain.

Conflict of Interests

The authors declare that there is no conflict of interests regarding the publication of this paper.

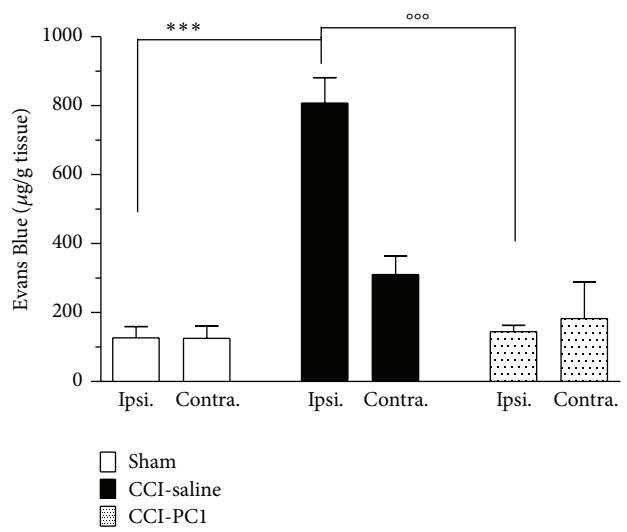

FIGURE 12: Evans Blue extravasation was measured at 3 dpi in injured and contralateral sciatic nerves. A significant increase in Evans Blue accumulation was evident in the injured nerve. The level of Evans Blue in the contralateral nerve was not significantly different from the level found in sham animals. Evans blue extravasation in the sciatic nerves of mice treated with PC1 (150 μg Kg^{-1}, twice/day, at 1 and 2 dpi) did not differ from sham mice. Data are expressed as mean ± SEM of 4-5 animals. One-way ANOVA was used for statistical evaluation, followed by Tukey test for multiple comparisons: $^{***}P < 0.001$ CCI-saline versus sham mice; $^{°°°}P < 0.001$ CCI-PC1 versus CCI-saline mice.

Acknowledgments

This work was supported by grants from the Italian Ministry of University and Scientific Research and from Sapienza University of Rome.

References

[1] C. Abbadie, "Chemokines, chemokine receptors and pain," *Trends in Immunology*, vol. 26, no. 10, pp. 529–534, 2005.

[2] L. Negri and R. Lattanzi, "Bv8/PK2 and prokineticin receptors: a druggable pronociceptive system," *Current Opinion in Pharmacology*, vol. 12, no. 1, pp. 62–66, 2012.

[3] E. Giannini, R. Lattanzi, A. Nicotra et al., "The chemokine Bv8/prokineticin 2 is up-regulated in inflammatory granulocytes and modulates inflammatory pain," *Proceedings of the National Academy of Sciences of the United States of America*, vol. 106, no. 34, pp. 14646–14651, 2009.

[4] J. LeCouter, C. Zlot, M. Tejada, F. Peale, and N. Ferrara, "Bv8 and endocrine gland-derived vascular endothelial growth factor stimulate hematopoiesis and hematopoietic cell mobilization," *Proceedings of the National Academy of Sciences of the United States of America*, vol. 101, no. 48, pp. 16813–16818, 2004.

[5] M. Dorsch, Y. Qiu, D. Soler et al., "PK1/EG-VEGF induces monocyte differentiation and activation," *Journal of Leukocyte Biology*, vol. 78, no. 2, pp. 426–434, 2005.

[6] S. Franchi, E. Giannini, D. Lattuada et al., "The prokineticin receptor agonist Bv8 decreases IL-10 and IL-4 production in mice splenocytes by activating prokineticin receptor-1," *BMC Immunology*, vol. 9, article 60, 2008.

[7] C. Martucci, S. Franchi, E. Giannini et al., "Bv8, the amphibian homologue of the mammalian prokineticins, induces a proinflammatory phenotype of mouse macrophages," *British Journal of Pharmacology*, vol. 147, no. 2, pp. 225–234, 2006.

[8] G. Moalem and D. J. Tracey, "Immune and inflammatory mechanisms in neuropathic pain," *Brain Research Reviews*, vol. 51, no. 2, pp. 240–264, 2006.

[9] L. Negri, R. Lattanzi, E. Giannini, and P. Melchiorri, "Modulators of Pain: Bv8 and prokineticins," *Current Neuropharmacology*, vol. 4, no. 3, pp. 207–215, 2006.

[10] M. Y. Cheng, F. M. Leslie, and Q.-Y. Zhou, "Expression of prokineticins and their receptors in the adult mouse brain," *Journal of Comparative Neurology*, vol. 498, no. 6, pp. 796–809, 2006.

[11] W.-P. Hu, C. Zhang, J.-D. Li et al., "Impaired pain sensation in mice lacking prokineticin 2," *Molecular Pain*, vol. 2, article 35, 2006.

[12] L. Negri, R. Lattanzi, E. Giannini, and P. Melchiorri, "Bv8/Prokineticin proteins and their receptors," *Life Sciences*, vol. 81, no. 14, pp. 1103–1116, 2007.

[13] V. Vellani, M. Colucci, R. Lattanzi et al., "Sensitization of transient receptor potential vanilloid 1 by the prokineticin receptor agonist Bv8," *The Journal of Neuroscience*, vol. 26, no. 19, pp. 5109–5116, 2006.

[14] M. de Felice, P. Melchiorri, M. H. Ossipov, T. W. Vanderah, F. Porreca, and L. Negri, "Mechanisms of Bv8-induced biphasic hyperalgesia: increased excitatory transmitter release and expression," *Neuroscience Letters*, vol. 521, no. 1, pp. 40–45, 2012.

[15] R. Lattanzi, C. Congiu, V. Onnis et al., "Halogenated triazinediones behave as antagonists of PKR1: in vitro and in vivo pharmacological characterization," *International Journal of Pharmaceutical Sciences and Research*. In press.

[16] D. Maftei, V. Marconi, F. Florenzano et al., "Controlling the activation of the Bv8/prokineticin system reduces neuroinflammation and abolishes thermal and tactile hyperalgesia in neuropathic animals," *British Journal of Pharmacology*, 2014.

[17] G. J. Bennett and Y.-K. Xie, "A peripheral mononeuropathy in rat that produces disorders of pain sensation like those seen in man," *Pain*, vol. 33, no. 1, pp. 87–107, 1988.

[18] J. W. Griffin and W. J. Thompson, "Biology and pathology of nonmyelinating schwann cells," *Glia*, vol. 56, no. 14, pp. 1518–1531, 2008.

[19] S. N. Lawson, A. A. Harper, E. I. Harper, J. A. Garson, and B. H. Anderton, "A monoclonal antibody against neurofilament protein specifically labels a subpopulation of rat sensory neurones," *Journal of Comparative Neurology*, vol. 228, no. 2, pp. 263–272, 1984.

[20] L. Negri, R. Lattanzi, E. Giannini et al., "Nociceptive sensitization by the secretory protein Bv8," *British Journal of Pharmacology*, vol. 137, no. 8, pp. 1147–1154, 2002.

[21] L. Negri, R. Lattanzi, E. Giannini et al., "Impaired nociception and inflammatory pain sensation in mice lacking the prokineticin receptor PKR1: focus on interaction between PKR1 and the capsaicin receptor TRPV1 in pain behavior," *The Journal of Neuroscience*, vol. 26, no. 25, pp. 6716–6727, 2006.

[22] K. Weller, P. W. Reeh, and S. K. Sauer, "TRPV1, TRPA1, and CB1 in the isolated vagus nerve—axonal chemosensitivity and control of neuropeptide release," *Neuropeptides*, vol. 45, no. 6, pp. 391–400, 2011.

[23] C. Sommer and M. Kress, "Recent findings on how proinflammatory cytokines cause pain: peripheral mechanisms in inflammatory and neuropathic hyperalgesia," *Neuroscience Letters*, vol. 361, no. 1–3, pp. 184–187, 2004.

[24] P. Sacerdote, S. Franchi, S. Moretti et al., "Cytokine modulation is necessary for efficacious treatment of experimental neuropathic pain," *Journal of Neuroimmune Pharmacology*, vol. 8, no. 1, pp. 202–211, 2013.

[25] S. Rotshenker, "Wallerian degeneration: the innate-immune response to traumatic nerve injury," *Journal of Neuroinflammation*, vol. 8, article 109, 2011.

[26] C. Kleinschnitz, H. H. Hofstetter, S. G. Meuth, S. Braeuninger, C. Sommer, and G. Stoll, "T cell infiltration after chronic constriction injury of mouse sciatic nerve is associated with interleukin-17 expression," *Experimental Neurology*, vol. 200, no. 2, pp. 480–485, 2006.

[27] N. Noma, J. Khan, I.-F. Chen et al., "Interleukin-17 levels in rat models of nerve damage and neuropathic pain," *Neuroscience Letters*, vol. 493, no. 3, pp. 86–91, 2011.

[28] C. Martucci, A. E. Trovato, B. Costa et al., "The purinergic antagonist PPADS reduces pain related behaviours and interleukin-1β, interleukin-6, iNOS and nNOS overproduction in central and peripheral nervous system after peripheral neuropathy in mice," *Pain*, vol. 137, no. 1, pp. 81–95, 2008.

[29] S. L. Kojundzic, I. Dujmovic, I. Grkovic, and D. Sapunar, "Regional differences in epidermal thickness and behavioral response following partial denervation of the rat paw," *International Journal of Neuroscience*, vol. 118, no. 12, pp. 1748–1762, 2008.

[30] J. C. Peleshok and A. Ribeiro-da-Silva, "Delayed reinnervation by nonpeptidergic nociceptive afferents of the glabrous skin of the rat hindpaw in a neuropathic pain model," *Journal of Comparative Neurology*, vol. 519, no. 1, pp. 49–63, 2011.

[31] S. Beggs, X. J. Liu, C. Kwan, and M. W. Salter, "Peripheral nerve injury and TRPV1-expressing primary afferent C-fibers cause opening of the blood-brain barrier," *Molecular Pain*, vol. 6, article 74, 2010.

[32] C. Guilini, K. Urayama, G. Turkeri et al., "Divergent roles of prokineticin receptors in the endothelial cells: angiogenesis and fenestration," *American Journal of Physiology: Heart and Circulatory Physiology*, vol. 298, no. 3, pp. H844–H852, 2010.

[33] F. Shojaei, X. Wu, C. Zhong et al., "Bv8 regulates myeloid-cell-dependent tumour angiogenesis," *Nature*, vol. 450, no. 7171, pp. 825–831, 2007.

[34] X. Qu, G. Zhuang, L. Yu, G. Meng, and N. Ferrara, "Induction of Bv8 Expression by granulocyte colony-stimulating factor in CD11b+Gr1+ cells: Key role of Stat3 signaling," *Journal of Biological Chemistry*, vol. 287, no. 23, pp. 19574–19584, 2012.

[35] B. Yan, J.-J. Wei, Y. Yuan et al., "IL-6 cooperates with G-CSF to induce protumor function of neutrophils in bone marrow by enhancing STAT3 activation," *The Journal of Immunology*, vol. 190, no. 11, pp. 5882–5893, 2013.

[36] H. Xin, R. Lu, H. Lee et al., "G-protein-coupled receptor agonist BV8/prokineticin-2 and STAT3 protein form a feed-forward loop in both normal and malignant myeloid cells," *The Journal of Biological Chemistry*, vol. 288, no. 19, pp. 13842–13849, 2013.

[37] M. Schweizerhof, S. Stösser, M. Kurejova et al., "Hematopoietic colony-stimulating factors mediate tumor-nerve interactions and bone cancer pain," *Nature Medicine*, vol. 15, no. 7, pp. 802–807, 2009.

[38] M. Tsuda, Y. Kohro, T. Yano et al., "JAK-STAT3 pathway regulates spinal astrocyte proliferation and neuropathic pain maintenance in rats," *Brain*, vol. 134, no. 4, pp. 1127–1139, 2011.

[39] S. Stösser, M. Schweizerhof, and R. Kuner, "Hematopoietic colony-stimulating factors: new players in tumor-nerve interactions," *Journal of Molecular Medicine*, vol. 89, no. 4, pp. 321–329, 2011.

[40] C. E. Egwuagu, "STAT3 in $CD4^+$ T helper cell differentiation and inflammatory diseases," *Cytokine*, vol. 47, no. 3, pp. 149–156, 2009.

[41] A. S. Chung, X. Wu, G. Zhuang et al., "An interleukin-17-mediated paracrine network promotes tumor resistance to anti-angiogenic therapy," *Nature Medicine*, vol. 19, no. 9, pp. 1114–1123, 2013.

Hindawi Publishing Corporation
BioMed Research International
Volume 2015, Article ID 394257, 13 pages
http://dx.doi.org/10.1155/2015/394257

Review Article

mTOR Kinase: A Possible Pharmacological Target in the Management of Chronic Pain

Lucia Lisi,[1] Paola Aceto,[2] Pierluigi Navarra,[1] and Cinzia Dello Russo[1]

[1]*Institute of Pharmacology, Catholic University Medical School, Largo F. Vito 1, 00168 Rome, Italy*
[2]*Department of Anesthesiology and Intensive Care, A. Gemelli Hospital, Catholic University Medical School, 00168 Rome, Italy*

Correspondence should be addressed to Cinzia Dello Russo; cinzia.dellorusso@rm.unicatt.it

Received 16 May 2014; Accepted 12 September 2014

Academic Editor: Livio Luongo

Chronic pain represents a major public health problem worldwide. Current pharmacological treatments for chronic pain syndromes, including neuropathic pain, are only partially effective, with significant pain relief achieved in 40–60% of patients. Recent studies suggest that the mammalian target of rapamycin (mTOR) kinase and downstream effectors may be implicated in the development of chronic inflammatory, neuropathic, and cancer pain. The expression and activity of mTOR have been detected in peripheral and central regions involved in pain transmission. mTOR immunoreactivity was found in primary sensory axons, in dorsal root ganglia (DRG), and in dorsal horn neurons. This kinase is a master regulator of protein synthesis, and it is critically involved in the regulation of several neuronal functions, including the synaptic plasticity that is a major mechanism leading to the development of chronic pain. Enhanced activation of this pathway is present in different experimental models of chronic pain. Consistently, pharmacological inhibition of the kinase activity turned out to have significant antinociceptive effects in several experimental models of inflammatory and neuropathic pain. We will review the main evidence from animal and human studies supporting the hypothesis that mTOR may be a novel pharmacological target for the management of chronic pain.

1. Introduction

Chronic pain represents a major public health problem worldwide, affecting approximately 37% of the US population, with an economic burden of up to US$ 635 billion per year [1]. In Europe, the prevalence of chronic pain syndromes ranges between 25 and 30% [2]. Physiologically, nociceptive pathways are activated in response to traumatic or noxious stimuli. Acute pain, which is primarily due to nociception, serves as an adaptive and protective mechanism to detect, localize, and limit tissue damage; on the contrary, chronic pain, which persists after a reasonable time for healing to occur (ranging between 1 and 6 months in most definitions), can be regarded as a form of maladaptive response, in which pain is no longer protective or strictly linked to the initial stimulus. After application of an intense and prolonged injury, ongoing excitation of primary nociceptive neurons leads to neuronal changes both in the primary afferents (peripheral sensitization) and in the spinal dorsal horn neurons (central sensitization), contributing to the development of chronic pain [3]. In this condition, pain arises in the absence of noxious stimulus, may be stimulated by normally innocuous stimuli (allodynia), is exaggerated and prolonged in response to noxious stimuli (primary hyperalgesia), and spreads beyond the site of injury (secondary hyperalgesia) [3]. Chronic pain has a neuropathic origin in approximately 20% of the patients [2]. Neuropathic pain may arise from a direct damage of somatosensory nerves or nerves innervating visceral organs or from a disease affecting the somatosensory nervous system which implies an indirect injury resulting from various causes, including metabolic stress, autoimmune, degenerative, or chronic inflammatory conditions, and idiopathic origins [4].

Neuropathic pain is characterized by pain hypersensitivity that is mediated by both peripheral and spinal neuronal synaptic plasticity (leading toperipheral and central sensitization, resp.), involving pre- and posttranslational changes in the expression and functions of receptors, enzymes, and voltage-dependent ion channels in sensory neurons [3]. In addition, other biochemical events contribute to the hyperactivity of the somatosensory system, including phenotypic

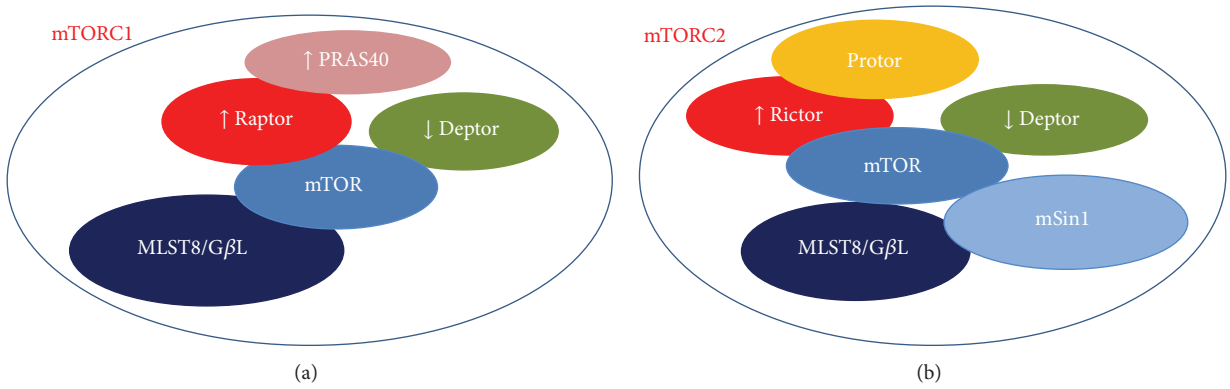

Figure 1: Schematic representing the molecular partners of mTOR forming (a) mTOR complex 1 (mTORC1) and (b) mTOR complex 2 (mTORC2). The down-arrows indicate the inhibitory proteins, whereas the up-arrows indicate activator factors on mTOR function.

neuronal switch (i.e., large myelinated Aβ fibers expressing neuropeptides directly involved in pain transmission, such as substance P and calcitonin gene-related peptide), sprouting of nerve endings (i.e., myelinated Aβ fibers establishing direct contacts with nociceptive projecting neurons in the lamina I-II of the spinal dorsal horn), loss of spinal inhibitory control, and increased activity of descending excitatory pathways [3]. Moreover, synaptic plasticity within key cortical regions involved in pain processing (i.e., the anterior cingulated cortex, the insular cortex, primary and secondary sensory cortices, and the amygdala) has been also observed in relation to neuropathic pain [4]. Finally, activation of glial cells with release of pronociceptive mediators can directly modulate neuronal excitability and thus pain transmission, contributing to central sensitization and to the occurrence of neuropathic pain [5].

Multimodal pharmacological treatments for chronic pain syndromes, including neuropathic pain, are based on the use of antiepileptics, antidepressants, local anesthetics, opioid analgesics, or tramadol. These treatments are only partially effective, with significant pain relief achieved in 40–60% of patients [4]. A relatively recent modality of neuropathic pain therapy, which represents the future challenge of upcoming researches, involves specific cellular targets implied in neuronal synaptic plasticity and/or glial activation [6]. Interestingly, recent studies show that the mammalian target of rapamycin (mTOR) kinase and downstream effectors may be implicated in the development of chronic inflammatory, neuropathic, and cancer pain. This kinase is a master regulator of protein synthesis, and it is critically involved in the regulation of several neuronal functions, including synaptic plasticity and memory formation in the central nervous system (CNS) [7]. As mentioned above, neuronal synaptic plasticity both at peripheral level and in the CNS is a major mechanism leading to the development of chronic pain, thus suggesting that mTOR may be a novel pharmacological target for the management of chronic pain. In addition, mTOR has been also reported to regulate astrocyte and microglial activity (as we have recently reviewed [8]), thus suggesting an additional therapeutic target in the treatment of chronic pain syndromes that involve increased glial activation. The main evidence from animal studies as well as clinical reports supporting this hypothesis is reviewed in the present paper.

2. mTOR, the "Mechanistic" Target of Rapamycin

The mTOR kinase, now officially known as "mechanistic" TOR, is a conserved serine/threonine protein kinase belonging to the phosphoinositide 3-kinase (PI3K) family that regulates multiple intracellular processes [9]. In mammals, mTOR is encoded by a single gene [10] and interacts with several proteins to form two distinct complexes, referred to as mTORC1 and mTORC2. These complexes display different sensitivity to the inhibitory action of rapamycin, which mainly suppresses mTORC1-dependent activities in acute treatments [11]. Notably, the two complexes promote the activation of different signalling pathways and recognize distinct upstream regulators as well as downstream targets, whose specificity is determined by the specificity of the interacting proteins. Both complexes include the inhibitory protein DEPTOR and the adaptor protein mLST8/GβL (mammalian LST8/G-protein β-subunit like protein) [12]. However, the role of mLST8/GβL in the regulation of mTORC1 function remains unclear at present, since its chronic loss does not affect mTORC1 activity *in vivo* [13]. As shown in Figure 1, mTORC1 specifically contains the regulatory-associated protein of mTOR (raptor) and the inhibitory protein PRAS40 (proline-rich AKT substrate of 40 KDa) [14]. Raptor regulates mTORC1 assembly and serves as a scaffold for the recruitment of specific substrates, such as the eukaryotic initiation factor-4E-binding protein 1 (4E-BP1) [15, 16]. Similarly, other proteins reside uniquely within complex 2, that is, the rapamycin-insensitive companion of mTOR (rictor), the protein observed with rictor (PROTOR), and the stress-activated protein kinase-interacting protein 1 (mSIN1) (Figure 1) [17]. Much like raptor, rictor is necessary for mTORC2 assembly together with mSIN1, for mTORC2 catalytic activity, and it may also be involved in the selective recruitment of specific substrates [14].

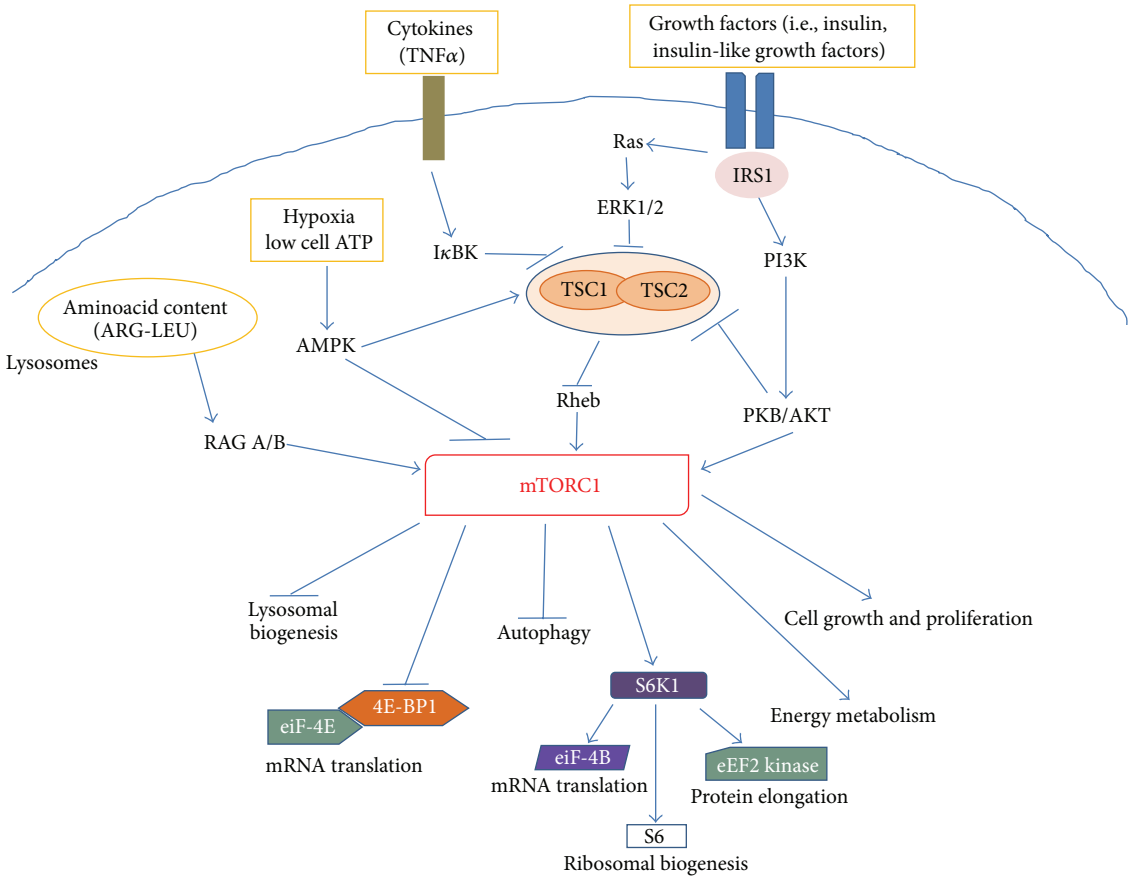

Figure 2: Schematic representing the main intracellular targets as well as the main cellular processes regulated by mTORC1.

The mTOR complex 1 is activated in response to different intracellular and extracellular cues, that is, growth factors, cytokines, energy status, oxygen, and amino acids, to control multiple functions related to cell growth and metabolism [12]. As shown in Figure 2, several upstream regulators of mTORC1 activity converge on theheterodimer consisting of tuberous sclerosis 1 (TSC1, also known as hamartin) and TSC2 (also known as tuberin). In this complex, TSC1 stabilizes TSC2 by preventing its degradation, while TSC2 acts as a GTPase-activating protein (GAP) for the small GTPase protein, Rheb (Ras homolog enriched in brain) [18]. Rheb in its GTP-bound state binds to and activates mTORC1, whereas the TSC1/2 complex normally inhibits mTORC1 activity by favoring the GDP-bound inactive state of Rheb. As recently reviewed by Laplante and Sabatini [12], growth factors (such as insulin and insulin-like growth factors) increase mTORC1 activity, by promoting the phosphorylation and degradation of the TSC1/2 complex. This occurs via ligand-dependent activation of receptor tyrosine kinases (RTKs), like the insulin receptors, followed by activation of the PI3K and Ras pathways. The effector kinases of these pathways, namely, the protein kinase B (PKB/AKT) and the extracellular-signal-regulated kinases (ERK) 1 and 2, induce TSC1/2 phosphorylation (Figure 2). In addition, AKT can directly phosphorylate the inhibitory protein PRAS40, promoting its dissociation from raptor and further contributing to mTORC1 activation. Proinflammatory cytokines, like TNFα, increase mTORC1 activity via IκB kinase- (IKK-) dependent inactivation of the TSC1/2 complex, whereas, in response to hypoxia or low energy status, the adenosine monophosphate activated kinase (AMPK) blocks mTORC1 activity, by increasing TSC2 function and directly inhibiting raptor (Figure 2). Finally, increased intracellular levels of aminoacids, particularly arginine and leucine, promote mTORC1 activation, by inducing its binding to a distinct family of GTPases, the Rag GTPases, together with its translocation to the lysosomal surface [19, 20]. It has been hypothesized that translocation of mTORC1 to the lysosomes allows GTP-bound Rheb to interact with mTORC1, promoting its activation only when aminoacids are available. Additional details on the regulation of mTORC1 can be retrieved in the above mentioned review article [12].

Protein synthesis is the best-characterized intracellular process regulated by mTORC1, whose activation generally increases the cellular capacity of protein generation [14]. The two main downstream targets of mTORC1, 4E-BP1 and the ACG-family protein, S6 kinase 1 (S6K1), are key components of the protein translation machinery. Phosphorylation of 4E-BP1 causes its dissociation from the eukaryotic translation initiation factor- (eIF-) 4E (Figure 2). This allows eIF-4E to associate with eIF-4G leading to the formation of eIF-4F, which facilitates the loading of ribosomes onto the mRNA. By this molecular mechanism, mTORC1 can control the

translation of specific mRNAs, including the so-called 5′-TOP mRNAs that mostly encode for components of the translational machinery. In addition, phosphorylation and activation of S6K1 promote protein translation by phosphorylation of several substrates, including eIF-4B, the eukaryotic elongation factor 2 (eEF2) kinase, and the ribosomal S6 protein (Figure 2). Local protein synthesis within sensory neurons contributes to their nociceptive functions both under physiological conditions and during chronic pain. As described in detail in Section 4, by controlling protein translation mTORC1 can regulate the activity of sensory neurons, in periphery as well as in the CNS. The activity of S6K1 is also important in the control of RTK activation. In fact, S6K1 (activated by mTORC1) promotes also the phosphorylation and inactivation of IRS1, the insulin receptor substrate 1. The latter is a docking protein that in its tyrosine-phosphorylated form couples the insulin receptor to its downstream effectors [21]. This is part of a retroinhibitory feedback mechanism that reduce RTK activation, thus the activity of AKT and ERK [12]. The latter is also a kinase critically involved in the regulation of pain processing (see Section 4). The mTOR complex 1 is also involved in the regulation of several metabolic pathways, regulating the expression of genes encoding different steps of glycolysis and the pentose phosphate pathway, as well as critical enzymes in the *de novo* biosynthesis of lipids [22]. Finally, mTORC1 can favor cell growth by negatively regulating macroautophagy (autophagy), the central degradative process in cells, and lysosome biogenesis [12, 14]. As discussed in detail in Section 4, the activation of autophagy in Schwann cells can limit the extent of axonal degeneration after nerve injury and promote regeneration and myelination, thus favoring analgesic effects.

In contrast to mTORC1, mechanisms leading to mTORC2 activation are less characterized. It seems that mTORC2 activation is directly promoted by PI3K via phosphorylation of specific mTORC2 interactors, including rictor (Figure 3) [17]. Thus, mTORC2 appears to be also responsive to growth factors, but insensitive to nutrients. mTORC2 regulates the activity of several proteins belonging to the ACG family, including AKT, the serum- and glucocorticoid-induced protein kinase (SGK1), and protein kinase C- (PKC-) α. AKT is a key regulator of cell survival and proliferation, with mTORC2 promoting its phosphorylation at Ser_{473} in the hydrophobic motif and maximal activation [23, 24]. In this way, mTOR appears to be both a downstream effector of AKT (i.e., mTORC1) and an important upstream regulator of the kinase activity (i.e., mTORC2) (Figure 4). Moreover, it has been shown that an intricate crosstalk exists between the two complexes (Figure 4), since S6K can negatively control the activation of mTORC2 [24], whereas TSC1/2 positively contributes to mTORC2 activation [25]. The mTOR complex 2 also promotes the activity of SGK1, another important kinase in the control of cell proliferation [26]. Finally, activation of PKCα by mTORC2, along with other effectors (like paxillin and Rho GTPases), regulates the dynamic of actin cytoskeleton [27, 28]. Direct regulation of AKT activity together with a role in the control of actin dynamics suggests a possible involvement of mTORC2 in the control of neuronal function, as discussed in Section 4.

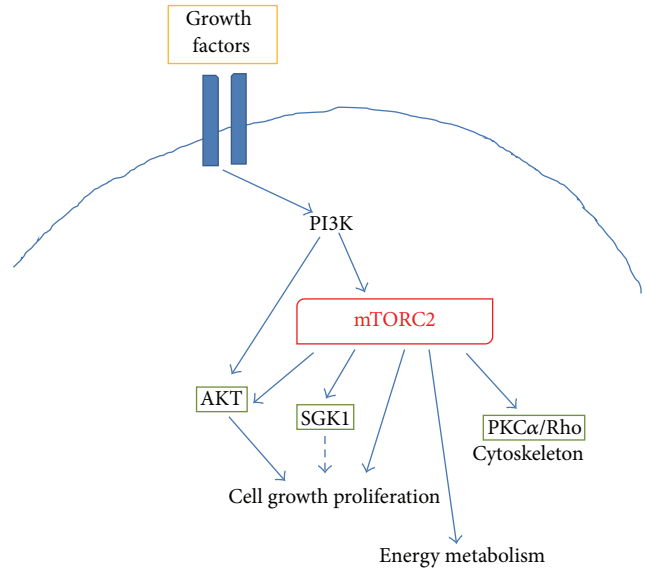

Figure 3: Schematic representing the main intracellular targets as well as the main cellular processes regulated by mTORC2.

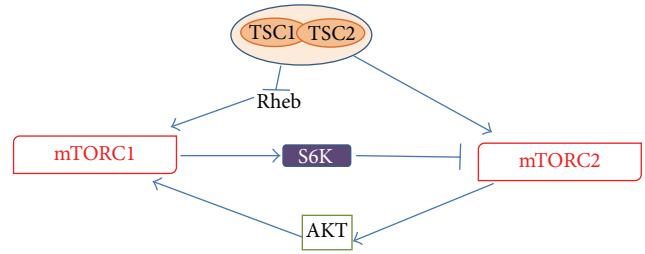

Figure 4: Schematic representing the main mTORC1-mTORC2 crosstalks.

3. mTOR Inhibitors

The mTOR kinase, now officially known as "mechanistic" TOR, was initially identified as "mammalian target of rapamycin," because the kinase is the main target of an antifungal compound derived from *Streptomyces hygroscopicus*, rapamycin [29]. This drug, discovered in soil samples collected from Easter Island (Rapa Nui, from where the name), was originally found to have antifungal proprieties, but rapidly its immunosuppressive activity became its more important property. Actually, rapamycin is widely used in preventing clinical allograft rejection and in treating some autoimmune diseases [30]. In the 1980s, rapamycin was also found to have anticancer activity, although the exact mechanism of action remained unknown until many years later.

Rapamycin (or sirolimus) mainly inhibits mTORC1 activity by forming a trimolecular complex with mTOR and the immunophilin, FKBP12 (FK506-binding protein of 12 kDa; also known as PPIase FKBP1A). The drug associates with FKBP12, and the resulting complex interacts with the FRB (FKBP12-rapamycin binding) domain located in the carboxyl terminus of mTOR: the interaction disrupts the association with raptor and thus uncouples mTORC1 from its substrates

inducing a block of mTORC1 signaling [31, 32]. However, not all the functions mediated by mTORC1 are sensitive to rapamycin; the inhibition of cap-dependent translation and the induction of autophagy are in part resistant to rapamycin [33]. Originally, the effects of rapamycin were thought to be only related to the inhibition of mTORC1, but studies of Sabatini's group have shown that rapamycin given at higher concentrations and in chronic treatments also interferes with mTORC2 regulatory functions [11]. In particular, high intracellular levels of rapamycin inhibit the binding and subsequent assembly of mTORC2-specific components mSIN1 and rictor [11].

Rapamycin readily crosses the blood brain barrier (BBB), thus exerting direct effects within the CNS [34]. However, in order to ameliorate the pharmacokinetic profile of rapamycin, novel drugs have been developed. This first generation of mTOR inhibitors displays the same binding sites for mTOR and FKBP12 and is thus so-called rapalogs (i.e., rapamycin and its analogs). Rapalogs includes CCI-779 (temsirolimus), RAD-001 (everolimus), and AP23573 (ridaforolimus or deforolimus) (Table 1). Among these mTOR inhibitors, CCI-779 is a prodrug of rapamycin, which delays tumor proliferation [35], and it is actually used for the treatment of renal cell carcinoma, whereas RAD-001, a 40-O-(2-hydroxyethyl) derivative of rapamycin, is currently used as an immunosuppressant to prevent rejection of organ transplants and, like CCI-779, for the treatment of renal cell cancer and subependymal giant cell astrocytoma [36].

However, the use of rapalogs unmasked the feedback loop between mTORC1 and AKT in certain type of cells. The mTORC1 inhibition induced by these drugs fails to repress the negative feedback loop that results in phosphorylation and activation of AKT, and it is unable to block the mTORC2 positive feedback to AKT [37]. The elevation of AKT activity can promote a longer survival in some cell types and may also be associated to pain hypersensitivity (as described in Section 4). These limitations have led to the development of a second generation of mTOR inhibitors: the ATP-competitive mTOR inhibitors, which block both mTORC1 and mTORC2 activity [38]. Unlike rapamycin, which is a specific allosteric inhibitor of mTORC1, these ATP-competitive inhibitors target the catalytic site of the enzyme, thus promoting a broader, more potent, and sustained inhibition of mTOR and preventing the activation of PI3K/AKT caused by the derepression of negative feedbacks [39]. This is due to the effective inhibition of rapamycin-insensitive mTORC2 activity in addition to mTORC1 inhibition and also to a more comprehensive and sustained mTORC1 inhibition as demonstrated by sustained reduction of 4E-BP1 phosphorylation [38]. Actually, many compounds with different chemical structures show these functions (see Table 1) and some of them are being tested in clinical trials.

Finally, the close interaction of mTOR with the PI3K pathway has also led to the development of mTOR/PI3K dual inhibitors [40]. Compared with drugs that inhibit either mTORC1 or PI3K, these drugs have the benefit of inhibiting both mTORC1 and mTORC2 and all the catalytic isoforms of PI3K. Interestingly, because of the high sequence homology between mTOR and PI3K, some compounds (like wortmannin), originally identified as PI3K inhibitors, were later shown to inhibit mTOR as well [41]. The activity of these small molecules differs from rapalog activity, for a more specific block of both mTORC1-dependent phosphorylation of S6K1 and mTORC2-dependent phosphorylation of AKT at the Ser_{473} residue. Dual mTOR/PI3K inhibitors include NVP-BEZ235, BGT226, SF1126, and PKI-587 (Table 1), and many of them are being tested in early-stage of preclinical trials.

A detailed list of mTOR inhibitor drugs is provided in Table 1, together with specific information on their molecular properties (including *in vitro* mTOR IC50 and cellular potency towards mTORC1 and mTORC2). Dual mTORC1/mTORC2 inhibitors have been developed by counterscreening their inhibitory activity against the most closely related kinases, class I and class III PI3K lipid kinases and the PI3K-related kinase (PIKK) family members [42], whereas dual PI3K/mTORC inhibitors were optimized to inhibit class I PI3Ks [43]. Thus, the *in vitro* inhibitory potency against class I PI3Ks has been also included in Table 1. As far as the ATP-competitive mTOR inhibitors (first generation and second generation) are concerned, we calculated the ratio between PI3K and mTOR IC50 and marked those drugs with a ratio <500 since inhibition of PI3K by these drugs may become relevant in cellular or *in vivo* systems. This information should provide the reader with a better understanding of the biological effects of these novel drugs.

4. mTOR in the Control of Chronic Pain

4.1. Histology. The expression and activity of mTOR have been extensively detected in peripheral and in central regions involved in pain transmission, both under physiological conditions and in several experimental models of inflammatory and neuropathic pain. In the adult rat and mouse cutaneous tissue, mTOR immunoreactivity was found in a subset of primary sensory axons and in nonneuronal cells surrounding the peripheral axons in the dermis [44, 45]. Using specific markers that distinguish between C- and A-fibers, it has been shown that mTOR positive axons are mainly myelinated A-fibers, and only less than 5% are peptidergic fibers, coexpressing CGRP. Interestingly, these fibers were stained also for the active form of mTOR, evaluated by measurement of mTOR phosphorylation at Ser_{2448}. This phosphorylation primarily reflects a feedback signal from the mTORC1 downstream target S6K1 (also known as p70S6 kinase, p70S6K), and it is therefore considered a reliable marker of mTORC1 activation within the cells [46]. Moreover, myelinated sensory fibers in the rat skin also express phosphorylated downstream targets of mTORC1, including 4E-BP1, S6K, and the S6 ribosomal protein [44], suggesting that mTORC1 may regulate local protein synthesis within these axons thus contributing to their nociceptive functions under physiological conditions. These fibers, particularly the large A-beta (Aβ) fibers, are normally involved in the conduction of nonnociceptive inputs such as light touch, movement, or vibration [47]. However, amplification of their signals by sensitized dorsal horn

Table 1: mTOR inhibitor drugs.

Classes	Drugs	mTOR (*in vitro* kinase IC50)	mTORC1 (cellular potency EC50)	mTORC2 (cellular potency EC50)	Class I PI3K (*in vitro* kinase IC50)	References
	Rapamycin	1.74 μM (2 nM[1], in presence of FKBP12)	0.4–3.5 nM[2]			[82–84]
Rapalogs	RAD001		0.4–3.5 nM[2]			[82]
	CCI-779	1.76 μM	<20 nM	10–20 μM		[84]
	AP23573		0.2 nM			[85]
ATP-competitive mTOR inhibitors (*first generation*)	KU-0063794	2.5 nM[1]	660 nM[3]	240 nM[3]	>5.3–>30 μM	[86–88]
	PP242[4]	8 nM		300–400 nM	0.10–2.2 μM	[89, 90]
	PP30[4]	80 nM			0.68–5.8 μM	[89]
	Torin 1[4]	4.3 nM	2–10 nM	2–10 nM	0.17–>10 μM	[90, 91]
	WEY-600[4]	9 nM[1]	300 nM	1 μM	1.96–8.45 μM	[92]
	WYE-354[4]	5 nM[1]	300 nM	1 μM	1.89–7.37 μM	[92]
	CC214-1	2 nM	40 nM	18 nM	1.38 μM	[93]
	OSI-027[4]	4 nM			0.42–>30 μM	[94]
	X-387[4]	23 nM[1]			0.12–>0.3 μM	[95]
ATP-competitive mTOR inhibitors (*second generation*)	AZ8055	0.13 nM[1]	27 nM[3]	24 nM[3]	3.2–18.9 μM	[42, 88]
	AZ2014	2.8 nM[1]	200 nM[3]	80 nM[3]	3.8–>30 μM	[88]
	INK128/MLN0128[4]	1 nM	<10 nM	<10 nM	0.22–5.29 μM	[96]
	WYE-125132	0.19 nM[1]	20 nM	200 nM	1.18–>10 μM	[97]
	CC214-2	106 nM	386 nM	315 nM	>30 μM	[93]
ATP-competitive mTOR/PI3K dual inhibitors	Wortmannin	0.2 μM[1]			0.1 nM	[83, 98]
	LY294002/SF1101[5]	1.5 μM[1]			0.5–1.6 μM	[83, 99–101]
	PI-103[5]		*In vitro* kinase IC50: 20 nM	*In vitro* kinase IC50: 83 nM	2–15 nM	[40, 100, 101]
	Torin 2	2.81 nM	0.25 nM	10 nM	4.68–17.5 nM	[102, 103]
	GSK2126458	ND	Low nM	0.18–0.41 nM	0.04 nM	[104]
	NVP-BEZ235[5]	20.7 nM	<250 nM	8 nM	4–75 nM	[43, 101]
	NVP-BGT226[6]				4–63 nM	[105]
	SF1126 (RDGS conjugated SF1101)				Not significant inhibitory activity until hydrolyzed to SF1101	[106]
	PKI587	1.4 nM[1]	<30 nM	<10 nM	0.6–8 nM	[107]

In vitro mTOR kinase IC50 was evaluated using either the immunoprecipitated or the recombinant full length enzyme. Cellular potency for the two different mTOR complexes was calculated after short term incubation, ranging between 30 min and 2 h, of different cell lines with mTOR inhibitors and subsequent analysis of the phosphorylation status of specific mTORC1 (S6K or S6) or mTORC2 (AKT, at Ser_{473}) substrates. *In vitro* PI3K and PIKK IC50 were measured using specific biochemical assays.

[1]A truncated mTOR enzyme was used in the *in vitro* kinase assay.

[2]Cellular potency was evaluated by inhibition of cell proliferation, using vascular smooth muscle cells stimulated by fetal calf serum.

[3]Cellular potency was evaluated using a high throughput immunocytochemical assay, carried out in the MDA-MB-468 cell line.

[4]Ratio between PI3K and mTOR IC50 is <500.

[5]The reader should also consider IC50 values reported by Hayakawa et al., 2007 [99], and Kong et al., 2009 [101].

[6]NVP-226 is considered a dual mTOR/PI3K inhibitor. However, *in vitro* preclinical data on the mTOR inhibitory activity for this compound were not found through Medline Search.

neurons is thought to account for secondary hyperalgesia and allodynia, clinical features of chronic pain (as summarized in Section 1). Consistently, active mTORC1 and its downstream phosphorylated targets (4E-BP1 and the S6 ribosomal protein) have been also detected in the adult rat dorsal roots, mostly in myelinated axons [48]. Local or intrathecal administration of rapamycin significantly reduced phosphorylation of downstream targets of mTORC1 both in the peripheral fibers [44] and in the central spinal cord neurons [48]. Similarly to these data, phospho-mTOR was also found to be expressed by a subset of myelinated fibers in the adult mouse dorsal roots [45], whereas, in rat dorsal root ganglia (DRG), positive immunoreactivity for mTOR and S6K1 was detected mainly in the cell body of small nociceptors, coexpressing

substance P or IB4 positive [49]. These data suggest that mTOR and its downstream targets are mostly transported to myelinated peripheral and central fibers in the medium and large (but not small) DRG neurons [44, 48]. In addition, at the DRG level, a predominant expression of 4E-BP1 has been detected in GFAP positive satellite cells [49]. Satellite cells are specialized glial cells that surround the cell body of sensory neurons both in DRG and in trigeminal ganglia and, like central glia, are involved in the development of chronic pain [50]. Studies from our laboratory have shown that satellite glial cells contribute to neuronal sensitization of trigeminal neurons *in vitro* [51] and that they can express functional CGRP receptors which increase the stimulatory effects of cytokines [52]. Finally, Xu et al. [49] have documented the expression of mTOR and mTORC1 downstream targets in the dorsal horn of rat spinal cord.However, these authors failed to detect the phosphorylated proteins both at the DRG and spinal cord level. On the other hand, Géranton et al. [48], using a tyramide signal amplification- (TSA-) enhanced immunofluorescent staining, demonstrated that phospho-mTOR, phospho-S6 ribosomal protein, and phospho-4E-BP1 are strongly expressed in lamina I/III projection neurons of the dorsal horn, that is, those neurons critically involved in the development and maintenance of chronic pain [53].

Consistently with a possible involvement of mTOR in chronic pain processes, it has been shown that peripheral inflammation increases mTOR activation in the spinal cord dorsal horn. In particular, intraplantar injection of capsaicin significantly increased the phosphorylation level of the S6 ribosomal protein after 2 h in the dorsal horn neurons, an effect abolished by intrathecal administration of rapamycin [48]. Intraplantar injection of carrageenan increased the magnitude of S6 phosphorylation in the ipsilateral spinal cord dorsal horn but not in the contralateral one, 4 h after treatment. In these animals, phospho-S6 together with Rheb, the positive regulator of mTOR activity, was mainly detected in neurons, but not in spinal glia (astrocytes and microglia). Moreover, basal S6 activity was also detected in larger motor neurons in the ventral horn, but it was not modified by carrageenan peripheral administration [54]. Finally, peripheral inflammation due to intraplantar injection of complete Freund's adjuvant significantly increased mTOR activation in DRG neurons, with a minor increase observed in spinal cord dorsal horn [55]. Enhanced activation of the mTOR pathway was also found in different experimental models of neuropathic pain. In adult male rat undergoing L5-L6 spinal nerve ligation (SNL), increased phospho-mTOR staining was detected in sensory neurons mainly in myelinated fibers of injured nerves [56]. However, Asante et al. [57] in the same model measured reduced levels of CGRP and S6K1 in the superficial dorsal horn neurons, just at the ligated L5-L6 nerves, but not in the uninjured L4 spinal cord. Increased mTOR activation was instead found in a mouse model of chronic crush injury (CCI) at the spinal cord level, and it was significantly reduced by intrathecal administration of rapamycin. In particular, rapamycin reduced phospho-mTOR expression at 7 and 14 days after surgery, together with significant reduction of the phosphorylation level of S6K1 and 4E-BP1 at 7 (but not 14) days after surgery [58]. In contrast, no differences in the level of mTOR activation were detected in the spinal cord dorsal horn 7 days after surgery, in a different model of neuropathic pain induced by spared nerve injury (SNI) of the sciatic nerve [48]. All together these data suggest that mTORC1 activity is significantly elevated in dorsal horn neurons in different models of chronic pain (even tough not in all models), thus suggesting a possible involvement in mediating central neuronal plasticity and thus pain hypersensitivity. In support of this hypothesis, a recent paper by Xu et al. [59] has demonstrated increased mTORC1 activation in the spinal cord dorsal horn (at the lumbar level, but not at cervical and thoracic level) in a rat model of morphine induced tolerance and hyperalgesia, thus suggesting that the reduced analgesic effects of morphine observed in long-term treatments may be due to the upregulation of mTORC1 activity within the spinal cord. It is, therefore, possible that inhibition of mTORC1 activity may have beneficial effects in chronic pain syndromes.

4.2. Electrophysiology. In addition to these data, there is also consistent electrophysiological evidence which point out mTOR signaling pathways as important modulators of chronic pain [44, 57, 60]. The electrophysiological analysis conducted by Jiménez-Díaz et al. [44] revealed an increased mechanical threshold of subsets of myelinated fibers, the A-fiber nociceptors, after intraplantar injection of rapamycin, following capsaicin induced injury in rats. The authors proposed that ongoing local protein synthesis is essential for the complete response of this subset of nociceptors and were pioneers in supposing the possibility that a similar process is operating at the sites of termination of sensory afferents within the dorsal horn [44]. The role of mTOR in the neuron injury-induced hyperexcitability was demonstrated later in a study conducted by Asante et al., in which rapamycin (50 μL of 250 nM), directly applied on the spinal cord at L4-L5 level, was found to produce inhibitory effects on nociceptive C-fiber activity in lamina V wide dynamic range (WDR) neurons, in response to mechanically and thermally stimulus in rats after removal of lumbar vertebral segments L1–L3 of the spinal cord [60]. For the thermally induced response, a significant inhibition was only found at 35°C, with a trend towards reduction at higher temperatures. Also formalin-induced hyperexcitability was attenuated by spinally administered rapamycin, with significant effects only in the second phase of formalin test, which is thought to be due to central sensitization of dorsal horn neurons as a result of the initial attenuation of input from nociceptive C-fiber afferents occurring during the first phase. The same authors demonstrated similar effects of anisomycin, a general inhibitor of protein translation, on the formalin test, confirming that these effects were indeed due to inhibition of mRNA translation [60]. In a second paper, Asante et al. demonstrated the spinal effects of the rapamycin analogue CCI-779 on neuronal responses by using *in vivo* single-unit extracellular recordings from spinal cord neurons of rats following L5-L6 SNL [57]. The authors found that spinal administration of 250 μM CCI-779 significantly attenuated specific neuronal responses to mechanical stimuli from SNL rats compared

to predrug responses and sham rats, whereas no effect was established on thermally evoked responses. In particular, CCI-779 inhibited C-fiber-mediated transmission onto WDR neurons. A further significant inhibitory effect was seen on WDR neuronal postdischarge and on "wind-up" phenomenon, a potentiated response mediated by nociceptive C-fibers activity and a measure of central hypersensitivity mechanisms. The limitation of this study is represented by the fact that no differences in electrophysiological responses were found between sham and neuropathic rats before drug injection. The authors stated that the increased excitability of L4 WDR neurons in neuropathic rats could have masked the adjacent L5 ligation, according to a previous study in which periphery connected spinal neurons were shown to expand their receptive fields after the same nerve ligation [61]. The observation that CCI-779 was quite ineffective on neuronal responses in the absence of nerve injury [57] allows to confirm that mTOR signaling at the spinal level is an integral element of nociception and that its role in central sensitization likely contributes to the persistence of pain.

4.3. Behavioral Studies. The antinociceptive effects of rapamycin and its analogous CCI-779 (thus mTOR inhibition) have been documented in several experimental models of inflammatory and neuropathic pain. Using the formalin test, it has been shown that rapamycin (administered both intrathecally or locally in the paw) significantly reduced the second phase of behavioral pain in mice [62]. Similarly, in adult rats, intrathecal administration of rapamycin produced a significant inhibition of formalin-induced second phase flinches [63]. The formalin test is a well-characterized behavioral model of chemically induced pain consisting of two consecutive pain behavior phases, of which the second one has been suggested to involve central sensitization of the nociceptive system [64], thus suggesting an involvement of spinal mTOR in inflammation induced hyperalgesia. On the other hand, rapamycin, injected directly through the skin at L5-L6 spinal cord level 30 minutes before the formalin test, was shown to significantly reduce both pain behavioral phases of the formalin test in adult rats, indicating an involvement of mTOR in peripheral sensitization as well [60]. A possible role of mTOR kinase (and thus local protein translation) in mediating both peripheral and central neuronal sensitization is also suggested by other studies based on different models of inflammatory pain. Inflammatory pain can be induced by intradermal injection of other nociceptive and algogenic substances including capsaicin, carrageenan, and the complete Freund's adjuvant (CFA) [64]. For example, the injection of capsaicin produces both peripheral sensitization of C- and Aδ-nociceptors and central sensitization of dorsal horn neurons [48]. The hallmark of peripheral sensitization is represented by increased thermal sensitivity, most likely supported by ERK activation in the cell body of nociceptors followed by synthesis of TRPV1 receptors and their transport to the axon terminals in the inflamed cutaneous tissue, whereas increased mechanical sensitivity is mainly due to central sensitization of spinal cord neurons [65]. In this experimental model (in adult rats), rapamycin administered either centrally or locally significantly reduced mechanical hyperalgesia without affecting thermal hypersensitivity in adult rats [44, 48]. In a similar manner, local and central injection of CCI-779 reduced mechanical hyperalgesia, but not thermal hypersensitivity developing in response to intradermal injection of carrageenan in adult mice [45]. The mechanical hypersensitivity that occurs in the undamaged area surrounding the site of injury, in these models, is known to be mostly transmitted by A-fibers and amplified by sensitized dorsal horn neurons.

In this regard, electromyographic studies have shown that both local and intrathecal injection of rapamycin significantly increased threshold temperatures for paw withdrawal evoked by fast heat ramps (activating A-fiber nociceptors) compared to control injections of vehicle, thus suggesting a direct effect on this subset of myelinated nociceptors known to be important for the increased mechanical sensitivity that follows injury [44, 48]. However, intrathecal injections of rapamycin inhibited the activation of downstream targets of mTOR in dorsal horn and dorsal roots, thus suggesting a modulatory effect on both primary afferents and central neurons [48]. Consistently with these observations, centrally administered rapamycin was shown to reduce mechanical allodynia in several models of inflammatory pain [54, 55, 59]. However, these studies reported variable effects on thermal sensitivity, with inhibitory effects observed after intraplantar injections of carrageenan [54, 63], and minor albeit significant reductions of thermal hyperalgesia induced by intraplantar injection of CFA [55]. Considering that the expression of mTOR and other components of the translational machinery has not been detected in C-nociceptors, these results further suggest a direct role of spinal mTOR in the modulation of central pain processing. Interestingly, the PI3K inhibitor, wortmannin, was more effective at reducing pain hypersensitivity in response to carrageenan, thus suggesting the involvement of other pathways (including ERK) in the development of central sensitization [63]. Moreover, intradermal injection of carrageenan increased the phosphorylation level of AKT at Ser_{473} in the dorsal horn of spinal cord thus suggesting a concomitant activation of mTORC2 in parallel with development of hyperalgesia in response to peripheral inflammation [63]. Therefore, wortmannin by inhibiting PI3K can simultaneously affect both mTOR complexes and other signaling pathways (including ERK; as described in Sections 2 and 3) potentially important in mediating peripheral and central sensitization thus resulting more effective than rapamycin in chronic pain.

mTOR inhibitors also display beneficial effects in several models of neuropathic pain, which are also characterized by the development of secondary hyperalgesia. In summary, intraplantar or intrathecal administration of rapamycin significantly reduced mechanical allodynia developing after SNI in rats [44, 48]. This model consists in a tightly ligation followed by distal sectioning of the common peroneal and tibial branches of the sciatic nerve, with preservation of the sural nerve. It is characterized by increased mechanical sensitivity observed 6 days after surgery in the spared sural territory, that is, the lateral part of the hind paw [44, 48]. Similarly in mice, intraplantar or intraperitoneal injection of CCI-779

significantly reduced mechanical allodynia observed in the lateral part of the hind paw three days after surgery [45]. Interestingly, in this study, the authors also evaluated the effect of repeated administration of CCI-779 (4 injections every 24 hours) observing a persistent reduction in mechanical allodynia which was gradually lost 48 hours after the last administration [45]. Moreover, in agreement with a possible role of mTORC2 in mediating central neuronal plasticity, the dual mTOR inhibitor Torin 1 appeared to be more effective than rapamycin in this experimental model, either after one injection or after repeated administrations [45]. Interestingly, daily administration of metformin (which also inhibits mTOR by promoting AMPK activation (see Section 2)) reduced mechanical allodynia in a mouse model of SNI [56]. In addition to these data, mTOR inhibitors were found to exert beneficial effects in other models of neuropathic pain. For example, CCI-779 or metformin significantly reduced mechanical allodynia in a model of persistent pain caused by SNL [56, 57], and rapamycin reduced mechanical hypersensitivity in mouse models of CCI [58, 66]. In agreement with these observations, Cui et al. have shown, using adult female Sprague Dawley, which chronic (14 days) intrathecal administration of rapamycin reduced both the mechanical allodynia and the thermal hypersensitivity induced by CCI [67]. However, variable effects of rapamycin on thermal sensitivity have been reported in this experimental model as well [58], suggesting a main role of mTOR in the regulation of central sensitization. Notably, peripheral nerve injury can induce a different spectrum of glial (both microglia and astrocytes) activation in the dorsal horn of the spinal cord. These cells can release inflammatory and pronociceptive mediators, thus significantly contributing to neuronal sensitization and to the establishment of chronic pain syndromes [5]. Recent experimental evidence from our group and others suggest a direct role of mTOR in the regulation of glial inflammatory responses and a potential beneficial role of rapamycin in neuroinflammatory based diseases [8], including chronic pain syndromes. In fact, rapamycin (centrally administered) reduced CCI induced astrogliosis [67] but did not modify microglial activation when injected peripherally in the affected hind paw [66]. These data suggest that rapamycin may have multiple cellular and molecular targets that can contribute to the therapeutic effects observed *in vivo*. In this regard, Marinelli et al. have demonstrated the critical role of autophagy, particularly in Schwann cells (SCs), in reducing neuronal damage, clearing myelin debris, and facilitating neuronal regeneration after injury [66]. In these animals, rapamycin significantly increased the autophagic flux in SCs, their proliferation, and improved myelination in injured nerves [66]. Consistently, rapamycin improved myelination in explant cultures from neuropathic mice by activating autophagic mechanisms [68]. However, mice lacking mTOR in SCs display hypomyelinated sciatic nerves [69], further underlying the relevance of the mTOR pathway in the regulation of myelination in both peripheral and central nervous system [70, 71].

In this field, recent evidence from our group suggests that mTOR inhibitors can reduce signs of neuropathic pain in a chronic model of a demyelinating disease, the experimental autoimmune encephalomyelitis (EAE). We have shown that chronic administration of rapamycin was able to increase the sensitivity threshold for mechanical allodynia, which is usually reduced at the clinical onset of disease [72]. In this study, we observed that rapamycin ameliorates clinical and histological signs of EAE when administered to already ill animals, at the peak of disease (therapeutic approach). Interestingly, the histological study of the brains at the end of the experiment revealed a significant improvement in the myelination of the corpus callosum in the rapamycin treated animals, which may be the consequence of reduced neuroinflammation as well as a direct effect of rapamycin [72]. In addition, rapamycin was also found beneficial in a mouse model of cancer metastatic pain. In fact, repeated treatment with rapamycin reduced both thermal and mechanical hypersensitivity developing in response to intratibial injection of prostate cancer cells. In this model of chronic cancer pain, rapamycin was also effective when administered in a therapeutic manner, that is, once daily 5 days after injection of cancer cells within the tibia [73]. Rapamycin was also effective in a similar model of metastatic cancer pain induced by intratibial inoculation of breast cancer cells [74]. Finally, rapamycin reduced hyperalgesia associated with chronic administration of morphine in rats [59], thus further supporting a potential clinical use of mTOR inhibitors in the management of chronic pain syndromes.

4.4. Preclinical and Clinical Evidence of a Pronociceptive Role for mTOR Inhibitors. Despite the promising results from the preclinical studies reviewed above, the role of rapamycin and rapalogs in the clinical treatment of chronic pain is undermined by the clinical evidence that chronic treatment of patients with these mTORC1 inhibitors is associated with increases in the incidence of pain [75, 76], including the possible development of complex regional pain syndrome (CRPS) [77]. In addition, the anticancer agents, RAD001 or AP23573, are associated with a number of unique toxicities, with one of the most significant being the so-called painful mTOR inhibitor-associated stomatitis (mIAS) [78]. However, mechanistic data are lacking concerning whether and how rapalogs are linked to the development of pain in patients chronically treated with these drugs; hence more and appropriate clinical studies are necessary to clarify this important issue. In this regard, the only preclinical study carried out in C57bl/6 mice that show possible negative effects of long-term mTOR inhibition with respect to pain hypersensitivity is a recent paper from Melemedjian et al. [79]. These authors demonstrated that chronic rapamycin treatment (intraperitoneally injected for 9 days) induced mechanical allodynia in sham-operated animals, while reducing mechanical hypersensitivity in SNL animals in agreement with data reviewed in Section 4.3. Similarly, rapamycin partially reversed mechanical allodynia in mice with SNI, while producing mechanical allodynia in sham animals. Chronic administration of rapamycin appeared to increase ERK and AKT phosphorylation in sham animal sciatic nerves, thus suggesting that the abrogation of the negative feedback loops on these other pathways due to the incomplete blocking of mTORC1 (see Sections 2 and 3)

may cause activation of other signaling pathways responsible for pain development [79]. For example, increased ERK activity can induce sensory neuron sensitization, mechanical hypersensitivity, and spontaneous pain. Interestingly, the clinically available antidiabetic drug metformin, which is also a AMPK activator thus mTOR inhibitor (see above), prevents rapamycin-induced ERK activation and the development of mechanical hypersensitivity and spontaneous pain [79]. These data suggest that a more complete inhibition of the mTOR pathway can overcome these side effects of rapamycin and its analogs. In this regard, in a retrospective study conducted on diabetic patients, the use of metformin has been found significantly associated with reduction of pain symptoms in patients affected by lumbar radiculopathy, a very frequent form of chronic pain syndrome [80, 81].

5. Conclusions

Data presented in this review paper strongly suggest that mTOR has a critical role in several mechanism of pain processing, including a role in the development of chronic pain. However, clinical evidence suggests that chronic use of first generation mTOR inhibitors may be associated with development of pain hypersensitivity, thus underlying the involvement of other signaling pathways including PI3K downstream effectors (ERK, AKT, and more interestingly mTORC2). A more comprehensive understanding of these signaling pathways may lead to improved treatments for the management of chronic pain. A vast array of novel inhibitors, with a broader range of activity, is becoming available for clinical testing. These have been mostly developed for cancer treatment, but may also be employed in the management of chronic pain.

Conflict of Interests

The authors declare that there is no conflict of interests regarding the publication of this paper.

References

[1] P. A. Pizzo and N. M. Clark, "Alleviating suffering 101—pain relief in the United States," *The New England Journal of Medicine*, vol. 366, no. 3, pp. 197–199, 2012.

[2] S. P. Cohen and J. Mao, "Neuropathic pain: mechanisms and their clinical implications," *British Medical Journal*, vol. 348, Article ID f7656, 2014.

[3] A. Latremoliere and C. J. Woolf, "Central sensitization: a generator of pain hypersensitivity by central neural plasticity," *Journal of Pain*, vol. 10, no. 9, pp. 895–926, 2009.

[4] B. Xu, G. Descalzi, H.-R. Ye, M. Zhuo, and Y.-W. Wang, "Translational investigation and treatment of neuropathic pain," *Molecular Pain*, vol. 8, article 15, 2012.

[5] P. M. Grace, M. R. Hutchinson, S. F. Maier, and L. R. Watkins, "Pathological pain and the neuroimmune interface," *Nature Reviews Immunology*, vol. 14, no. 4, pp. 217–231, 2014.

[6] C. Voscopoulos and M. Lema, "When does acute pain become chronic?" *British Journal of Anaesthesia*, vol. 105, supplement 1, pp. i69–i85, 2010.

[7] C. A. Hoeffer and E. Klann, "mTOR signaling: at the crossroads of plasticity, memory and disease," *Trends in Neurosciences*, vol. 33, no. 2, pp. 67–75, 2010.

[8] C. D. Russo, L. Lisi, D. L. Feinstein, and P. Navarra, "mTOR kinase, a key player in the regulation of glial functions: relevance for the therapy of multiple sclerosis," *Glia*, vol. 61, no. 3, pp. 301–311, 2013.

[9] S. Wullschleger, R. Loewith, and M. N. Hall, "TOR signaling in growth and metabolism," *Cell*, vol. 124, no. 3, pp. 471–484, 2006.

[10] N. Hay and N. Sonenberg, "Upstream and downstream of mTOR," *Genes and Development*, vol. 18, no. 16, pp. 1926–1945, 2004.

[11] D. D. Sarbassov, S. M. Ali, S. Sengupta et al., "Prolonged rapamycin treatment inhibits mTORC2 assembly and Akt/PKB," *Molecular Cell*, vol. 22, no. 2, pp. 159–168, 2006.

[12] M. Laplante and D. M. Sabatini, "MTOR signaling in growth control and disease," *Cell*, vol. 149, no. 2, pp. 274–293, 2012.

[13] D. A. Guertin, D. M. Stevens, C. C. Thoreen et al., "Ablation in mice of the mTORC components raptor, rictor, or mLST8 reveals that mTORC2 is required for signaling to Akt-FOXO and PKCα, but Not S6K1," *Developmental Cell*, vol. 11, no. 6, pp. 859–871, 2006.

[14] S. Sengupta, T. R. Peterson, and D. M. Sabatini, "Regulation of the mTOR complex 1 pathway by nutrients, growth factors, and stress," *Molecular Cell*, vol. 40, no. 2, pp. 310–322, 2010.

[15] K. Hara, Y. Maruki, X. Long et al., "Raptor, a binding partner of target of rapamycin (TOR), mediates TOR action," *Cell*, vol. 110, no. 2, pp. 177–189, 2002.

[16] D.-H. Kim, D. D. Sarbassov, S. M. Ali et al., "mTOR interacts with raptor to form a nutrient-sensitive complex that signals to the cell growth machinery," *Cell*, vol. 110, no. 2, pp. 163–175, 2002.

[17] C. A. Sparks and D. A. Guertin, "Targeting mTOR: prospects for mTOR complex 2 inhibitors in cancer therapy," *Oncogene*, vol. 29, no. 26, pp. 3733–3744, 2010.

[18] J. Huang and B. D. Manning, "The TSC1-TSC2 complex: a molecular switchboard controlling cell growth," *Biochemical Journal*, vol. 412, no. 2, pp. 179–190, 2008.

[19] E. Kim, P. Goraksha-Hicks, L. Li, T. P. Neufeld, and K.-L. Guan, "Regulation of TORC1 by Rag GTPases in nutrient response," *Nature Cell Biology*, vol. 10, no. 8, pp. 935–945, 2008.

[20] Y. Sancak, L. Bar-Peled, R. Zoncu, A. L. Markhard, S. Nada, and D. M. Sabatini, "Ragulator-rag complex targets mTORC1 to the lysosomal surface and is necessary for its activation by amino acids," *Cell*, vol. 141, no. 2, pp. 290–303, 2010.

[21] T. Brummer, C. Schmitz-Peiffer, and R. J. Daly, "Docking proteins," *FEBS Journal*, vol. 277, no. 21, pp. 4356–4369, 2010.

[22] K. Düvel, J. L. Yecies, S. Menon et al., "Activation of a metabolic gene regulatory network downstream of mTOR complex 1," *Molecular Cell*, vol. 39, no. 2, pp. 171–183, 2010.

[23] R. C. Hresko and M. Mueckler, "mTOR·RICTOR is the Ser^{473} kinase for Akt/protein kinase B in 3T3-L1 adipocytes," *The Journal of Biological Chemistry*, vol. 280, no. 49, pp. 40406–40416, 2005.

[24] D. D. Sarbassov, D. A. Guertin, S. M. Ali, and D. M. Sabatini, "Phosphorylation and regulation of Akt/PKB by the rictor-mTOR complex," *Science*, vol. 307, no. 5712, pp. 1098–1101, 2005.

[25] P. Liu, J. Guo, W. Gan, and W. Wei, "Dual phosphorylation of Sin1 at T86 and T398 negatively regulates mTORC2 complex integrity and activity," *Protein and Cell*, vol. 5, no. 3, pp. 171–177, 2014.

[26] J. M. García-Martínez and D. R. Alessi, "mTOR complex 2 (mTORC2) controls hydrophobic motif phosphorylation and activation of serum- and glucocorticoid-induced protein kinase 1 (SGK1)," *Biochemical Journal*, vol. 416, no. 3, pp. 375–385, 2008.

[27] E. Jacinto, R. Loewith, A. Schmidt et al., "Mammalian TOR complex 2 controls the actin cytoskeleton and is rapamycin insensitive," *Nature Cell Biology*, vol. 6, no. 11, pp. 1122–1128, 2004.

[28] S. M. Ali, D.-H. Kim, D. A. Guertin et al., "Rictor, a novel binding partner of mTOR, defines a rapamycin-insensitive and raptor-independent pathway that regulates the cytoskeleton," *Current Biology*, vol. 14, no. 14, pp. 1296–1302, 2004.

[29] P. B. Dennis, S. Fumagalli, and G. Thomas, "Target of rapamycin (TOR): balancing the opposing forces of protein synthesis and degradation," *Current Opinion in Genetics and Development*, vol. 9, no. 1, pp. 49–54, 1999.

[30] P. A. Kelly, S. A. Gruber, F. Behbod, and B. D. Kahan, "Sirolimus, a new, potent immunosuppressive agent," *Pharmacotherapy*, vol. 17, no. 6, pp. 1148–1156, 1997.

[31] C. M. Hartford and M. J. Ratain, "Rapamycin: something old, something new, sometimes borrowed and now renewed," *Clinical Pharmacology and Therapeutics*, vol. 82, no. 4, pp. 381–388, 2007.

[32] C. K. Yip, K. Murata, T. Walz, D. M. Sabatini, and S. A. Kang, "Structure of the human mTOR complex I and its implications for rapamycin inhibition," *Molecular Cell*, vol. 38, no. 5, pp. 768–774, 2010.

[33] C. C. Thoreen and D. M. Sabatini, "Rapamycin inhibits mTORC1, but not completely," *Autophagy*, vol. 5, no. 5, pp. 725–726, 2009.

[34] K. Pong and M. M. Zaleska, "Therapeutic implications for immunophilin ligands in the treatment of neurodegenerative diseases," *Current Drug Targets: CNS and Neurological Disorders*, vol. 2, no. 6, pp. 349–356, 2003.

[35] F. Stenner-Liewen, V. Grünwald, R. Greil, and C. Porta, "The clinical potential of temsirolimus in second or later lines of treatment for metastatic renal cell carcinoma," *Expert Review of Anticancer Therapy*, vol. 13, no. 9, pp. 1021–1033, 2013.

[36] M. P. Curran, "Everolimus: in patients with subependymal giant cell astrocytoma associated with tuberous sclerosis complex," *Pediatric Drugs*, vol. 14, no. 1, pp. 51–60, 2012.

[37] J. Huang, C. C. Dibble, M. Matsuzaki, and B. D. Manning, "The TSC1-TSC2 complex is required for proper activation of mTOR complex 2," *Molecular and Cellular Biology*, vol. 28, no. 12, pp. 4104–4115, 2008.

[38] D. Benjamin, M. Colombi, C. Moroni, and M. N. Hall, "Rapamycin passes the torch: a new generation of mTOR inhibitors," *Nature Reviews Drug Discovery*, vol. 10, no. 11, pp. 868–880, 2011.

[39] S. A. Wander, B. T. Hennessy, and J. M. Slingerland, "Next-generation mTOR inhibitors in clinical oncology: how pathway complexity informs therapeutic strategy," *Journal of Clinical Investigation*, vol. 121, no. 4, pp. 1231–1241, 2011.

[40] Z. A. Knight, B. Gonzalez, M. E. Feldman et al., "A pharmacological map of the PI3-K family defines a role for p110α in insulin signaling," *Cell*, vol. 125, no. 4, pp. 733–747, 2006.

[41] S. Schenone, C. Brullo, F. Musumeci, M. Radi, and M. Botta, "ATP-competitive inhibitors of mTOR: an update," *Current Medicinal Chemistry*, vol. 18, no. 20, pp. 2995–3014, 2011.

[42] C. M. Chresta, B. R. Davies, I. Hickson et al., "AZD8055 is a potent, selective, and orally bioavailable ATP-competitive mammalian target of rapamycin kinase inhibitor with *in vitro* and *in vivo* antitumor activity," *Cancer Research*, vol. 70, no. 1, pp. 288–298, 2010.

[43] S.-M. Maira, F. Stauffer, J. Brueggen et al., "Identification and characterization of NVP-BEZ235, a new orally available dual phosphatidylinositol 3-kinase/mammalian target of rapamycin inhibitor with potent in vivo antitumor activity," *Molecular Cancer Therapeutics*, vol. 7, no. 7, pp. 1851–1863, 2008.

[44] L. Jiménez-Díaz, S. M. Géranton, G. M. Passmore et al., "Local translation in primary afferent fibers regulates nociception," *PLoS ONE*, vol. 3, no. 4, Article ID e1961, 2008.

[45] I. Obara, K. K. Tochiki, S. M. Géranton et al., "Systemic inhibition of the mammalian target of rapamycin (mTOR) pathway reduces neuropathic pain in mice," *Pain*, vol. 152, no. 11, pp. 2582–2595, 2011.

[46] G. G. Chiang and R. T. Abraham, "Phosphorylation of mammalian target of rapamycin (mTOR) at Ser-2448 is mediated by p70S6 kinase," *Journal of Biological Chemistry*, vol. 280, no. 27, pp. 25485–25490, 2005.

[47] V. Gangadharan and R. Kuner, "Pain hypersensitivity mechanisms at a glance," *DMM Disease Models and Mechanisms*, vol. 6, no. 4, pp. 889–895, 2013.

[48] S. M. Géranton, L. Jiménez-Díaz, C. Torsney et al., "A rapamycin-sensitive signaling pathway is essential for the full expression of persistent pain states," *Journal of Neuroscience*, vol. 29, no. 47, pp. 15017–15027, 2009.

[49] J.-T. Xu, X. Zhao, M. Yaster, and Y.-X. Tao, "Expression and distribution of mTOR, p70S6K, 4E-BP1, and their phosphorylated counterparts in rat dorsal root ganglion and spinal cord dorsal horn," *Brain Research*, vol. 1336, pp. 46–57, 2010.

[50] M. Hanani, "Intercellular communication in sensory ganglia by purinergic receptors and gap junctions: implications for chronic pain," *Brain Research*, vol. 1487, pp. 183–191, 2012.

[51] A. Capuano, A. de Corato, L. Lisi, G. Tringali, P. Navarra, and C. Dello Russo, "Proinflammatory-activated trigeminal satellite cells promote neuronal sensitization: relevance for migraine pathology," *Molecular Pain*, vol. 5, article 43, 2009.

[52] A. De Corato, L. Lisi, A. Capuano et al., "Trigeminal satellite cells express functional calcitonin gene-related peptide receptors, whose activation enhances interleukin-1β pro-inflammatory effects," *Journal of Neuroimmunology*, vol. 237, no. 1-2, pp. 39–46, 2011.

[53] M. L. Nichols, B. J. Allen, S. D. Rogers et al., "Transmission of chronic nociception by spinal neurons expressing the substance P receptor," *Science*, vol. 286, no. 5444, pp. 1558–1561, 1999.

[54] E. N. Gregory, S. Codeluppi, J. A. Gregory, J. Steinauer, and C. I. Svensson, "Mammalian target of rapamycin in spinal cord neurons mediates hypersensitivity induced by peripheral inflammation," *Neuroscience*, vol. 169, no. 3, pp. 1392–1402, 2010.

[55] L. Liang, B. Tao, L. Fan, M. Yaster, Y. Zhang, and Y.-X. Tao, "mTOR and its downstream pathway are activated in the dorsal root ganglion and spinal cord after peripheral inflammation, but not after nerve injury," *Brain Research*, vol. 1513, pp. 17–25, 2013.

[56] O. K. Melemedjian, M. N. Asiedu, D. V. Tillu et al., "Targeting adenosine monophosphate-activated protein kinase (AMPK) in preclinical models reveals a potential mechanism for the treatment of neuropathic pain," *Molecular Pain*, vol. 7, article 70, 2011.

[57] C. O. Asante, V. C. Wallace, and A. H. Dickenson, "Mammalian target of rapamycin signaling in the spinal cord is required for neuronal plasticity and behavioral hypersensitivity associated

with neuropathy in the rat," *Journal of Pain*, vol. 11, no. 12, pp. 1356–1367, 2010.

[58] W. Zhang, X.-F. Sun, J.-H. Bo et al., "Activation of mTOR in the spinal cord is required for pain hypersensitivity induced by chronic constriction injury in mice," *Pharmacology Biochemistry and Behavior*, vol. 111, pp. 64–70, 2013.

[59] J.-T. Xu, J.-Y. Zhao, X. Zhao et al., "Opioid receptor-triggered spinal mTORC1 activation contributes to morphine tolerance and hyperalgesia," *The Journal of Clinical Investigation*, vol. 124, no. 2, pp. 592–603, 2014.

[60] C. O. Asante, V. C. Wallace, and A. H. Dickenson, "Formalin-induced behavioural hypersensitivity and neuronal hyperexcitability are mediated by rapid protein synthesis at the spinal level," *Molecular Pain*, vol. 5, article 27, 2009.

[61] R. Suzuki, V. K. Kontinen, E. Matthews, E. Williams, and A. H. Dickenson, "Enlargement of the receptive field size to low intensity mechanical stimulation in the rat spinal nerve ligation model of neuropathy," *Experimental Neurology*, vol. 163, no. 2, pp. 408–413, 2000.

[62] T. J. Price, M. H. Rashid, M. Millecamps, R. Sanoja, J. M. Entrena, and F. Cervero, "Decreased nociceptive sensitization in mice lacking the fragile X mental retardation protein: role of mGluR1/5 and mTOR," *Journal of Neuroscience*, vol. 27, no. 51, pp. 13958–13967, 2007.

[63] Q. Xu, B. Fitzsimmons, J. Steinauer et al., "Spinal phosphinositide 3-kinase-Akt-mammalian target of rapamycin signaling cascades in inflammation-induced hyperalgesia," *Journal of Neuroscience*, vol. 31, no. 6, pp. 2113–2124, 2011.

[64] D. Le Bars, M. Gozariu, and S. W. Cadden, "Animal models of nociception," *Pharmacological Reviews*, vol. 53, no. 4, pp. 597–652, 2001.

[65] I. Obara, S. M. Géranton, and S. P. Hunt, "Axonal protein synthesis: a potential target for pain relief?" *Current Opinion in Pharmacology*, vol. 12, no. 1, pp. 42–48, 2012.

[66] S. Marinelli, F. Nazio, A. Tinari et al., "Schwann cell autophagy counteracts the onset and chronification of neuropathic pain," *Pain*, vol. 155, no. 1, pp. 93–107, 2014.

[67] J. Cui, W. He, B. Yi et al., "mTOR pathway is involved in ADP-evoked astrocyte activation and ATP release in the spinal dorsal horn in a rat neuropathic pain model," *Neuroscience*, vol. 275, pp. 395–403, 2014.

[68] S. Rangaraju, J. D. Verrier, I. Madorsky, J. Nicks, W. A. Dunn Jr., and L. Notterpek, "Rapamycin activates autophagy and improves myelination in explant cultures from neuropathic mice," *The Journal of Neuroscience*, vol. 30, no. 34, pp. 11388–11397, 2010.

[69] D. L. Sherman, M. Krols, L.-M. N. Wu et al., "Arrest of myelination and reduced axon growth when Schwann cells lack mTOR," *Journal of Neuroscience*, vol. 32, no. 5, pp. 1817–1825, 2012.

[70] C. Norrmen and U. Suter, "Akt/mTOR signalling in myelination," *Biochemical Society Transactions*, vol. 41, no. 4, pp. 944–950, 2013.

[71] T. L. Wood, K. K. Bercury, S. E. Cifelli et al., "mTOR: a link from the extracellular milieu to transcriptional regulation of oligodendrocyte development," *ASN Neuro*, vol. 5, no. 1, Article ID e00108, 2013.

[72] L. Lisi, P. Navarra, R. Cirocchi et al., "Rapamycin reduces clinical signs and neuropathic pain in a chronic model of experimental autoimmune encephalomyelitis," *Journal of Neuroimmunology*, vol. 243, no. 1-2, pp. 43–51, 2012.

[73] M.-H. Shih, S.-C. Kao, W. Wang, M. Yaster, and Y.-X. Tao, "Spinal cord NMDA receptor-mediated activation of mammalian target of rapamycin is required for the development and maintenance of bone cancer-induced pain hypersensitivities in rats," *Journal of Pain*, vol. 13, no. 4, pp. 338–349, 2012.

[74] D. M. Abdelaziz, L. S. Stone, and S. V. Komarova, "Osteolysis and pain due to experimental bone metastases are improved by treatment with rapamycin," *Breast Cancer Research and Treatment*, vol. 143, no. 2, pp. 227–237, 2014.

[75] K. Budde, "How to use mTOR inhibitors? The search goes on," *American Journal of Transplantation*, vol. 11, no. 8, pp. 1551–1552, 2011.

[76] F. X. McCormack, Y. Inoue, J. Moss et al., "Efficacy and safety of sirolimus in lymphangioleiomyomatosis," *The New England Journal of Medicine*, vol. 364, no. 17, pp. 1595–1606, 2011.

[77] C. Massard, K. Fizazi, M. Gross-Goupil, and B. Escudier, "Reflex sympathetic dystrophy in patients with metastatic renal cell carcinoma treated with Everolimus," *Investigational New Drugs*, vol. 28, no. 6, pp. 879–881, 2010.

[78] M. A. De Oliveira, F. M. E. Martins, Q. Wang et al., "Clinical presentation and management of mTOR inhibitor-associated stomatitis," *Oral Oncology*, vol. 47, no. 10, pp. 998–1003, 2011.

[79] O. K. Melemedjian, A. Khoutorsky, R. E. Sorge et al., "MTORC1 inhibition induces pain via IRS-1-dependent feedback activation of ERK," *Pain*, vol. 154, no. 7, pp. 1080–1091, 2013.

[80] A. Taylor, A. H. Westveld, M. Szkudlinska et al., "The use of metformin is associated with decreased lumbar radiculopathy pain," *Journal of Pain Research*, vol. 6, pp. 755–763, 2013.

[81] A. Taylor, A. H. Westveld, M. Szkudlinska et al., "The use of metformin is associated with decreased lumbar radiculopathy pain [Erratum]," *Journal of Pain Research*, vol. 2014, no. 7, pp. 89–90, 2014.

[82] W. Schuler, R. Sedrani, S. Cottens et al., "SDZ RAD, a new rapamycin derivative: pharmacological properties in vitro and in vivo," *Transplantation*, vol. 64, no. 1, pp. 36–42, 1997.

[83] L. Toral-Barza, W.-G. Zhang, C. Lamison, J. LaRocque, J. Gibbons, and K. Yu, "Characterization of the cloned full-length and a truncated human target of rapamycin: activity, specificity, and enzyme inhibition as studied by a high capacity assay," *Biochemical and Biophysical Research Communications*, vol. 332, no. 1, pp. 304–310, 2005.

[84] B. Shor, W.-G. Zhang, L. Toral-Barza et al., "A new pharmacologic action of CCI-779 involves FKBP12-independent inhibition of mTOR kinase activity and profound repression of global protein synthesis," *Cancer Research*, vol. 68, no. 8, pp. 2934–2943, 2008.

[85] V. M. Rivera, R. M. Squillace, D. Miller et al., "Ridaforolimus (AP23573; MK-8669), a potent mtor inhibitor, has broad antitumor activity and can be optimally administered using intermittent dosing regimens," *Molecular Cancer Therapeutics*, vol. 10, no. 6, pp. 1059–1071, 2011.

[86] J. M. García-Martínez, J. Moran, R. G. Clarke et al., "Ku-0063794 is a specific inhibitor of the mammalian target of rapamycin (mTOR)," *Biochemical Journal*, vol. 421, no. 1, pp. 29–42, 2009.

[87] K. Malagu, H. Duggan, K. Menear et al., "The discovery and optimisation of pyrido[2,3-d]pyrimidine-2,4-diamines as potent and selective inhibitors of mTOR kinase," *Bioorganic and Medicinal Chemistry Letters*, vol. 19, no. 20, pp. 5950–5953, 2009.

[88] K. G. Pike, K. Malagu, M. G. Hummersone et al., "Optimization of potent and selective dual mTORC1 and mTORC2 inhibitors:

the discovery of AZD8055 and AZD2014," *Bioorganic & Medicinal Chemistry Letters*, vol. 23, no. 5, pp. 1212–1216, 2013.

[89] M. E. Feldman, B. Apsel, A. Uotila et al., "Active-site inhibitors of mTOR target rapamycin-resistant outputs of mTORC1 and mTORC2," *PLoS Biology*, vol. 7, no. 2, article e38, 2009.

[90] Q. Liu, S. Kirubakaran, W. Hur et al., "Kinome-wide selectivity profiling of ATP-competitive mammalian target of rapamycin (mTOR) inhibitors and characterization of their binding kinetics," *The Journal of Biological Chemistry*, vol. 287, no. 13, pp. 9742–9752, 2012.

[91] C. C. Thoreen, S. A. Kang, J. W. Chang et al., "An ATP-competitive mammalian target of rapamycin inhibitor reveals rapamycin-resistant functions of mTORC1," *The Journal of Biological Chemistry*, vol. 284, no. 12, pp. 8023–8032, 2009.

[92] K. Yu, L. Toral-Barza, C. Shi et al., "Biochemical, cellular, and *in vivo* activity of novel ATP-competitive and selective inhibitors of the mammalian target of rapamycin," *Cancer Research*, vol. 69, no. 15, pp. 6232–6240, 2009.

[93] D. S. Mortensen, J. Sapienza, B. G. S. Lee et al., "Use of core modification in the discovery of CC214-2, an orally available, selective inhibitor of mTOR kinase," *Bioorganic and Medicinal Chemistry Letters*, vol. 23, no. 6, pp. 1588–1591, 2013.

[94] S. V. Bhagwat, P. C. Gokhale, A. P. Crew et al., "Preclinical characterization of OSI-027, a potent and selective inhibitor of mTORC1 and mTORC2: distinct from rapamycin," *Molecular Cancer Therapeutics*, vol. 10, no. 8, pp. 1394–1406, 2011.

[95] S.-M. Chen, J.-L. Liu, X. Wang, C. Liang, J. Ding, and L.-H. Meng, "Inhibition of tumor cell growth, proliferation and migration by X-387, a novel active-site inhibitor of mTOR," *Biochemical Pharmacology*, vol. 83, no. 9, pp. 1183–1194, 2012.

[96] A. C. Hsieh, Y. Liu, M. P. Edlind et al., "The translational landscape of mTOR signalling steers cancer initiation and metastasis," *Nature*, vol. 485, no. 7396, pp. 55–61, 2012.

[97] K. Yu, C. Shi, L. Toral-Barza et al., "Beyond rapalog therapy: preclinical pharmacology and antitumor activity of WYE-125132, an ATP-competitive and specific inhibitor of mTORC1 and mTORC2," *Cancer Research*, vol. 70, no. 2, pp. 621–631, 2010.

[98] A. Arcaro and M. P. Wymann, "Wortmannin is a potent phosphatidylinositol 3-kinase inhibitor: the role of phosphatidylinositol 3,4,5-trisphosphate in neutrophil responses," *Biochemical Journal*, vol. 296, no. 2, pp. 297–301, 1993.

[99] M. Hayakawa, H. Kaizawa, K.-I. Kawaguchi et al., "Synthesis and biological evaluation of imidazo[1,2-a]pyridine derivatives as novel PI3 kinase p110α inhibitors," *Bioorganic and Medicinal Chemistry*, vol. 15, no. 1, pp. 403–412, 2007.

[100] F. I. Raynaud, S. Eccles, P. A. Clarke et al., "Pharmacologic characterization of a potent inhibitor of class I phosphatidylinositide 3-kinases," *Cancer Research*, vol. 67, no. 12, pp. 5840–5850, 2007.

[101] D. Kong, S.-I. Yaguchi, and T. Yamori, "Effect of ZSTK474, a novel phosphatidylinositol 3-kinase inhibitor, on DNA-dependent protein kinase," *Biological and Pharmaceutical Bulletin*, vol. 32, no. 2, pp. 297–300, 2009.

[102] Q. Liu, J. Wang, S. A. Kang et al., "Discovery of 9-(6-aminopyridin-3-yl)-1-(3-(trifluoromethyl)phenyl)benzo[h][1,6]naphthyridin-2(1 H)-one (torin2) as a potent, selective, and orally available mammalian target of rapamycin (mTOR) inhibitor for treatment of cancer," *Journal of Medicinal Chemistry*, vol. 54, no. 5, pp. 1473–1480, 2011.

[103] Q. Liu, C. Xu, S. Kirubakaran et al., "Characterization of Torin2, an ATP-competitive inhibitor of mTOR, ATM, and ATR," *Cancer Research*, vol. 73, no. 8, pp. 2574–2586, 2013.

[104] S. D. Knight, N. D. Adams, J. L. Burgess et al., "Discovery of GSK2126458, a highly potent inhibitor of PI3K and the mammalian target of rapamycin," *ACS Medicinal Chemistry Letters*, vol. 1, no. 1, pp. 39–43, 2010.

[105] B. Markman, J. Tabernero, I. Krop et al., "Phase I safety, pharmacokinetic, and pharmacodynamic study of the oral phosphatidylinositol-3-kinase and mTOR inhibitor BGT226 in patients with advanced solid tumors," *Annals of Oncology*, vol. 23, no. 9, pp. 2399–2408, 2012.

[106] J. R. Garlich, P. De, N. Dey et al., "A vascular targeted pan phosphoinositide 3-kinase inhibitor prodrug, SF1126, with antitumor and antiangiogenic activity," *Cancer Research*, vol. 68, no. 1, pp. 206–215, 2008.

[107] A. M. Venkatesan, C. M. Dehnhardt, E. D. Delos Santos et al., "Bis(morpholino-l,3,5-triazine) derivatives: potent adenosine 5'-triphosphate competitive phosphatidylinositol-3-kinase/mammalian target of rapamycin inhibitors: discovery of compound 26 (PKI-587), a highly efficacious dual inhibitor," *Journal of Medicinal Chemistry*, vol. 53, no. 6, pp. 2636–2645, 2010.

Hindawi Publishing Corporation
BioMed Research International
Volume 2014, Article ID 498410, 11 pages
http://dx.doi.org/10.1155/2014/498410

Research Article

Proteomic Identification of Altered Cerebral Proteins in the Complex Regional Pain Syndrome Animal Model

Francis Sahngun Nahm,[1] Zee-Yong Park,[2] Sang-Soep Nahm,[3] Yong Chul Kim,[4] and Pyung Bok Lee[1]

[1] *Department of Anesthesiology and Pain Medicine, Seoul National University Bundang Hospital, Seongnam 463707, Republic of Korea*
[2] *School of Life Science, Gwangju Institute of Science and Technology, Gwangju 500712, Republic of Korea*
[3] *Laboratory of Veterinary Anatomy, College of Veterinary Medicine, Konkuk University, Seoul 143701, Republic of Korea*
[4] *Department of Anesthesiology and Pain Medicine, Seoul National University Hospital, Seoul 110744, Republic of Korea*

Correspondence should be addressed to Pyung Bok Lee; painfree@snubh.org

Received 6 March 2014; Revised 14 August 2014; Accepted 25 August 2014; Published 16 September 2014

Academic Editor: Livio Luongo

Background. Complex regional pain syndrome (CRPS) is a rare but debilitating pain disorder. Although the exact pathophysiology of CRPS is not fully understood, central and peripheral mechanisms might be involved in the development of this disorder. To reveal the central mechanism of CRPS, we conducted a proteomic analysis of rat cerebrum using the chronic postischemia pain (CPIP) model, a novel experimental model of CRPS. *Materials and Methods*. After generating the CPIP animal model, we performed a proteomic analysis of the rat cerebrum using a multidimensional protein identification technology, and screened the proteins differentially expressed between the CPIP and control groups. *Results*. A total of 155 proteins were differentially expressed between the CPIP and control groups: 125 increased and 30 decreased; expressions of proteins related to cell signaling, synaptic plasticity, regulation of cell proliferation, and cytoskeletal formation were increased in the CPIP group. However, proenkephalin A, cereblon, and neuroserpin were decreased in CPIP group. *Conclusion*. Altered expression of cerebral proteins in the CPIP model indicates cerebral involvement in the pathogenesis of CRPS. Further study is required to elucidate the roles of these proteins in the development and maintenance of CRPS.

1. Introduction

Complex regional pain syndrome (CRPS) is a rare but serious and painful disorder. Although CRPS can occur following a minor injury, such as a sprain or even soft-tissue blunt trauma, severe intractable pain from CRPS can impair the quality of life. Symptoms and signs of CRPS include sensory changes (allodynia/hyperalgesia), vasomotor changes (temperature asymmetry/skin color change or asymmetry), sudomotor changes (edema/sweating change or asymmetry), and motor or trophic changes [1]. Although the exact pathophysiology of CRPS is not fully understood, several pathological mechanisms, including oxidative stress [2], neurogenic inflammation [3], and alteration in the autonomic nervous system [4, 5], are known to play some roles in its development. Also, psychophysical studies show that CRPS patients have distorted body image and have difficulty in recognizing the size or the position of the affected extremity [6]. The patients get worse when they think about moving the body part, even if they do not move it [7]. Mechanical stimulation of the "virtual (unaffected)" limb reflected in the mirror results in allodynia, which suggests that allodynia and paresthesia can be mediated by the brain [8]. Thus, the distorted body representation of CRPS patients can be treated with mirror therapy [9, 10]. Also, the spreading of symptoms and signs of CRPS from the initial site of presentation to another limb is a well-known phenomenon, which may be due to aberrant central regulation of neurogenic inflammation [11]. These findings highlight the contribution of a cortical pain mechanism in patients with CRPS. Moreover, functional imaging studies provide supporting evidence for the important role of the central nervous system in the

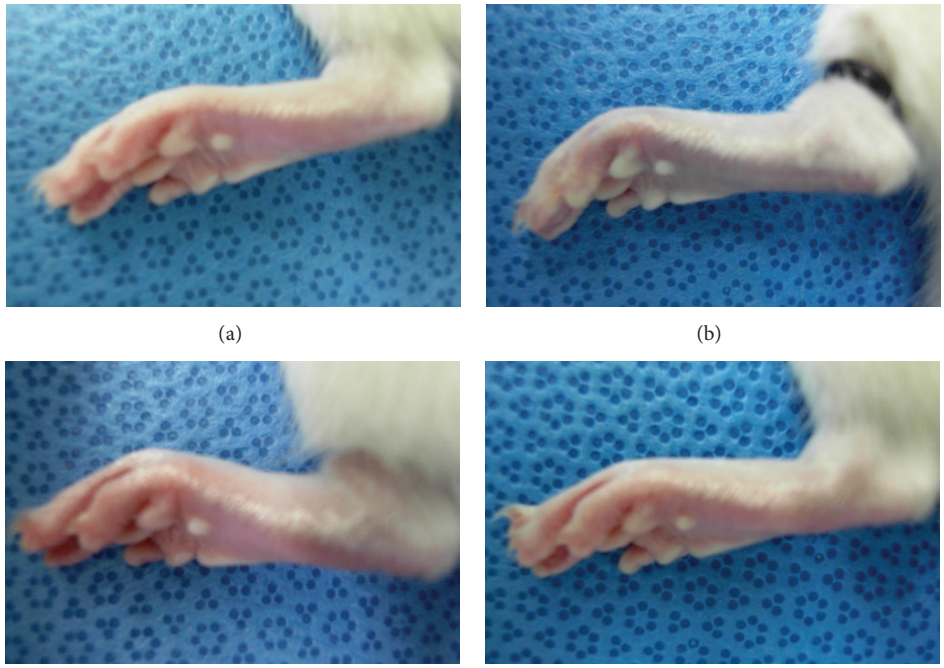

Figure 1: Plantar skin color changes in chronic postischemia pain model rats. (a) Before O-ring application, (b) during O-ring application, (c) 1 hour after reperfusion, and (d) 4 h after reperfusion.

pathogenesis of CRPS [12–14], and recent research suggests that changes in cortical structures can contribute to the pathophysiology of CRPS [15].

Thus, the brain seems to play an important role in the development and maintenance of symptoms and signs in patients with CRPS. Some researchers insist that the peripheral changes in CRPS must be understood as a manifestation of changes in the brain [16]. Therefore, we postulated that protein expression would be altered in the CRPS-affected brain. However, there have been no studies on the changes of cerebral protein expression in CRPS. Therefore, to verify our hypothesis, we conducted a proteomic analysis using multidimensional protein identification technology (MudPIT) in a chronic postischemia perfusion (CPIP) rat model, a novel and widely used experimental model of CRPS type 1 [17].

2. Materials and Methods

2.1. Animals. This study was approved by the Institutional Animal Care and Use Committee of Seoul National University Bundang Hospital (IACUC number 52-2009-033). Male Sprague-Dawley rats weighing 200–250 g had free access to food and water and were housed individually in cages with soft bedding under a 12 h night/day light cycle at a constant temperature of 20–22°C and a humidity level of 55–60%. The animals were acclimatized for at least 1 week prior to the CPIP procedure.

2.2. CPIP Model Generation. The CPIP animal model was generated according to previous methods [17]. Briefly, after induction of anesthesia with isoflurane, a tight fitting O-ring (O-ring West, Seattle, WA, USA) with a 5.5 mm internal diameter was applied to the left hind limb of each anesthetized rat just proximal to the left ankle joint for 3 h. The O-ring was then removed from the anesthetized rat, allowing reperfusion of the hind limb (Figure 1). The animals in the control group underwent anesthesia similar to the CPIP animals, but the O-ring was not placed around the hind limb.

2.3. Behavioral Tests. All behavioral tests were performed during the daylight portion of the regulated circadian cycle between 9 a.m. and 3 p.m. To assess the mechanical threshold, the rats were placed in individual plastic cages with wire mesh bottoms. After 20 min acclimatization, calibrated von Frey filaments (Stoelting Co., Wood Dale, IL, USA) with logarithmically increasing stiffness of 0.41, 0.70, 1.20, 2.00, 3.63, 5.50, 8.50, and 15.10 g were applied to the midplantar surface of the hind paw. The mechanical threshold was assessed using an up-down statistical method [18]. Then, the change in the mechanical threshold (CMT, %) was calculated. The mechanical threshold was examined during the postreperfusion period: 1 h, 4 h, 24 h, 48 h, day 7, and day 21. The CMT was calculated by following equation:

$$\text{CMT}\,(\%) = \frac{M_{\text{post}} - M_{\text{pre}}}{M_{\text{pre}}} \times 100. \quad (1)$$

We used the findings from the neurobehavioral test on day 21 to classify the animals into groups: rats whose CMT was decreased 50% or more after the CPIP procedure were classified as the successful CPIP (A) group. The mechanical

threshold of the animals in the control (C) group was also examined and compared using repeated-measures analysis of variance. All animals were sacrificed 3 weeks after the CPIP procedure for proteomic analysis.

2.4. Proteomic Analysis. The difference in cerebral protein expression between Groups A and C was explored using a MudPIT as follows.

2.4.1. Protein Extraction. A total of six animals (three from Groups A and C) were used for the mass spectrometry analysis. On the day 21, right half of each rat cerebrum was grinded using a mortar in liquid nitrogen. The tissue powder was kept at −80°C. The tissue powder was resolubilized in a small volume of 8 M urea, 100 mM Tris-HCl, pH 8.5, and 1 mM dithiothreitol (DTT) for two hours. The homogenates were sonicated and centrifuged at 100,000 ×g for 1 h. Next, 5 mM DTT was added to the homogenate for 30 min at 37°C and alkylated with 25 mM iodoacetamide for 30 min at 37°C in the dark. The samples were then diluted with 2 M urea and with 50 mM Tris-HCl, pH 8.0, and digested at 37°C overnight with sequence grade trypsin (Promega Co., Fitchburg, MA, USA) diluted 1 : 50 in 5 mM $CaCl_2$.

2.4.2. MudPIT. Peptides were separated with an Agilent 1100 series high-performance liquid chromatography (HPLC) pump (Agilent technologies, Santa Clara, CA, USA) connected to a linear quadruple ion-trap mass spectrometer (MS, LTQ, Thermo-Finnigan, San Jose, CA, USA) using an in-house-built nanoelectrospray ionization interface. To identify peptides, the ion-trap mass spectrometer was operated in a data-dependent MS/MS mode (m/z 400–2000), in which a full MS scan was followed by 10 MS/MS scans and the temperature of the heated capillary was 200°C. MS/MS spectra were generated in the positive ion mode at an electrospray voltage of 2.5 kV and normalized collision energy of 35%. An analytical column-fused (100 μm internal diameter) silica capillary microcolumn (Polymicro technologies, Phoenix, AZ, USA) was pulled to a fine tip using a laser puller and packed with 7 cm of 5 μm C18 reverse-phase resin, which was connected to an internal diameter of 250 μm fused-silica trapping column packed with 2 cm of SCX followed by 2 cm of C18 resin. Each 30 μg peptide mixture was manually loaded onto separate columns using a pressure vessel. A seven-step chromatography run was carried out on each sample and three buffers were used (buffer A: 5% ACN/0.1% formic acid, buffer B: 80% ACN/0.1% formic acid, and buffer C: 5% ACN/0.1% formic acid/500 mM ammonium acetate).

2.4.3. Data Searching and Analysis. Acquired MS/MS spectra were searched against an international protein index "rat v. 3.78 FASTA-format decoy database" downloaded from European Bioinformatics Institute (EBI, http://www.ebi.ac.uk/). The SEQUEST algorithm [19] was used to find the best matching sequences from the database with BioWorks 3.3 (Thermo Fisher Scientific Inc., Rockford, IL, USA) for fully tryptic peptides. The mass of the amino acid cysteine was statically modified by +57 Da and the differential modification search was performed for oxidation (+16 Da on Met). Xcorr values were based on tryptic peptides and charge states following 1.8 for singly charged peptides, 2.5 for doubly charged peptides, 3.5 for triply charged peptides, and 0.08 for ΔCn (DTASelect v. 2.0.39). The analysis of protein fold-change was quantified by an overall spectral counting method comparison of label-free methods for quantifying human proteins [20].

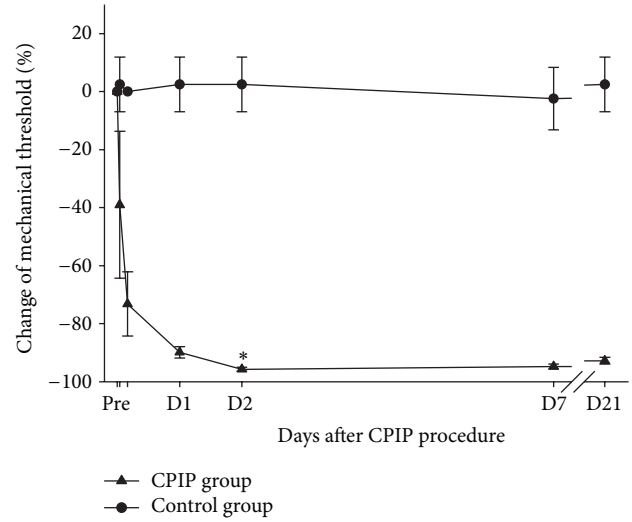

Figure 2: Change in mechanical threshold (%). Group A showed a significant decrease in mechanical threshold compared to group C ($n = 7$ in each group). Asterisk (*) indicates $P < 0.05$ at each time point. Group A: CPIP group and Group C: control group.

3. Results

3.1. Behavioral Tests. A total of 14 animals ($n = 7$ per group) were included in the behavioral test. Before the CPIP procedure, there were no differences in the mechanical threshold between the groups. However, Group A exhibited a significant decrease in the mechanical threshold compared to Group C after the CPIP procedure ($P < 0.01$, Figure 2). The mean differences of CMT (%) in Group A compared to Group C were −41.5, −73.2, −92.3, −98.2, −92.2, and −95.3 after CPIP procedure 1 h, 4 h, day 1, day 2, day 7, and day 21, respectively.

3.2. Differential Protein Expression in the Rat Cerebrum. A total of 454 proteins were differentially expressed between Groups A and C under the criterion of P value <0.1. Among the 454 proteins, we selected those found in the cerebrum of all study animals in either group and excluded "uncharacterized proteins" and "hypothetical proteins." Finally, we found 155 differentially expressed proteins between Group A and Group C: 125 increased (Table 6) and 30 decreased (Table 7). Specifically, expression of proteins related to cell signaling (Table 1), synaptic plasticity (Table 2), regulation of cell proliferation (Table 3), and cytoskeletal formation (Table 4) was increased in Group A. Also, expression of a group of protein kinases (calmodulin dependent protein kinase II beta M isoform, casein kinase 2, phosphoenolpyruvate carboxykinase 2, mitogen-activated protein kinase 4, protein

Table 1: Increased cerebral proteins in the chronic post-ischemia pain group; proteins which might be related to cell signaling.

Number	Symbol	Description	*P* value
1	Kctd12	Potassium channel tetramerisation domain containing 12	0.004
2	Ecsit	Evolutionarily conserved signaling intermediate in Toll pathway, mitochondrial	0.004
3	Tns1	Tensin 1	0.004
4	Ccbp2	Chemokine-binding protein 2	0.004
5	Apba1	Amyloid beta A4 precursor protein-binding family A member 1	0.008
6	Tnc	Tenascin C	0.008
7	Rabl2b	RAB, member of RAS oncogene family-like 2B	0.008
8	Epha4	Eph receptor A4	0.035
9	Rab6a	Ras-related protein Rab-6A	0.038
10	Gpr158	G protein-coupled receptor 158	0.042
11	Anxa2	Isoform Short of Annexin A2	0.043
12	Hgs	Isoform 1 of hepatocyte growth factor-regulated tyrosine kinase substrate	0.054
13	Prkcd	Isoform 1 of protein kinase C delta type	0.060
14	Gabarapl2	Gamma-aminobutyric acid receptor-associated protein-like 2	0.065
15	Map2k4	Dual specificity mitogen-activated protein kinase 4	0.066
16	Cacng2	Voltage-dependent calcium channel gamma-2 subunit	0.083
17	Phb2	Prohibitin-2	0.086
18	Camk2b	Calmodulin-dependent protein kinase II beta M isoform	0.086
19	Anxa5	Annexin A5	0.093
20	Scn2a1	Sodium channel Nav1.2	0.095
21	Rab10	Ras-related protein Rab-10	0.097

Table 2: Increased cerebral proteins in the chronic postischemia pain group; proteins which might be related to synaptic plasticity.

Number	Symbol	Description	*P* value
1	Itpr2	Inositol 1,4,5-trisphosphate receptor type 2	0.001
2	Kctd12	Potassium channel tetramerisation domain containing 12	0.004
3	Grid2	Glutamate receptor delta-2 subunit	0.004
4	Baiap3	BAI1-associated protein 3-like isoform 2	0.008
5	Atad1	ATPase family, AAA domain containing 1	0.008
6	Pick1	PRKCA-binding protein	0.008
7	Nlgn3	Isoform 1 of Neuroligin-3	0.056
8	Nudc	Nuclear migration protein nudC	0.085
9	Camk2b	Calmodulin-dependent protein kinase II beta M isoform	0.086

Table 3: Increased cerebral proteins in the chronic postischemia pain group; proteins which might be related to regulation of cell proliferation.

Number	Symbol	Description	*P* value
1	Pik3r4	Phosphoinositide 3-kinase regulatory subunit 4	0.001
2	Itpr2	Inositol 1,4,5-trisphosphate receptor type 2	0.001
3	Anp32b	Acidic leucine-rich nuclear phosphoprotein 32 family member B	0.002
4	Plk1	Serine/threonine-protein kinase	0.004
5	Drg2	Developmentally regulated GTP binding protein 2-like	0.004
6	Dmwd	Dystrophia myotonica-containing WD repeat motif	0.008
7	Acin1	Apoptotic chromatin condensation inducer 1 protein	0.008
8	Pole2	Polymerase (DNA directed), epsilon 2	0.008
9	Cyld	Ubiquitin carboxyl-terminal hydrolase	0.076
10	Csnk2a2	Casein kinase 2, alpha prime polypeptide	0.084
11	Rab10	Ras-related protein Rab-10	0.097

Table 4: Increased cerebral proteins in the chronic postischemia pain group; proteins which might be related to cytoskeletal formation.

Number	Symbol	Description	*P* value
1	Krt4	Keratin, type II cytoskeletal 4	0.008
2	Sntb2	Syntrophin, beta 2	0.008
3	Ckap5	Cytoskeleton associated protein 5	0.038
4	Fermt2	Fermitin family homolog 2	0.063
5	Cotl1	Coactosin-like protein	0.065
6	Rps5	40S ribosomal protein S5	0.072
7	Col1a2	Collagen alpha-2(I) chain	0.079
8	Actr10	Actin-related protein 10 homolog	0.080
9	Etl4	Enhancer trap locus 4-like	0.083
10	Farp1	FERM, RhoGEF (Arhgef), and pleckstrin domain protein 1	0.094

Table 5: Decreased cerebral proteins in the chronic postischemia pain group; proteins which might be related to cell signaling.

Number	Symbol	Description	*P* value
1	Vwa1	Von Willebrand factor A domain-containing protein 1	0.002
2	Ppp1r10	Serine/threonine-protein phosphatase 1 regulatory subunit 10	0.003
3	Slc4a8	Isoform 2 of electroneutral sodium bicarbonate exchanger 1	0.003
4	Daam2	Dishevelled associated activator of morphogenesis 2	0.003
5	Trim32	Tripartite motif protein 32	0.007
6	Slc1a1	Excitatory amino acid transporter 3	0.007
7	Spn	Sialophorin	0.007
8	Crbn	Cereblon	0.007
9	Thoc1	Da2-19 THO complex subunit 1	0.007
10	Lmo7	Lim domain only protein 7	0.007
11	Rps27a	Ribosomal protein S27a	0.007
12	Sema4d	Sema domain	0.043
13	Sec3l1	SEC3-like 1	0.047
14	Spna2	Alpha II spectrin	0.065
15	Pde10a	Isoform 3 of cAMP- and cAMP-inhibited cGMP 3′,5′-cyclic phosphodiesterase 10A	0.065
16	Snx2	Sorting nexin 2	0.067
17	Slc25a3	Phosphate carrier protein, mitochondrial	0.068
18	Cox6a1	Cytochrome c oxidase subunit 6A1, mitochondrial	0.090

kinase C delta, N-terminal kinase like protein, uridine kinase-like 1, serine/threonine protein kinase PLK 1, and phosphoinositide 3 kinase regulatory subunit 4) and calcium-related proteins (inositol 1,4,5-triphosphate receptor type 2, annexin A1, annexin A2, annexin A5, voltage-dependent Ca^{2+} channel gamma-2 subunit, and voltage-dependent Ca^{2+} channel beta-3 subunit, and coiled-coil domain-containing protein 47) was also elevated in Group A. However, several proteins were decreased in group A. Specifically, expression of proteins related to cell signaling (Table 5) and metabolism of fatty acid (peroxisomal 3,2-trans-enoyl Co A isomerase, acetyl-CoA acyltransferase 1b, and acetyl-CoA acetyltransferase 2) were decreased. Also, proenkephalin A, protein cereblon, and neuroserpin were decreased in Group A.

4. Discussion

In our study, various proteins were differentially expressed in the cerebrum of CPIP animals. Specifically, expressions of proteins related to cell signaling, synaptic plasticity, regulation of cell proliferation, and cytoskeletal formation were increased in Group A. These findings suggest that both functional and structural changes may occur in the cerebrum of CPIP animals, and altered protein expression can be related to the development of CRPS. This is the first study of cerebral protein expression changes in the CPIP rat model.

We also found that inositol 1,4,5-triphosphate (IP3) receptor type 2 and phosphoinositide 3 kinase (PI3K) regulatory subunit were also increased in Group A. IP3 receptor is intracellular calcium release channel and is regulated by calcium and calmodulin (CaM) [21]. And it is known that PI3K is an important mediator of central sensitization in painful inflammatory condition [22], and many tumorous conditions are related to this enzyme [23, 24]. Based on these findings, cerebral overexpression of IP3 receptor type 2 and PI3K can be related to the sustained pain after rat CPIP model.

Table 6: Cerebral proteins with increased expression in the chronic postischemia pain (CPIP) group.

Number	Symbol	Description	*P* value
1	Itpr2	Inositol 1,4,5-trisphosphate receptor type 2	0.001
2	Pik3r4	Phosphoinositide 3-kinase regulatory subunit 4	0.001
3	Exoc7	Exocyst complex component 7	0.001
4	Rcor2	REST corepressor 2	0.001
5	Anp32b	Acidic leucine-rich nuclear phosphoprotein 32 family member B	0.002
6	Qrich2	Glutamine rich 2-like	0.002
7	Dnah11	Dynein, axonemal, heavy chain 11	0.002
8	Plk1	Serine/threonine-protein kinase PLK1	0.004
9	Ephx1	Epoxide hydrolase 1	0.004
10	Cacnb3	Voltage-dependent L-type calcium channel subunit beta-3	0.004
11	Anxa1	Annexin A1	0.004
12	Tns1	Tensin 1	0.004
13	Hdac4	Histone deacetylase 4	0.004
14	Osbpl7	Oxysterol binding protein like 7	0.004
15	Ecsit	Evolutionarily conserved signaling intermediate in Toll pathway, mitochondrial	0.004
16	Sorbs3	Sorbin and SH3 domain containing 3, isoform CRA_b	0.004
17	Kctd12	Potassium channel tetramerisation domain containing 12	0.004
18	Ccbp2	Chemokine-binding protein 2	0.004
19	Drg2	Developmentally regulated GTP binding protein 2-like	0.004
20	Grid2	Glutamate receptor delta-2 subunit	0.004
21	Safb	Scaffold attachment factor B1	0.008
22	Dnm3	Isoform 1 of Dynamin-3	0.008
23	Dnajc16	DnaJ homolog subfamily C member 16	0.008
24	Sntb2	Syntrophin, beta 2	0.008
25	Pnpt1	Polyribonucleotide nucleotidyltransferase 1	0.008
26	Eif3g	Eukaryotic translation initiation factor 3 subunit G	0.008
27	Pole2	Polymerase (DNA directed), epsilon 2	0.008
28	Scyl1	N-terminal kinase-like protein	0.008
29	Atad1	ATPase family, AAA domain containing	0.008
30	Krt4	Keratin, type II cytoskeletal 4	0.008
31	Ctsa	Protective protein for beta-galactosidase	0.008
32	Abca1	5 ATP-binding cassette, subfamily A (ABC1), member 15	0.008
33	Dmwd	Dystrophia myotonica-containing WD repeat motif	0.008
34	Baiap3	BAI1-associated protein 3-like isoform 2	0.008
35	Znf512b	Uridine kinase-like 1	0.008
36	Gale	Gale protein	0.008
37	Pick1	PRKCA-binding protein	0.008
38	Acin1	Acin1 protein	0.008
39	Chid1	Chitinase domain containing 1	0.008
40	Pcyox1l	Pcyox1l protein	0.008
41	Rabl2b	RAB, member of RAS oncogene family-like 2B	0.008
42	Serpina3k	Serine protease inhibitor A3K	0.008
43	Glg1	Golgi apparatus protein 1	0.008
44	Tnc	Tenascin C	0.008
45	Lysmd1	LysM and putative peptidoglycan-binding domain-containing protein 1	0.008
46	Apba1	Amyloid beta A4 precursor protein-binding family A member 1	0.008
47	Ckap5	Cytoskeleton associated protein 5	0.038
48	Ndufab1	Acyl carrier protein	0.035
49	Epha4	Eph receptor A4	0.035
50	Kalrn	Isoform 2 of Kalirin	0.035
51	Myh14	Myosin, heavy chain 14	0.035

Table 6: Continued.

Number	Symbol	Description	*P* value
52	Anxa2	Isoform Short of Annexin A2	0.043
53	Ccdc47	Coiled-coil domain-containing protein 47	0.043
54	Gpr158	G protein-coupled receptor 158	0.042
55	Cugbp1	CUGBP Elav-like family member 1	0.041
56	Hba2	Hemoglobin alpha 2 chain	0.040
57	Acsl3	Isoform long of long-chain-fatty-acid-CoA ligase 3	0.040
58	Rab6a	Ras-related protein Rab-6A	0.038
59	Hbb	Hemoglobin subunit beta-1	0.048
60	Hbb-b1	Zero beta-1 globin	0.044
61	Khsrp	Far upstream element-binding protein 2	0.043
62	Scamp5	Secretory carrier-associated membrane protein 5	0.048
63	Aldh3a2	Fatty aldehyde dehydrogenase	0.049
64	Mesdc2	LDLR chaperone MESD	0.049
65	Rab3d	GTP-binding protein Rab-3D	0.051
66	Vps29	Isoform 2 of vacuolar protein sorting-associated protein 29	0.051
67	Psma3l	Psma3 Proteasome subunit alpha type-3	0.053
68	Hgs	Isoform 1 of hepatocyte growth factor-regulated tyrosine kinase	0.054
69	Nlgn3	Isoform 1 of neuroligin-3	0.056
70	Cygb	Cytoglobin	0.060
71	Pcsk2	Neuroendocrine convertase 2	0.060
72	Prkcd	Isoform 1 of Protein kinase C delta	0.060
73	Fnbp4	Formin binding protein 4	0.062
74	Eif2s3x	Eukaryotic translation initiation factor 2 subunit 3	0.063
75	Fermt2	Fermitin family homolog 2	0.063
76	Vps33a	Vacuolar protein sorting-associated protein 33A	0.063
77	SNX3	Sorting nexin-3	0.063
78	Exoc8	Exocyst complex component 8	0.063
79	Thrap3	Thyroid hormone receptor-associated protein 3	0.063
80	Ndufa1	NADH dehydrogenase (ubiquinone) 1 alpha subcomplex, 1	0.063
81	Gabarapl2	Gamma-aminobutyric acid receptor-associated protein-like 2	0.065
82	Cotl1	Coactosin-like protein	0.065
83	Gad1	Glutamate decarboxylase 1	0.065
84	Ehd1	EH domain-containing protein 1	0.066
85	Map2k4	Mitogen-activated protein kinase 4	0.066
86	Mug1	Murinoglobulin (alpha-1-inhibitor 3)	0.070
87	Pck2	Phosphoenolpyruvate carboxykinase 2	0.072
88	Rps5	40S ribosomal protein S5	0.072
89	Ap2s1	Adaptor protein complex 2 subunit sigma	0.075
90	Tpp1	Tripeptidyl-peptidase 1	0.076
91	Cyld	Ubiquitin carboxyl-terminal hydrolase	0.076
92	Nuc	Nucleolin-like protein	0.079
93	Col1a2	Collagen alpha-2(I) chain	0.079
94	Slc6a17	Orphan sodium- and chloride-dependent neurotransmitter transporter NTT4	0.079
95	Actr10	Actin-related protein 10 homolog	0.080
96	Cacng2	Voltage-dependent calcium channel gamma-2 subunit	0.083
97	Ampd3	AMP deaminase 3	0.083
98	Eif5b-ps1	Eif5b Eukaryotic translation initiation factor 5B	0.083
99	Timm9	Mitochondrial import inner membrane translocase subunit Tim9	0.083
100	Etl4	Enhancer trap locus 4-like	0.083
101	Csnk2a2	Casein kinase 2, alpha prime polypeptide	0.084
102	Cct6a	Chaperonin containing TCP1 subunit 6a	0.084
103	Nudc	Nuclear migration protein nud	0.085

Table 6: Continued.

Number	Symbol	Description	*P* value
104	Ndufa13	NADH dehydrogenase (ubiquinone) 1 alpha subcomplex 13	0.085
105	Camk2b	Calmodulin-dependent protein kinase II beta M isoform	0.086
106	Clta	Isoform brain of clathrin light chain A	0.086
107	Asah1	Acid ceramidase	0.086
108	Phb2	Prohibitin-2	0.086
109	Sod1	Superoxide dismutase [Cu-Zn]	0.088
110	Ndufs8	NADH dehydrogenase (ubiquinone) 1 alpha subcomplex subunit 8	0.090
111	Slc17a7	Isoform 1 of vesicular glutamate transporter 1	0.091
112	Ugp2	UDP-glucose pyrophosphorylase 2, isoform CRA-b	0.091
113	Rala	Ras-related protein Ral-A	0.091
114	Anxa5	Annexin A5	0.093
115	Hnrph1	Isoform 1 of heterogeneous nuclear ribonucleoprotein H	0.093
116	Stxbp5l	Syntaxin binding protein 5-like	0.093
117	Abcd3	ATP-binding cassette subfamily D member 3	0.094
118	Farp1	FERM, RhoGEF (Arhgef), and pleckstrin domain protein 1	0.094
119	Leng4	Leng4 protein	0.094
120	Scn2a1	Sodium channel Nav1.2	0.095
121	Rab10	Ras-related protein Rab-10	0.097
122	Aldh7a1	Alpha-aminoadipic semialdehyde dehydrogenase	0.097
123	Cltb	Isoform Brain of Clathrin light chain B	0.097
124	Phyhipl	Isoform 1 of phytanoyl-CoA hydroxylase-interacting protein-like	0.098
125	Synpo	Isoform 1 of synaptopodin	0.099

Among the 155 proteins expressed differentially, calcium related proteins, including calcium calmodulin kinase II (CaMKII), were increased in group A. Calcium plays a crucial role in many physiological processes, including signal transduction, cell growth, and proliferation. CaMKII is one of the most prominent protein kinases, present in every tissue, but most concentrated in the brain. CaMKII plays various roles, including synthesis and release of neurotransmitter modulation of ion channel activity, synaptic plasticity, learning, and memory [25–28]. Moreover, CaMKII is thought to be important in central sensitization [29–31] and is implicated in central neuropathic pain [31] and long term potentiation (LTP) [32]. LTP is initiated when NMDA receptors allow Ca^{2+} into the postsynaptic neuron, and this Ca^{2+} influx activates CaMKII. LTP in nociceptive spinal pathways shares several features with hyperalgesia, and LTP at synapses constitutes a contemporary cellular model for pain [33, 34]. And it was reported that the overexpression of CaMKII was observed in the dorsal root ganglia of rat model of type 1 diabetes [35], and the inhibition of CaMKII can reverse the chronic inflammatory pain [36]. These findings are consistent with the result of our study. Therefore, overexpression of cerebral CaMKII implicates cerebral involvement in CRPS, and CaMKII can be a target for the prevention and treatment of CRPS.

In addition, we observed that proenkephalin A, cereblon, and neuroserpin decreased in CPIP animals. Proenkephalin is an endogenous opioid hormone which produces the enkephalin peptide. Enkephalin provides a role as inhibiting neurotransmitters in the pathway for pain perception to reduce pain perception. Therefore, decreased proenkephalin A in the cerebrum of CPIP animals seems to reflect the blunted ability to pain modulation and exaggerated response to the pain. For the cereblon, it is known to be related to memory, learning, and intelligence [37], and anomalous cereblon expression can lead to memory and learning deficit [38]. The defect in cereblon gene is associated with mental retardation [39]. Therefore, decreased expression of cereblon in CPIP animals in our study might be related to the deficit in the learning and memory. Neuroserpin, which was known to be related to neurogenesis [40] was decreased in CPIP animals in our study. Neuroserpin plays a role of neuronal protection in pathologic state, and point mutation can cause encephalopathy [41]. Also it has been known that deficiency in neuroserpin exacerbates ischemic brain injury [42]. Therefore, the decreased expression of neuroserpin in CPIP animals in our study might be related to the altered or defected cerebral function.

In our study, we used the CPIP model because CRPS develops after a minor injury without distinguishable nerve lesions. This model is considered a novel animal model of CRPS type 1, in which nerve injury or bone fracture usually does not exist. The previous proteomic studies in neuropathic pain research usually used the nerve ligation model or nerve crush injury model [43, 44]. Since the CPIP model exhibits similar features of human CRPS type 1, our results may have an implication for cerebral involvement in human CRPS. The mechanical threshold was similar at the beginning (day 1) and after 21 days. This is because we took no actions for treatment on the CPIP animals and therefore the initial pain seemed to persist without change. We did not measure the mechanical threshold in the contralateral paws, because it has

Table 7: Cerebral proteins with decreased expression in the chronic postischemia pain (CPIP) group.

Number	Symbol	Description	*P* value
1	Vwa1	Von Willebrand factor A domain-containing protein 1	0.002
2	Ppp1r10	Serine/threonine-protein phosphatase 1 regulatory subunit 10	0.003
3	Poldip2	DNA-directed polymerase delta interacting protein 2	0.003
4	Slc4a8	Isoform 2 of electroneutral sodium bicarbonate exchanger 1	0.003
5	Daam2	Dishevelled associated activator of morphogenesis 2	0.003
6	Cep350	Centrosome-associated protein 350	0.003
7	Tra2b	Transformer-2 protein homolog beta	0.007
8	Epb4.1l1	Isoform L of band 4.1-like protein 1	0.007
9	Trim32	Tripartite motif protein 32	0.007
10	Slc1a1	Excitatory amino acid transporter 3	0.007
11	Spn	Sialophorin	0.007
12	Crbn	Cereblon	0.007
13	Thoc1	Da2-19 THO complex subunit 1	0.007
14	Lmo7	Lim domain only protein 7	0.007
15	Rps27a	Ribosomal protein S27a	0.007
16	Sema4d	Sema domain, immunoglobulin domain (Ig), transmembrane domain	0.043
17	Sec3l1	SEC3-like 1	0.047
18	Ikbkap	Elongator complex protein 1	0.058
19	Peci	Peroxisomal 3,2-trans-enoyl-CoA isomerase	0.058
20	Penk	Proenkephalin-A	0.058
21	Bles03	basophilic leukemia expressed protein	0.058
22	Spna2	Alpha II spectrin	0.065
23	Pde10a	Isoform 3 of cAMP and cAMP-inhibited cGMP 3′,5′-cyclic phosphodiesterase 10A	0.065
24	Snx2	Sorting nexin 2	0.067
25	Slc25a3	Phosphate carrier protein, mitochondrial	0.068
26	Serpini1	Neuroserpin	0.070
27	Acaa1b	Acetyl-CoA acyltransferase 1b	0.077
28	H2afz	Histone H2A.Z	0.079
29	Cox6a1	Cytochrome c oxidase subunit 6A1, mitochondrial	0.090
30	Acat2	Acetyl-CoA acetyltransferase 2	0.094

been already known that the mechanical threshold decreases in the contralateral paws of the CPIP animals, and ipsilateral plantar allodynia is known to be the most characteristic feature of the CPIP animals [17]. The CMT in the ipsilateral paw was used for the criterion of the successful establishment of the animal model.

This study had some limitations. First, the differentially expressed cerebral proteins may not be specific to CPIP animals. These proteins may also change in response to peripheral noxious stimuli. However, CPIP animals exhibit many features of human CRPS type 1, and thus our findings can be extrapolated to human CRPS. Second, because of the complexity of protein interactions in many physiologic pathways in the brain, it is still unclear which is the key protein in the development of CRPS.

Third, we performed proteomic analysis only 21 days after CPIP model generation. However, protein expression related to the development and maintenance of CRPS can differ according to the time course. A proper time course to evaluate a possible correlation between pain behavior development and protein modulation may be useful to discriminate protein changes associated with the early inflammation from that one responsible for possible structural or functional alterations (neural sensitization) occurring at central level. Further investigation of the cerebral mechanism of CRPS is required.

5. Conclusion

In conclusion, the cerebral proteome is altered after CPIP injury; many functional and structural changes seem to occur in the cerebrum. These findings support the notion of cerebral involvement in CRPS. Therefore, treatment of CRPS should target not only the periphery, but also the brain.

Conflict of Interests

The authors have no conflict of interests to declare.

Acknowledgment

This study was financially supported by Grant no. 02-2009-038 from the Seoul National University Bundang Hospital.

References

[1] R. N. Harden, S. Bruehl, M. Stanton-Hicks, and P. R. Wilson, "Proposed new diagnostic criteria for complex regional pain syndrome," *Pain Medicine*, vol. 8, no. 4, pp. 326–331, 2007.

[2] E. Eisenberg, S. Shtahl, R. Geller et al., "Serum and salivary oxidative analysis in Complex Regional Pain Syndrome," *Pain*, vol. 138, no. 1, pp. 226–232, 2008.

[3] F. Birklein and M. Schmelz, "Neuropeptides, neurogenic inflammation and complex regional pain syndrome (CRPS)," *Neuroscience Letters*, vol. 437, no. 3, pp. 199–202, 2008.

[4] J. Schulze and C. Troeger, "Increased sympathetic activity assessed by spectral analysis of heart rate variability in patients with CRPS I," *Handchirurgie, Mikrochirurgie, Plastische Chirurgie*, vol. 42, pp. 44–48, 2010.

[5] J. Schattschneider, A. Binder, D. Siebrecht, G. Wasner, and R. Baron, "Complex regional pain syndromes: the influence of cutaneous and deep somatic sympathetic innervation on pain," *Clinical Journal of Pain*, vol. 22, no. 3, pp. 240–244, 2006.

[6] G. L. Moseley, "Distorted body image in complex regional pain syndrome," *Neurology*, vol. 65, no. 5, p. 773, 2005.

[7] G. L. Moseley, N. Zalucki, F. Birklein, J. Marinus, J. J. van Hilten, and H. Luomajoki, "Thinking about movement hurts: the effect of motor imagery on pain and swelling in people with chronic arm pain," *Arthritis Care & Research*, vol. 59, no. 5, pp. 623–631, 2008.

[8] N. E. Acerra and G. L. Moseley, "Dysynchiria: watching the mirror image of the unaffected limb elicits pain on the affected side," *Neurology*, vol. 65, no. 5, pp. 751–753, 2005.

[9] J. H. Bultitude and R. D. Rafal, "Derangement of body representation in complex regional pain syndrome: report of a case treated with mirror and prisms," *Experimental Brain Research*, vol. 204, no. 3, pp. 409–418, 2010.

[10] C. S. McCabe, R. C. Haigh, E. F. J. Ring, P. W. Halligan, P. D. Wall, and D. R. Blake, "A controlled pilot study of the utility of mirror visual feedback in the treatment of complex regional pain syndrome (type 1)," *Rheumatology*, vol. 42, no. 1, pp. 97–101, 2003.

[11] J. Maleki, A. A. LeBel, G. J. Bennett, and R. J. Schwartzman, "Patterns of spread in complex regional pain syndrome, type I (reflex sympathetic dystrophy)," *Pain*, vol. 88, no. 3, pp. 259–266, 2000.

[12] P. Schwenkreis, C. Maier, and M. Tegenthoff, "Functional imaging of central nervous system involvement in complex regional pain syndrome," *American Journal of Neuroradiology*, vol. 30, no. 7, pp. 1279–1284, 2009.

[13] W. Freund, A. P. Wunderlich, G. Stuber et al., "Different activation of opercular and posterior cingulate cortex (pcc) in patients with complex regional pain syndrome (crps i) compared with healthy controls during perception of electrically induced pain: a functional MRI study," *Clinical Journal of Pain*, vol. 26, no. 4, pp. 339–347, 2010.

[14] P. Y. Geha, M. N. Baliki, R. N. Harden, W. R. Bauer, T. B. Parrish, and A. V. Apkarian, "The brain in chronic CRPS pain: abnormal gray-white matter interactions in emotional and autonomic regions," *Neuron*, vol. 60, no. 4, pp. 570–581, 2008.

[15] C. M. Swart, J. F. Stins, and P. J. Beek, "Cortical changes in complex regional pain syndrome (CRPS)," *European Journal of Pain*, vol. 13, no. 9, pp. 902–907, 2009.

[16] W. Jänig and R. Baron, "Complex regional pain syndrome is a disease of the central nervous system," *Clinical Autonomic Research*, vol. 12, no. 3, pp. 150–164, 2002.

[17] T. J. Coderre, D. N. Xanthos, L. Francis, and G. J. Bennett, "Chronic post-ischemia pain (CPIP): a novel animal model of complex regional pain syndrome-Type I (CRPS-I; reflex sympathetic dystrophy) produced by prolonged hindpaw ischemia and reperfusion in the rat," *Pain*, vol. 112, no. 1-2, pp. 94–105, 2004.

[18] S. R. Chaplan, F. W. Bach, J. W. Pogrel, J. M. Chung, and T. L. Yaksh, "Quantitative assessment of tactile allodynia in the rat paw," *Journal of Neuroscience Methods*, vol. 53, no. 1, pp. 55–63, 1994.

[19] J. K. Eng, A. L. McCormack, and J. R. Yates, "An approach to correlate tandem mass spectral data of peptides with amino acid sequences in a protein database," *Journal of the American Society for Mass Spectrometry*, vol. 5, no. 11, pp. 976–989, 1994.

[20] W. M. Old, K. Meyer-Arendt, L. Aveline-Wolf et al., "Comparison of label-free methods for quantifying human proteins by shotgun proteomics," *Molecular and Cellular Proteomics*, vol. 4, no. 10, pp. 1487–1502, 2005.

[21] N. Nadif Kasri, G. Bultynck, I. Sienaert et al., "The role of calmodulin for inositol 1,4,5-trisphosphate receptor function," *Biochimica et Biophysica Acta*, vol. 1600, no. 1-2, pp. 19–31, 2002.

[22] S. Pezet, F. Marchand, R. D'Mello et al., "Phosphatidylinositol 3-kinase is a key mediator of central sensitization in painful inflammatory conditions," *Journal of Neuroscience*, vol. 28, no. 16, pp. 4261–4270, 2008.

[23] W.-P. Fung-Leung, "Phosphoinositide 3-kinase delta (PI3Kδ) in leukocyte signaling and function," *Cellular Signalling*, vol. 23, no. 4, pp. 603–608, 2011.

[24] P. M. Lorusso and S. A. Boerner, "The role of phosphoinositide 3-kinase in breast cancer: an overview," *Clinical Breast Cancer*, vol. 10, supplement 3, pp. S56–S58, 2010.

[25] T. Yamauchi, "Neuronal Ca^{2+}/calmodulin-dependent protein kinase II-discovery, progress in a quarter of a century, and perspective: implication for learning and memory," *Biological and Pharmaceutical Bulletin*, vol. 28, no. 8, pp. 1342–1354, 2005.

[26] C. Solà, S. Barrón, J. M. Tusell, and J. Serratosa, "The Ca^{2+}/calmodulin system in neuronal hyperexcitability," *The International Journal of Biochemistry & Cell Biology*, vol. 33, no. 5, pp. 439–455, 2001.

[27] A. R. Halt, R. F. Dallapiazza, Y. Zhou et al., "CaMKII binding to GluN2B is critical during memory consolidation," *EMBO Journal*, vol. 31, no. 5, pp. 1203–1216, 2012.

[28] S. J. Coultrap and K. U. Bayer, "CaMKII regulation in information processing and storage," *Trends in Neurosciences*, vol. 35, no. 10, pp. 607–618, 2012.

[29] L. Fang, J. Wu, Q. Lin, and W. D. Willis, "Calcium-calmodulin-dependent protein kinase II contributes to spinal cord central sensitization," *The Journal of Neuroscience*, vol. 22, no. 10, pp. 4196–4204, 2002.

[30] Y. Dai, H. Wang, A. Ogawa et al., "Ca^{2+}/calmodulin-dependent protein kinase II in the spinal cord contributes to neuropathic pain in a rat model of mononeuropathy," *European Journal of Neuroscience*, vol. 21, no. 9, pp. 2467–2474, 2005.

[31] E. D. Crown, Y. S. Gwak, Z. Ye et al., "Calcium/calmodulin dependent kinase II contributes to persistent central neuropathic pain following spinal cord injury," *Pain*, vol. 153, no. 3, pp. 710–721, 2012.

[32] J. Lisman, R. Yasuda, and S. Raghavachari, "Mechanisms of CaMKII action in long-term potentiation," *Nature Reviews Neuroscience*, vol. 13, no. 3, pp. 169–182, 2012.

[33] R. Ruscheweyh, O. Wilder-Smith, R. Drdla, X.-G. Liu, and J. Sandkühler, "Long-term potentiation in spinal nociceptive pathways as a novel target for pain therapy," *Molecular Pain*, vol. 7, article 20, 2011.

[34] J. Sandkühler and D. Gruber-Schoffnegger, "Hyperalgesia by synaptic long-term potentiation (LTP): an update," *Current Opinion in Pharmacology*, vol. 12, no. 1, pp. 18–27, 2012.

[35] L. Ferhatovic, A. Banozic, S. Kostic et al., "Expression of calcium/calmodulin-dependent protein kinase II and pain-related behavior in rat models of type 1 and type 2 diabetes," *Anesthesia & Analgesia*, vol. 116, no. 3, pp. 712–721, 2013.

[36] F. Luo, C. Yang, Y. Chen et al., "Reversal of chronic inflammatory pain by acute inhibition of Ca^{2+}/calmodulin-dependent protein kinase II," *Journal of Pharmacology and Experimental Therapeutics*, vol. 325, no. 1, pp. 267–275, 2008.

[37] J. J. Higgins, A. L. Tal, X. Sun et al., "Temporal and spatial mouse brain expression of cereblon, an ionic channel regulator involved in human intelligence," *Journal of Neurogenetics*, vol. 24, no. 1, pp. 18–26, 2010.

[38] A. M. Rajadhyaksha, S. Ra, S. Kishinevsky et al., "Behavioral characterization of cereblon forebrain-specific conditional null mice: a model for human non-syndromic intellectual disability," *Behavioural Brain Research*, vol. 226, no. 2, pp. 428–434, 2012.

[39] J. J. Higgins, J. Pucilowska, R. Q. Lombardi, and J. P. Rooney, "A mutation in a novel ATP-dependent Lon protease gene in a kindred with mild mental retardation," *Neurology*, vol. 63, no. 10, pp. 1927–1931, 2004.

[40] M. Yaamada, K. Takaehashi, W. Ukai, E. Hashimoto, T. Saito, and M. Yamada, "Neuroserpin is expressed in early stage of neurogenesis in adult rat hippocampus," *NeuroReport*, vol. 21, no. 2, pp. 138–142, 2010.

[41] E. Miranda and D. A. Lomas, "Neuroserpin: a serpin to think about," *Cellular and Molecular Life Sciences*, vol. 63, no. 6, pp. 709–722, 2006.

[42] M. Gelderblom, M. Neumann, P. Ludewig et al., "Deficiency in serine protease inhibitor neuroserpin exacerbates ischemic brain injury by increased postischemic inflammation," *PLoS ONE*, vol. 8, no. 5, Article ID e63118, 2013.

[43] C. R. Jiménez, F. J. Stam, K. W. Li et al., "Proteomics of the injured rat sciatic nerve reveals protein expression dynamics during regeneration," *Molecular and Cellular Proteomics*, vol. 4, no. 2, pp. 120–132, 2005.

[44] O. Alzate, S.-R. A. Hussain, V. M. Goettl et al., "Proteomic identification of brainstem cytosolic proteins in a neuropathic pain model," *Molecular Brain Research*, vol. 128, no. 2, pp. 193–200, 2004.

Hindawi Publishing Corporation
BioMed Research International
Volume 2014, Article ID 495789, 13 pages
http://dx.doi.org/10.1155/2014/495789

Review Article

The Purinergic System and Glial Cells: Emerging Costars in Nociception

Giulia Magni[1,2] and Stefania Ceruti[1]

[1] *Department of Pharmacological and Biomolecular Sciences, Università degli Studi di Milano, Via Balzaretti, 9-20133 Milan, Italy*
[2] *Department of Drug Discovery and Development (D3), Italian Institute of Technology (IIT), Via Morego, 30-16163 Genoa, Italy*

Correspondence should be addressed to Stefania Ceruti; stefania.ceruti@unimi.it

Received 28 May 2014; Accepted 8 July 2014; Published 3 September 2014

Academic Editor: Livio Luongo

It is now well established that glial cells not only provide mechanical and trophic support to neurons but can directly contribute to neurotransmission, for example, by release and uptake of neurotransmitters and by secreting pro- and anti-inflammatory mediators. This has greatly changed our attitude towards acute and chronic disorders, paving the way for new therapeutic approaches targeting activated glial cells to indirectly modulate and/or restore neuronal functions. A deeper understanding of the molecular mechanisms and signaling pathways involved in neuron-to-glia and glia-to-glia communication that can be pharmacologically targeted is therefore a mandatory step toward the success of this new healing strategy. This holds true also in the field of pain transmission, where the key involvement of astrocytes and microglia in the central nervous system and satellite glial cells in peripheral ganglia has been clearly demonstrated, and literally hundreds of signaling molecules have been identified. Here, we shall focus on one emerging signaling system involved in the cross talk between neurons and glial cells, the purinergic system, consisting of extracellular nucleotides and nucleosides and their membrane receptors. Specifically, we shall summarize existing evidence of novel "druggable" glial purinergic targets, which could help in the development of innovative analgesic approaches to chronic pain states.

1. Chronic Pain: Neurons Need Costars to Be Sensitized

Several lines of evidence from basic pain research using diverse animal models indicate that an aberrant excitability of doreceptor agonists, such asrsal horn neurons evoked by peripheral sensory inputs is at the basis of both neuropathic and inflammatory pain [1, 2]. While neurons have long been considered the only cell type involved in pain development and transmission, recent studies have shown that pathologically altered neurotransmission requires communication with glial cells [3].

Microglia show a long-term response to a wide range of stimuli controlling physiological homeostasis, including peripheral nerve injury (PNI). In response to PNI, microglia activation in the spinal cord leads to cell hypertrophy, increase in cell number, and altered gene expression [4–6]. By responding to extracellular stimuli, activated glial cells evoke various cellular responses, such as production and release of bioactive factors including cytokines and neurotrophic factors [7], which in turn lead to the hyperexcitability of dorsal horn neurons and, consequently, to the development of neuropathic pain.

Not only spinal microglia but also astrocytes are involved in neuronal sensitization in the spinal cord. In fact, it has been hypothesized that microglia sense nerve damage or proalgogenic inputs from the periphery, and as a consequence they release several mediators that either act directly on dorsal horn neurons or promote reactive astrogliosis [8]. Reactive astrogliosis is a typical double-edged sword phenomenon, showing both neurotoxic and neuroprotective features, depending upon the type of injury and the basal conditions of the affected tissue [9]. This is possibly true also in pain models, where both astrocyte-derived proalgogenic and analgesic molecules have been detected [8].

Glial cells are directly involved in nociception not only in the central nervous system (CNS), but also in the periphery. In fact, a peculiar type of glial cells, named satellite glial

cells (SGCs), is located in peripheral sensory ganglia, where they enwrap neuronal bodies, thus constituting distinct morphological and functional units [10]. In the past few years, their central role in the development and maintenance of chronic pain has been clearly demonstrated by several authors, reporting an increased expression and release of mediators such as interleukin-1β (IL-1β) and tumor necrosis factor alpha (TNFα) [11, 12], as well as their increased gap junction-mediated coupling following nerve injury [13]. In response to chronic pain, SGCs also upregulate the expression of glial fibrillary acidic protein (GFAP) and undergo cell division [14, 15].

The currently established role of glial cells in nociception suggests that the pharmacological manipulation of their reactivity might represent a groundbreaking analgesic strategy, as an alternative to a classical "neuron-centric" approach. It is therefore mandatory to identify the most promising key signaling pathways contributing to glial cell reaction to painful stimulation, which could be exploited pharmacologically. Here, we shall focus on the purinergic system, which in recent years has emerged as one of the most innovative and yet partially unexplored signaling systems controlling glial cell function under various pathological conditions, including pain. Far from being exhaustive in reviewing the exponentially growing number of publications in this field, this review aims at convincing the pain community that extracellular nucleotides and nucleosides are fundamental pro- and antinociceptive signals, mostly through their activity on peripheral and central glial cells.

2. Ionic Receptors Activated by Extracellular Nucleotides: The P2X Receptor Family

Extracellular nucleotides, mostly ATP but possibly also UTP, are costored in synaptic vesicles and actively released during physiological or pathological (i.e., excitotoxic) neurotransmission [16]. Glial sources of ATP have been also demonstrated, which contribute to physiological cell-to-cell communication [17]. Additionally, extracellular concentrations of nucleotides increase severalfold at sites of tissue damage, due to leakage of the intracellular nucleotide pool and degradation of nucleic acids [16, 17].

P2X receptors are membrane ion channels that open in response to the binding of extracellular ATP and elicit rapid responses (<10 ms), resulting in selective permeability to Na^+, K^+, and Ca^{2+} cations [18]. In vertebrates, seven genes encode P2X receptor subunits, which are 40–50% identical in their amino acidic sequence. Each subunit has two transmembrane domains, separated by an extracellular domain (~280 amino acids). Channels function as trimers of several subunits, and the extracellular domain is the portion containing the binding sites for nucleotides. To date, 7 homomeric (P2X1, P2X2, P2X3, P2X4, P2X5, P2X6, and P2X7), and 6 heteromeric P2X receptors (P2X1/2, P2X1/4, P2X1/5, P2X2/3, P2X2/6, and P2X4/6) have been identified, the latter showing specific pharmacological differences compared to their homomerical counterpart [18]. P2X receptors are differentially distributed among the cell types in different brain areas. Peripheral neurons mainly express the P2X3 and P2X2/3 receptor subtypes, which are involved in pain and temperature perception (see below) [19]. All P2X receptor subtypes can modulate membrane action potential. They are expressed either at the presynaptic level, regulating neurotransmitters release through the modulation of intracellular levels of Ca^{2+} ions, or postsynaptically, where they interact with ionotropic receptors (i.e., nicotinic; gamma-aminobutyric acid, GABA; N-Methyl-D-Aspartate, NMDA) via Ca^{2+}-dependent kinases [16]. P2X receptors are involved in a variety of physiological processes, including the modulation of cardiac rhythm and contractility, vascular tone, platelet aggregation, macrophage activation, apoptosis, neuron-glia communication, and modulation of nociception [20].

3. P2X Receptors and Chronic Pain: Not Only a Matter of Neurons

Since the first publications demonstrating the involvement of ATP in pain transmission [21], the expression levels and functions of P2X receptors have been characterized in neurons from dorsal root ganglia (DRG) and in the trigeminal nerve [22]. All P2X receptor subtypes, with the exception of P2X7, are expressed in sensory neurons; among these, the P2X3 subtype showed the highest expression levels [23]. To date, the most important P2X receptor subtypes involved in pain transmission are (i) the P2X3 and P2X2/3 receptor subtypes, expressed by sensory neurons, (ii) the P2X4 receptor, expressed by CNS microglia, and (iii) the P2X7 receptor, expressed by CNS microglia and astrocytes and by SGCs in sensory ganglia [24].

4. Neuronal P2X3 Receptors: Key Players in Nociception

Although this review article is focused on glial purinergic receptors involved in pain transmission, a brief summary of data on neuronal P2X3 subtype, the most studied P2X receptor subtype involved in nociception, cannot be omitted. P2X3 receptors are selectively expressed at high levels in nociceptive primary sensory neurons in trigeminal, nodose, and dorsal root ganglia [25]. The selective expression of P2X3 receptors in these areas involved in pain transmission suggested that they may be crucial in processing pain signals, and several studies have evaluated the relationships between P2X3 receptors and pain sensation.

P2X3 receptors have been initially cloned and functionally characterized from rat DRG [26], showing their unique expression in small and medium size sensory neurons and their absence in large diameter neurons [27, 28]. On the other hand, P2X3 has never been found to be expressed by glial cells, by either immunohistochemical analysis or calcium imaging [29]. P2X3 immunoreactivity has also been observed in other structures indirectly involved in nociceptive transmission, such as the nucleus of the solitary tract, and the spinal trigeminal nucleus [30].

A number of *in vitro* and *in vivo* studies have evaluated the relationships between P2X3 receptors and pain transmission.

Local injection of P2X3 receptor agonists, such as ATP or α,β-methyleneATP, into the hind paws of rats induced nociceptive behaviors and reduced thermal and mechanical thresholds [31, 32]. During inflammation and chronic constriction injuries, ATP concentrations and neuronal expression of P2X3 receptors are upregulated in DRG, trigeminal ganglion (TG), and spinal cord [33, 34]. In animal models of inflammatory and neuropathic pain, P2X3 receptor knockout or its downregulation by antisense oligonucleotides or by short interfering RNA significantly attenuated painful behaviors, including tactile allodynia and mechanical hyperalgesia [35]. In addition, the nonselective P2X3 receptor antagonists TNP-ATP [2′,3′-O-(2,4,6 trinitrophenyl) adenosine-5′-triphosphate] and PPADS pyridoxal phosphate-6-azophenyl-2′,4′ disulfonic acid reduced the excitability of DRG neurons and neuropathic pain [36]. Overall, these findings suggest that neuronal P2X3 receptors play a crucial role in the development and maintenance of chronic pain.

Despite the above-mentioned results, more recent studies have shown a transient decrease in P2X3 expression in a model of partial damage of the mental nerve (belonging to the mandibular branch of the trigeminal nerve), or no significant expression changes following resection of the lingual nerve [37]. It is possible that these differences reflect the type of lesion: after a constriction (i.e., application of a ligature) an increase in the expression levels is observed, while nerve injury or full axotomy leads to reduction or no changes of receptor expression. More importantly, it has been observed that variations in P2X3 expression levels are modulated at different time points after the lesion; a transient decrease in the expression was observed in the first two weeks after nerve injury, followed by an increase during the following weeks, paralleled by the increased expression of glial cell-derived neurotrophic factor (GDNF) and the generation of new neuronal branches (sprouting) in the damaged sensory areas [38]. Therefore, the timing and the type of lesion are critical for the observed results. Finally, it is also worth mentioning that P2X3 receptors are involved in the mechanism of action of known analgesics, as recently shown for the nonsteroidal anti-inflammatory drug naproxen, which inhibits P2X3 activation in the TG [39]. Moreover, it is now emerging that bioactive molecules contained in analgesic preparation from traditional Chinese medicine (such as tetramethylpyrazine, sodium ferulate, and puerarin) can inhibit P2X3-mediated transmission in primary afferent neurons [40].

5. Glial P2X4 and P2X7 Receptors

Microglia-neuron communication is bidirectional, and several lines of evidence implicate ATP as a critical signaling molecule [41–43]. Microglia expression of P2X receptors is restricted to the P2X4 and P2X7 subtypes [42, 44], whose activation evokes current responses, increases intracellular $[Ca^{2+}]$, and causes the release of signaling molecules affecting neuronal functions [45, 46].

The central role of P2X4 receptor subtype in neuropathic pain was first reported by [47]. In this paper, authors showed that intrathecal injection of TNP-ATP, acting as antagonist at P2X1-4 receptor subtypes, reverted tactile allodynia in nerve-injured rats. On the contrary, treatment with PPADS, antagonist at P2X1-3, 5, and 7 but not at P2X4 receptor, had no effect. Authors therefore concluded that the main P2X receptor subtype involved in central responses to peripheral nerve injury is the P2X4 receptor, and the development and maintenance of tactile allodynia require its activation. To confirm this hypothesis, targeting P2X4 receptors with antisense oligonucleotides [47] or the genetic deletion of the *P2rx4* gene [48] significantly attenuated nerve injury-induced pain phenotypes. Moreover, the development of tactile allodynia correlated with a progressive increase in spinal P2X4 receptor expression, which is generally low in naïve CNS [48].

Further immunohistochemical analysis of wild-type (wt) mice, and studies on transgenic mice selectively expressing the green fluorescent protein in microglial cells revealed that this cell population rather than neurons or astrocytes was expressing the P2X4 receptor subtype [48] and that the increase in P2X4 receptor expression temporally correlated with the development of tactile allodynia. P2X4 receptor upregulation was a consequence, rather than a cause of microglia activation; in fact, preventing the increase in P2X4 receptor did not affect the expression of protein markers of microglia activation, such as complement receptor 3 or the ionized calcium binding adaptor molecule-1 (Iba-1) [47, 48]. Interestingly, activation of microglial P2X4 receptor is sufficient to elicit pain, since the intrathecal injection of P2X4 receptor-stimulated cultured microglia induced mechanical allodynia in naïve animals [41, 47, 49]. Taken together, pharmacological, genetic, and behavioral findings indicate that activation of P2X4 receptor subtype expressed by spinal microglia is both necessary and sufficient to induce tactile allodynia after peripheral nerve injury.

Concerning the bidirectional cross talk between activated microglia and dorsal horn neurons, the chemokine (C-C motif) ligand 21 (CCL21) released from injured neurons has been demonstrated to act as an upstream activator of P2X4 receptor [50], in close collaboration with interferon γ, a cytokine converting resting spinal microglia into its activated state [51], and tryptase, a protease released from mast cells that activates proteinase-activated receptor 2 in microglia [52] (Figure 1). Another critical element for the upregulation of P2X4 receptors expression is the extracellular matrix molecule fibronectin, which modulates the transcriptional and posttranscriptional levels of P2X4 receptor expression in microglia through the activity of Lyn kinase and the downstream activation of intracellular signaling pathways involving phosphatidylinositol 3-kinase- (PI3 K-) Akt and mitogen-activated protein kinase kinase- (MAPK kinase, MEK-) extracellular signal-regulated kinase (ERK) [49, 53, 54]. The implications of this wide modulation network and whether these elements are connected into a common pathway controlling P2X4 receptor expression are still not known.

On the other way around, it has been reported that the activation of microglial P2X4 receptor promoted the synthesis and release of brain-derived neurotrophic factor (BDNF), through the activation of p38 MAPkinase [48, 55].

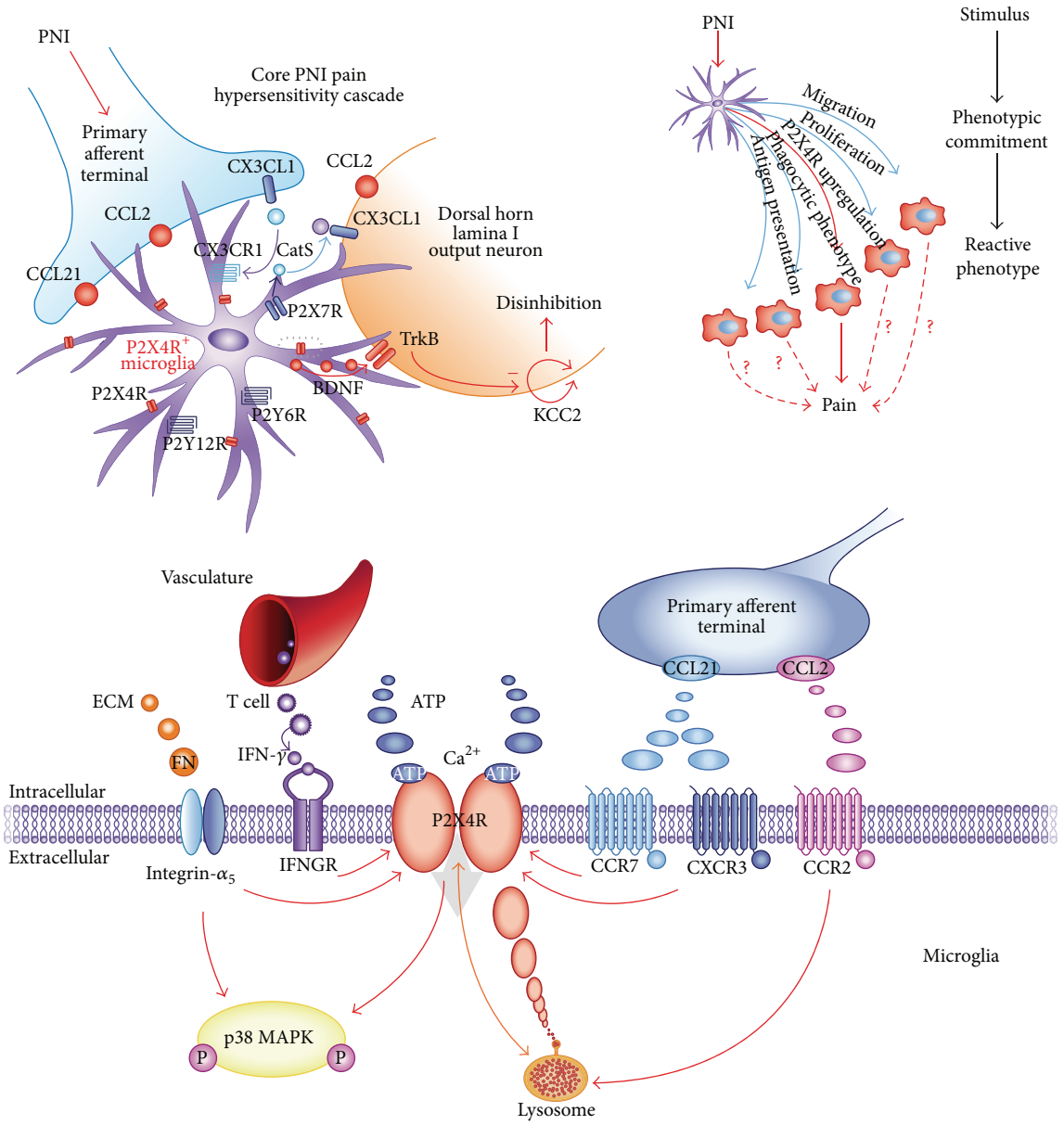

Figure 1: Central role of microglial P2X4 receptors in mediating a molecular cascade leading to hypersensitivity after peripheral nerve injury (PNI). The upper left cartoon shows the neuron-to-microglia cross talk triggered by neuronal injury, leading to the appearance of an "activated" microglia phenotype, which expresses higher levels of the P2X4 receptor. The dotted rectangle is expanded in the lower panel, showing the complex molecular network responsible for P2X4 receptor upregulation and involving chemokines, growth factors, and integrins. Activation of the P2X4 receptor ultimately leads to the recruitment and activation of p38 MAP kinase. Reproduced from [56] with permission from Nature Publishing Group.

BDNF in turn altered the transmembrane anion gradient in a subpopulation of dorsal horn lamina I neurons, through the downregulation of the neuronal chloride transporter KCC2. This makes GABA and glycine act as depolarizing rather than hyperpolarizing neurotransmitters, causing an aberrant nociceptive output that contributes to the development of neuropathic pain [41, 56].

In addition to the P2X4 subtype, microglial cells also express functional P2X7 receptors. The P2X7 receptor is a unique member of the P2X receptor family, since it is only activated by high concentrations of ATP (>100 μM) and can open a much larger membrane pore than any other P2X channel [57]. Stimulation of P2X7 receptors is implicated in microglia response to inflammation, release of proinflammatory cytokines, like IL-1β, and proliferation [58], underlining the involvement of this receptor subtype in inflammatory diseases and pain.

Although P2X7 receptors are expressed on a wide variety of cell types, evidence for involvement of microglial P2X7 receptors in chronic neuropathic pain stems from findings

that its activation causes the p38 MAPkinase-dependent release of IL-1β and cathepsin S, which contribute to the maintenance of mechanical hypersensitivity in the spinal cord [59, 60]. Additional hints on the role of P2X7 receptors in neuropathic pain have been provided by the demonstration of reduced pain sensitivity in P2X7 receptor-deficient mice [61] and by the analgesic effects exerted by P2X7 receptor antagonists [62, 63]. In fact, authors demonstrated the absence of inflammatory and neuropathic hypersensitivity In fact, in mice lacking the P2X7 receptor, authors demonstrated the absence of inflammatory and neuropathic hypersensitivity after both mechanical and thermal stimuli, accompanied by a reduction of adjuvant-induced increases in IL-1β, IL-6, IL-10, and macrophage chemoattractant protein-1, while normal nociceptive processing is preserved [61]. Moreover, P2X7 receptor was upregulated in human DRG and injured nerves from chronic neuropathic pain patients [61]. Recent studies also showed that P2X7 receptor expression is increased in the ipsilateral spinal cord after sciatic nerve ligation and is highly restricted to microglia; moreover, chronic constriction injury- (CCI-) induced mechanical allodynia and thermal hypersensitivity are reversed by intrathecal administration of the selective P2X7 antagonist Brilliant Blue G [64].

Interestingly, a correlation between single nucleotide polymorphisms (SNPs) within the coding sequence of the *P2rx7* gene and the sensitivity to chronic pain has been provided in both mice and humans. In fact, mice in which P2X7 receptors have impaired pore formation due to the P451L mutation showed less allodynia than mice with the wt pore-forming *P2rx7* allele. Indeed, administration of a peptide, which blocked pore formation but not cation channel activity, selectively reduced nerve injury and inflammatory allodynia only in wt mice. Moreover, in two independent human chronic pain cohorts, a cohort with pain after mastectomy and a cohort with osteoarthritis, authors observed a genetic association between lower pain intensity and the hypofunctional His270 allele of P2X7 receptor, further suggesting that selectively targeting P2X7 pore formation may be a new strategy for individualizing the treatment of chronic pain [65].

Several lines of evidence suggest a functional convergence between the signaling pathways activated by P2X4 and P2X7 receptors in microglia. As previously mentioned, p38 MAPkinase is involved in both the P2X4 receptor-mediated release of BDNF and the P2X7-induced release of IL-1β and cathepsin S (see above). Moreover, a recent paper showed that phosphorylation of p38 MAPK via P2X7 receptor may induce tactile allodynia/hyperalgesia in an orofacial pain model based on the CCI of the infraorbital nerve (CCI-ION), which is most likely mediated by soluble TNF-α released by microglia [66]. Thus, activation of p38 MAPK may be a critical mechanistic step of convergence in the P2X7 and P2X4 receptor signaling pathways in neuropathic pain. P2X7 and P2X4 receptors also interact to form complexes with unique channel properties [44, 67]. This raises the interesting possibility that structural and functional interactions, as well as converging signaling pathways, might be critical cellular mechanisms that underlie the involvement of microglial P2X7 and P2X4 receptors in neuropathic pain. The expression of P2X4 and P2X7 receptors subtype in a variety of cell types involved in pain transmission represents a promising target for pharmacological intervention. For example, locally administered oxidized ATP, an irreversible inhibitor of P2X7 receptors, had an antihyperalgesic effect on complete Freund's adjuvant-induced mechanical hyperalgesia (paw pressure test) [68].

An important role has been also disclosed for the P2X7 receptor subtype in the modulation of reactive astrogliosis. Following trauma, an upregulation of its expression on astrocytes has been demonstrated, and its activation by extracellular ATP or by synthetic agonists led to the release of proinflammatory IL-1β, ATP itself, and glutamate [17]. These molecules can further sustain and propagate astrocytic reaction to injury and can also sensitize nearby neurons in the spinal cord, thus contributing to nociception. More recently, the P2X7-mediated astrocytic release of dynorphins has been demonstrated in the spinal cord [69], thus further corroborating the notion of a direct involvement of astrocytic P2X7 receptor subtype in nociception.

The role of glial P2X7 in nociception is not restricted to the CNS, since recent data established its expression in SGCs, the specialized population of glial cells that enwrap neuronal bodies in peripheral sensory ganglia [10]. In sensory ganglia, ATP released from neuronal somata engages P2X7 receptors expressed by surrounding SGCs [12], which in turn inhibits back neuronal algogenic P2X3 receptors [70]. Additional P2X receptor subtypes are upregulated in SGCs upon exposure to proinflammatory conditions [71], but their role in nociception still remains elusive.

6. G Protein-Coupled Receptors Activated by Extracellular Nucleotides: The P2Y Receptor Family

The first P2Y receptor (currently named as the $P2Y_1$ subtype) was cloned in 1993 [76, 77], and since then a total of eight human P2Y receptor subtypes have been identified: the $P2Y_1$, $P2Y_2$, $P2Y_4$, $P2Y_6$, $P2Y_{11}$, $P2Y_{12}$, $P2Y_{13}$, and $P2Y_{14}$ receptors [78]. The various P2Y receptor subtypes are functionally coupled to different G proteins, and, consequently, downstream signaling pathways, either phospholipase C, with inositol 3 phosphate (IP_3) formation and intracellular calcium increase, or adenylyl cyclase, leading to modulation of cyclic adenosine monophosphate (cAMP) production [78]. From a pharmacological point of view, P2Y receptors can be broadly subdivided into four groups based on their responsivity to nucleotides: (i) adenine nucleotide-preferring receptors, mainly responding to ADP and ATP; this group includes human and rodent $P2Y_1$, $P2Y_{12}$, and $P2Y_{13}$, and human $P2Y_{11}$; (ii) uracil nucleotide-preferring receptors, including the human $P2Y_4$ and $P2Y_6$ responding to either UTP or UDP; (iii) receptors of mixed selectivity (the human and rodent $P2Y_2$, the rodent $P2Y_4$ and, possibly, $P2Y_{11}$); and (iv) the $P2Y_{14}$ receptor, responding to both UDP and sugar nucleotides (mainly UDP-glucose and UDP-galactose) [78, 79].

7. Glial P2Y Receptors and Chronic Pain: Still Elusive but Promising Targets for New Analgesic Strategies

Unlike the key and quite well defined role played by P2X receptors in pain transmission, controversial information is currently available concerning P2Y receptor contribution to nociception. Nevertheless, it is well known that these receptors are widely expressed by neurons and glial cells in both the central and the peripheral nervous systems [16], thus leading to hypothesize that their activity is integrated in the complex molecular network associated with the transmission of nociceptive signals. The comprehension of their role in pain pathogenesis is therefore of paramount importance for the discovery of new potential drug targets for pain therapy.

As for P2Y receptors expressed by sensory neurons, the $P2Y_1$ receptor subtype is often coexpressed with the P2X3 receptor, acting as its functional antagonist in DRG [80], while the $P2Y_{12,13}$ subtypes can inhibit N-type voltage-gated calcium channels [81]. Taken together, these data suggest an overall analgesic profile for ADP-sensitive P2Y receptor activation. Surprisingly, $P2Y_1$ receptors were also reported to mediate hyperalgesia, possibly through the sensitization of transient receptor potential vanilloid 1 ($TRPV_1$) channels [82], thus suggesting that the functional outcome of $P2Y_1$ receptor activation could depend upon the specific tissue conditions. The same hyperalgesic potentiation of TRPV1 receptors has been later demonstrated for the UTP-sensitive $P2Y_2$ receptor subtype in rat lumbar DRGs [83].

Increasing evidence is highlighting a role for glial P2Y receptors in chronic pain. Microglia express a wide range of P2Y receptors ($P2Y_{1,2,4,6,12}$), with the $P2Y_6$ and $P2Y_{12}$ receptor subtypes mediating chemotaxis and migration towards the site of damage [43, 84]. To date, only the $P2Y_{12}$ receptor subtype is clearly known to be involved in neuropathic pain onset. In fact, in response to peripheral nerve injury, microglial $P2Y_{12}$ receptor expression was upregulated, and its activation was critical for microglial engulfment of myelinated axons in the spinal dorsal horn [43]. Moreover, pharmacological blockade, antisense knockdown of $P2Y_{12}$ receptor expression, or genetic deletion of the *P2ry12* gene suppresses both mechanical allodynia and thermal hyperalgesia in nerve-injured rats [85, 86]. Conversely, intrathecal administration of the $P2Y_{12}$ receptor agonist 2Me-SADP elicits pain behavior in naïve rats, mimicking what is observed in nerve-injured rats [85]. Moreover, mRNA not only for the $P2Y_{12}$, but also for the $P2Y_{6,13,14}$ receptor subtypes was upregulated in microglia in the ipsilateral spinal cord following nerve injury, and a mixture of $P2Y_6$, $P2Y_{12}$, and $P2Y_{13}$ selective antagonists showed a longer suppressive effect on pain behavior compared to every single treatment itself [87].

The $P2Y_6$ receptor can be considered a sensor for microglial cell phagocytosis by sensing diffusible UDP signals in primary cultured microglial cells [84]. Although microglial $P2Y_6$ receptors expression markedly increases in the spinal cord after peripheral nerve injury [87], its specific role under neuropathic pain conditions still remains unclear. As already mentioned, ATP-gated P2X4 receptor channels expressed in spinal microglia actively participate in central sensitization, making their functional regulation a key process in chronic pain pathologies (see above); interestingly, it has been recently reported that P2X4 receptors function is inhibited by the $P2Y_6$ receptor subtype, highlighting its possible critical role in regulating neuropathic pain-induced microglial responses [88].

Although not directly associated with pain signaling to date, it is conceivable that also P2Y receptors expressed by astrocytes could significantly contribute to nociception, especially in the spinal cord. P2Y receptors have been directly implicated in the modulation of reactive astrogliosis since the 1990s, also thanks to the contribution of our laboratory (for reviews, see [9, 89]). In particular, activation of the $P2Y_1$ receptor subtype has been directly correlated with the release of prostaglandins and other proinflammatory mediators [90, 91] and directly or indirectly correlated with the transmission of painful sensations. Targeting astrocytic P2Y receptors could therefore represent an innovative approach to pain, specifically neuropathic pain, through the modulation of astroglial inputs controlling second order spinal neurons firing.

Very few data are currently available on the role of the P2Y receptor family in SGCs, and the vast majority of the available data concerns expression rather than functional studies (for reviews see [75, 92]). Under basal conditions, SGCs in the trigeminal ganglion express functional $P2Y_{1,2,4,6,13}$ receptor subtypes [28, 93], whereas glial P2Y expression in DRG cells has been only evaluated at the mRNA level [94], with the exception of $P2Y_1$ receptors protein which has been detected by immunofluorescence studies [70].

Within the TG, the close interplay between the purinergic system and other classical pain transducing signals has been recently elucidated, starting from the observation that chronic exposure of TG cultures to the algogenic mediator bradykinin induced the upregulation of P2Y-mediated calcium signaling in SGCs [28, 95], thus prompting us to speculate that P2Y receptors expressed by SGCs could represent possible pharmacological targets for the development of innovative therapies against migraine and trigeminal pain in general (for review see [75]). From then on, *in vitro* and *in vivo* studies have revealed that those specific glial P2Y receptors potentiated under proalgogenic conditions are the $P2Y_1$ and $P2Y_2$ subtypes (Magni et al., manuscript in preparation). These results have been partially confirmed by a recent paper showing that $P2Y_2$ receptor inhibition induces analgesia in a rat model of neuropathic pain based on CCI-ION [96], although authors mostly focused on $P2Y_2$ receptors expressed by trigeminal sensory neurons. Altogether, these data highlight the key role of P2Y purinergic receptors, and especially of the $P2Y_2$ subtype, as promising targets for the development of new analgesic drugs.

An emerging role for the glial $P2Y_{12}$ receptor subtype has been demonstrated in an animal model of trigeminal neuropathic pain [97]. In fact, although not expressed in the TG upon control conditions [14], expression of the $P2Y_{12}$ receptor subtype was detected in activated SGCs after unilateral lingual nerve crush. Interestingly, administration

of a $P2Y_{12}$-selective antagonist significantly reverted glial cell activation and alleviated animals' sensitivity to mechanical and heat stimulation of the tongue [97]. These data further sustain the hypothesis that a shift and/or upregulation in purinergic receptor expression can be observed within sensory ganglia, and especially on SGCs, upon proalgogenic conditions (Figure 2). This observation opens up the possibility that drugs selectively targeting specific purinergic receptors could exert their analgesic activity at the site of receptor upregulation, thus limiting the occurrence of systemic and unwanted side effects.

8. Adenosine Exerts Analgesic Effects through Its Glial Receptors: An Additional Component of Its Neuromodulatory Actions

Adenosine is the major metabolite of the ectonucleotidase-mediated sequential dephosphorylation of ATP. Therefore, it cannot be classified as a true neurotransmitter, but rather as a neuromodulator, through the activation of 4 subtypes of G protein-coupled receptors, that is, the A_1, A_{2A}, A_{2B}, and A_3 adenosine receptor subtypes, collectively referred to as P1 receptors [98]. The temporal relationship between ATP release and subsequent adenosine generation from its hydrolysis guarantees the generation of a feedback inhibitory loop, which overall counteracts the excitatory effects of ATP. This is particularly true for the A_1 receptor subtype, which is coupled with inhibition of cAMP synthesis and with the activation of potassium conductance, with consequent inhibition of neuronal firing and neurotransmitter release, reduction of heart rate, and other inhibitory effects.

A key role for the A_1 receptor subtype in the modulation of painful sensations has been hypothesized more than 15 years ago. Both spinal and peripheral A_1 receptors have been found directly involved in the analgesic effects exerted by several known drugs, like tramadol, acetaminophen, and amitriptyline, often in close interconnection with 5-HT_7 serotonin receptors [99–101]. Moreover, recent studies also suggest that the analgesic efficacy of some herbal preparations long utilized in traditional Chinese medicine can be at least in part due to a modulation of the adenosine system. In fact, norisoboldine (the major active alkaloid component isolated from the dry roots of *Lindera aggregata* often utilized for chest and abdomen pain, indigestion, cold hernia, and frequent urination) was shown to promote analgesia in both the formalin and the writhing tests in rodents through the activation of A_1 receptor subtype [102].

The cell population expressing the A_1 receptor subtype involved in pain transmission was not clearly identified, until the publication of papers suggesting its microglial identity. An A_1 receptor subtype selective agonist was in fact shown to alleviate neuropathic pain and to reduce spinal microglia activation in the spared nerve injury rat model [103]. Most interestingly, authors later demonstrated that exposure to proalgogenic ATP induced a significant increase in A_1 receptor subtype expression in microglia, whose activation in turn led to inhibition of microglial phenotypic changes and to the reduction of the ability of microglia to promote neuronal firing [104]. Thus, it can be envisaged that microglial A_1 receptors are upregulated and engaged to counteract the algogenic actions induced by massive ATP release at injury or inflammation sites.

The role of additional adenosine receptor subtypes in nociception is much less clear. Conflicting results have been obtained by administering either A_{2A} receptor subtype-selective agonists or antagonists in animal pain models, showing both analgesia and hyperalgesia [105]. In fact, it has been demonstrated that A_{2A} receptor knock-out mice have a reduced sensitivity to pronociceptive stimuli, which seems to be mediated by the loss of pronociceptive A_{2A} receptors on DRG primary sensory neurons [106]. It should be mentioned, however, that microglia express A_{2A} receptors, which are directly involved in the modulation of the release of proalgogenic stimuli, like nerve growth factor (NGF), prostaglandin E2 (PGE_2), and nitric oxide (NO) [107]. Based on the above-mentioned data, it can therefore be envisaged that selective A_{2A} receptor antagonists could counteract the proinflammatory and proalgogenic features of microglial cells and ultimately prove to be useful as antialgogenic agents, at least in inflammatory pain conditions. Conversely, the intrathecal injection of a selective A_{2A} receptor agonist produced a significant and long-lasting reversal of mechanical allodynia and thermal hyperalgesia consequent to the CCI of the sciatic nerve [108]. A reduction of glial cell activation and a significant upregulation in the production of anti-inflammatory IL-10 in the spinal cord were also observed, thus suggesting that activating rather than inhibiting the A_{2A} receptor subtype could represent a better option for neuropathic pain states [108].

Finally, the availability of selective agonist ligands has allowed demonstrating an antialgogenic role for the A_3 receptor subtype in neuropathic pain induced either by the CCI of the sciatic nerve or by chemotherapic agents in rodents [109]. The cellular localization of the target receptors involved in nociception has not been directly identified, although it has been demonstrated that the A_3 receptor subtype is involved in ADP-mediated microglia chemotaxis and process extension [110].

Although their direct role in pain transmission has not been proven yet, it is worth mentioning that all the four adenosine receptor subtypes are expressed by spinal cord and brain astrocytes and significantly contribute to the modulation of reactive astrogliosis (for review see [111]). It is therefore conceivable that they can participate to astrocytic modulation of neuronal functions, especially under chronic pain conditions, when high amounts of adenosine are produced as a consequence of the hydrolysis of extracellular nucleotides and of the leakage of nucleic acids from damaged cells [111]. To date the role of adenosine receptors in peripheral ganglia has not been studied in detail.

A major limitation to the systemic use of drugs acting on adenosine receptors is represented by their wide distribution, especially in the CNS and in the cardiovascular system, which could account for significant and harmful side effects. Specifically, activation of the A_1 adenosine receptors in the CNS could lead to inhibition of locomotor activity

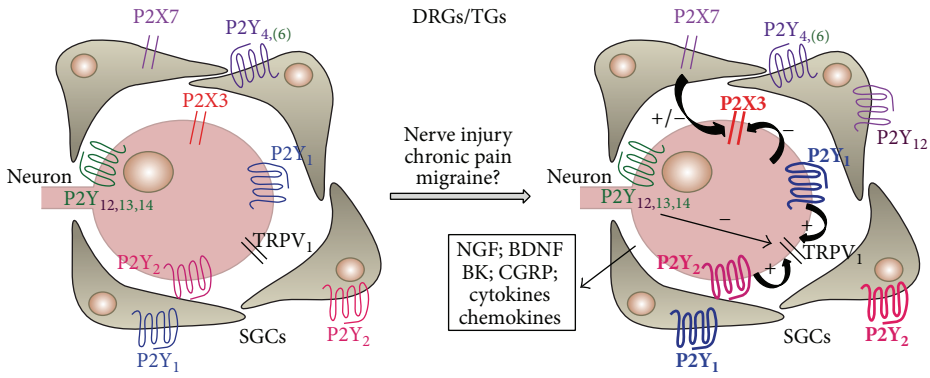

FIGURE 2: Plasticity of purinergic signaling within sensory ganglia upon proinflammatory conditions. The cartoon schematically summarizes currently available data on the modulation of P2 receptor expression by proalgogenic and proinflammatory conditions in sensory ganglia. An increased line weight indicates receptor upregulation, which has been observed in both sensory neurons and surrounding satellite glial cells. Some receptor subtypes (i.e., glial $P2Y_{12}$ receptor subtype) are only detected upon algogenic conditions. Activation of P2 receptors by extracellular nucleotides leads to the modulation of other systems involved in nociception, like TRPV1 receptors, and in the release of additional cytokines, growth factors, and other substances (see box), further contributing to the development and maintenance of a proalgogenic milieu. Reproduced from [75] with permission from Elsevier.

and catalepsy, whereas in the heart severe bradycardia and atrioventricular block may occur [112]. Acting on the A_{2A} subtype with selective agonists may lead to a significant drop in blood pressure, accompanied by tachycardia [112]. Conversely, despite the significant increase of circulating histamine that was observed in mice, clinical studies in cancer patients have shown no significant side effects after administration of selective A_3 receptor agonists [112].

9. When Will an Analgesic Drug Targeting Glial Purinergic Receptors Be Finally Available?

The incomplete and still growing list of scientific studies reviewed in this paper clearly demonstrates that targeting glial purinergic receptors might significantly improve the currently available armamentarium of analgesic drugs to be utilized in chronic pain state, still lacking a satisfactory pharmacological control. Nevertheless, to date no new purinergic drug entities have reached the market. This is mostly due to (i) the widespread expression of all the different receptor subtypes, which renders the discrimination between beneficial and side effects extremely complicated, (ii) the lack of good subtype-selective agents, and (iii) when selective ligands are available, the lack of an acceptable route of administration to humans.

Concerning the most studied purinergic receptor in nociception, the neuronal P2X3 subtype, no clinical studies were available so far, despite the massive preclinical *in vivo* and *in vitro* efforts. This was mainly due to the lack of selective antagonists with a chemical structure suitable for administration to humans [37]. Very recently, however, two clinical trials employing the new orally active P2X3-selective antagonist AF-219 [113] were concluded (see Table 1), although results have not been disclosed yet. Recently, the extensive use of high-throughput screening followed by a hit-to-lead program has prompted a number of pharmaceutical companies to identify highly selective, potent, and metabolically stable small-molecule inhibitors for both P2X4 and P2X7 receptor, which provide a novel therapeutic approach to the treatment of pain and inflammatory disorders [114, 115]. Nevertheless, no significant results have emerged from the first clinical trials performed with different P2X7-selective antagonists (Table 1), thus suggesting that the role of this receptor subtype should be reconsidered, at least in rheumatoid arthritis-related pain.

As for P2Y receptors, although important progress in exploring structure-activity relationships has been recently achieved with the publication of the first crystal structure of a member of the family [116], most of the P2Y receptor subtypes are still lacking potent and selective synthetic agonists and antagonists [78], which has greatly hampered both research in this field, and the translation of *in vitro* data to *in vivo* and clinical settings. Additionally, the only P2Y-selective antagonists available so far, acting on the $P2Y_{12}$ receptor subtype, are widely utilized for their strong antiplatelet activity [116], which poses serious concerns about possible side effects in case of their administration for painful conditions.

Finally, in the case of the A_1 adenosine receptor subtype, its widespread distribution has greatly limited the preclinical and clinical use of the available A_1-selective agonists, due to significant systemic side effects (see above). Recently, it has been demonstrated that a novel and potent A_1 receptor allosteric modulator, named TRR469, exhibits antinociceptive activity in the formalin and writhing tests in mice, without showing the usual side effects of A_1-selective agonists (see above) [117].

It is also worth reaffirming that expression of purinergic receptor on glial cells is highly plastic and can therefore significantly change during the course of chronic pain conditions (Figure 2). For example, it has been hypothesized that the purinergic system is fundamental for the so-called "modal shift" of microglia, namely, their acquisition of different

Table 1: Summary of past and current clinical trials evaluating purinergic ligands in pain.

Name of ligand	Company	Clinical trial number	Type of pain	Main outcomes
AF219 (P2X3 antagonist)	Afferent Pharmaceuticals	NCT01554579	Osteoarthritis of the knee	No published results yet
		NCT01569438	Interstitial cystitis/bladder pain syndrome	No published results yet
CE-224,535 (P2X7 antagonist)	Pfizer	NCT00628095	Rheumatoid arthritis	CE-224,535 was not efficacious, compared with placebo, for the treatment of RA in patients with an inadequate response to metotrexate [72]
		NCT00418782	Osteoarthritis of the knee	CE-224,535 failed to demonstrate efficacy in a 2-week study of knee pain in osteoarthritis patients
AZD9056	AstraZeneca	NCT00520572	Rheumatoid arthritis	AZD9056 does not have significant efficacy in the treatment of RA [73]
GSK1482160 (P2X7 antagonist)	GlaxoSmithKline	NCT00849134	"First-in-human" study to assess the pharmacokinetic profile of the drug	No major safety or tolerability concerns were identified in this study. Nevertheless, monitoring the release of IL-1β in subjects led to the decision to discontinue drug development for inflammatory pain conditions [74]
Adenosine (e.v.)	Wake Forest School of Medicine	NCT00349921	Neuropathic pain (comparison with clonidine)	No published results yet
	Xsira Pharmaceuticals	NCT00298636	Perioperative pain (hysterectomy/myomectomy)	No published results yet
GW493838	GlaxoSmithKline	NCT00376454	Neuropathic pain as a result of postherpetic neuralgia or nerve injury	No published results yet

phenotypes over time, based on the time-dependent modification of the expression profile of P1 and P2 receptors [118]. This additional fascinating, but complicating, issue should be taken into consideration when deciding which is the best target option for the development of an antihyperalgesic rather than an antiallodynic purinergic-based agent.

Therefore, based on these promises and pitfalls, a closer collaboration among pharmacology, biochemistry, molecular biology, and pharmaceutical chemistry is highly recommended to clearly identify and target the most promising "druggable" receptors, which could be successfully utilized in preclinical and clinical studies to accelerate the process towards new therapeutic options for chronic pain patients.

Conflict of Interests

The authors declare that there is no conflict of interests regarding the publication of this paper.

Acknowledgment

The financial contribution of the Fondazione Cariplo (Grant no. 2011-0505) is gratefully acknowledged.

References

[1] C. J. Woolf and M. W. Salter, "Neuronal plasticity: increasing the gain in pain," *Science*, vol. 288, no. 5472, pp. 1765–1768, 2000.

[2] F. Xu, Y. Li, S. Li et al., "Complete Freund's adjuvant-induced acute inflammatory pain could be attenuated by triptolide via inhibiting spinal glia activation in rats," *Journal of Surgical Research*, vol. 188, pp. 174–182, 2014.

[3] R. Ji, T. Berta, and M. Nedergaard, "Glia and pain: is chronic pain a gliopathy?" *Pain*, vol. 154, supplement 1, pp. S10–S28, 2013.

[4] M. Tsuda, K. Inoue, and M. W. Salter, "Neuropathic pain and spinal microglia: a big problem from molecules in "small" glia," *Trends in Neurosciences*, vol. 28, no. 2, pp. 101–107, 2005.

[5] M. R. Suter, Y. Wen, I. Decosterd, and R. Ji, "Do glial cells control pain?" *Neuron Glia Biology*, vol. 3, no. 3, pp. 255–268, 2007.

[6] I. Kazuhide and T. Makoto, "Microglia and neuropathic pain," *Glia*, vol. 57, no. 14, pp. 1469–1479, 2009.

[7] K. Inoue, "ATP receptors of microglia involved in pain," *Novartis Foundation Symposium*, vol. 276, pp. 263–272, 2006.

[8] V. Tiwari, Y. Guan, and S. N. Raja, "Modulating the delicate glial-neuronal interactions in neuropathic pain: promises and potential caveats," *Neuroscience & Biobehavioral Reviews*, vol. 45, pp. 19–27, 2014.

[9] A. Buffo, C. Rolando, and S. Ceruti, "Astrocytes in the damaged brain: molecular and cellular insights into their reactive

response and healing potential," *Biochemical Pharmacology*, vol. 79, no. 2, pp. 77–89, 2010.

[10] M. Hanani, "Satellite glial cells in sympathetic and parasympathetic ganglia: in search of function," *Brain Research Reviews*, vol. 64, no. 2, pp. 304–327, 2010.

[11] M. Takeda, T. Tanimoto, J. Kadoi et al., "Enhanced excitability of nociceptive trigeminal ganglion neurons by satellite glial cytokine following peripheral inflammation," *Pain*, vol. 129, no. 1-2, pp. 155–166, 2007.

[12] X. Zhang, Y. Chen, C. Wang, and L.-Y. M. Huang, "Neuronal somatic ATP release triggers neuron-satellite glial cell communication in dorsal root ganglia," *Proceedings of the National Academy of Sciences of the United States of America*, vol. 104, no. 23, pp. 9864–9869, 2007.

[13] M. Ledda, E. Blum, S. de Palo, and M. Hanani, "Augmentation in gap junction-mediated cell coupling in dorsal root ganglia following sciatic nerve neuritis in the mouse," *Neuroscience*, vol. 164, no. 4, pp. 1538–1545, 2009.

[14] G. Villa, S. Ceruti, M. Zanardelli et al., "Temporomandibular joint inflammation activates glial and immune cells in both the trigeminal ganglia and in the spinal trigeminal nucleus," *Molecular Pain*, vol. 6, article 89, 2010.

[15] M. Donegan, M. Kernisant, C. Cua et al., "Satellite glial cell proliferation in the trigeminal ganglia after chronic constriction injury of the infraorbital nerve," *Glia*, vol. 61, pp. 2000–2008, 2013.

[16] M. P. Abbracchio, G. Burnstock, A. Verkhratsky, and H. Zimmermann, "Purinergic signalling in the nervous system: an overview," *Trends in Neurosciences*, vol. 32, no. 1, pp. 19–29, 2009.

[17] G. Burnstock, U. Krügel, M. P. Abbracchio, and P. Illes, "Purinergic signalling: from normal behaviour to pathological brain function," *Progress in Neurobiology*, vol. 95, no. 2, pp. 229–274, 2011.

[18] R. A. North and M. F. Jarvis, "P2X receptors as drug targets," *Molecular Pharmacology*, vol. 83, no. 4, pp. 759–769, 2013.

[19] V. Khmyz, O. Maximyuk, V. Teslenko, A. Verkhratsky, and O. Krishtal, "$P2X_3$ receptor gating near normal body temperature," *Pflugers Archiv European Journal of Physiology*, vol. 456, no. 2, pp. 339–347, 2008.

[20] S. P. H. Alexander, H. E. Benson, E. Faccenda et al., "The concise guide to PHARMACOLOGY 2013/14: ligand-gated ion channels," *British Journal of Pharmacology*, vol. 170, no. 8, pp. 1582–1606, 2013.

[21] T. Bleehen and C. A. Keele, "Observations on the algogenic actions of adenosine compounds on the human blister base preparation," *Pain*, vol. 3, no. 4, pp. 367–377, 1977.

[22] P. M. Dunn, Y. Zhong, and G. Burnstock, "P2X receptors in peripheral neurons," *Progress in Neurobiology*, vol. 65, no. 2, pp. 107–134, 2001.

[23] Y. S. Kim, S. K. Paik, Y. S. Cho et al., "Expression of P2X3 receptor in the trigeminal sensory nuclei of the rat," *Journal of Comparative Neurology*, vol. 506, no. 4, pp. 627–639, 2008.

[24] G. Burnstock, "Purines and sensory nerves," *Handbook of Experimental Pharmacology*, vol. 194, pp. 333–392, 2009.

[25] J. H. Cho, K. Y. Jung, Y. Jung et al., "Design and synthesis of potent and selective P2X3 receptor antagonists derived from PPADS as potential pain modulators," *European Journal of Medicinal Chemistry*, vol. 70, pp. 811–830, 2013.

[26] C. C. Chen, A. N. Akopian, L. Sivilotti, D. Colquhoun, G. Burnstock, and J. N. Wood, "A P2X purinoceptor expressed by a subset of sensory neurons," *Nature*, vol. 377, no. 6548, pp. 428–431, 1995.

[27] R. A. North, "P2X3 receptors and peripheral pain mechanisms," *The Journal of Physiology*, vol. 554, no. 2, pp. 301–308, 2004.

[28] S. Ceruti, M. Fumagalli, G. Villa, C. Verderio, and M. P. Abbracchio, "Purinoceptor-mediated calcium signaling in primary neuron-glia trigeminal cultures," *Cell Calcium*, vol. 43, no. 6, pp. 576–590, 2008.

[29] S. K. Hullugundi, M. D. Ferrari, A. M. J. M. van den Maagdenberg, and A. Nistri, "The mechanism of functional upregulation of P2X3 receptors of trigeminal sensory neurons in a genetic mouse model of familial hemiplegic migraine type 1 (FHM-1)," *PLoS ONE*, vol. 8, no. 4, Article ID e60677, 2013.

[30] I. J. Llewellyn-Smith and G. Burnstock, "Ultrastructural localization of P2X3 receptors in rat sensory neurons," *NeuroReport*, vol. 9, no. 11, pp. 2545–2550, 1998.

[31] M. Tsuda, S. Koizumi, A. Kita, Y. Shigemoto, S. Ueno, and K. Inoue, "Mechanical allodynia caused by intraplantar injection of P2X receptor agonist in rats: involvement of heteromeric P2X2/3 receptor signaling in capsaicin-insensitive primary afferent neurons," *Journal of Neuroscience*, vol. 20, no. 15, article RC90, 2000.

[32] Y. Chen, G. W. Li, C. Wang, Y. Gu, and L. M. Huang, "Mechanisms underlying enhanced P2X receptor-mediated responses in the neuropathic pain state," *Pain*, vol. 119, no. 1–3, pp. 38–48, 2005.

[33] K. Kage, W. Niforatos, C. Z. Zhu, K. J. Lynch, P. Honore, and M. F. Jarvis, "Alteration of dorsal root ganglion P2X3 receptor expression and function following spinal nerve ligation in the rat," *Experimental Brain Research*, vol. 147, no. 4, pp. 511–519, 2002.

[34] R. D. Cheng, W. Z. Tu, W. S. Wang et al., "Effect of electroacupuncture on the pathomorphology of the sciatic nerve and the sensitization of $P2X_3$ receptors in the dorsal root ganglion in rats with chronic constrictive injury," *Chinese Journal of Integrative Medicine*, vol. 19, no. 5, pp. 374–379, 2013.

[35] J. Barclay, S. Patel, G. Dorn et al., "Functional downregulation of P2X3 receptor subunit in rat sensory neurons reveals a significant role in chronic neuropathic and inflammatory pain," *The Journal of Neuroscience*, vol. 22, no. 18, pp. 8139–8147, 2002.

[36] P. Honore, J. Mikusa, B. Bianchi et al., "TNP-ATP, a potent P2X3 receptor antagonist, blocks acetic acid-induced abdominal constriction in mice: comparison with reference analgesics," *Pain*, vol. 96, no. 1-2, pp. 99–105, 2002.

[37] A. P. Ford, "In pursuit of P2X3 antagonists: novel therapeutics for chronic pain and afferent sensitization," *Purinergic Signalling*, vol. 8, no. 1, pp. 3–26, 2012.

[38] A. M. W. Taylor and A. Ribeiro-da-Silva, "GDNF levels in the lower lip skin in a rat model of trigeminal neuropathic pain: implications for nonpeptidergic fiber reinnervation and parasympathetic sprouting," *Pain*, vol. 152, no. 7, pp. 1502–1510, 2011.

[39] T. Hautaniemi, N. Petrenko, A. Skorinkin, and R. Giniatullin, "The inhibitory action of the antimigraine nonsteroidal anti-inflammatory drug naproxen on P2X3 receptor-mediated responses in rat trigeminal neurons," *Neuroscience*, vol. 209, pp. 32–38, 2012.

[40] S. Liang, C. Xu, G. Li, and Y. Gao, "P2X receptors and modulation of pain transmission: focus on effects of drugs and compounds used in traditional Chinese medicine," *Neurochemistry International*, vol. 57, no. 7, pp. 705–712, 2010.

[41] J. A. M. Coull, S. Beggs, D. Boudreau et al., "BDNF from microglia causes the shift in neuronal anion gradient underlying

neuropathic pain," *Nature*, vol. 438, no. 7070, pp. 1017–1021, 2005.

[42] M. F. Jarvis, "The neural-glial purinergic receptor ensemble in chronic pain states," *Trends in Neurosciences*, vol. 33, no. 1, pp. 48–57, 2010.

[43] M. Maeda, M. Tsuda, H. Tozaki-Saitoh, K. Inoue, and H. Kiyama, "Nerve injury-activated microglia engulf myelinated axons in a $P2Y_{12}$ signaling-dependent manner in the dorsal horn," *Gila*, vol. 58, no. 15, pp. 1838–1846, 2010.

[44] T. Trang, S. Beggs, and M. W. Salter, "ATP receptors gate microglia signaling in neuropathic pain," *Experimental Neurology*, vol. 234, no. 2, pp. 354–361, 2012.

[45] T. Trang, S. Beggs, and M. W. Salter, "Brain-derived neurotrophic factor from microglia: a molecular substrate for neuropathic pain," *Neuron Glia Biology*, vol. 7, no. 1, pp. 99–108, 2012.

[46] M. R. Bianco, G. Cirillo, V. Petrosino et al., "Neuropathic pain and reactive gliosis are reversed by dialdehydic compound in neuropathic pain rat models," *Neuroscience Letters*, vol. 530, no. 1, pp. 85–90, 2012.

[47] M. Tsuda, Y. Shigemoto-Mogami, S. Koizumi et al., "P2X4 receptors induced in spinal microglia gate tactile allodynia after nerve injury," *Nature*, vol. 424, no. 6950, pp. 778–783, 2003.

[48] L. Ulmann, J. P. Hatcher, J. P. Hughes et al., "Up-regulation of P2X4 receptors in spinal microglia after peripheral nerve injury mediates BDNF release and neuropathic pain," *Journal of Neuroscience*, vol. 28, no. 44, pp. 11263–11268, 2008.

[49] M. Tsuda, E. Toyomitsu, T. Komatsu et al., "Fibronectin/integrin system is involved in P2X(4) receptor upregulation in the spinal cord and neuropathic pain after nerve injury," *Glia*, vol. 56, no. 5, pp. 579–585, 2008.

[50] K. Biber, M. Tsuda, H. Tozaki-Saitoh et al., "Neuronal CCL21 up-regulates microglia P2X4 expression and initiates neuropathic pain development," *EMBO Journal*, vol. 30, no. 9, pp. 1864–1873, 2011.

[51] M. Tsuda, T. Masuda, J. Kitano, H. Shimoyama, H. Tozaki-Saitoh, and K. Inoue, "IFN-γ receptor signaling mediates spinal microglia activation driving neuropathic pain," *Proceedings of the National Academy of Sciences of the United States of America*, vol. 106, no. 19, pp. 8032–8037, 2009.

[52] H. Yuan, X. Zhu, S. Zhou et al., "Role of mast cell activation in inducing microglial cells to release neurotrophin," *Journal of Neuroscience Research*, vol. 88, no. 6, pp. 1348–1354, 2010.

[53] K. Nasu-Tada, S. Koizumi, M. Tsuda, E. Kunifusa, and K. Inoue, "Possible involvement of increase in spinal fibronectin following peripheral nerve injury in upregulation of microglial P2X4, a key molecule for mechanical allodynia," *Glia*, vol. 53, no. 7, pp. 769–775, 2006.

[54] M. Tsuda, H. Tozaki-Saitoh, T. Masuda et al., "Lyn tyrosine kinase is required for P2X4 receptor upregulation and neuropathic pain after peripheral nerve injury," *GLIA*, vol. 56, no. 1, pp. 50–58, 2008.

[55] T. Trang, S. Beggs, X. Wan, and M. W. Salter, "P2X4-receptor-mediated synthesis and release of brain-derived neurotrophic factor in microglia is dependent on calcium and p38-mitogen-activated protein kinase activation," *Journal of Neuroscience*, vol. 29, no. 11, pp. 3518–3528, 2009.

[56] S. Beggs, T. Trang, and M. W. Salter, "P2X4R + microglia drive neuropathic pain," *Nature Neuroscience*, vol. 15, no. 8, pp. 1068–1073, 2012.

[57] R. A. North, "Molecular physiology of P2X receptors," *Physiological Reviews*, vol. 82, no. 4, pp. 1013–1067, 2002.

[58] M. Monif, G. Burnstock, and D. A. Williams, "Microglia: proliferation and activation driven by the P2X7 receptor," *International Journal of Biochemistry and Cell Biology*, vol. 42, no. 11, pp. 1753–1756, 2010.

[59] A. K. Clark, A. A. Staniland, F. Marchand, T. K. Y. Kaan, S. B. McMahon, and M. Malcangio, "P2X7-dependent release of interleukin-1β and nociception in the spinal cord following lipopolysaccharide," *Journal of Neuroscience*, vol. 30, no. 2, pp. 573–582, 2010.

[60] A. K. Clark, R. Wodarski, F. Guida, O. Sasso, and M. Malcangio, "Cathepsin S release from primary cultured microglia is regulated by the P2X7 receptor," *Glia*, vol. 58, no. 14, pp. 1710–1726, 2010.

[61] I. P. Chessell, J. P. Hatcher, C. Bountra et al., "Disruption of the P2X7 purinoceptor gene abolishes chronic inflammatory and neuropathic pain," *Pain*, vol. 114, no. 3, pp. 386–396, 2005.

[62] S. McGaraughty, K. L. Chu, M. T. Namovic et al., "P2X7-related modulation of pathological nociception in rats," *Neuroscience*, vol. 146, no. 4, pp. 1817–1828, 2007.

[63] A. Perez-Medrano, D. L. Donnelly-Roberts, P. Honore et al., "Discovery and biological evaluation of novel cyanoguanidine P2X7 antagonists with analgesic activity in a rat model of neuropathic pain," *Journal of Medicinal Chemistry*, vol. 52, no. 10, pp. 3366–3376, 2009.

[64] W. He, J. Cui, L. Du et al., "Spinal P2X 7 receptor mediates microglia activation-induced neuropathic pain in the sciatic nerve injury rat model," *Behavioural Brain Research*, vol. 226, no. 1, pp. 163–170, 2012.

[65] R. E. Sorge, T. Trang, R. Dorfman et al., "Genetically determined P2X7 receptor pore formation regulates variability in chronic pain sensitivity," *Nature Medicine*, vol. 18, no. 4, pp. 595–599, 2012.

[66] G. Ito, Y. Suekawa, M. Watanabe et al., "P2X7 receptor in the trigeminal sensory nuclear complex contributes to tactile allodynia/hyperalgesia following trigeminal nerve injury," *European Journal of Pain*, vol. 17, no. 2, pp. 185–199, 2013.

[67] C. Guo, M. Masin, O. S. Qureshi, and R. D. Murrell-Lagnado, "Evidence for functional P2X4/P2X7 heteromeric receptors," *Molecular Pharmacology*, vol. 72, no. 6, pp. 1447–1456, 2007.

[68] G. Dell'Antonio, A. Quattrini, E. Dal Cin, A. Fulgenzi, and M. E. Ferrero, "Antinociceptive effect of a new P2Z/P2X7 antagonist, oxidized ATP, in arthritic rats," *Neuroscience Letters*, vol. 327, no. 2, pp. 87–90, 2002.

[69] A. Wahlert, L. Funkelstein, B. Fitzsimmons, T. Yaksh, and V. Hook, "Spinal astrocytes produce and secrete dynorphin neuropeptides," *Neuropeptides*, vol. 47, no. 2, pp. 109–115, 2013.

[70] Y. Chen, X. Zhang, C. Wang, G. Li, Y. Gu, and L. M. Huang, "Activation of $P2X_7$ receptors in glial satellite cells reduces pain through downregulation of $P2X_3$ receptors in nociceptive neurons," *Proceedings of the National Academy of Sciences of the United States of America*, vol. 105, no. 43, pp. 16773–16778, 2008.

[71] R. Kushnir, P. S. Cherkas, and M. Hanani, "Peripheral inflammation upregulates P2X receptor expression in satellite glial cells of mouse trigeminal ganglia: a calcium imaging study," *Neuropharmacology*, vol. 61, no. 4, pp. 739–746, 2011.

[72] T. C. Stock, B. J. Bloom, N. Wei et al., "Efficacy and safety of CE-224,535, an antagonist of $P2X_7$ receptor, in treatment of patients with rheumatoid arthritis inadequately controlled by methotrexate," *Journal of Rheumatology*, vol. 39, no. 4, pp. 720–727, 2012.

[73] E. C. Keystone, M. M. Wang, M. Layton, S. Hollis, and I. B. McInnes, "Clinical evaluation of the efficacy of the P2X7

purinergic receptor antagonist AZD9056 on the signs and symptoms of rheumatoid arthritis in patients with active disease despite treatment with methotrexate or sulphasalazine," *Annals of the Rheumatic Diseases*, vol. 71, no. 10, pp. 1630–1635, 2012.

[74] Z. Ali, B. Laurijssens, T. Ostenfeld et al., "Pharmacokinetic and pharmacodynamic profiling of a $P2X_7$ receptor allosteric modulator GSK1482160 in healthy human subjects," *British Journal of Clinical Pharmacology*, vol. 75, no. 1, pp. 197–207, 2013.

[75] G. Magni and S. Ceruti, "P2Y purinergic receptors: new targets for analgesic and antimigraine drugs," *Biochemical Pharmacology*, vol. 85, no. 4, pp. 466–477, 2013.

[76] K. D. Lustig, A. K. Shiau, A. J. Brake, and D. Julius, "Expression cloning of an ATP receptor from mouse neuroblastoma cells," *Proceedings of the National Academy of Sciences of the United States of America*, vol. 90, no. 11, pp. 5113–5117, 1993.

[77] T. E. Webb, J. Simon, B. J. Krishek et al., "Cloning and functional expression of a brain G-protein-coupled ATP receptor," *FEBS Letters*, vol. 324, no. 2, pp. 219–225, 1993.

[78] M. P. Abbracchio, G. Burnstock, J. Boeynaems et al., "International Union of Pharmacology LVIII: update on the P2Y G protein-coupled nucleotide receptors: from molecular mechanisms and pathophysiology to therapy," *Pharmacological Reviews*, vol. 58, no. 3, pp. 281–341, 2006.

[79] R. L. Carter, I. P. Fricks, M. O. Barrett et al., "Quantification of Gi-mediated inhibition of adenylyl cyclase activity reveals that UDP is a potent agonist of the human $P2Y_{14}$ receptor," *Molecular Pharmacology*, vol. 76, no. 6, pp. 1341–1348, 2009.

[80] Z. Gerevich, C. Müller, and P. Illes, "Metabotropic $P2Y_1$ receptors inhibit P2X3 receptor-channels in rat dorsal root ganglion neurons," *European Journal of Pharmacology*, vol. 521, no. 1-3, pp. 34–38, 2005.

[81] S. A. Malin and D. C. Molliver, "Gi- and Gq-coupled ADP (P2Y) receptors act in opposition to modulate nociceptive signaling and inflammatory pain behavior," *Molecular Pain*, vol. 6, article 21, 2010.

[82] M. Tominaga, M. Wada, and M. Masu, "Potentiation of capsaicin receptor activity by metabotropic ATP receptors as a possible mechanism for ATP-evoked pain and hyperalgesia," *Proceedings of the National Academy of Sciences of the United States of America*, vol. 98, no. 12, pp. 6951–6956, 2001.

[83] T. Moriyama, T. Iida, K. Kobayashi et al., "Possible involvement of $P2Y_2$ metabotropic receptors in ATP-induced transient receptor potential vanilloid receptor 1-mediated thermal hypersensitivity," *Journal of Neuroscience*, vol. 23, no. 14, pp. 6058–6062, 2003.

[84] S. Koizumi, Y. Shigemoto-Mogami, K. Nasu-Tada et al., "UDP acting at $P2Y_6$ receptors is a mediator of microglial phagocytosis," *Nature*, vol. 446, no. 7139, pp. 1091–1095, 2007.

[85] K. Kobayashi, H. Yamanaka, T. Fukuoka, Y. Dai, K. Obata, and K. Noguchi, "$P2Y_{12}$ receptor upregulation in activated microglia is a gateway of p38 signaling and neuropathic pain," *Journal of Neuroscience*, vol. 28, no. 11, pp. 2892–2902, 2008.

[86] H. Tozaki-Saitoh, M. Tsuda, H. Miyata, K. Ueda, S. Kohsaka, and K. Inoue, "$P2Y_{12}$ receptors in spinal microglia are required for neuropathic pain after peripheral nerve injury," *Journal of Neuroscience*, vol. 28, no. 19, pp. 4949–4956, 2008.

[87] K. Kobayashi, H. Yamanaka, F. Yanamoto, M. Okubo, and K. Noguchi, "Multiple P2Y subtypes in spinal microglia are involved in neuropathic pain after peripheral nerve injury," *Glia*, vol. 60, no. 10, pp. 1529–1539, 2012.

[88] L. P. Bernier, A. R. Ase, É. Boué-Grabot, and P. Séguéla, "Inhibition of P2X4 function by P2Y6 UDP receptors in microglia," *Glia*, vol. 61, no. 12, pp. 2038–2049, 2013.

[89] F. Di Virgilio, S. Ceruti, P. Bramanti, and M. P. Abbracchio, "Purinergic signalling in inflammation of the central nervous system," *Trends in Neurosciences*, vol. 32, no. 2, pp. 79–87, 2009.

[90] M. Xia and Y. Zhu, "Signaling pathways of ATP-induced PGE_2 release in spinal cord astrocytes are EGFR transactivation-dependent," *GLIA*, vol. 59, no. 4, pp. 664–674, 2011.

[91] M. Boccazzi, C. Rolando, M. P. Abbracchio et al., "Purines regulate adult brain subventricular zone cell functions: contribution of reactive astrocytes," *Glia*, vol. 62, pp. 428–439, 2014.

[92] K. Kobayashi, H. Yamanaka, and K. Noguchi, "Expression of ATP receptors in the rat dorsal root ganglion and spinal cord," *Anatomical Science International*, vol. 88, no. 1, pp. 10–16, 2013.

[93] G. Villa, M. Fumagalli, C. Verderio, M. P. Abbracchio, and S. Ceruti, "Expression and contribution of satellite glial cells purinoceptors to pain transmission in sensory ganglia: an update," *Neuron Glia Biology*, vol. 6, no. 1, pp. 31–42, 2010.

[94] K. Kobayashi, T. Fukuoka, H. Iyamanaka et al., "Neurons and glial cells differentially express P2Y receptor mRNAs in the rat dorsal root ganglion and spinal cord," *Journal of Comparative Neurology*, vol. 498, no. 4, pp. 443–454, 2006.

[95] S. Ceruti, G. Villa, M. Fumagalli et al., "Calcitonin gene-related peptide-mediated enhancement of purinergic neuron/glia communication by the algogenic factor bradykinin in mouse trigeminal ganglia from wild-type and R192Q $Ca_v2.1$ knock-in mice: Implications for basic mechanisms of migraine pain," *Journal of Neuroscience*, vol. 31, no. 10, pp. 3638–3649, 2011.

[96] N. Li, Z. Y. Lu, L. H. Yu et al., "Inhibition of G protein-coupled $P2Y_2$ receptor induced analgesia in a rat model of trigeminal neuropathic pain," *Molecular Pain*, vol. 10, article 21, 2014.

[97] A. Katagiri, M. Shinoda, K. Honda, A. Toyofuku, B. J. Sessle, and K. Iwata, "Satellite glial cell $P2Y_{12}$ receptor in the trigeminal ganglion is involved in lingual neuropathic pain mechanisms in rats," *Molecular Pain*, vol. 8, article 23, 2012.

[98] J. F. Chen, H. K. Eltzschig, and B. B. Fredholm, "Adenosine receptors as drug targets-what are the challenges?" *Nature Reviews Drug Discovery*, vol. 12, no. 4, pp. 265–286, 2013.

[99] J. Sawynok, A. R. Reid, and J. Liu, "Spinal and peripheral adenosine A_1 receptors contribute to antinociception by tramadol in the formalin test in mice," *European Journal of Pharmacology*, vol. 714, no. 1–3, pp. 373–378, 2013.

[100] J. Liu, A. R. Reid, and J. Sawynok, "Antinociception by systemically-administered acetaminophen (paracetamol) involves spinal serotonin 5-HT7 and adenosine A_1 receptors, as well as peripheral adenosine A1 receptors," *Neuroscience Letters*, vol. 536, no. 1, pp. 64–68, 2013.

[101] J. Liu, A. R. Reid, and J. Sawynok, "Spinal serotonin 5-HT7 and adenosine A_1 receptors, as well as peripheral adenosine A_1 receptors, are involved in antinociception by systemically administered amitriptyline," *European Journal of Pharmacology*, vol. 698, no. 1–3, pp. 213–219, 2013.

[102] X. Gao, Q. Lu, G. Chou et al., "Norisoboldine attenuates inflammatory pain via the adenosine A_1 receptor," *European Journal of Pain*, vol. 18, no. 7, pp. 939–948, 2014.

[103] L. Luongo, R. Petrelli, L. Gatta et al., "5'-Chloro-5'-deoxy-(±)-ENBA, a potent and selective adenosine A_1 receptor agonist, alleviates neuropathic pain in mice through functional glial and microglial changes without affecting motor or cardiovascular functions," *Molecules*, vol. 17, no. 12, pp. 13712–13726, 2012.

[104] L. Luongo, F. Guida, R. Imperatore et al., "The A_1 adenosine receptor as a new player in microglia physiology," *Glia*, vol. 62, no. 1, pp. 122–132, 2014.

[105] S. Ferré, I. Diamond, S. R. Goldberg et al., "Adenosine A_{2A} receptors in ventral striatum, hypothalamus and nociceptive circuitry: implications for drug addiction, sleep and pain," *Progress in Neurobiology*, vol. 83, no. 5, pp. 332–347, 2007.

[106] L. Li, J. X. Hao, B. B. Fredholm, G. Schulte, Z. Wiesenfeld-Hallin, and X. J. Xu, "Peripheral adenosine A_{2A} receptors are involved in carrageenan-induced mechanical hyperalgesia in mice," *Neuroscience*, vol. 170, no. 3, pp. 923–928, 2010.

[107] J. M. Pocock and H. Kettenmann, "Neurotransmitter receptors on microglia," *Trends in Neurosciences*, vol. 30, no. 10, pp. 527–535, 2007.

[108] L. C. Loram, F. R. Taylor, K. A. Strand et al., "Intrathecal injection of adenosine 2A receptor agonists reversed neuropathic allodynia through protein kinase (PK)A/PKC signaling," *Brain, Behavior, and Immunity*, vol. 33, pp. 112–122, 2013.

[109] Z. Chen, K. Janes, C. Chen et al., "Controlling murine and rat chronic pain through A_3 adenosine receptor activation," *The FASEB Journal*, vol. 26, no. 5, pp. 1855–1865, 2012.

[110] K. Ohsawa, T. Sanagi, Y. Nakamura, E. Suzuki, K. Inoue, and S. Kohsaka, "Adenosine A_3 receptor is involved in ADP-induced microglial process extension and migration," *Journal of Neurochemistry*, vol. 121, no. 2, pp. 217–227, 2012.

[111] E. Daré, G. Schulte, O. Karovic, C. Hammarberg, and B. B. Fredholm, "Modulation of glial cell functions by adenosine receptors," *Physiology and Behavior*, vol. 92, no. 1-2, pp. 15–20, 2007.

[112] L. Antonioli, B. Csóka, M. Fornai et al., "Adenosine and inflammation: what's new on the horizon?" *Drug Discovery Today*, vol. 19, no. 8, pp. 1051–1068, 2014.

[113] A. P. Ford, "P2X3 antagonists: novel therapeutics for afferent sensitization and chronic pain," *Pain Management*, vol. 2, pp. 267–277, 2012.

[114] M. Furber, L. Alcaraz, J. E. Bent et al., "Discovery of potent and selective adamantane-based small-molecule P2X7 receptor antagonists/interleukin-1β inhibitors," *Journal of Medicinal Chemistry*, vol. 50, no. 24, pp. 5882–5885, 2007.

[115] V. Hernandez-Olmos, A. Abdelrahman, A. El-Tayeb, D. Freudendahl, S. Weinhausen, and C. E. Müller, "N-substituted phenoxazine and acridone derivatives: structure-activity relationships of potent P2X4 receptor antagonists," *Journal of Medicinal Chemistry*, vol. 55, no. 22, pp. 9576–9588, 2012.

[116] K. Zhang, J. Zhang, Z. G. Gao et al., "Structure of the human $P2Y_{12}$ receptor in complex with an antithrombotic drug," *Nature*, vol. 509, pp. 115–118, 2014.

[117] F. Vincenzi, M. Targa, R. Romagnoli et al., "TRR469, a potent A_1 adenosine receptor allosteric modulator, exhibits anti-nociceptive properties in acute and neuropathic pain models in mice," *Neuropharmacology*, vol. 81, pp. 6–14, 2014.

[118] S. Koizumi, K. Ohsawa, K. Inoue, and S. Kohsaka, "Purinergic receptors in microglia: functional modal shifts of microglia mediated by P2 and P1 receptors," *Glia*, vol. 61, no. 1, pp. 47–54, 2013.

Hindawi Publishing Corporation
BioMed Research International
Volume 2014, Article ID 982121, 11 pages
http://dx.doi.org/10.1155/2014/982121

Research Article

Remote Dose-Dependent Effects of Dry Needling at Distant Myofascial Trigger Spots of Rabbit Skeletal Muscles on Reduction of Substance P Levels of Proximal Muscle and Spinal Cords

Yueh-Ling Hsieh,[1] Chen-Chia Yang,[2] Szu-Yu Liu,[1] Li-Wei Chou,[3,4,5] and Chang-Zern Hong[6]

[1] *Department of Physical Therapy, Graduate Institute of Rehabilitation Science, China Medical University, Taichung 40402, Taiwan*
[2] *Department of Physical Medicine and Rehabilitation, Cheng Ching General Hospital, Taichung 40407, Taiwan*
[3] *School of Chinese Medicine, College of Chinese Medicine, China Medical University, Taichung 40402, Taiwan*
[4] *Department of Physical Medicine and Rehabilitation, China Medical University Hospital, Taichung 40402, Taiwan*
[5] *Research Center for Chinese Medicine and Acupuncture, China Medical University, Taichung 40402, Taiwan*
[6] *Department of Physical Therapy, Hungkuang University, Taichung 43302, Taiwan*

Correspondence should be addressed to Li-Wei Chou; chouliwe@gmail.com and Chang-Zern Hong; cczzhhoonngg@yahoo.com.tw

Received 13 February 2014; Accepted 15 August 2014; Published 3 September 2014

Academic Editor: Katarzyna Starowicz

Background. Dry needling at distant myofascial trigger points is an effective pain management in patients with myofascial pain. However, the biochemical effects of remote dry needling are not well understood. This study evaluates the remote effects of dry needling with different dosages on the expressions of substance P (SP) in the proximal muscle, spinal dorsal horns of rabbits. *Methods*. Male New Zealand rabbits (2.5–3.0 kg) received dry needling at myofascial trigger spots of a gastrocnemius (distant muscle) in one (1D) or five sessions (5D). Bilateral biceps femoris (proximal muscles) and superficial laminaes of L5-S2, T2-T5, and C2-C5 were sampled immediately and 5 days after dry needling to determine the levels of SP using immunohistochemistry and western blot. *Results*. Immediately after dry needling for 1D and 5D, the expressions of SP were significantly decreased in ipsilateral biceps femoris and bilateral spinal superficial laminaes ($P < .05$). Five days after dry needling, these reduced immunoactivities of SP were found only in animals receiving 5D dry needling ($P < .05$). *Conclusions*. This remote effect of dry needling involves the reduction of SP levels in proximal muscle and spinal superficial laminaes, which may be closely associated with the control of myofascial pain.

1. Introduction

Myofascial trigger points (MTrPs), a source of musculoskeletal pain, has been defined as a hyperirritable (hypersensitive) spot in a taut band of skeletal muscle fibers and may play a key role in the pathophysiology of myofascial pain syndrome [1].

Dry needling targeting directly the primary MTrP, if performed appropriately, is one of the effective therapies for inactivating MTrPs and alleviating pain [2–10]. However, repetitive and intensive needling manipulation may cause excess damage and increase inflammatory nociception in skeletal muscle fibers [11]. Therefore, acupuncture-like needling at a region some distance away from the painful MTrPs can provide an alternative approach to remote pain relief [12–16]. In an electrophysiological study investigating the neural mechanism of remote effects of dry needling, it has found that these effects are mediated via intact afferent neural pathways from the stimulated site to the spinal cord segments of the proximally responded affected muscle [17] and may also involve the possible effects from extrasegments of the spinal cord, such as descending pain inhibitory systems [17].

But the biochemical mechanisms underlying the nociception transmission modulated by remote effects of dry needling are still unclear.

An animal model for MTrP study on rabbit was established by Hong and Torigoe [18]. A certain hyperirritable spot (myofascial trigger spot, MTrS) in the rabbit biceps femoris muscle is similar to that in human MTrP. In this spot, local twitch responses can be elicited when the needle tip encountered a sensitive locus. As in human MTrP, spontaneous electrical activity including endplate noise (EPN) and endplate spike can also be frequently recorded within this sensitive spot [19, 20]. This animal model had been used for many studies on myofascial pain syndrome [17, 19, 21–24].

The aim of the present study was to evaluate the remote effects of dry needling treatment on the pain-related peptide, substance P (SP), in a rabbit model of MTrSs. The analgesic mechanism of remote dry needling was further elucidated by additional studies of electrophysiological EPN recordings and measurements of SP immunolabeling expressions in this rabbit model to assess and compare the alterations of SP levels in the proximally affected muscle and to explore the corresponding neuronal circuits affected by remote dry needling. This study is also designed to further investigate the dose-dependent effect of remote dry needling treatment.

2. Materials and Methods

2.1. General Design. The current experiment was designed to confirm the remote analgesic effects of dry needling at a distal muscle containing MTrSs (i.e., unilateral gastrocnemius) by quantifying the expressions of SP in the proximally affected muscles (i.e., bilateral bicep femoris muscles) and in the dorsal horns of the corresponding spinal segment (where the needling stimulation input reaches) and their suprasegments (C2-C5 and T2-T5). The MTrS of the gastrocnemius (i.e., distant muscles) on a randomly selected side was treated with predetermined dosages of dry needling. A total of 48 rabbits were randomly and equally assigned into one of the following two major groups: dry needling group (experimental) and sham-operated needling group (control). Then the animals in each group were further divided into four subgroups according to the treatment dosages at distant MTrSs of gastrocnemius. The subgroups are (1) 1D group with animals submitted to one dosage of dry needling (one session), (2) s1D group with animals submitted to one dosage of sham-operated dry needling, (3) 5D group with animals submitted to one dosage of dry needling for five consecutive days (five daily sessions), and (4) s5D group with animals submitted to one dosage of sham-operated dry needling for five consecutive days. Animals were sacrificed at two examined timepoints for SP immunoanalysis, half of the animals in each group on the day immediately after dry needling and the remaining animals on the fifth day after cessation of dry needling. The experimental design is presented in Figure 1.

2.2. Animal Care. The experiments were performed on adult male New Zealand rabbits (aged from 16 to 20 weeks, body weight of 2.5–3.0 kg). The animals were housed individually in standard polycarbonate tub cages lined with wood chip beddings and had free access to food and water. The cages were placed in an air-conditioned room (25 ± 1°C), with 40 dBA and a 12-hour alternating light-dark cycle (6:00 am to 6:00 pm). Each animal was housed and cared for according to the ethical guidelines of the International Association for Study of Pain in Animals [25, 26]. Effort was made to minimize discomfort and to reduce the number of animals used. All animal experiments were conducted following the procedure approved by the Animal Care and Use Committee of a university in accordance with the Guidelines for Animal Experimentation. The general experimental conditions were essentially the same as those previously described [11, 17, 27].

2.3. Identification and Stimulation of Myofascial Trigger Spots. Before an anesthetic is given, the most sensitive spots (i.e., MTrSs) of biceps femoris and gastrocnemius muscles were identified by finger pinch. The animal's reactions were observed (such as withdrawal of lower limb, head turning, and screaming) to confirm the exact location of an MTrS. These painful regions were marked on the skin with an indelible marker. Then the animals were anesthetized with 2% isoflurane (AErrane, Baxter Healthcare of Puerto Rico, PR, USA) in oxygen flow for induction followed by a 0.5% maintenance dose. Body temperature, monitored by a thermistor probe of a thermometer (Physiotemp Instrument, Clifton, NJ, USA) in the rectum, was maintained at approximately 37.5°C using a body temperature control system comprising a thermostatically regulated DC current heating pad and an infrared lamp. The muscle of each marked site was grasped between the fingers from behind the muscle and the muscle is palpated by gently rubbing (rolling) it between the fingers to find a taut band, which feels like a clearly delineated "rope" of muscle fibers and is roughly 10 mm in diameter. The marked sites were areas designated for dry needling treatment of gastrocnemius or electrophysiological and immunolabeling studies of biceps femoris.

2.4. Dry Needling of Gastrocnemius Muscle. Dry needling technique was similar to that used in our previous study [11]. For needling in MTrS of gastrocnemius, the needle (300 μm in diameter and 1.5 inches in length, Yu-Kuang Industrial Co., Ltd., Taiwan) was first inserted through the skin perpendicularly at the center of the marked spot and advanced slowly and gently into the muscle. Then simultaneous needle rotation was performed to facilitate fast "in-and-out" needle movement in order to elicit as many local twitch responses as possible. For sham-operated needling, the needle was inserted into the subcutaneous layer of the marked MTrS region at a depth approximately 1-2 mm from the skin surface, without penetrating into the muscle tissues. After insertion, the needle stayed there without further movement for the same period of duration as in dry needling.

2.5. Recording of Endplate Noise. This procedure was performed by an investigator who was blind to the group assignment. For EPN assessment, a digital EMG machine (Neuro-EMG-Micro; Neurosoft, Ivanovo, Russia) and monopolar

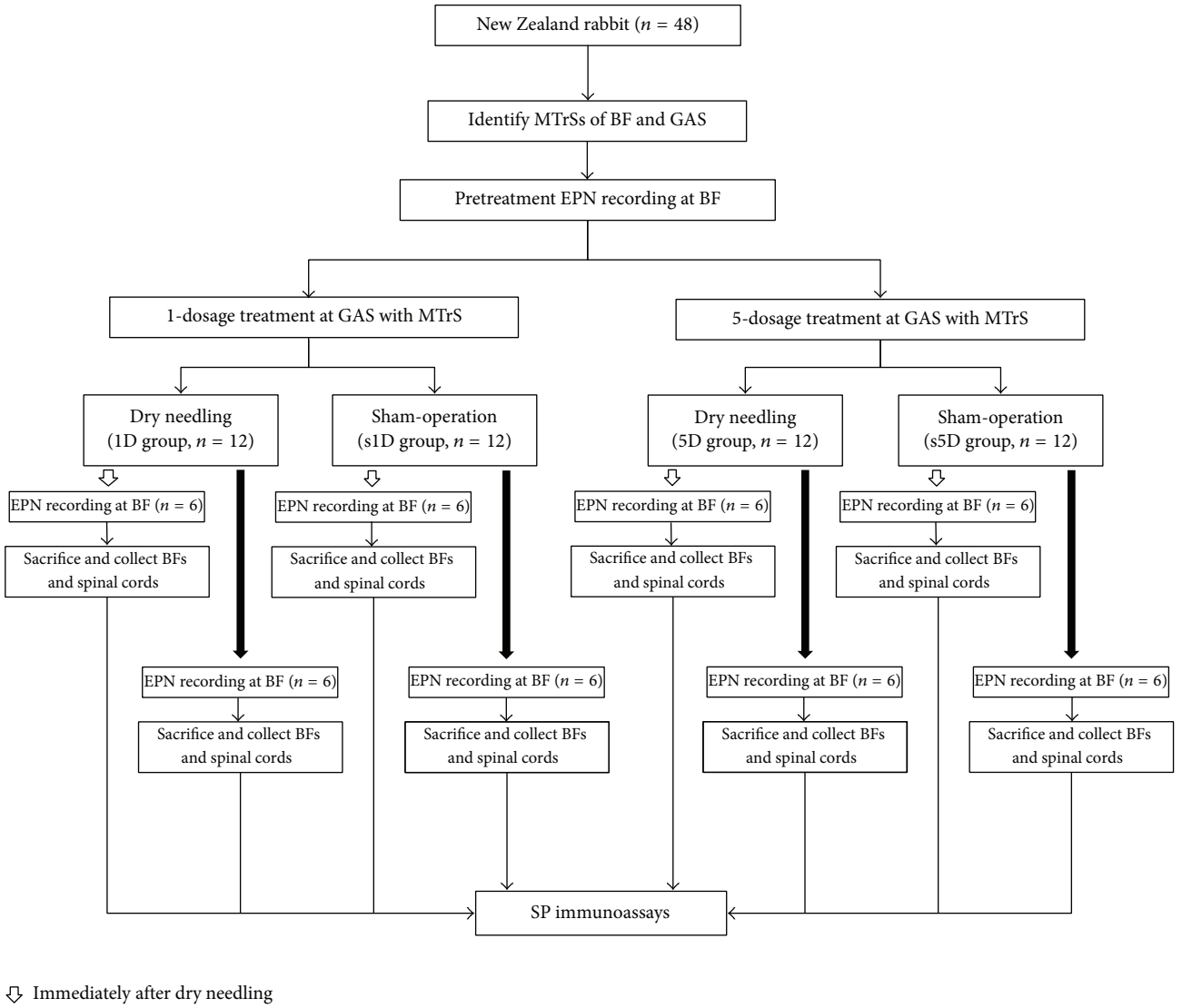

Figure 1: Flow chart for the animal study. Abbreviations: 1D, one-dosage dry needling; 5D, five-dosage dry needling; BF, biceps femoris; Gastrocnemius, GAS; MTrS, myofascial trigger spots, SP, substance P; s1D, sham one-dosage dry needling; and s5D, sham five-dosage dry needling.

needle electrodes (37 mm disposable Teflon-coated model) were used. The gain was set at 20 μV per division for recordings from both channels. Low-cut frequency filter was set at 100 Hz and the high-cut one was set at 1,000 Hz. Sweep speed was 10 ms per division.

The search needle was inserted into the MTrS region in a direction parallel to the muscle fibers at an angle of approximately 60° to the surface of the muscle. After initial insertion just short of the depth of the MTrS, the needle was advanced very slowly with simultaneous slow rotation to prevent it from "grabbing" and releasing the tissue suddenly to advance in a large jump. When the needle approached an active locus (EPN locus), the continuous electrical activity with amplitude higher than 10 μV, that is, EPN, can be recorded. Then the needle was fixed in place to ensure that this EPN can run continuously on the recording screen with constant amplitudes for at least 3 minutes.

Five EPN recordings (25 ms each) taken before and 3 minutes after the needling treatment were randomly selected for all groups. The mean amplitude of the five random EPN recordings was analyzed and calculated for a certain measurement point for each animal.

2.6. Tissue Preparation. Half of the animals in each group were sacrificed on the day immediately after dry needling, and the remaining animals were sacrificed 5 days after dry needling for SP immunoassays. Animals were sacrificed under strong anesthesia by injection of saturated KCl (300 g/mL, intraperitoneal injection). Bilateral biceps femoris muscles, their corresponding segments of L5-S2,

and extrasegmentsof T2-T5 and C2-C5 spinal cords were harvested. The spinal cord specimens were fixed in 4% paraformaldehyde (diluted in 0.1 mol/L PBS) and then immersed in 30% sucrose in 0.1 mol/L PBS for 2 days at 4°C for immunohistochemical staining. The muscle specimens were homogenized in T-PER tissue protein extraction reagent (Pierce Chemical Co., IL, USA) and the complete cocktail of protease inhibitors (Sigma, NY, USA) for western blot immunoassay.

2.7. Western Blot Analysis. Equal amounts of protein were loaded and separated in 10% Tris-Tricine SDS-PAGE gels. The resolved proteins were transferred onto polyvinylidene fluoride membranes (Millipore, Bedford, MA, USA). The membranes were blocked in 5% nonfat milk for 1 hour at room temperature and incubated overnight with primary antibodies against SP (1 : 500, Cat. # orb11399, Biorbyt, Cambridge, UK) and GAPDH (1 : 2000, ab8245, Abcam Inc. MA, USA) at a dilution of 1 : 2500 in blocking solution. The blots were then incubated with the horseradish peroxidase-conjugated goat anti-rabbit and anti-mouse IgG secondary antibody (1 : 2000, Jackson ImmunoResearch Laboratories, Inc., West Grove, PA, USA) for 1 hour at room temperature. The signals were finally visualized using an enhanced chemiluminescence detection system (Fujifilm LAS-3000 Imager, Tokyo, Japan), and the blots were exposed to X-ray. All western blot analyses were performed at least three times, and consistent results were obtained. The immunoreactive bands were analyzed using a computer-based densitometry Gel-Pro Analyzer (version 6.0, Media Cybernetics, Inc. USA). Relative intensity of western blot band for each protein was normalized to the level of GAPDH protein and presented as percentage of its sham value.

2.8. Immunohistochemistry for Substance P and Quantitative Analysis. The frozen spinal cord tissues were cut serially and coronally into sections of 4 μm thickness by a freezing microtome. Each spinal cord specimen produced approximately 100 sections. Each staining assay was examined in 10 alternate sections per rabbit, which were selected by a systematic-random series with a random start for analysis. The sections were first mounted on poly L-lysine (Sigma, P8920)-coated slides and then blocked in 10% normal goat serum (in PBS with 0.3% Triton X-100, Jackson ImmunoResearch Laboratories, Inc., West Grove, PA, USA). Subsequently, they were incubated overnight at 4°C with rat monoclonal anti-SP antibody (1 : 200, MAB356, Millipore, CA, USA). The sections were then incubated with biotinylated goat anti-rat IgG secondary antibody (1 : 500, Jackson ImmunoResearch Laboratories, Inc., West Grove, PA, USA) for 1 hour at room temperature. After being washed, the sections were incubated with a streptavidin-horseradish peroxidase conjugate (Jackson ImmunoResearch Laboratories, Inc., West Grove, PA, USA). The sections were visualized as brown precipitates by adding 0.2 mg/mL 3,3′-diaminobenzidine (DAB, Pierce, Rockford, IL, USA) as a substrate. Negative control slides omitting either primary antibodies or secondary antibodies were also prepared for comparison.

The slides were examined and photographed at three randomly selected fields of superficial dorsal horn (laminae I-II; superficial, the localization of nociresponsive neurons) at 200x magnification using a light microscope (BX43, Olympus America Inc. NY, USA) and a cooled digital color camera with a resolution of 1360 × 1024 pixels (DP70, Olympus America Inc. NY, USA). Images were saved and adjusted to equalize contrast and brightness with Adobe Photoshop (CS3, San Jose, CA); no other modifications were made.The digital images were analyzed using a computer-based morphometry, Image-Pro Plus 4.5 software (Media Cybernetics, Silver Spring, USA). According to the automatically calculated parameters, the area labeled by DAB-stained strong-positive staining cells for SP immunoreactivity (SP-IR) was measured. The percentage of the positive and strong SP-IR pixels to total stained pixels in superficial lamina of spinal dorsal horn (%) was analyzed.

2.9. Statistical Analysis. All data were expressed as mean ± standard deviation (SD). The differences in SP-IR levels in animals submitted to dry needling and sham operation were calculated. One-way analysis of variance (ANOVA) was employed to determine the differences in SP-IR levels among groups. Post hoc comparisons between groups were examined using Scheffe's method. A P value of <.05 was considered statistically significant. All data were analyzed using SPSS version 12.0 for Windows (SPSS Inc., IL, USA).

3. Results

3.1. Changes in Amplitudes of EPN in Biceps Femoris Induced by Dry Needling at Distant MTrSs. Figure 2 shows the alterations of mean EPN amplitude recorded from biceps femoris ipsilaterally and contralaterally to the dry needling side at gastrocnemius muscle. As can be seen, there were significant differences among the four groups at any examined timepoint (ANOVA, all $P < .05$). Compared with the pretreatment levels, the EPN amplitudes of ipsilateral biceps femoris were significantly decreased immediately after dry needling treatment ($P < .05$; Figure 2(a)). However, the EPN amplitudes after sham-operated needling showed no marked changes ($P > .05$).

There were also significant differences in EPN amplitudes recorded immediately after treatment between dry needling and sham-operation groups at any dosage (1D versus s1D, 5D versus s5D, all $P < .05$; Figure 2(a)). Five days after treatment, the marked reduction in EPN amplitude was no longer observed in the 1D group (1D versus s1D, $P > .05$). However, the 5D group showed significant decrease in EPN amplitude when compared with the s5D group (5D versus s5D, $P < .05$; Figure 2(a)) and the 1D group (1D versus 5D, $P < .05$; Figure 2(b)). The EPN recordings from biceps femoris contralateral to the dry needling side presented similar trends of amplitude changes (Figure 2(c)).

3.2. Changes in SP-IR of Biceps Femoris Induced by Dry Needling at Distant MTrSs. Figure 3 presents the SP-IR in biceps femoris immediately and 5 days after treatments for

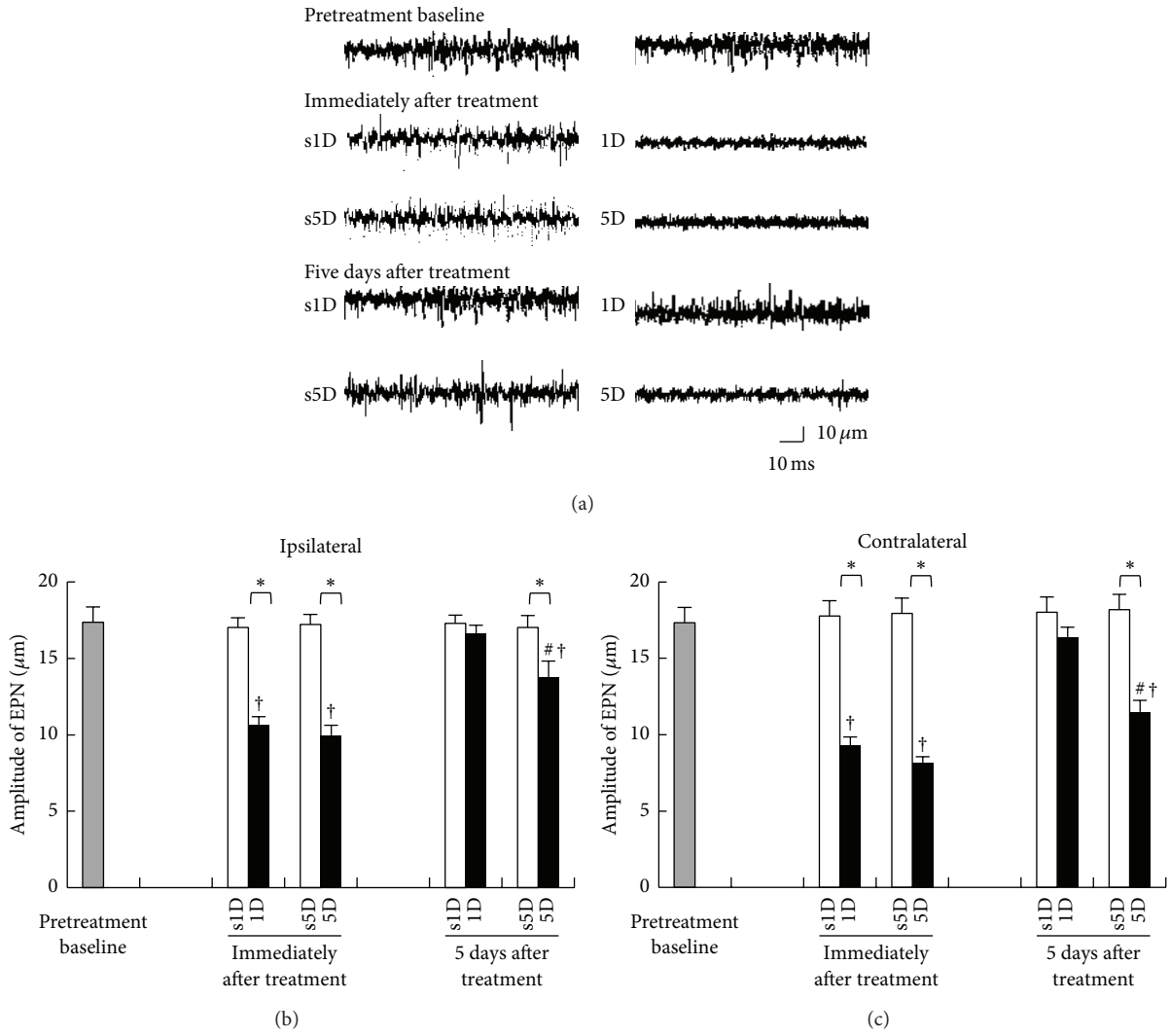

Figure 2: Changes in EPN amplitude measured at MTrS of biceps femoris before, immediately, and 5 days after one-(1D) and five-dosage (5D) of dry needling at gastrocnemius in experimental (1D and 5D groups) and sham-operated groups (s1D and s5D groups). Sample EPN recordings (a) in rabbits from 1D, s1D, 5D, and s5D groups. (b) Quantification of EPN amplitude in biceps femoris ipsilateral (b) and contralateral (c) to dry needling side expressed as mean ± SD. ∗ represents significant difference ($P < .05$) compared with sham-operated groups (s1D and s5D). # represents significant difference ($P < .05$) between 1D and 5D groups. †: $P < .05$ represent significant differences compared with pretreatment values.

all groups. As can be seen, there were significant differences among the four groups at any examined timepoint (ANOVA, all $P < .05$). Immediately after treatment, 1D and 5D groups showed significant decrease in SP-IR levels in biceps femoris ipsilaterally to the needling side when compared with s1D and s5D groups, respectively (Scheffe's method, 1D versus s1D, 5D versus s5D, all $P < .05$; Figures 3(a) and 3(b)).

Five days after treatment, the 5D group still showed marked decrease in SP-IR levels when compared with the s5D group (Scheffe's method, $P < .05$) but there was no difference in SP-IR levels between 1D and s1D groups ($P > .05$; Figure 3(b)). Moreover, there were no significant differences in SP-IR in biceps femoris contralaterally to the needling side between 1D and s1D, as well as 5D and s5D groups at any examined timepoint (Scheffe's method, 1D versus s1D, 5D versus s5D, all $P > .05$; Figure 3(c)).

3.3. Changes in SP-IR Cells of Spinal Dorsal Horns Induced by Dry Needling at Distant MTrSs

3.3.1. SP Expressions in L5-S2 Segments. The SP-IR patterns in L5-S2 segments for the four groups immediately and 5 days after treatments are presented in Figures 4(a) and 4(b), respectively. Qualitative analysis of the SP-IR in superficial laminae of the L5-S2 dorsal horn showed different patterns of reactivity between dry needling and sham-operation groups (Figure 4(c)). There were significant differences among the four groups at any examined timepoint (ANOVA, all $P < .05$).

In sham-operated controls, SP-IR was expressed bilaterally in the nuclei of cells of the superficial laminae in L5-S2 dorsal horn spinal cords, which showed no statistically significant differences between s1D and s5D groups at each

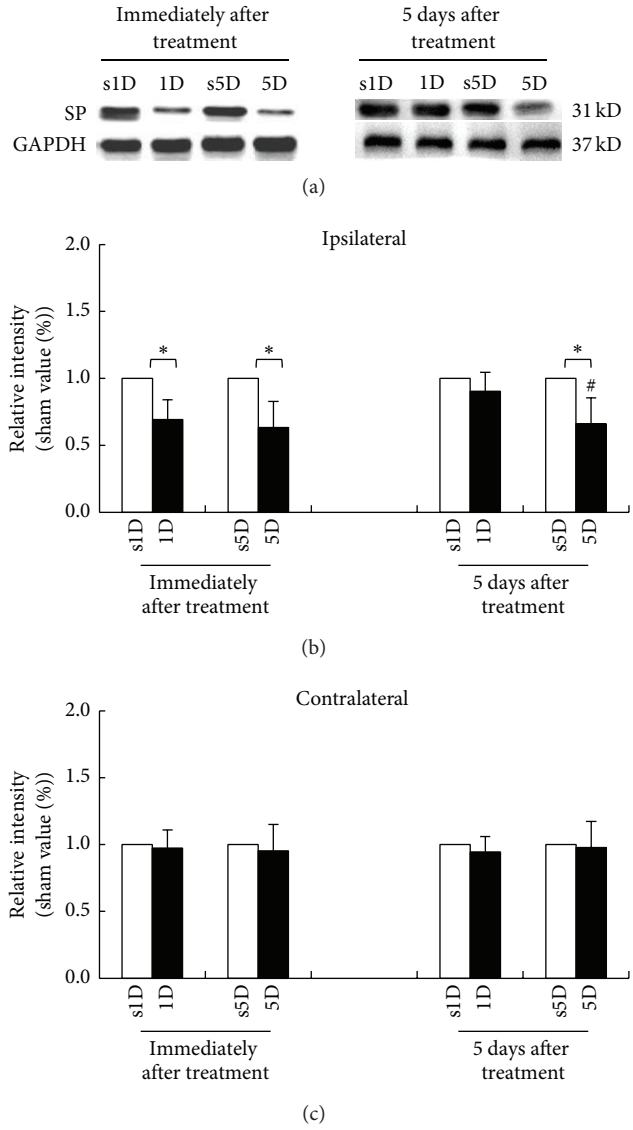

Figure 3: Alterations of substance P (SP) level at biceps femoris muscle after one-(1D) and five-dosage (5D) of dry needling at gastrocnemius in experimental (1D and 5D groups) and sham-operated groups (s1D and s5D groups). Representative western blot photographs (a) in ipsilateral biceps femoris immediately and 5 days after dry needling at gastrocnemius. Quantification of SP levels in biceps femoris ipsilateral (b) and contralateral (c) to dry needling side expressed as mean ± SD. ∗ represents significant difference ($P < .05$) compared with sham-operated groups (s1D and s5D). # represents significant difference ($P < .05$) between 1D and 5D groups.

examined timepoint (Scheffe's method, $P > .05$; Figure 4(c)). The nuclei of SP-IR neurons were visualized as brown precipitates and there was also some cytoplasmic staining. Most of the SP-IR cells were distributed in the bilateral superficial laminae (I-II) of the dorsal horn. Immediately after treatment, 1D and 5D groups showed significant reduction in SP-IR levels in bilateral superficial laminae when compared with s1D and s5D groups, respectively (Scheffe's method, 1D versus s1D, 5D versus s5D; all $P < .05$; Figure 4(a)).

Overall, the spinal cord sections had faint SP labelings in bilateral superficial laminae of dorsal horns in both groups submitted to dry needling, as confirmed by the quantitative analysis, which also showed statistically significant differences between 1D and 5D groups (Scheffe's method, 1D versus 5D, $P < .05$; Figure 4(c)). Five days after treatment, there was no significant difference in SP-IR level between the 1D group and the s1D group (Scheffe's method, 1D versus s1D, $P > .05$; Figure 4(b)). However, the 5D group still showed significant reduction in the SP-IR level in bilateral superficial laminae when compared with the s5D group (Scheffe's method, 5D versus s5D, $P < .05$; Figure 4(b)) and the 1D group (Scheffe's method, 1D versus 5D, $P < .05$; Figure 4(c)).

3.3.2. SP Expressions in C2-C5 and T2-T5 Suprasegments. A similar trend of SP-IR expression at L5-S2 segments was also observed in bilateral superficial laminae at T2-T5 (Figure 5(a)) and C2-C5 levels (Figure 6(a)). There were significant differences in SP expressions among the four groups at any examined timepoint (ANOVA, all $P < .05$). Immediately after treatment, 1D and 5D groups showed statistically significant reduction in SP-IR levels in bilateral superficial laminae at T2-T5 and C2-C5 levels when compared with s1D and s5D groups, respectively (Scheffe's method, 1D versus s1D, 5D versus s5D, all $P < .05$). In contrast, there were no significant differences between 1D and 5D groups at any examined level (Scheffe's method, 1D versus 5D, T2-T5: $P > .05$; C2-C5: $P > .05$; Figures 5(c) and 6(c)).

Five days after treatments, the 1D group showed no significant change in SP-IR at T2-T5 and C2-C5 levels when compared with the s1D group (Scheffe's method, 1D versus s1D group, $P > .05$). However, the spinal sections in the 5D group showed a reduction in SP-IR expressions when compared with those in the s5D group (Scheffe's method, 5D versus s5D, $P < .05$; Figures 5(b) and 6(b)). The 5D group also showed significant reduction in SP-IR levels in bilateral superficial laminae when compared with the 1D group at each examined level (Scheffe's method, 1D versus 5D, T2-T5: $P < .05$; C2-C5: $P < .05$; Figures 5(c) and 6(c)).

3.3.3. Differences in SP-IR Patterns among Spinal Cord Levels. Comparison among SP-IR patterns of C2-C5, T2-T5, and L5-S2 levels shows no statistically significant differences in either 1D or s1D group at any examined timepoint (ANOVA, $P > .05$). However, the differences in SP-IR between 5D and s5D groups were significant among various spinal cord levels at all examined timepoints of either immediately or 5 days after treatments (ANOVA, $P < .05$). The reduction of SP-IR cells in the lumbosacral dorsal horn was significantly higher in comparison with that in cervical or thoracic cells (Scheffe's method, all $P < .05$, Figure 7).

4. Discussion

This is the first study showing that short-term and long-term dry needling at distant MTrSs can induce suppression of SP levels in the proximal muscle and spinal cord dorsal horns. The results also suggest that maintenance effects of remote

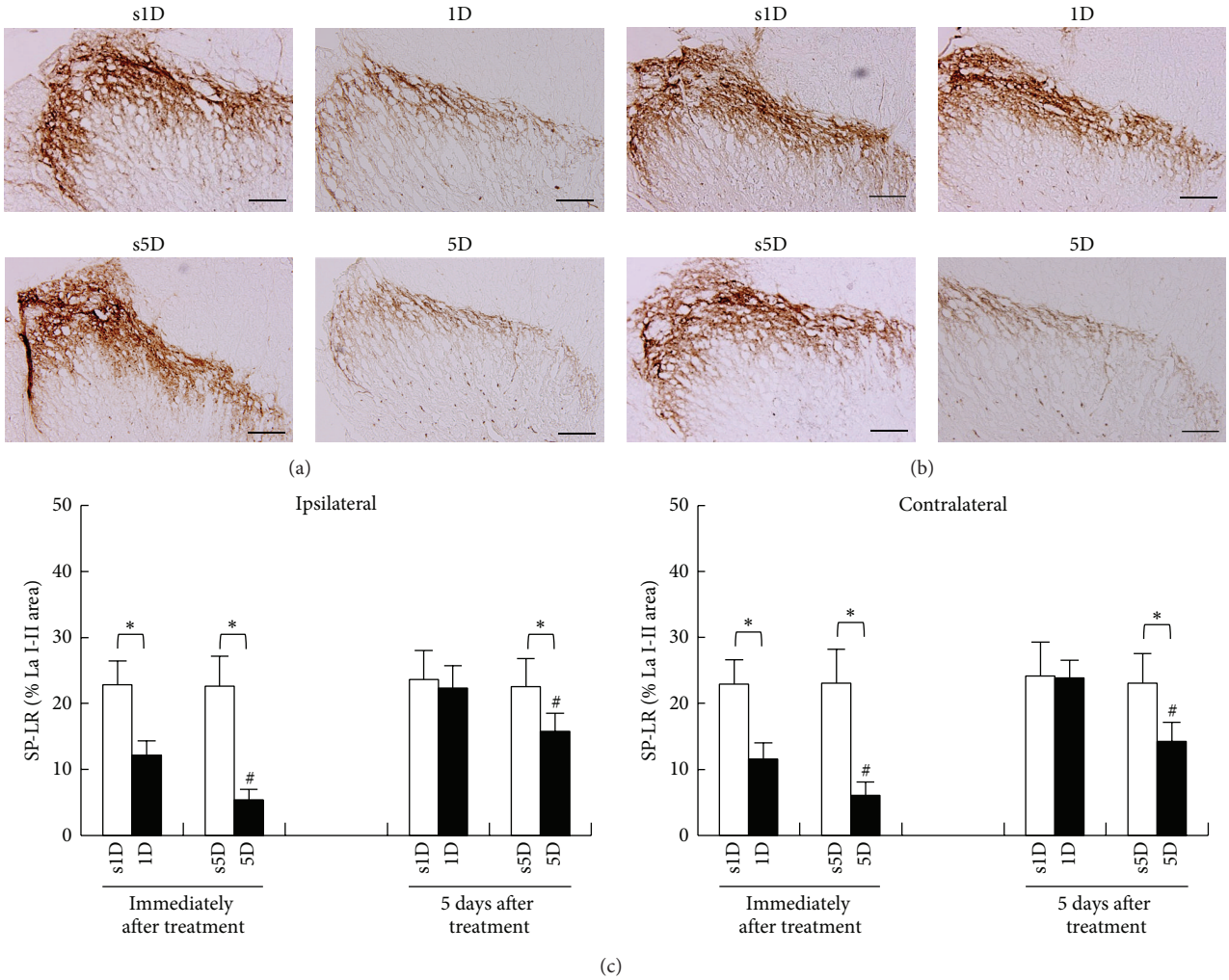

Figure 4: Alterations of substance P (SP) levels at superficial laminae of L5-S2 after one-(1D) and five-dosage (5D) of dry needling at gastrocnemius in experimental (1D and 5D groups) and sham-operated groups (s1D and s5D groups). The representative photomicrographs indicate immunohistochemical labeling for SP in ipsilateral dorsal horns of lumbosacral spinal cords at the timepoints immediately (a) and 5 days (b) after dry needling. Histograms indicate the quantitative analysis of SP immunoreactivity in ipsilateral and contralateral spinal cords (c). ∗ represents significant difference ($P < .05$) compared with sham-operated groups (s1D and s5D). # represents significant difference ($P < .05$) between 1D and 5D groups (scale bar = 100 μm).

dry needling may contribute to the extrasegmental desensitization effect. There is strong indication that both neural and biochemical effects are involved in the mechanisms of remote pain control.

Dry needling targeting the MTrPs for pain relief has its basis in theories similar, but not exclusive, to traditional acupuncture. The electrophysiological outcomes affected by acupuncture and dry needling are similar [17]. In our previous studies, decreases in EPN amplitude in proximal muscles containing MTrSs were found after dry needling at the MTrSs of a distant muscle when compared with pretreatment baseline EPN amplitude in animals with intact neural circuits [17]. Similar findings were found in humans receiving acupuncture at remote acupoints [15, 16]. Fernández-Carnero et al. also found an increase in spontaneous electrical activity at an MTrP region during persistent noxious stimulation at another distant MTrP, followed by suppression of electrophysiological irritability after cessation of needling [28]. The evidences reveal that dry needling at distant MTrS could decrease the irritability of the proximal MTrS by suppression of EPN in prevalence and amplitude. In the present study, the results obtained are in line with those of earlier studies, showing that EPN amplitudes were significantly reduced after a single or five dosages of dry needling when compared with those after sham operation.

SP has been widely proposed as being involved in delivering nociceptive information from the peripheral receptors to the spinal dorsal horn and supraspinal processing centers, thus leading to central sensitization [29–34]. Interventions that inhibit SP signaling pathways generally show antinociceptive effects in animal models [35, 36]. Electroacupuncture can reduce the noxious nerve stimulation-induced release of SP from both central terminals and peripheral endings of the primary sensory neurons [37]. Immunohistochemical

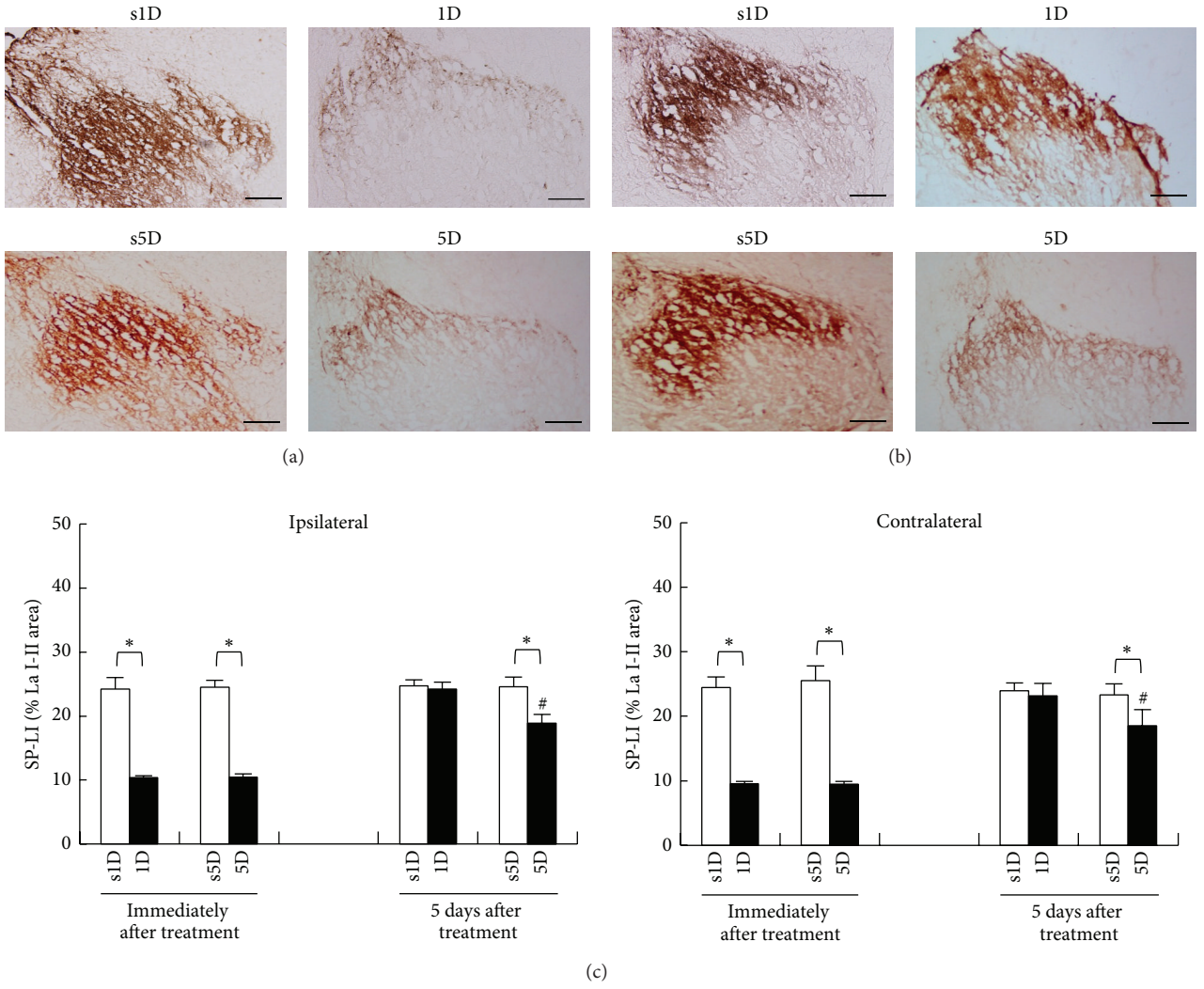

Figure 5: Alterations of substance P (SP) levels at superficial laminae of T2-T5 after one-(1D) and five-dosage (5D) of dry needling at gastrocnemius in experimental (1D and 5D groups) and sham-operated groups (s1D and s5D groups). The representative photomicrographs indicate immunohistochemical labeling for SP in ipsilateral dorsal horns of lumbosacral spinal cords at the timepoints immediately (a) and 5 days (b) after dry needling. Histograms indicate the quantitative analysis of SP immunoreactivity in ipsilateral and contralateral spinal cords (c). $*$ represents significant difference ($P < .05$) compared with sham-operated groups (s1D and s5D). # represents significant difference ($P < .05$) between 1D and 5D groups (scale bar = 100 μm).

studies showed that electroacupuncture of "Zusanli" (ST-36) could depress the pain response and inhibit spinal dorsal horn SP release [38]. Electroacupuncture can also suppress immunoreactive SP accumulation induced by tooth pulp stimulation in the superficial layers of the trigeminal nucleus caudalis [39]. Therefore, SP may be an important transmitter in mechanism of acupuncture analgesia. The present result on dry needling-induced suppression of spinal dorsal horn SP was consistent with those of previous studies described above, implying that short- and long-term remote dry needling probably produce analgesic effect. In addition, the finding of reduction in SP expression in extrasegments, dorsal horns of C2-C5, and T2-T5 after dry needling was similar to our previous results [17], which reported supraspinal control of spinal inhibitory interneurons induced by dry needling at distant MTrSs. The extrasegmental desensitization effect involving a more generalized system of analgesia is probably activated by remote dry needling.

SP is also likely to be involved in the pathogenesis of musculoskeletal pain. A recent study has also found higher SP levels in active MTrPs compared with control latent or absent MTPs [40]. Mean optical density of the immunostaining for SP was statistically greater in trapezius muscle of patients with myofascial pain syndrome when compared with specimens from patients with fibromyalgia. Extensive studies demonstrate that SP accumulated in MTrPs of skeletal muscles is associated with pain and inflammation [17, 40, 41]. The current findings of reduction in SP level in proximal

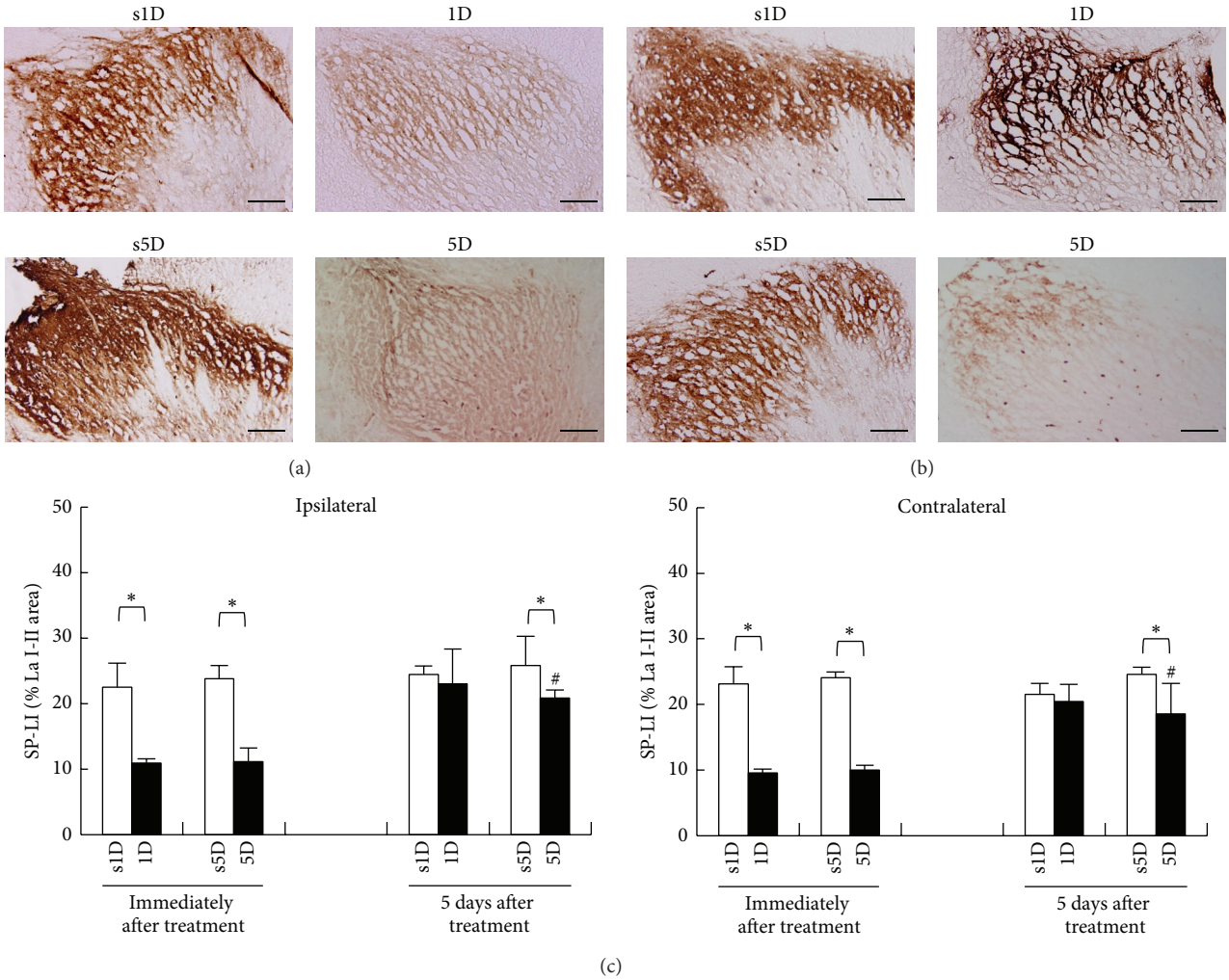

Figure 6: Alterations of substance P (SP) levels at superficial laminae of C2-C5 after one-(1D) and five-dosage (5D) of dry needling at gastrocnemius in experimental (1D and 5D groups) and sham-operated groups (s1D and s5D groups). The representative photomicrographs indicate immunohistochemical labeling for SP in ipsilateral dorsal horns of lumbosacral spinal cords at the timepoints immediately (a) and 5 days (b) after dry needling. Histograms indicate the quantitative analysis of SP immunoreactivity in ipsilateral and contralateral spinal cords (c). ∗ represents significant difference ($P < .05$) compared with sham-operated groups (s1D and s5D). # represents significant difference ($P < .05$) between 1D and 5D groups (scale bar = 100 μm).

muscle (biceps femoris) ipsilateral to the needling side after dry needling at a distant muscle containing MTrSs may be related to pain control.

Suppression of SP expressions was of a higher extent in animals submitted to 5D dry needling than those submitted to 1D dry needling, indicating immediate dose-dependent effects. On the other hand, five days after cessation of dry needling, the suppression effect persisted and even became more pronounced in laminae I to II at L5-S2 levels in animals submitted to 5D dry needling, demonstrating prolonged dose-dependent effects. The immediate pain relief by 1D dry needling is probably elicited by the neural effect as demonstrated by changes in EPN. However, the long-term or accumulated effect of pain relief by 5D dry needling may be accompanied by and mediated via biochemical changes in addition to neural effects. Therefore, repetitive or extensive remote needling may provide better effects on reduction in SP levels for control of myofascial pain. It is commonly accepted that electroacupuncture of higher intensities and longer pulse durations can produce persistent analgesia [42].

5. Conclusion

The hypothesis that dry needling at distant MTrSs could modulate irritability of proximal MTrSs by altering the EPN amplitude and SP levels of muscle and spinal cords is supported by the present results. The findings of this study might elucidate the biochemical mechanisms induced by remote effects of dry needling. Accordingly, the practice of dry needling at some distance away from the painful site may facilitate decreased MTrP sensitivity in any muscle within the same levels of spinal innervations via activating the mechanisms of segmental and extrasegmental desensitization.

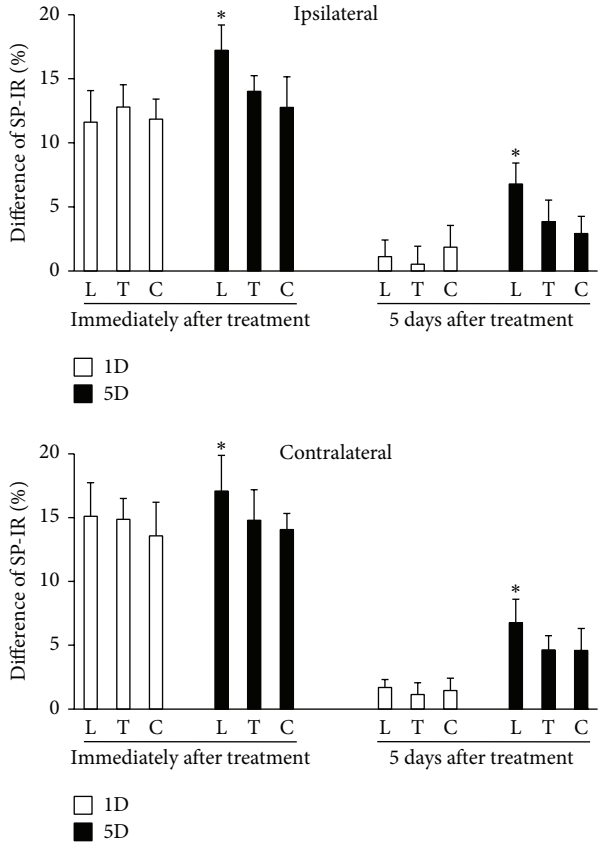

Figure 7: Differences in substance P (SP) levels at ipsilateral and contralateral superficial laminae of L5-S2 (L), T2-T5 (T), and C2-C5 (C) between animals after one-(1D) and five-dosage (5D) of dry needling at gastrocnemius in experimental (1D and 5D groups) and sham-operated groups (s1D and s5D groups). ∗ represents significant difference ($P < .05$) compared with SP levels of thoracic and cervical dorsal horns.

Further understanding of the analgesic action of dry needling in treating soft tissue pain can contribute to develop new therapeutic strategies for treating myofascial pain syndrome.

Conflict of Interests

No commercial party having a direct financial interest in the results of the research supporting this paper has or will confer a benefit upon the authors or upon any organization with which the authors are associated with.

Authors' Contribution

Li-Wei Chou had provided the same effort as Chang-Zern Hong.

Acknowledgment

This study was supported by a Grant from National Science Council (NSC 101-2314-B-241-001; 101-2314-B-039 -003 -MY2), China Medical University (CMU) (CMU-101-S-35), CMU under the Aim for Top University Plan of the Ministry of Education, and Cheng Ching General Hospital, Taiwan.

References

[1] J. G. Travell and D. G. Simons, *Myofascial Pain and Dysfunction: The Trigger Point Manual*, Williams & Wilkins, Baltimore, Md, USA, 1983.

[2] C. C. Gunn, W. E. Milbrandt, A. S. Little, and K. E. Mason, "Dry needling of muscle motor points for chronic low-back pain. A randomized clinical trial with long-term follow-up," *Spine*, vol. 5, no. 3, pp. 279–291, 1980.

[3] C.-Z. Hong, "New trends in myofascial pain syndrome," *Zhonghua Yi Xue Za Zhi*, vol. 65, no. 11, pp. 501–512, 2002.

[4] Y.-L. Hsieh, M.-J. Kao, T.-S. Kuan, S.-M. Chen, J.-T. Chen, and C.-Z. Hong, "Dry needling to a key myofascial trigger point may reduce the irritability of satellite MTrPs," *American Journal of Physical Medicine & Rehabilitation*, vol. 86, no. 5, pp. 397–403, 2007.

[5] D. M. Kietrys, K. M. Palombaro, and E. Azzaretto, "Effectiveness of dry needling for upper-quarter myofascial pain: a systematic review and meta-analysis," *The Journal of Orthopaedic and Sports Physical Therapy*, vol. 43, no. 9, pp. 620–634, 2013.

[6] J. Fernández-Carnero, R. la Touche, R. Ortega-Santiago et al., "Short-term effects of dry needling of active myofascial trigger points in the masseter muscle in patients with temporomandibular disorders," *Journal of Orofacial Pain*, vol. 24, no. 1, pp. 106–112, 2010.

[7] T. M. Cummings and A. R. White, "Needling therapies in the management of myofascial trigger point pain: a systematic review," *Archives of Physical Medicine and Rehabilitation*, vol. 82, no. 7, pp. 986–992, 2001.

[8] E. A. Tough, A. R. White, T. M. Cummings, S. H. Richards, and J. L. Campbell, "Acupuncture and dry needling in the management of myofascial trigger point pain: a systematic review and meta-analysis of randomised controlled trials," *European Journal of Pain*, vol. 13, no. 1, pp. 3–10, 2009.

[9] K. Itoh, Y. Katsumi, S. Hirota, and H. Kitakoji, "Randomised trial of trigger point acupuncture compared with other acupuncture for treatment of chronic neck pain," *Complementary Therapies in Medicine*, vol. 15, no. 3, pp. 172–179, 2007.

[10] K. Itoh, Y. Katsumi, and H. Kitakoji, "Trigger point acupuncture treatment of chronic low back pain in elderly patients—a blinded RCT," *Acupuncture in Medicine*, vol. 22, no. 4, pp. 170–177, 2004.

[11] Y.-L. Hsieh, S.-A. Yang, C.-C. Yang, and L.-W. Chou, "Dry needling at myofascial trigger spots of rabbit skeletal muscles modulates the biochemicals associated with pain, inflammation, and hypoxia," *Evidence-Based Complementary and Alternative Medicine*, vol. 2012, Article ID 342165, 12 pages, 2012.

[12] L.-W. Chou, M.-J. Kao, and J.-G. Lin, "Probable mechanisms of needling therapies for myofascial pain control," *Evidence-Based Complementary and Alternative Medicine*, vol. 2012, Article ID 705327, 11 pages, 2012.

[13] K.-H. Chen, K.-Y. Hsiao, C.-H. Lin, W.-M. Chang, H.-C. Hsu, and W.-C. Hsieh, "Remote effect of lower limb acupuncture on latent myofascial trigger point of upper trapezius muscle: a pilot study," *Evidence-based Complementary and Alternative Medicine*, vol. 2013, Article ID 287184, 8 pages, 2013.

[14] C.-T. Tsai, L.-F. Hsieh, T.-S. Kuan, M.-J. Kao, L.-W. Chou, and C.-Z. Hong, "Remote effects of dry needling on the irritability

of the myofascial trigger point in the upper trapezius muscle," *American Journal of Physical Medicine and Rehabilitation*, vol. 89, no. 2, pp. 133–140, 2010.

[15] L.-W. Chou, Y.-L. Hsieh, M.-J. Kao, and C.-Z. Hong, "Remote influences of acupuncture on the pain intensity and the amplitude changes of endplate noise in the myofascial trigger point of the upper trapezius muscle," *Archives of Physical Medicine and Rehabilitation*, vol. 90, no. 6, pp. 905–912, 2009.

[16] L.-W. Chou, Y.-L. Hsieh, H.-S. Chen, C.-Z. Hong, M.-J. Kao, and T.-I. Han, "Remote therapeutic effectiveness of acupuncture in treating myofascial trigger point of the upper trapezius muscle," *The American Journal of Physical Medicine and Rehabilitation*, vol. 90, no. 12, pp. 1036–1049, 2011.

[17] Y.-L. Hsieh, L.-W. Chou, Y.-S. Joe, and C.-Z. Hong, "Spinal cord mechanism involving the remote effects of dry needling on the irritability of myofascial trigger spots in rabbit skeletal muscle," *Archives of Physical Medicine & Rehabilitation*, vol. 92, no. 7, pp. 1098–1105, 2011.

[18] C.-Z. Hong and Y. Torigoe, "Electrophysiological characteristics of localized twitch responses in responsive taut bands of rabbit skeletal muscle fibers," *Journal of Musculoskeletal Pain*, vol. 2, no. 2, pp. 17–43, 1994.

[19] D. G. Simons, C.-Z. Hong, and L. S. Simons, "Prevalence of spontaneous electrical activity at trigger spots and at control sites in rabbit skeletal muscle," *Journal of Musculoskeletal Pain*, vol. 3, no. 1, pp. 35–48, 1995.

[20] D. G. Simons, C.-Z. Hong, and L. S. Simons, "Endplate potentials are common to midfiber myofacial trigger points," *American Journal of Physical Medicine and Rehabilitation*, vol. 81, no. 3, pp. 212–222, 2002.

[21] T.-S. Kuan, J. T. Chen, S. M. Chen, C. H. Chien, and C. Z. Hong, "Effect of botulinum toxin on endplate noise in myofascial trigger spots of rabbit skeletal muscle," *American Journal of Physical Medicine and Rehabilitation*, vol. 81, no. 7, pp. 512–520, 2002.

[22] K.-H. Chen, C.-Z. Hong, F.-C. Kuo, H.-C. Hsu, and Y.-L. Hsieh, "Electrophysiologic effects of a therapeutic laser on myofascial trigger spots of rabbit skeletal muscles," *American Journal of Physical Medicine and Rehabilitation*, vol. 87, no. 12, pp. 1006–1014, 2008.

[23] K.-H. Chen, C.-Z. Hong, H.-C. Hsu, S.-K. Wu, F.-C. Kuo, and Y.-L. Hsieh, "Dose-dependent and ceiling effects of therapeutic laser on myofascial trigger spots in rabbit skeletal muscles," *Journal of Musculoskeletal Pain*, vol. 18, no. 3, pp. 235–245, 2010.

[24] T.-S. Kuan, C.-Z. Hong, J.-T. Chen, S.-M. Chen, and C.-H. Chien, "The spinal cord connections of the myofascial trigger spots," *European Journal of Pain*, vol. 11, no. 6, pp. 624–634, 2007.

[25] M. Zimmermann, "Ethical considerations in relation to pain in animal experimentation," *Acta Physiologica Scandinavica*, vol. 128, no. 554, pp. 221–233, 1986.

[26] M. Zimmermann, "Ethical guidelines for investigations of experimental pain in conscious animals," *Pain*, vol. 16, no. 2, pp. 109–110, 1983.

[27] K.-H. Chen, C.-Z. Hong, F.-C. Kuo, H.-C. Hsu, and Y.-L. Hsieh, "Electrophysiologic effects of a therapeutic laser on myofascial trigger spots of rabbit skeletal muscles," *The American Journal of Physical Medicine and Rehabilitation*, vol. 87, no. 12, pp. 1006–1014, 2008.

[28] J. Fernández-Carnero, H.-Y. Ge, Y. Kimura, C. Fernández-De-Las-Peñas, and L. Arendt-Nielsen, "Increased spontaneous electrical activity at a latent myofascial trigger point after nociceptive stimulation of another latent trigger point," *Clinical Journal of Pain*, vol. 26, no. 2, pp. 138–143, 2010.

[29] S. Harrison and P. Geppetti, "Substance *P*," *International Journal of Biochemistry and Cell Biology*, vol. 33, no. 6, pp. 555–576, 2001.

[30] Y. Kobayashi, M. Sekiguchi, S.-I. Konno, and S.-I. Kikuchi, "Increased intramuscular pressure in lumbar paraspinal muscles and low back pain: model development and expression of substance P in the dorsal root ganglion," *Spine*, vol. 35, no. 15, pp. 1423–1428, 2010.

[31] A. W. Duggan, I. A. Hendry, C. R. Morton, W. D. Hutchison, and Z. Q. Zhao, "Cutaneous stimuli releasing immunoreactive substance P in the dorsal horn of the cat," *Brain Research*, vol. 451, no. 1-2, pp. 261–273, 1988.

[32] G.-Y. Xu, L.-Y. M. Huang, and Z.-Q. Zhao, "Activation of silent mechanoreceptive cat C and Aδ sensory neurons and their substance P expression following peripheral inflammation," *Journal of Physiology*, vol. 528, no. 2, pp. 339–348, 2000.

[33] T. Hokfelt, J. O. Kellerth, G. Nilsson, and B. Pernow, "Substance P: localization in the central nervous system and in some primary sensory neurons," *Science*, vol. 190, no. 4217, pp. 889–890, 1975.

[34] H. Zhang, C.-L. Cang, Y. Kawasaki et al., "Neurokinin-1 receptor enhances TRPV1 activity in primary sensory neurons via PKCε: a novel pathway for heat hyperalgesia," *Journal of Neuroscience*, vol. 27, no. 44, pp. 12067–12077, 2007.

[35] P. W. Mantyh, S. D. Rogers, P. Honore et al., "Inhibition of hyperalgesia by ablation of lamina I spinal neurons expressing the substance P receptor," *Science*, vol. 278, no. 5336, pp. 275–279, 1997.

[36] C. De Felipe, J. F. Herrero, J. A. O'Brien et al., "Altered nociception, analgesia and aggression in mice lacking the receptor for substance P," *Nature*, vol. 392, no. 6674, pp. 394–397, 1998.

[37] L.-X. Zhu, F.-Y. Zhao, and R.-L. Cui, "Effect of acupuncture on release of substance P," *Annals of the New York Academy of Sciences*, vol. 632, pp. 488–489, 1991.

[38] J. Du and L. He, "Alterations of spinal dorsal horn substance P following electroacupuncture analgesia—a study of the formalin test with immunohistochemistry and densitometry," *Acupuncture and Electro-Therapeutics Research*, vol. 17, no. 1, pp. 1–6, 1992.

[39] N. Yonehara, T. Sawada, H. Matsuura, and R. Inoki, "Influence of electro-acupuncture on the release of substance P and the potential evoked by tooth pulp stimulation in the trigeminal nucleus caudalis of the rabbit," *Neuroscience Letters*, vol. 142, no. 1, pp. 53–56, 1992.

[40] J. P. Shah, J. V. Danoff, M. J. Desai et al., "Biochemicals associated with pain and inflammation are elevated in sites near to and remote from active myofascial trigger points," *Archives of Physical Medicine and Rehabilitation*, vol. 89, no. 1, pp. 16–23, 2008.

[41] J. P. Shah, T. M. Phillips, J. V. Danoff, and L. H. Gerber, "An in vivo microanalytical technique for measuring the local biochemical milieu of human skeletal muscle," *Journal of Applied Physiology*, vol. 99, no. 5, pp. 1977–1984, 2005.

[42] V. V. Romita, A. Suk, and J. L. Henry, "Parametric studies on electroacupuncture-like stimulation in a rat model: effects of intensity, frequency, and duration of stimulation on evoked antinociception," *Brain Research Bulletin*, vol. 42, no. 4, pp. 289–296, 1997.

Hindawi Publishing Corporation
BioMed Research International
Volume 2014, Article ID 762930, 12 pages
http://dx.doi.org/10.1155/2014/762930

Research Article

Minocycline Enhances the Effectiveness of Nociceptin/Orphanin FQ during Neuropathic Pain

Katarzyna Popiolek-Barczyk,[1] Ewelina Rojewska,[1] Agnieszka M. Jurga,[1] Wioletta Makuch,[1] Ferenz Zador,[2] Anna Borsodi,[2] Anna Piotrowska,[1] Barbara Przewlocka,[1] and Joanna Mika[1]

[1] *Department of Pain Pharmacology, Institute of Pharmacology, Polish Academy of Sciences, 12 Smetna Street, 31-343 Cracow, Poland*
[2] *Institute of Biochemistry, Biological Research Center, Hungarian Academy of Sciences, Temesvári krt 62 Street, Szeged 6726, Hungary*

Correspondence should be addressed to Joanna Mika; joasia272@onet.eu

Received 14 May 2014; Accepted 1 August 2014; Published 3 September 2014

Academic Editor: Livio Luongo

Nociceptin/orphanin FQ (N/OFQ) antinociception, which is mediated selectively by the N/OFQ peptide receptor (NOP), was demonstrated in pain models. In this study, we determine the role of activated microglia on the analgesic effects of N/OFQ in a rat model of neuropathic pain induced by chronic constriction injury (CCI) to the sciatic nerve. Repeated 7-day administration of minocycline (30 mg/kg i.p.), a drug that affects microglial activation, significantly reduced pain in CCI-exposed rats and it potentiates the analgesic effects of administered N/OFQ (2.5–5 μg i.t.). Minocycline also downregulates the nerve injury-induced upregulation of NOP protein in the dorsal lumbar spinal cord. Our *in vitro* study showed that minocycline reduced *NOP* mRNA, but not protein, level in rat primary microglial cell cultures. In [^{35}S]GTPγS binding assays we have shown that minocycline increases the spinal N/OFQ-stimulated NOP signaling. We suggest that the modulation of the N/OFQ system by minocycline is due to the potentiation of its neuronal antinociceptive activity and weakening of the microglial cell activation. This effect is beneficial for pain relief, and these results suggest new targets for the development of drugs that are effective against neuropathic pain.

1. Introduction

Neuropathic pain is a common consequence of nervous tissue damage. The mechanisms underlying neuropathy still remain unclear, and the currently available drugs are frequently ineffective, making treatment a major clinical challenge [1, 2]. Nociceptin/orphanin FQ (N/OFQ) acts through the N/OFQ peptide receptor (NOP) [3] and can change responsiveness to painful stimuli in several models of pain [4–6]. Pro- and antinociceptive effects of N/OFQ have been reported in a variety of animal models depending on the route of administration. Intracerebroventricular (i.c.v.) administration was found to display hyperalgesic effects [3, 7, 8], which were mediated by NOP, as these effects are not present in NOP-knockout mice [9]. In contrast, N/OFQ administered intrathecally (i.t.) has been generally found to produce antinociceptive responses [4, 5, 10–16].

The role of N/OFQ in the development of neuropathic pain has been extensively studied. In recent studies, it has been found that the N/OFQ system influences glial cell functions [17–21] and now it is considered if neuroimmune interaction may be one of the mechanisms of its antinociceptive properties. We have shown that microglia are the glial cell type to be activated in response to peripheral nerve injury and that this activation is in parallel with changes in neuropeptide systems involved in nociceptive transmission (proenkephalin, prodynorphin, and pronociceptin) [17]. Biochemical studies revealed the presence of N/OFQ and its receptor in the CNS and peripheral tissues, particularly in regions associated with nociceptive pathways [22–28].

The NOP was demonstrated to be expressed not only on neurons but also on astrocytes and microglia [20, 21], which further suggest the involvement of these cells in the modulation of N/OFQ system. Fu et al. have [20] shown that spinal cord astrocyte activation and *in vitro* cytokine production by those glial cells are attenuated by N/OFQ through the astrocytic NOP. It was shown that LPS-induced IL-1β gene expression was reduced by N/OFQ in cultured primary microglia, but it was enhanced in neuronal cultures [21]. The regulatory effects of N/OFQ on glia-derived cytokines suggest that the action of the N/OFQ system is dependent on glial cell activation in the CNS.

The aim of the present study was to determine the role of activated microglia in the analgesic effects of N/OFQ in a rat model of neuropathic pain (achieved by chronic constriction injury to the sciatic nerve, CCI). In our studies, we used minocycline, a well-characterized drug for inhibiting microglial activation [29–32], viability, and migration [33, 34]. Minocycline (30 mg/kg) was intraperitoneally (i.p.) administered preemptively 16 h and 1 h before CCI and then twice daily for 7 days. On day 7 after injury, vehicle- or minocycline-treated CCI-exposed rats received intrathecally (i.t.) N/OFQ, and we examined the analgesic effects using von Frey and cold plate tests. In our biochemical studies, we analyzed molecular changes in mRNA and protein levels of the NOP in the dorsal horn of the lumbar spinal cord at day 7 after injury in vehicle- or minocycline-treated CCI-exposed rats using qRT-PCR and Western blot analysis, respectively. Additionally, using primary cultures of rat microglia, we investigated the effects of minocycline on mRNA and protein levels of NOP. We also investigated the effects of minocycline on NOP signaling in the spinal cord of the vehicle- or minocycline-treated CCI-exposed rats using a functional [^{35}S]GTPγS binding assay.

2. Methods

2.1. Animals. Male Wistar rats (200–350 g) were housed in cages that were lined with sawdust under a standard 12/12 h light/dark cycle (lights on at 08:00 h) with food and water available *ad lib*. Care was taken to reduce the number of animals used. All experiments were approved by the local bioethics committee (Cracow, Poland) and were performed according to the recommendations of IASP [35], ARRIVE guidelines [36], and the NIH Guide for the Care and Use of Laboratory Animals.

2.2. Surgical Preparations. Chronic constriction injury (CCI) was produced in rats according to Bennett and Xie [37], by tying four ligatures around the sciatic nerve under sodium pentobarbital anesthesia (60 mg/kg; i.p.). The *biceps femoris* and the *gluteus superficialis* were separated, and the right sciatic nerve was exposed. The ligatures (4/0 silk) were tied loosely around the nerve distal to the sciatic notch with 1-mm spacing until they elicited a brief twitch in the respective hind limb. After the surgery, all rats developed long-lasting neuropathic pain symptoms such as allodynia and hyperalgesia. Because we have shown in earlier studies that there are no differences between the nociceptive responses of naïve and sham animals [38], we used naïve animals for the behavioral experiments in the present study.

2.3. Intrathecal (i.t.) Injection. Rats were prepared for intrathecal (i.t.) injection by implanting catheters according to the method of Yaksh and Rudy [39] under pentobarbital (60 mg/kg i.p.) anesthesia. The intrathecal catheter consisted of polyethylene tubing that was 12 cm long (PE 10, Intramedic; Clay Adams, Parsippany, NJ) with an outside diameter of 0.4 mm and a dead space of 10 μL that had been sterilized by immersion in 70% (v/v) ethanol and been fully flushed with sterile water before insertion. Rats were placed on a stereotaxic table (David Kopf Instruments, Tujunga, CA), and an incision was made in the atlantooccipital membrane. The catheter (7.8 cm of its length) was carefully introduced into the subarachnoid space at the rostral level of the spinal cord lumbar enlargement (L4-L5). After the implantation, the first injection of 10 μL of water was performed slowly, and the catheter was tightened. After catheter implantation, the rats were monitored for physical impairments. Those showing motor deficits (ca 5%) were excluded from further study. Animals were allowed a minimum of 1 week to recover after the surgery before the experiment began. Water for injection or respective drugs were delivered slowly (1-2 min) in a volume of 5 μL through the i.t. catheter and were followed by 10 μL of water, which flushed the catheter.

2.4. Behavioral Tests

2.4.1. Tactile Allodynia (Von Frey Test). Allodynia was measured in rats subjected to CCI by the use of an automatic von Frey apparatus (Dynamic Plantar Aesthesiometer cat. no. 37400, Ugo Basile, Italy). Rats were placed in plastic cages with a wire net floor 5 min before the experiment. The von Frey filament (up to 26 g) was applied to the midplantar surface of the hind foot, and measurements were taken automatically [40].

2.4.2. Hyperalgesia (Cold Plate Test). Hyperalgesia was assessed using the cold plate test (Cold/Hot Plate Analgesia Meter no. 05044 Columbus Instruments, USA) as has been described previously [40, 41]. The temperature of the cold plate was maintained at 5°C, and the cut-off latency was 30 s. The rats were placed on the cold plate, and the time until lifting of the hind foot was recorded. The injured foot was the first to react in every case.

2.5. Drug Administration. The chemicals used in this study and their sources were as follows: N/OFQ (cat. no. 0910, TOCRIS, UK), and minocycline hydrochloride (cat. no. M9511, Sigma-Aldrich, USA). Minocycline (30 mg/kg; i.p.) was dissolved in sterile water and preemptively administered intraperitoneally 16 h and 1 h before CCI and then twice daily for 7 days. This method of minocycline administration was used throughout the work and is referred to in the text as "repeated administration". The control groups received a vehicle (water for injection) according to the same schedule.

One hour after the last morning of minocycline or vehicle administration on day 7 after CCI, N/OFQ (2.5 and 5 μg/5 μL) or a vehicle was i.t. injected. After vehicle or N/OFQ administration the von Frey test (20 and 40 min later) and cold plate tests (30 and 50 min later) were performed.

2.6. Microglial Cell Cultures and Treatments. Primary cultures of microglial cells were prepared from 1-day-old Wistar rat pups as previously described [42]. Briefly, cells were isolated from the rats' cerebral cortices and were plated at a density of 3×10^5 cells/cm^2 in a culture medium that consisted of DMEM/Glutamax/high glucose (Gibco, USA) supplemented with heat-inactivated 10% fetal bovine serum (Gibco, USA), 100 U/mL penicillin, and 0.1 mg/mL streptomycin (Gibco, USA) on poly-L-lysine coated 75 cm^2 culture flasks maintained at 37°C and 5% CO_2. The culture medium was changed after 4 days. The loosely adherent microglial cells were recovered after 9 days by mild shaking and centrifugation. Microglial cells were suspended in a culture medium and plated at a final density of 2×10^5 cells onto 24-well plates and 1.2×10^6 cells onto 6-well plates. Adherent cells were incubated for 48 h in a culture medium before being used for the analyses. Cell specificity was determined in cultures of primary microglia by Western blot assay using an antibody against OX-42 (a microglial marker) and qRT-PCR using primers for *C1q* (a microglial marker) and *GFAP* (an astrocyte marker). The homogeneity of microglial population was kept on high level (more than 95% positive for OX-42 and C1q), and our homogeneity was similar to those published by Mika et al. [41]. Primary microglial cell cultures were treated with minocycline (10 μM) or vehicle (water) for 6 h for mRNA analysis and for 24 h for protein analysis.

2.7. qRT-PCR Analysis of Gene Expression. Ipsilateral dorsal rat spinal cords (L4–L6) were collected 7 days after injury, 4 h after last morning minocycline treatment. Total RNA was extracted according to the method described by Chomczynski and Sacchi [43] using TRIzol reagent (Invitrogen) as previously described [6]. RNA concentration was measured using a NanoDrop ND-1000 Spectrometer (NanoDrop Technologies). Reverse transcription was performed on 500 ng (from cell cultures) or 1000 ng (from tissue) of total RNA using Omniscript reverse transcriptase (Qiagen Inc.) at 37°C for 60 min. cDNA was diluted 1 : 10 with H_2O. qRT-PCR was performed using Assay-On-Demand TaqMan probes according to the manufacturer's protocol (Applied Biosystems) and run on a Real-Time PCR iCycler (BioRad, Hercules, CA, USA). Rn01527838_g1 (*Hprt*) and Rn00440563_m1 (*Orl1*) were used as TaqMan primers and probes. The expression of HPRT (a housekeeping gene) was quantified to control group for variation in cDNA amounts. Cycle threshold values were calculated automatically by iCycler IQ 3.0 software with default parameters. Abundance of RNA was calculated as $2^{-(\text{threshold cycle})}$.

2.8. Western Blot Analysis. Ipsilateral dorsal rat spinal cords (L4–L6) were collected for protein analyses at day 7 after injury, 6 h after the last morning minocycline treatment. Cell and tissue lysates were collected in RIPA buffer with a protease inhibitor cocktail and cleared by centrifugation (14000 ×g for 30 min, 4°C). Samples containing 15 μg (cells lysates) and 20 μg (tissue lysates) of protein were heated in a loading buffer (50 mM Tris-HCl, 2% SDS, 2% β-mercaptoethanol, 4% glycerol, and 0.1% bromophenol blue) for 8 min at 98°C and resolved on 10–20% Criterion TGX precast polyacrylamide gels. Following gel electrophoresis, the proteins were transferred to Immune-Blot PVDF membranes (Bio-Rad) with semidry transfer (30 min, 25 V). The membranes were blocked for 1 h using 5% nonfat dry milk (Bio-Rad) in Tris-buffered saline with 0.1% Tween 20 (TBST), washed in TBST, incubated overnight at 4°C with primary antibodies (rabbit polyclonal anti-OPRL1, 1 : 600; rabbit polyclonal anti-IBA1, 1 : 500, ProteinTech), and incubated for 1 h at RT with a secondary goat polyclonal antibody that had been conjugated to horseradish peroxidase (goat anti-rabbit IgG, 1 : 5000, BioRad). Both primary and secondary antibodies were diluted in solutions from SignalBoost Immunoreaction Enhancer Kit (Merck Millipore). Membranes were washed 2×2 min and 3×5 min with TBST. Immunocomplexes were detected using a Immun-Star HRP Chemiluminescent Substrate Kit (BioRad) and visualized using a Fujifilm LAS-4000 FluorImager system. The blots were stripped using Restore Western Blot Stripping Buffer (ThermoScientific) for 15 min at RT, washed in TBST, and reprobed with a mouse antibody against GAPDH (1 : 5000, Millipore) as a loading control. The relative levels of immunoreactivity were quantified using Fujifilm Multi Gauge software.

2.9. Immunocytochemical Analysis. We used commercially available specific anti-NOP antibodies. Cells were fixed for 20 minutes in 4% paraformaldehyde in a 0.1 M phosphate buffer (pH 7.4) and incubated with primary antibodies (rabbit anti-ORL-1, 1 : 500, ProteinTech) for 2 days at 4°C. After three washes in phosphate buffered saline (PBS), immunofluorescence was revealed by incubation for 2 h in the fluorochrome-conjugated secondary antibody, Alexa Fluor555 donkey, antirabbit diluted 1 : 500 in 5% NDS. Sections were then washed with PB and coverslipped with an Aquatex mounting medium (Merck, Darmstadt, Germany). Sections without primary antibodies were used as negative controls.

2.10. Functional [^{35}S]GTPγS Binding Assay. Ipsilateral dorsal rat spinal cords (L4–L6) were collected 7 days after injury, 6 h after the last morning minocycline treatment and were prepared for the assay as previously described [44] with modifications. The membrane fractions of rat spinal cords were diluted in TEM buffer (50 mM Tris-HCl, 1 mM EGTA, and 5 mM $MgCl_2$; pH 7.4) to achieve the appropriate protein content for the assays (~10 μg of protein/sample).

The [^{35}S]GTPγS assays were prepared according to Sim et al. [45] and Traynor and Nahorski [46] with slight modifications. The membrane fractions were incubated at 30°C for 60 min in Tris-EGTA buffer (composed of 50 mM Tris-HCl, 1 mM EGTA, 3 mM $MgCl_2$, and 100 mM NaCl; pH 7.4). The buffer also contained 20 MBq/0.05 cm^3 [^{35}S]GTPγS (0.05 nM) and increasing concentrations (10^{-10}–10^{-5} M) of

N/OFQ 1–17 in the presence of excess GDP (30 μM) in a final volume of 1 mL. Total binding (T) was measured in the absence of N/OFQ 1–17, while nonspecific binding (NS) was determined in the presence of 10 μM unlabeled GTPγS and subtracted from the total binding. The difference (T-NS) represents basal activity. Bound and free [^{35}S]GTPγS were separated by vacuum filtration through Whatman GF/B filters with Brandel M24R cell harvester. Filters were washed three times with 5 mL ice-cold buffer (pH 7.4), and the radioactivity of the filters was detected in UltimaGold MV aqueous scintillation cocktail with Packard Tricarb 2300TR liquid scintillation counter. [^{35}S]GTPγS binding experiments were performed in triplicates and repeated at least three times.

2.11. Data Analysis. The behavioral data are presented as the mean ± SEM of 8–16 rats per group. The results of the experiments were statistically evaluated using one-way analysis of variance (ANOVA). All of the differences between the treatment groups were further analyzed with Bonferroni's *post hoc* tests. Significant differences in comparisons with vehicle-treated CCI-exposed rats are indicated by $^{*}P(< 0.05)$, $^{**}P(< 0.01)$, and $^{***}P(< 0.001)$. Significant differences between vehicle-treated CCI-exposed rats that had received a single dose of N/OFQ and minocycline-treated CCI-exposed rats that had received a single dose of N/OFQ are indicated by $^{\#}P(< 0.05)$ and $^{\#\#\#}P(< 0.001)$.

The qRT-PCR analyses from the tissue were performed in three groups: naïve, vehicle-treated CCI-exposed, and minocycline-treated CCI-exposed rats. The results from 6–8 animals are presented as fold changes compared with the naïve rats in the ipsilateral dorsal lumbar spinal cord. The results from 4 cell cultures are presented as fold changes compared with vehicle-treated cells. The qRT-PCR data are presented as the mean ± SEM and represent the normalized averages that were derived from the threshold qRT-PCR cycles from four to eight samples for each group. Intergroup differences were analyzed using ANOVAs followed by Bonferroni's multiple comparison tests. In the cell cultures analysis, the intergroup differences were analyzed by *t*-test; significant differences resulting from comparisons with nonstimulated cells are indicated by $^{*}P(< 0.05)$.

The protein analyses were performed using Western blots. The analyses from the tissue were performed in three groups: naïve, vehicle-treated CCI-exposed, and minocycline-treated CCI-exposed rats. The results are presented as fold changes compared to the naïve rats in the ipsilateral dorsal lumbar spinal cord. The results from cell cultures are presented as fold changes compared with vehicle-treated cells. The data are presented as the mean ± SEM and represent the normalized averages derived from analyses of four to five samples for each group (for tissue analysis) and four cell cultures performed with the Multi Gauge analysis program. Intergroup differences were analyzed using ANOVA followed by Bonferroni's multiple comparison tests. $^{**}P(< 0.01)$ indicates significant differences compared to naïve rats. $^{\#}P(< 0.05)$ indicates significant differences compared to the CCI-treated group. In cell cultures analysis intergroup differences were analyzed with *t*-test.

In the [^{35}S]GTPγS binding assays, the specifically bound [^{35}S]GTPγS were presented as percentages as the function of the applied concentrations of N/OFQ 1–17 in logarithmic scale. Basal activity was settled as 100%; experimental data are presented as the mean ± S.E.M. The data were fitted with GraphPad Prism 5.0 (GraphPad Prism Software Inc., San Diego, CA) curve fitting program to determine the maximal stimulation or efficacy ($E_{\max}$) of the receptor mediated G-protein and the potency (EC_{50}) of the stimulator ligand. Statistical analysis was performed using one-way ANOVA with Bonferroni's multiple comparison *post hoc* test to determine the significance level. Significance was accepted at the $^{*}P(< 0.05)$ level.

3. Results

3.1. Repeated Minocycline Administration Diminished the Development of Neuropathic Pain and Enhanced the Effectiveness of Nociceptin/Orphanin FQ. In the behavioral tests, all vehicle-treated CCI-exposed rats exhibited neuropathic pain symptoms. Seven days after injury, rats exhibited strong allodynia as measured by the von Frey test (11.7 g ± 0.6 compared with 25.8 g ± 0.2 for naïve rats) (Figure 1(a)) and potent hyperalgesia as measured by the cold plate test (7.6 s ± 0.9 compared with 29.7 s ± 0.3 for naïve rats) (Figure 1(b)). Minocycline (30 mg/kg; i.p.) administered repeatedly was effective in reducing mechanical allodynia as measured by the von Frey test (vehicle-treated 11.7 g ± 0.6 versus minocycline-treated 18.0 g ± 0.6) (Figure 1(a)) and also in reducing cold hyperalgesia as measured by the cold plate test (vehicle-treated 7.6 s ± 0.9 versus 12.1 s ± 0.9 minocycline-treated) (Figure 1(b)).

N/OFQ (2.5 and 5 μg; i.t.) was injected at day 7 at one hour after the last morning dose of minocycline (30 mg/kg; i.p.) or vehicle. The effect of N/OFQ (2.5 μg; 5 μg/μL; i.t.) in minocycline-treated rats as compared with vehicle-treated ones was significantly increased in the von Frey test 20 and 40 minutes after injection (Figure 1(a)). The antihyperalgesic effect of the lower dose of N/OFQ (2.5 μg/μL; i.t.) in minocycline-treated rats compared with vehicle-treated rats was significantly upregulated only after 50 minutes, while at a higher dose (5 μg/μL; i.t.) the antihyperalgesic effect was potentiated at both times (Figure 1(b)).

3.2. Repeated Minocycline Administration Influenced the Nociceptin/Orphanin FQ System Parallel to Microglia Regulation in the Spinal Cord Level under Neuropathic Pain. Seven days after CCI in the ipsilateral lumbar dorsal spinal cord an increase of 60% of NOP protein was observed compared with naive animals (Figure 2(b)). Repeated administration of minocycline reduced the upregulation of NOP protein level (by 24%) in comparison with naive rats (Figure 2(b)). No changes in *NOP* mRNA were seen in the vehicle- or the minocycline-treated rats compared with naive animals (Figure 2(a)). Parallel to NOP protein regulation, we observed the upregulation of protein by 185% for IBA-1

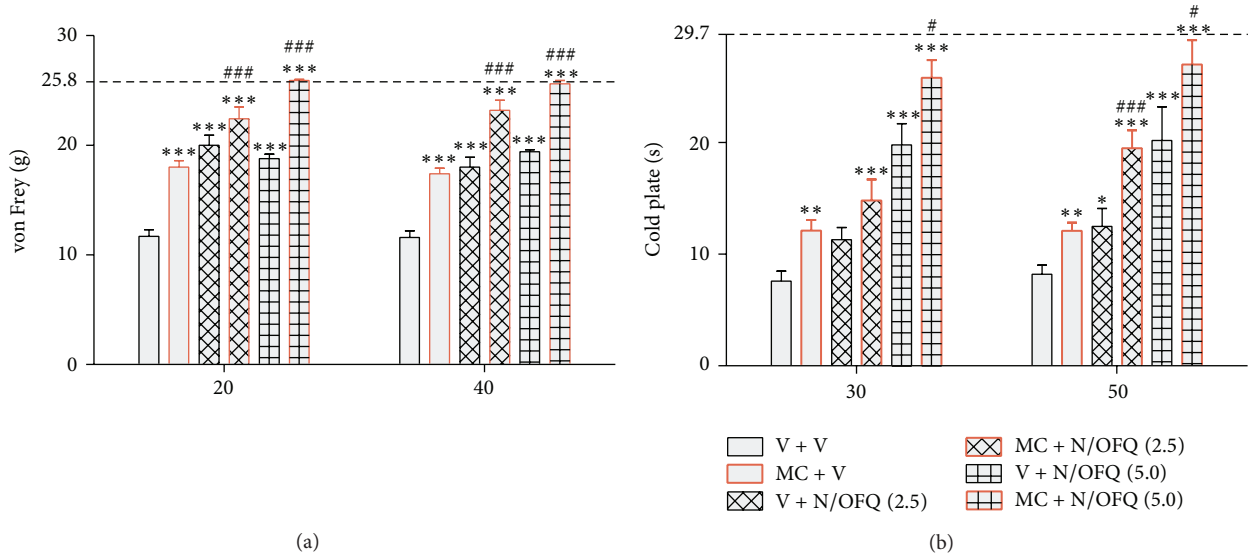

Figure 1: Repeated minocycline administration diminished the development of neuropathic pain and enhanced the effectiveness of N/OFQ. The response to N/OFQ was measured 20 and 40 minutes after administration by the von Frey test (a) and 30 and 50 minutes after administration by the cold plate test (b). Minocycline (MC; 30 mg/kg; i.p.) was administered intraperitoneally preemptively 16 h and 1 h before CCI and then repeatedly twice daily for 7 days. Vehicle-treated and minocycline-treated rats received intrathecal N/OFQ (2.5; 5 μg/5 μL) one hour after the last morning administration on day 7 after CCI. The data are presented as the mean response ± SEM. (8–16 rats per group). The results of the experiments were statistically evaluated using one-way analyses of variance (ANOVA). The differences between the treatment groups throughout the study were further analyzed with Bonferroni's *post hoc* tests. $^{*}P < 0.05$, $^{**}P < 0.01$, and $^{***}P < 0.001$ indicate significant differences compared with vehicle-treated CCI-exposed rats; $^{\#}P < 0.05$ and $^{\#\#\#}P < 0.001$ indicate significant differences between vehicle-treated CCI-exposed rats that received a single dose of N/OFQ and minocycline-treated CCI-exposed rats that received a single dose of N/OFQ. The dotted line is a value for naïve animals (von Frey test 25.8 g; cold plate test 29.7 s).

(a microglial marker) in the ipsilateral lumbar dorsal spinal cord in the vehicle-treated rats (Figure 2(c)). Repeated administration of minocycline diminished the level of microglial activation marker to 57% in comparison with naive rats (Figure 2(c)).

3.3. Repeated Minocycline Administration Influenced Nociceptin/Orphanin FQ Peptide Receptor Signaling under Neuropathic Pain. In the [^{35}S]GTPγS binding assay, during N/OFQ stimulation in the ipsilateral lumbar dorsal rat spinal cord CCI-exposed rats remained unaffected compared to the naive group. However, repeated minocycline treatment markedly increased the specific binding of the nucleotide analogue during NOP-mediated G-protein activation (Figure 3(b)). This resulted in a significant increase in the maximal activation (or efficacy, E_{max}) of NOP-mediated G-protein compared with the vehicle-treated CCI-exposed group (Figure 3(a)). The potency (pEC_{50}) of the ligand remained unaltered (data not shown; the curves did not shift to either side to a significant degree) compared to naive either to vehicle treated CCI-exposed animals (Figure 3(b)).

3.4. Minocycline Influenced the Nociceptin/Orphanin FQ Peptide Receptor mRNA but Not Protein Levels in Rat Primary Microglial Cell Cultures. Rat primary microglial cell cultures were treated with minocycline (10 μM) for 6 h and 24 h for mRNA and protein analysis, respectively. The qRT-PCR analysis shows that minocycline downregulates *NOP* mRNA in comparison with vehicle-treated cells (Figure 4(a)). Using Western blot analysis we have shown that minocycline did not have influence on the protein level of NOP after 24 h treatment in primary microglial cell cultures in comparison with vehicle-treated cells (Figure 4(b)). The presence of NOP in microglial cells was confirmed by immunocytochemistry (Figure 4(c)).

4. Discussion

Numerous pain studies are focused on the N/OFQ system because it is known that at the spinal cord level N/OFQ shows antinociceptive action through NOP, present in sensory neurons. NOP is considered as a novel potential target in the pain therapy. However, the role played by microglia in the functioning of this system has not been studiedthus far. In the present study, we have shown for the first time the important influence of microglial activation on the effectiveness of the N/OFQ system. We demonstrated that repeated administration of minocycline potentiated the analgesic effects of N/OFQ in neuropathic rats and the effect seems to be additive. Chronic minocycline administration reduced the elevated spinal level of NOP protein of CCI-exposed rats, and it significantly increased NOP signaling possibly through the upregulation of NOP coupled G_i protein activation. Interestingly, in our *in vitro* studies we had shown that minocycline downregulates mRNA level for NOP in primary microglial cell cultures.

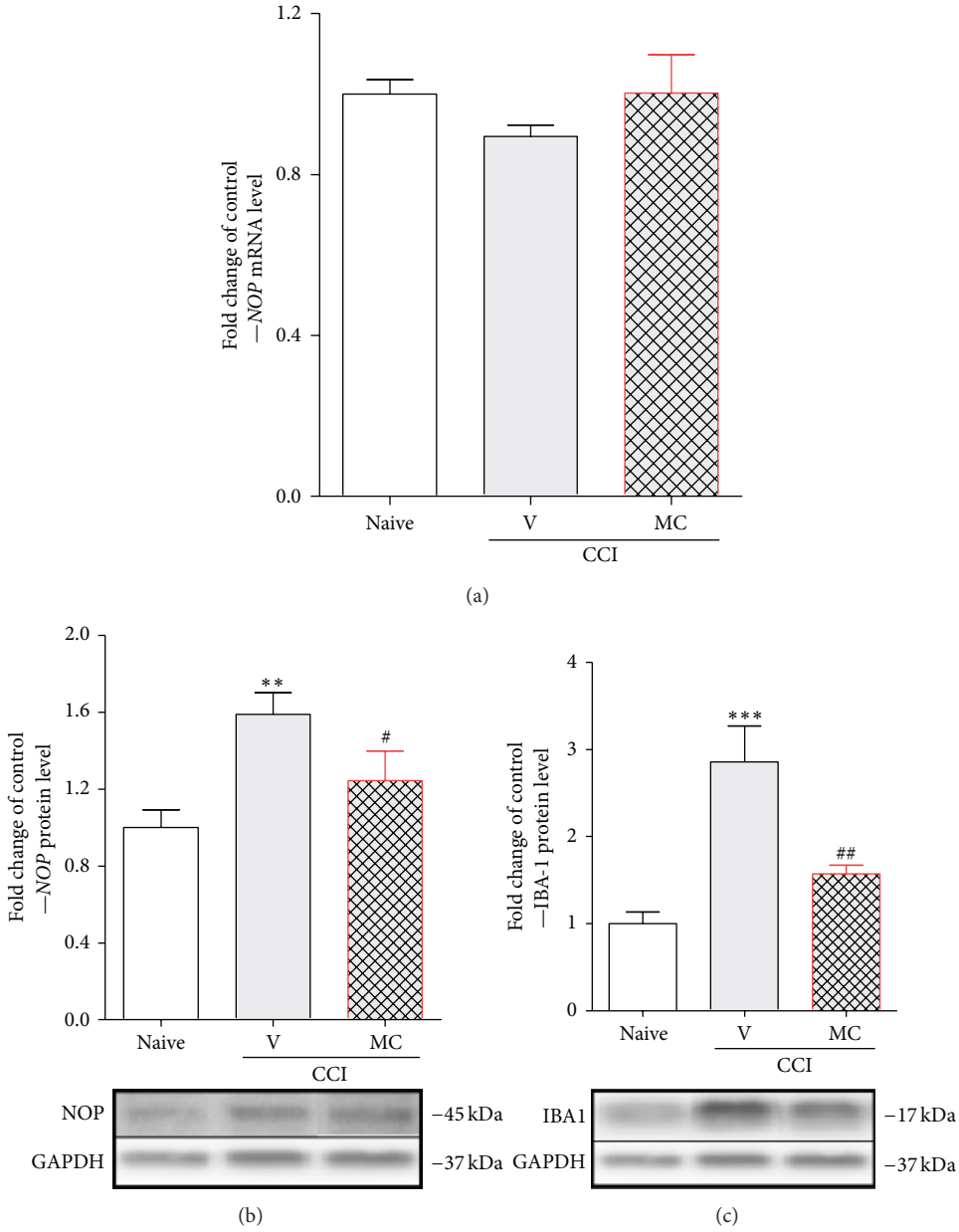

Figure 2: Repeated minocycline administration influenced the N/OFQ system parallel to microglia regulation in the spinal cord level under the neuropathic pain. Seven days after CCI in the ipsilateral dorsal spinal cord, minocycline-treatment diminished the level of NOP (b) and IBA-1 (c) proteins levels that were upregulated by nerve injury. The *NOP* mRNA level was unchanged by nerve injury and minocycline treatment (a). The qRT-PCR and Western blot data are presented as the mean ± SEM and represent the normalized averages derived from analyses of 4–8 samples for each group. Intergroup differences were analyzed using ANOVA followed by Bonferroni's multiple comparison test. $^{**}P < 0.01$ and $^{***}P < 0.001$ indicate significant differences compared with naïve rats. $^{\#}P < 0.05$ and $^{\#\#}P < 0.01$ indicate significant differences comp ared with the CCI-treated group. V: vehicle, MC: minocycline.

The N/OFQ analgesic activity is mediated selectively by NOP [3, 47, 48], which has been shown to act through the same intracellular pathway as classical opioid receptors [3, 7]. In healthy animals, N/OFQ administered i.t. has been generally found to produce antinociceptive responses that are similar to classical opioid receptor agonists without inducing signs of sedation or motor impairment [3, 10–14, 49, 50] which is why this system seems to be a promising target for chronic pain treatment. N/OFQ administered i.t. in neuropathic pain strongly alleviates both allodynia and hyperalgesia [4, 5, 48, 51, 52], and these results are in agreement with our behavioral results shown in the present paper. Additionally, electrophysiological studies have confirmed that the antinociceptive potency of spinally administered N/OFQ is maintained or even enhanced after nerve injury [14]. This is in contrast with classic opioid receptor agonists,

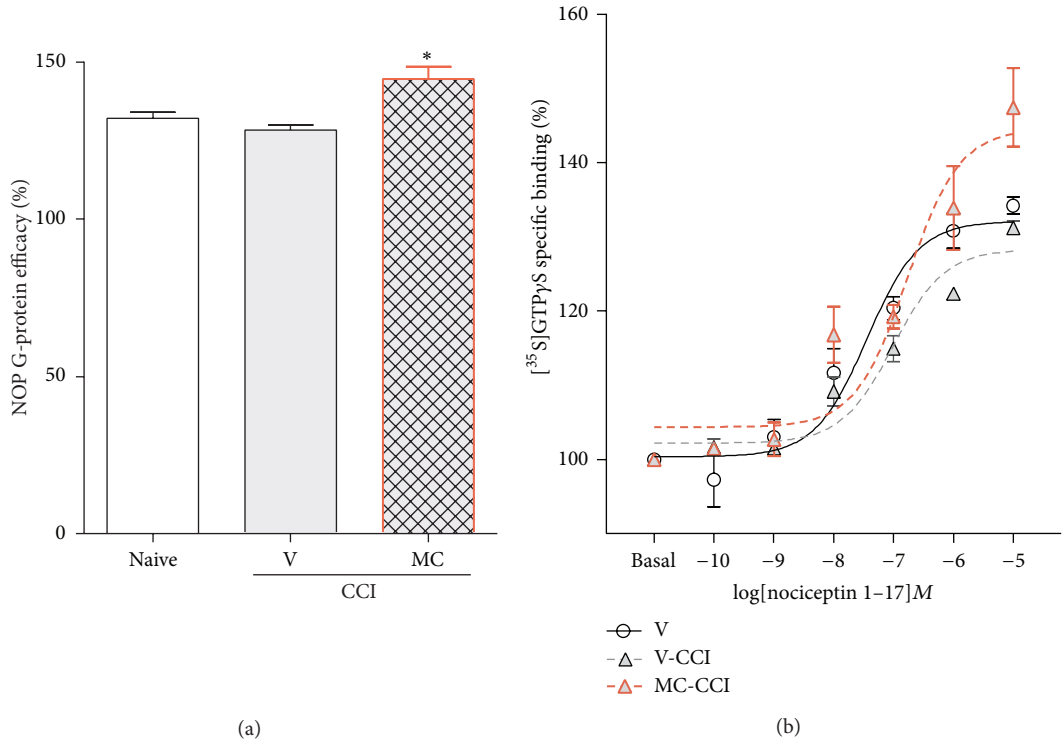

Figure 3: Repeated minocycline administration influenced NOP signaling. Chronic i.p. (30 mg/kg) minocycline treatment significantly increased the specific binding of the nucleotide analogue on NOP G-protein compared to vehicle-treated CCI-exposed rats. (a) The figure represents the calculated efficacy (or E_{max}) of the NOP-mediated G-protein during ligand stimulation. (b) The figure represents the specifically bound [^{35}S]GTPγS as a percentage in the presence of increasing concentrations (10^{10}–10^{-5} M) of N/OFQ 1–17. Basal activity was settled as 100%. Points and columns represent mean ± SEM. for at least three experiments performed in triplicates. Intergroup differences were analyzed using ANOVA followed by Bonferroni's multiple comparison test. $^{*}P < 0.05$ indicates significant differences compared with naïve rats. V: vehicle, MC: minocycline.

such as morphine, which are less effective in neuropathic than in acute pain conditions, making the N/OFQ system a much more effective target in neuropathic pain treatment [53].

N/OFQ and its receptor are localized in nervous system regions that are associated with nociception [22–24, 54]. Using immunoreactivity-based approaches, NOP protein has been detected in the gray matter of the spinal cord, particularly in the superficial layer II of the lumbar dorsal horn [9, 27]. Therefore, for our biochemical analysis we used dorsal part of the lumbar spinal cord L4–L6. Luo et al. [55] have shown that in the dorsal horn N/OFQ suppresses excitatory, but not inhibitory (glycinergic or GABAergic), synaptic transmission to substantia gelatinosa neurons. It has been clearly documented that the induction of chronic pain states, especially neuropathy, is associated with a regulation of the N/OFQ system [51, 56, 57].

It is suggested that the development of neuropathic pain conditions is caused by abnormal glial cell activation, especially microglia [58–62]. However, there is a lack of information on whether NOP can be expressed and regulated on microglial cells in the spinal cord during neuropathy. It is well known that microglial cells in the spinal cord become activated in response to injury [17, 61, 63–65] and may modulate pain by producing pronociceptive substances, such as cytokines (IL-1beta, TNFalpha, IL-6, fractalkine, MIP-1alpha, MIP-1beta, and MCP-1), cytokine receptors (TNFRI, TNFRII, IL-1RI, and CX3CR1), cytotoxic compounds (iNOS, NO, ROS, and ATP), prostaglandins, and excitatory amino acids [62, 66–71]. In our previous studies, we have shown that minocycline diminished the development of neuropathic pain in CCI-exposed rats [41, 64]. In our experiments, we used minocycline, which besides some influence on neurons [72, 73], is considered as an inhibitor of the microglial activation [29–32], viability, and migration [33, 34] during neuropathic pain. In our previous experiments, we observed that minocycline can enhance the antiallodynic and antihyperalgesic effects of morphine, DAMGO, and U50,488H but not DPDPE, deltorphin II, or SNC80 [74]. In the present study, we demonstrated for the first time that in CCI-exposed rats the antiallodynic and antihyperalgesic effects of N/OFQ were significantly potentiated by minocycline, similar to opioid agonists.

Our biochemical study shows strong ipsilateral upregulation of protein for NOP parallel to microglial cell activation, while fewer changes are observed in minocycline-treated rats. In our earlier experiments using *in situ* hybridization, we have shown that the upregulation of *NOP* mRNA occurred only in the ventral but not the dorsal horn of ipsilateral lumbar part of

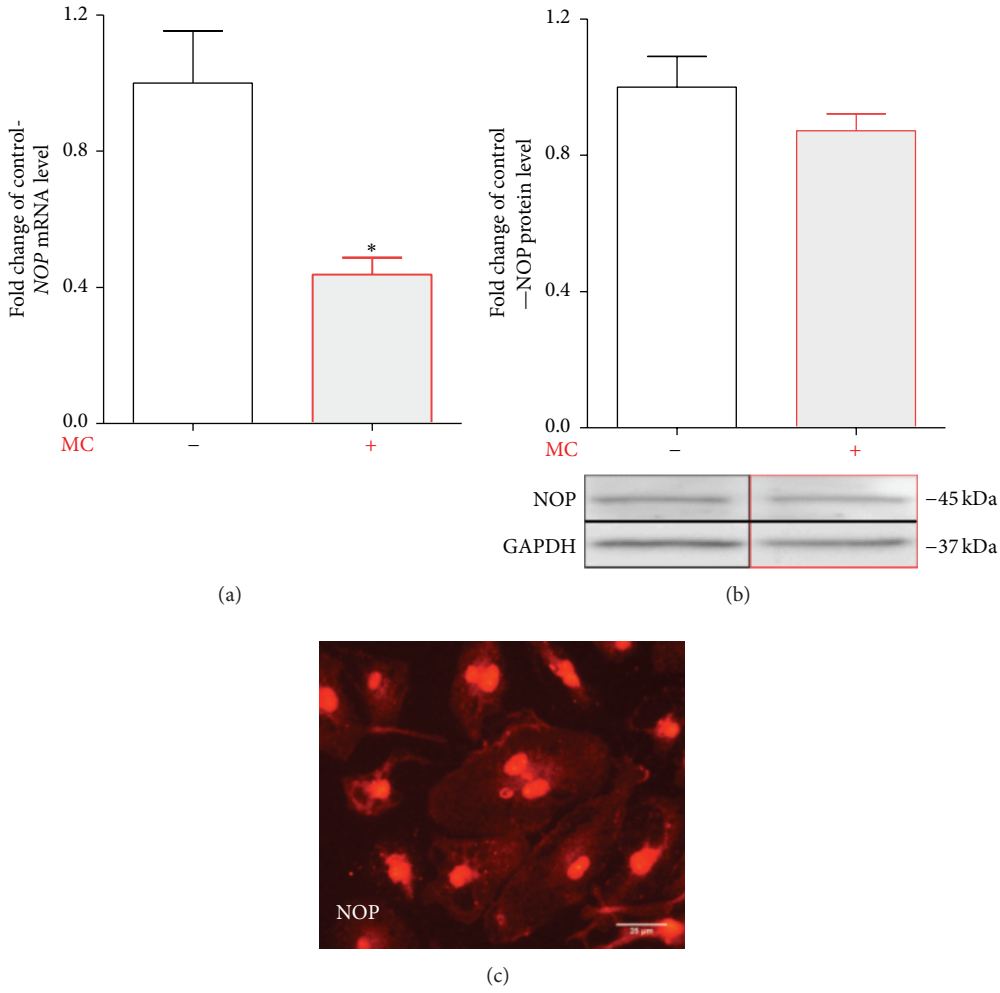

Figure 4: Minocycline diminished the mRNA but not protein NOP level in primary microglial cells. Primary microglial cell cultures were treated with minocycline [MC; 10 μM] for 6 h for mRNA analysis (a) and 24 h for protein analysis (b). The qRT-PCR analysis shows that minocycline [10 μM] downregulates *NOP* mRNA in primary microglial cell cultures (a). The Western blot analysis shows that minocycline did not change the protein level of NOP in primary microglia cultures (b). The qRT-PCR and Western blot data are presented as the mean ± SEM and represent the normalized averages derived from the analyses of four experiments. The intergroup differences were analyzed with a *t*-test; significant differences resulting from comparison with nonstimulated cells are indicated by $^{*}P < 0.05$. The presence of NOP on microglial cells was confirmed by immunocytochemistry (c). The scale bar for all microphotographs is 25 μm.

the spinal cord, suggesting it is increased in motoneurons [6]. Similarly, Briscini et al. [51] showed the upregulation of *NOP* mRNA in the whole (dorsal and ventral) ipsilateral lumbar enlargement. In our present study, no changes in *NOP* mRNA level were observed in the spinal dorsal part at L4–L6 in either vehicle- or minocycline-treated rats compared to naive animals.

Our results suggest that the alterations in the spinal N/OFQ signaling by minocycline treatment change the effectiveness of coupled G_i proteins which in turn compensates for neuropathic pain. G-protein activation was monitored in functional [^{35}S]GTPγS binding assays using N/OFQ 1–17 to activate the receptor. The unaffected potency of N/OFQ shows that the binding site of the receptor is unaltered in CCI-exposed rats after vehicle or minocycline injection. We have shown that minocycline caused an increase in N/OFQ-stimulated NOP signaling and influenced the N/OFQ system functionality during neuropathic pain.

The downregulation of the NOP by minocycline is in parallel with a reduced level of IBA-1 protein, which suggests that microglia play an important role in this phenomenon. In 2010, Mika et al. [17] demonstrated by using immunohistochemistry that repeated minocycline treatment reversed the injury-induced activation of microglia/macrophages in the dorsal lumbar spinal cord. Our present data suggest that the changes in the NOP affect not only neurons but also results from glial cells activation, which is in agreement with previous reports [20, 21, 72]. Using primary microglial cell cultures, we have shown for the first time that minocycline downregulates the level of *NOP* mRNA in microglial cells.

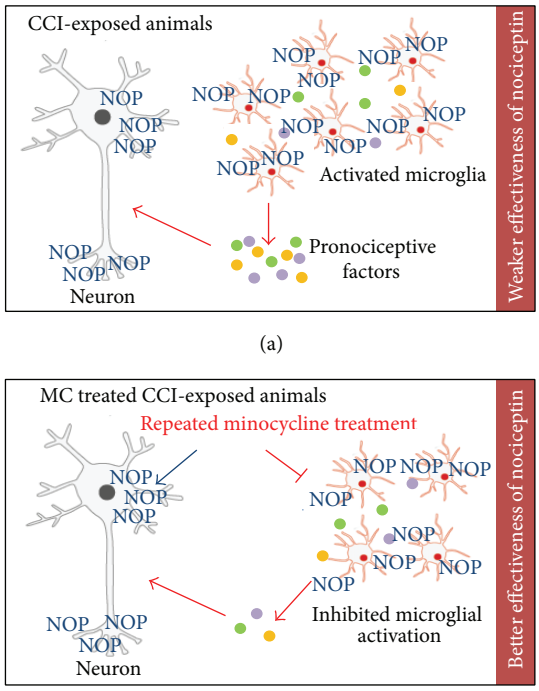

Scheme 1: Based on our results, we hypothesize the possible influence of minocycline on the N/OFQ system during neuropathic pain. Activated spinal microglia are key factors in the development of neuropathic pain by producing pronociceptive substances [65] and they play a role in the efficacy of analgesics (a). Minocycline (MC) potentiated the effects of N/OFQ through the downregulation of microglial activation, which leads to decrease of the microglial pool of NOP at the spinal cord level. This action of minocycline leads to increasing the analgesic effects of N/OFQ through neuronal receptors (b).

Our results may suggest that observed changes in NOP protein level after minocycline administration in a rat model of neuropathic pain can occur as result of the inhibition of microglial activation.

5. Summary

Minocycline potentiates the effects of N/OFQ through the downregulation of microglial activation and also by decreasing the microglial pool of NOP. Thus, it increases the analgesic action of N/OFQ through neuronal receptors, and it also potentiates the receptor-ligand signaling through the upregulation of G-protein activation. The results of the present study provide evidence that minocycline not only diminishes neuropathic pain-related behavior, but also enhances the effectiveness of N/OFQ by modulation of NOP expression and activity (Scheme 1). Our findings suggest that activated spinal microglial cells, which are the key factors in the development of neuropathic pain, play an important role in the function of the N/OFQ system. Therefore, specific microglial modulators, such as minocycline, combined with N/OFQ may be an interesting target to develop new therapy that would be effective against neuropathic pain.

Conflict of Interests

The authors declare that there is no conflict of interests regarding the publication of this paper.

Acknowledgments

This work was supported by Grant OPUS NCN 2011/03/B/NZ4/00042, Grant PRELUDIUM NCN 2012/07/N/NZ3/00379, and statutory funds. Katarzyna Popiolek-Barczyk and Agnieszka M. Jurga are recipients of a scholarship from the KNOW sponsored by the Ministry of Science and Higher Education, Poland.

References

[1] S. Arner and B. A. Meyerson, "Lack of analgesic effect of opioids on neuropathic and idiopathic forms of pain," *Pain*, vol. 33, no. 1, pp. 11–23, 1988.

[2] M. H. Ossipov, Y. Lopez, M. L. Nichols, D. Bian, and F. Porreca, "The loss of antinociceptive efficacy of spinal morphine in rats with nerve ligation injury is prevented by reducing spinal afferent drive," *Neuroscience Letters*, vol. 199, no. 2, pp. 87–90, 1995.

[3] R. K. Reinscheid, H. Nothacker, A. Bourson et al., "Orphanin FQ: a neuropeptide that activates an opioidlike G protein-coupled receptor," *Science*, vol. 270, no. 5237, pp. 792–794, 1995.

[4] C. Courteix, M. Coudoré-Civiale, A. Privat, T. Pélissier, A. Eschalier, and J. Fialip, "Evidence for an exclusive antinociceptive effect of nociceptin/orphanin FQ, an endogenous ligand for the ORL1 receptor, in two animal models of neuropathic pain," *Pain*, vol. 110, no. 1-2, pp. 236–245, 2004.

[5] T. Yamamoto, N. Nozaki-Taguchi, and S. Kimura, "Effects of intrathecally administered nociceptin, an opioid receptor-like1 (ORL1) receptor agonist, on the thermal hyperalgesia induced by unilateral constriction injury to the sciatic nerve in the rat," *Neuroscience Letters*, vol. 224, no. 2, pp. 107–110, 1997.

[6] J. Mika, I. Obara, and B. Przewlocka, "The role of nociceptin and dynorphin in chronic pain: Implications of neuro-glial interaction," *Neuropeptides*, vol. 45, no. 4, pp. 247–261, 2011.

[7] J. Meunier, C. Mollereau, L. Toll et al., "Isolation and structure of the endogenous agonist of opioid receptor-like ORL1 receptor," *Nature*, vol. 377, no. 6549, pp. 532–535, 1995.

[8] C. Suaudeau, S. Florin, J.-C. Meunier, and J. Costentin, "Nociceptin- induced apparent hyperalgesia in mice as a result of the prevention of opioid autoanalgesicmechanisms triggered by the stress of an intracerebroventricular injection," *Fundamental and Clinical Pharmacology*, vol. 12, no. 4, pp. 420–425, 1998.

[9] G. Calo, R. Guerrini, A. Rizzi, S. Salvadori, and D. Regoli, "Pharmacology of nociceptin and its receptor: a novel therapeutic target," *British Journal of Pharmacology*, vol. 129, no. 7, pp. 1261–1283, 2000.

[10] K. H. Jhamandas, M. Sutak, and G. Henderson, "Antinociceptive and morphine modulatory actions of spinal orphanin FQ," *Canadian Journal of Physiology and Pharmacology*, vol. 76, no. 3, pp. 314–324, 1998.

[11] J. Tian, W. Xu, W. Zhang et al., "Involvement of endogenous orphanin FQ in electroacupuncture-induced analgesia," *NeuroReport*, vol. 8, no. 2, pp. 497–500, 1997.

[12] Y. Wang, C. Zhu, X. Cao, and G. Wu, "Supraspinal hyperalgesia and spinal analgesia by [Phe1ψ(CH2-NH)Gly2]nociceptin-(1-13)-NH2 in rat," *European Journal of Pharmacology*, vol. 376, no. 3, pp. R1–R3, 1999.

[13] X. Xu, J. Hao, and Z. Wiesenfeld-Hallin, "Nociceptin or antinociceptin: potent spinal antinociceptive effect of orphanin FQ/nociceptin in the rat," *NeuroReport*, vol. 7, no. 13, pp. 2092–2094, 1996.

[14] X. Xu, S. Grass, J. Hao, I. Shi Xu, and Z. Wiesenfeld-Hallin, "Nociceptin/orphanin FQ in spinal nociceptive mechanisms under normal and pathological conditions," *Peptides*, vol. 21, no. 7, pp. 1031–1036, 2000.

[15] J. Mika, Y. Li, E. Weihe, and M. K. Schafer, "Relationship of pronociceptin/orphanin FQ and the nociceptin receptor ORL1 with substance P and calcitonin gene-related peptide expression in dorsal root ganglion of the rat," *Neuroscience Letters*, vol. 348, no. 3, pp. 190–194, 2003.

[16] J. Mika, M. K. H. Schäfer, I. Obara, E. Weihe, and B. Przewlocka, "Morphine and endomorphin-1 differently influence pronociceptin/orphanin FQ system in neuropathic rats," *Pharmacology Biochemistry and Behavior*, vol. 78, no. 1, pp. 171–178, 2004.

[17] J. Mika, E. Rojewska, W. Makuch, and B. Przewlocka, "Minocycline reduces the injury-induced expression of prodynorphin and pronociceptin in the dorsal root ganglion in a rat model of neuropathic pain," *Neuroscience*, vol. 165, no. 4, pp. 1420–1428, 2010.

[18] A. C. Eschenroeder, A. A. Vestal-Laborde, E. S. Sanchez, S. E. Robinson, and C. Sato-Bigbee, "Oligodendrocyte responses to buprenorphine uncover novel and opposing roles of μ-opioid- and nociceptin/orphanin FQ receptors in cell development: implications for drug addiction treatment during pregnancy," *GLIA*, vol. 60, no. 1, pp. 125–136, 2012.

[19] K. Sakoori and N. P. Murphy, "Reduced degeneration of dopaminergic terminals and accentuated astrocyte activation by high dose methamphetamine administration in nociceptin receptor knock out mice," *Neuroscience Letters*, vol. 469, no. 3, pp. 309–313, 2010.

[20] X. Fu, Z.-H. Zhu, Y.-Q. Wang, and G.-C. Wu, "Regulation of proinflammatory cytokines gene expression by nociceptin/orphanin FQ in the spinal cord and the cultured astrocytes," *Neuroscience*, vol. 144, no. 1, pp. 275–285, 2007.

[21] H. Zhao, G. Wu, and X. Cao, "Immunomodulatory activity of orphanin FQ/nociceptin on traumatic rats," *Acta Pharmacologica Sinica*, vol. 23, no. 4, pp. 343–348, 2002.

[22] B. Anton, J. Fein, T. To, X. Li, L. Silberstein, and C. J. Evans, "Immunohistochemical localization of ORL-1 in the central nervous system of the rat," *The Journal of Comparative Neurology*, vol. 368, no. 2, pp. 229–251, 1996.

[23] J. R. Bunzow, C. Saez, M. Mortrud et al., "Molecular cloning and tissue distribution of a putative member of the rat opioid receptor gene family that is not a mu, delta or kappa opioid receptor type," *FEBS Letters*, vol. 347, no. 2-3, pp. 284–288, 1994.

[24] M. J. Wick, S. R. Minnerath, X. Lin, R. Elde, P. Law, and H. H. Loh, "Isolation of a novel cDNA encoding a putative membrane receptor with high homology to the cloned μ, δ, and κ opioid receptors," *Molecular Brain Research*, vol. 27, no. 1, pp. 37–44, 1994.

[25] K. Fukuda, "cDNA cloning and regional distribution of a novel member of the opioid receptor family," *FEBS Letters*, vol. 343, no. 1, pp. 42–46, 1994.

[26] J. Meunier, L. Mouledous, and C. M. Topham, "The nociceptin (ORL1) receptor: molecular cloning and functional architecture," *Peptides*, vol. 21, no. 7, pp. 893–900, 2000.

[27] C. Mollereau and L. Mouledous, "Tissue distribution of the opioid receptor-like (ORL1) receptor," *Peptides*, vol. 21, no. 7, pp. 907–917, 2000.

[28] H. Nothacker, R. K. Reinscheid, A. Mansour et al., "Primary structure and tissue distribution of the orphanin FQ precursor," *Proceedings of the National Academy of Sciences of the United States of America*, vol. 93, no. 16, pp. 8677–8682, 1996.

[29] J. Mika, M. Zychowska, W. Makuch, E. Rojewska, and B. Przewlocka, "Neuronal and immunological basis of action of antidepressants in chronic pain—clinical and experimental studies," *Pharmacological Reports*, vol. 65, no. 6, pp. 1611–1121, 2013.

[30] F. Zhu, Y. Zheng, Y. Q. Ding et al., "Minocycline and risperidone prevent microglia activation and rescue behavioral deficits induced by neonatal intrahippocampal injection of lipopolysaccharide in rats," *PLoS ONE*, vol. 9, no. 4, Article ID e93966, 2014.

[31] F. Zhu, Y. Liu, J. Zhao, and Y. Zheng, "Minocycline alleviates behavioral deficits and inhibits microglial activation induced by intrahippocampal administration of Granulocyte-Macrophage Colony-Stimulating Factor in adult rats," *Neuroscience*, vol. 266, pp. 275–281, 2014.

[32] K. Liaury, T. Miyaoka, T. Tsumori et al., "Minocycline improves recognition memory and attenuates microglial activation in Gunn rat: a possible hyperbilirubinemia-induced animal model of schizophrenia," *Progress in Neuro-Psychopharmacology and Biological Psychiatry*, vol. 50, pp. 184–190, 2014.

[33] N. Nutile-McMenemy, A. Elfenbein, and J. A. DeLeo, "Minocycline decreases *in vitro* microglial motility, β_1- integrin, and Kv1.3 channel expression," *Journal of Neurochemistry*, vol. 103, no. 5, pp. 2035–2046, 2007.

[34] V. W. Yong, F. Giuliani, M. Xue, A. Bar-Or, and L. M. Metz, "Experimental models of neuroprotection relevant to multiple sclerosis," *Neurology*, vol. 68, no. 22, supplement 3, pp. S32–S37, 2007.

[35] M. Zimmermann, "Ethical guidelines for investigations of experimental pain in conscious animals," *Pain*, vol. 16, no. 2, pp. 109–110, 1983.

[36] C. Kilkenny, W. Browne, I. C. Cuthill, M. Emerson, and D. G. Altman, "Animal research: reporting in vivo experiments: the ARRIVE guidelines," *British Journal of Pharmacology*, vol. 160, no. 7, pp. 1577–1579, 2010.

[37] G. J. Bennett and Y. K. Xie, "A peripheral mononeuropathy in rat that produces disorders of pain sensation like those seen in man," *Pain*, vol. 33, no. 1, pp. 87–107, 1988.

[38] M. Osikowicz, J. Mika, W. Makuch, and B. Przewlocka, "Glutamate receptor ligands attenuate allodynia and hyperalgesia and potentiate morphine effects in a mouse model of neuropathic pain," *Pain*, vol. 139, no. 1, pp. 117–126, 2008.

[39] T. L. Yaksh and T. A. Rudy, "Chronic catheterization of the spinal subarachnoid space," *Physiology and Behavior*, vol. 17, no. 6, pp. 1031–1036, 1976.

[40] W. Makuch, J. Mika, E. Rojewska, M. Zychowska, and B. Przewlocka, "Effects of selective and non-selective inhibitors of nitric oxide synthase on morphine- and endomorphin-1-induced analgesia in acute and neuropathic pain in rats," *Neuropharmacology*, vol. 75, pp. 445–447, 2013.

[41] J. Mika, M. Osikowicz, W. Makuch, and B. Przewlocka, "Minocycline and pentoxifylline attenuate allodynia and hyperalgesia and potentiate the effects of morphine in rat and mouse

models of neuropathic pain," *European Journal of Pharmacology*, vol. 560, no. 2-3, pp. 142–149, 2007.

[42] M. Zawadzka and B. Kaminska, "A novel mechanism of FK506-mediated neuroprotection: downregulation of cytokine expression in glial cells," *GLIA*, vol. 49, no. 1, pp. 36–51, 2005.

[43] P. Chomczynski and N. Sacchi, "Single-step method of RNA isolation by acid guanidinium thiocyanate-phenol-chloroform extraction," *Analytical Biochemistry*, vol. 162, no. 1, pp. 156–159, 1987.

[44] S. Benyhe, J. Farkas, G. Tóth, and M. Wollemann, "Met5-enkephalin-Arg6-Phe7, an endogenous neuropeptide, binds to multiple opioid and nonopioid sites in rat brain," *Journal of Neuroscience Research*, vol. 48, no. 3, pp. 249–258, 1997.

[45] L. J. Sim, D. E. Selley, and S. R. Childers, "In vitro autoradiography of receptor-activated G proteins in rat brain by agonist-stimulated guanylyl 5′-[γ-[35S]thio]-triphosphate binding," *Proceedings of the National Academy of Sciences of the United States of America*, vol. 92, no. 16, pp. 7242–7246, 1995.

[46] J. R. Traynor and S. R. Nahorski, "Modulation by μ-opioid agonists of guanosine-5′-O-(3-[35S]thio)triphosphate binding to membranes from human neuroblastoma SH-SY5Y cells," *Molecular Pharmacology*, vol. 47, no. 4, pp. 848–854, 1995.

[47] F. A. Abdulla and P. A. Smith, "Axotomy reduces the effect of analgesic opioids yet increases the effect of nociceptin on dorsal root ganglion neurons," *Journal of Neuroscience*, vol. 18, no. 23, pp. 9685–9694, 1998.

[48] I. Obara, R. Przewlocki, and B. Przewlocka, "Spinal and local peripheral antiallodynic activity of Ro64-6198 in neuropathic pain in the rat," *Pain*, vol. 116, no. 1-2, pp. 17–25, 2005.

[49] X. Zhang, C. Zhu, S. Xu et al., "Effect of intrathecal or intracerebroventricular administration of OFQ on pain threshold and acpuncture analgesia in rats," *Acta Physiologica Sinica*, vol. 49, no. 5, pp. 575–580, 1997.

[50] C. Zhu, X. Zhang, S. Xu et al., "Antagonistic effect of orphanin FQ on opioid analgesia in rat," *Acta Pharmacologica Sinica*, vol. 19, no. 1, pp. 10–14, 1998.

[51] L. Briscini, L. Corradini, E. Ongini, and R. Bertorelli, "Up-regulation of ORL-1 receptors in spinal tissue of allodynic rats after sciatic nerve injury," *European Journal of Pharmacology*, vol. 447, no. 1, pp. 59–65, 2002.

[52] T. Yamamoto, S. Ohtori, and T. Chiba, "Inhibitory effect of intrathecally administered nociceptin on the expression of Fos-like immunoreactivity in the rat formalin test," *Neuroscience Letters*, vol. 284, no. 3, pp. 155–158, 2000.

[53] W. Schröder, D. G. Lambert, M. C. Ko, and T. Koch, "Functional plasticity of the N/OFQ-NOP receptor system determines analgesic properties of NOP receptor agonists," *The British Journal of Pharmacology*, vol. 171, no. 16, pp. 3777–3800, 2014.

[54] J. S. Mogil and G. W. Pasternak, "The molecular and behavioral pharmacology of the orphanin FQ/nociceptin peptide and receptor family," *Pharmacological Reviews*, vol. 53, no. 3, pp. 381–415, 2001.

[55] C. Luo, E. Kumamoto, H. Furue, J. Chen, and M. Yoshimura, "Nociceptin inhibits excitatory but not inhibitory transmission to substantia gelatinosa neurones of adult rat spinal cord," *Neuroscience*, vol. 109, no. 2, pp. 349–358, 2002.

[56] A. Rosén, T. Lundeberg, B. Bytner, and I. Nylander, "Central changes in nociceptin dynorphin B and Met-enkephalin-Arg-Phe in different models of nociception," *Brain Research*, vol. 857, no. 1-2, pp. 212–218, 2000.

[57] Y. Chen and C. Sommer, "Nociceptin and its receptor in rat dorsal root ganglion neurons in neuropathic and inflammatory pain models: Implications on pain processing," *Journal of the Peripheral Nervous System*, vol. 11, no. 3, pp. 232–240, 2006.

[58] V. Raghavendra, M. D. Rutkowski, and J. A. Deleo, "The role of spinal neuroimmune activation in morphine tolerance/hyperalgesia in neuropathic and sham-operated rats," *Journal of Neuroscience*, vol. 22, no. 22, pp. 9980–9989, 2002.

[59] V. Raghavendra, F. Tanga, and J. A. Deleo, "Inhibition of microglial activation attenuates the development but not existing hypersensitivity in a rat model of neuropathy," *Journal of Pharmacology and Experimental Therapeutics*, vol. 306, no. 2, pp. 624–630, 2003.

[60] C. Sommer, "Painful neuropathies," *Current Opinion in Neurology*, vol. 16, no. 5, pp. 623–628, 2003.

[61] L. R. Watkins and S. F. Maier, "Glia: a novel drug discovery target for clinical pain," *Nature Reviews Drug Discovery*, vol. 2, no. 12, pp. 973–985, 2003.

[62] J. Mika, M. Korostynski, D. Kaminska et al., "Interleukin-1alpha has antiallodynic and antihyperalgesic activities in a rat neuropathic pain model," *Pain*, vol. 138, no. 3, pp. 587–597, 2008.

[63] S. B. McMahon, W. B. J. Cafferty, and F. Marchand, "Immune and glial cell factors as pain mediators and modulators," *Experimental Neurology*, vol. 192, no. 2, pp. 444–462, 2005.

[64] J. Mika, M. Osikowicz, E. Rojewska et al., "Differential activation of spinal microglial and astroglial cells in a mouse model of peripheral neuropathic pain," *European Journal of Pharmacology*, vol. 623, no. 1–3, pp. 65–72, 2009.

[65] A. K. Clark, E. A. Old, and M. M. Malcangio, "Neuropathic pain and cytokines: current perspectives," *Journal of Pain Research*, vol. 21, no. 6, pp. 803–814, 2013.

[66] F. Aloisi, "Immune function of microglia," *GLIA*, vol. 36, no. 2, pp. 165–179, 2001.

[67] F. J. P. M. Huygen, N. Ramdhani, A. Van Toorenenbergen, J. Klein, and F. J. Zijlstra, "Mast cells are involved in inflammatory reactions during Complex Regional Pain Syndrome type 1," *Immunology Letters*, vol. 91, no. 2-3, pp. 147–154, 2004.

[68] D. Irnich, D. J. Tracey, J. Polten, R. Burgstahler, and P. Grafe, "ATP stimulates peripheral axons in human, rat and mouse—differential involvement of A2B adenosine and P2X purinergic receptors," *Neuroscience*, vol. 110, no. 1, pp. 123–129, 2002.

[69] J. M. Jimenez-Andrade, C. M. Peters, N. A. Mejia, J. R. Ghilardi, M. A. Kuskowski, and P. W. Mantyh, "Sensory neurons and their supporting cells located in the trigeminal, thoracic and lumbar ganglia differentially express markers of injury following intravenous administration of paclitaxel in the rat," *Neuroscience Letters*, vol. 405, no. 1-2, pp. 62–67, 2006.

[70] X. Jin and R. W. Gereau, "Acute p38-mediated modulation of tetrodotoxin-resistant sodium channels in mouse sensory neurons by tumor necrosis factor-α," *Journal of Neuroscience*, vol. 26, no. 1, pp. 246–255, 2006.

[71] L. R. Watkins, M. R. Hutchinson, A. Ledeboer, J. Wieseler-Frank, E. D. Milligan, and S. F. Maier, "Glia as the "bad guys": implications for improving clinical pain control and the clinical utility of opioids," *Brain, Behavior, and Immunity*, vol. 21, no. 2, pp. 131–146, 2007.

[72] H. M. Wu, L. F. Zhang, P. S. Ding, Y. J. Liu, X. Wu, and J. N. Zhou, "Microglial activation mediates host neuronal survival induced by neural stem cells," *Journal of Cellular and Molecular Medicine*, vol. 18, no. 7, pp. 1300–1312, 2014.

[73] G. B. Oliveira, A. Fontes Ede Jr., S. de Carvalho et al., "Minocycline mitigates motor impairments and cortical neuronal loss induced by focal ischemia in rats chronically exposed to ethanol during adolescence," *Brain Research*, vol. 1561, pp. 23–34, 2014.

[74] J. Mika, K. Popiolek-Barczyk, E. Rojewska, W. Makuch, K. Starowicz, and B. Przewlocka, "Delta-opioid receptor analgesia is independent of microglial activation in a rat model of neuropathic pain," *PLoS One*, vol. 9, pp. 1–9, 2014.

Hindawi Publishing Corporation
BioMed Research International
Volume 2014, Article ID 686908, 12 pages
http://dx.doi.org/10.1155/2014/686908

Research Article

Alterations in the Anandamide Metabolism in the Development of Neuropathic Pain

Natalia Malek, Mateusz Kucharczyk, and Katarzyna Starowicz

Laboratory of Pain Pathophysiology, Department of Pain Pharmacology, Institute of Pharmacology, Polish Academy of Sciences, Smetna Street 12, 31-343 Krakow, Poland

Correspondence should be addressed to Katarzyna Starowicz; starow@if-pan.krakow.pl

Received 28 May 2014; Revised 4 July 2014; Accepted 6 July 2014; Published 2 September 2014

Academic Editor: Livio Luongo

Endocannabinoids (EC), particularly anandamide (AEA), released constitutively in pain pathways might be accountable for the inhibitory effect on nociceptors. Pathogenesis of neuropathic pain may reflect complex remodeling of the dorsal root ganglia (DRGs) and spinal cord EC system. Multiple pathways involved both in the biosynthesis and degradation of AEA have been suggested. We investigated the local synthesis and degradation features of AEA in DRGs and spinal cord during the development and maintenance of pain in a model of chronic constriction injury (CCI). All AEA synthesis and degradation enzymes are present on the mRNA level in DRGs and lumbar spinal cord of intact as well as CCI-treated animals. Deregulation of EC system components was consistent with development of pain phenotype at days 3, 7, and 14 after CCI. The expression levels of enzymes involved in AEA degradation was significantly upregulated ipsilateral in DRGs and spinal cord at different time points. Expression of enzymes of the alternative, sPLA2-dependent and PLC-dependent, AEA synthesis pathways was elevated in both of the analyzed structures at all time points. Our data have shown an alteration of alternative AEA synthesis and degradation pathways, which might contribute to the variation of AEA levels and neuropathic pain development.

1. Background

The development of neuropathic pain after nerve injury occurs when peripheral nerve fibers are damaged or dysfunctional, which results in incorrect signals being sent to the brain and loss of afferent sensory function with typical features such as allodynia and hyperalgesia [1, 2]. Chronic pain serves no protective biological function unlike a symptom of a disease process, and there is a strong need to identify novel therapeutic targets [3]. Among the many suggested strategies to treat neuropathic pain, cannabinoids have the potential to become analgesic targets for drug development. Indeed cannabinoid agonists suppress neuropathic symptoms in animal models of neuropathic pain evoked by chronic constriction injury (CCI) to the sciatic nerve [4–6] or spinal nerve ligation [7–10]. Yet, this therapeutic intervention is also associated with a number of adverse effects, including sedation, motor impairment, and cognitive impairment. Therefore, an alternative approach to target endocannabinoid (EC) signaling has been proposed [11], which may provide a more effective strategy in relieving neuropathic pain [12–14]. Anandamide (AEA), the first discovered and best studied EC, acts via cannabinoid 1 (CB1) and cannabinoid 2 (CB2) receptors in a manner similar to naturally derived and synthetic cannabinoid agonists, but it may also modulate nociception via other receptors, that is, transient receptor potential vanilloid 1 (TRPV1) [15–18].

ECs are present in multiple pain-modulating regions throughout the central nervous system (CNS), including the dorsal horn of the spinal cord and the dorsal root ganglia (DRGs), where their levels are modified by acute nociceptive stimuli and stress [19–23]. Tissue concentrations of AEA in the spinal cord become altered [14, 23–25] as an adaptive response to neuropathic pain, which further confirms the significant role of the AEA in chronic pain development.

Previous reports suggest that AEA is synthesized "on demand" [26] in regions of cellular stress (such as injured tissues or nerves). Although AEA is mainly generated from

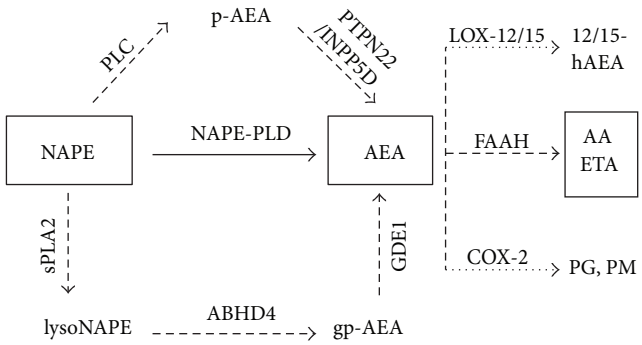

Figure 1: *Schematic illustration of parallel AEA synthesis and degradation pathways.* NAPE-PLD represents a Ca^{2+}-dependent route of AEA formation (—), while other enzymes (- - -) act in a Ca^{2+}-insensitive manner. Main route of AEA degradation is hydrolysis by FAAH (- - -). High AEA tissue concentration triggers parallel catabolic pathways through LOX-12/15 and COX-2 enzymes (· · ·). AEA: anandamide, NAPE: N-acylphosphatidylethanolamine, NAPE-PLD: N-acylphosphatidylethanolamine phospholipase D, GDE1: glycerophosphodiester phosphodiesterase 1, ABHD4: α/β hydrolase domain containing protein 4, PTPN22: protein tyrosine phosphatase nonreceptor type 22, sPLA2: soluble phospholipase A2, INPP5D: inositol 5-phosphatase, PLC: phospholipase C, FAAH: fatty acid amide hydrolase, COX-2: cycloxygenase 2, LOX-12: arachidonate 12-lipoxygenase, LOX-15: arachidonate 15-lipoxygenase, gp-AEA: glycerophosphoanandamide, p-AEA: phospho-anandamide, lysoNAPE: lyso-N-acylphosphatidylethanolamine, AA: arachidonic acid, ETA: ethanolamine, PG: prostaglandins, PM: prostamides, and 12/15-hAEA: 12/15-hydroxyanandamide.

phospholipid precursor N-arachidonoylphosphatidylethanolamine (NAPE) through hydrolysis by a N-arachidonoylphosphatidylethanolamine phospholipase D (NAPE-PLD) [27] in a Ca^{2+}-sensitive manner, recent evidence [28] indicates the existence of two parallel, additional, phospholipase C (PLC) and secreted phospholipase A2 (sPLA2)—catalyzed, Ca^{2+}-independent pathways. The PLC pathway involves PLC itself and two other enzymes with parallel activity: protein tyrosine phosphatase non-receptor type 22 (PTPN22) and phosphatidylinositol-3,4,5-trisphosphate 5-phosphatase 1 (INPP5D) [29, 30]. The sPLA2 pathway also includes the α/β hydrolase domain containing protein 4 (ABHD4) and glycerophosphodiesterphosphodiesterase 1 (GDE1) [31] (Figure 1). Similarly, multiple pathways involved in the degradation of AEA have been suggested [27, 32, 33]. Due to the efficient enzymatic degradation mainly by fatty acid amide hydrolase (FAAH) and also cyclooxygenase 2 (COX-2) as well as arachidonate lipoxygenases 12 and 15 (LOX-12/15), locally released ECs have a short half-life [34, 35]; thus, corrective relevance is limited.

Deregulation of the EC system underlies several neurological disorders including chronic pain; thus, there is a strong need for detailed characterization of the changes in the EC system during the development of neuropathic pain. Therefore, the aim of our studies was to investigate the role of multiple AEA production (both in Ca^{2+}-dependent and Ca^{2+}-independent manners) and degradation pathways as well as the possible consequences of altering its signaling during the development of neuropathic pain. We examined mRNA expression of EC system elements in DRGs and lumbar spinal cord, as both of these structures play a critical role in the integration and modulation of nociceptive signals from the peripheral nervous system. Additionally, changes at the site of nerve injury and in DRGs may give rise to the perception of pain in conditions such as neuropathy, which modifies the transmission of pain from peripheral tissues through the spinal cord to higher centers of the brain.

2. Results

2.1. Rats Subjected to CCI Showed Signs of Allodynia on the Operated Paw at 3, 7, and 14 Days after Induction of Injury. Presurgery thresholds reached the cut-off values for both thermal and mechanical allodynia, for both animals which undergo CCI procedure and intact. Cut-off values were also reached for intact animals in all tested time points. Neuropathic animals developed thermal allodynia as indicated by the cold plate test thermal withdrawal latency observed at day 3 after CCI (18.88 ± 2.88 s; $^{*}P < 0.01$; Figure 2(a)) and progressed at days 7 and 14 (12.85 ± 1.61 s, $^{*}P < 0.001$ and 16.63 ± 1.64 s, $^{*}P < 0.001$, resp.; Figure 2(a)). Mechanical allodynia was observed as decreased mechanical withdrawal threshold ipsilateral to injury in all time points tested (18.18 ± 1.88 g, $^{*}P < 0.001$; 11.68 ± 1.54, $^{*}P < 0.001$; 12.75 ± 1.40, $^{*}P < 0.001$; 3, 7, and 14 days after sciatic nerve injury, resp.; Figure 2(b)). In both tests, allodynia was maximal at day 7. The thresholds to mechanical stimulation were unaffected in contralateral paws and sham-operated rats (data not shown).

2.2. CCI Rats Exhibited a Significant Decrease in Thermal Hyperalgesia Thresholds after Nerve Ligation. Thermal ipsi-/contralateral withdrawal latency did not significantly change in intact animals or in the contralateral side of the CCI operated rats in all time points tested (Figure 2(c)). CCI to the sciatic nerve reduced ipsilateral thermal withdrawal latency compared with both the intact animals and the contralateral paw of CCI animals at all-time points tested. It reached the lowest values at day 7 after the procedure (6.77 ± 0.46 s, $^{\#}P < 0.05$; 4.83 ± 0.50 s, $^{*\#}P < 0.001$; 5.25 ± 0.52 s, $^{*\#}P < 0.001$; at day 3, 7 and 14 after CCI, resp.; Figure 2(c)).

2.3. Alteration of CB2 Expression Was Observed in DRGs (L4-L6) and Lumbar Spinal Cord during the Development of Neuropathic Pain, While No Changes Were Observed in the Expression of CB1 and TRPV1. CB1, CB2, and TRPV1 receptor transcripts were detected both in the DRGs and in the lumbar spinal cord of intact and neuropathic rats. Higher levels of *Cnr1* (CB1) receptor transcripts were detected contralateral to the injury in the DRGs throughout the development of neuropathic pain in comparison with the ipsilateral side (1.31 ± 0.11, $^{\#}P < 0.05$; 1.78 ± 0.14, $^{*\#}P < 0.001$; 1.35 ± 0.09, $^{\#}P < 0.01$; fold change at days 3, 7, and 14 in CCI rats, resp.; Figure 3(a)). Although there were significant differences in *Cnr1* expression in ipsilateral versus contralateral DRGs at respective days, only day 7 was characterized by a significant upregulation in the contralateral versus intact. No

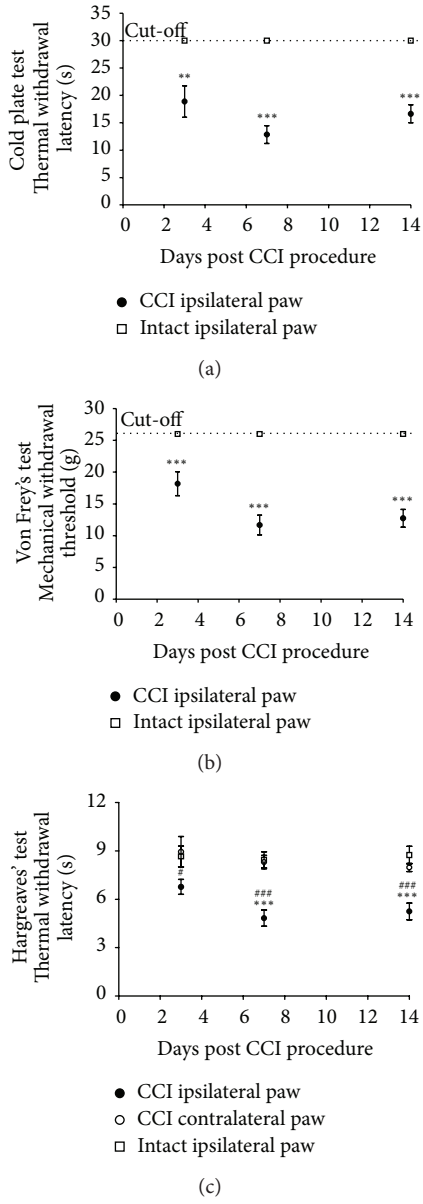

Figure 2: Thermal (a) and mechanical (b) allodynia and thermal hyperalgesia (c) in intact or CCI animals at 3, 7, and 14 days after CCI of the sciatic nerve. Thermal allodynia and hyperalgesia were measured as thermal withdrawal latency in seconds (mean ± SEM) and mechanical allodynia as mechanical withdrawal threshold in grams (mean ± SEM). Cut-off values were 30 s, 26 g, and 20 s for the cold plate, von Frey's and Hargreaves' tests, respectively. Statistical analysis was performed using a one-way ANOVA followed by Bonferroni post hoc tests. Values with $P < 0.05$ were considered significant. ∗ denotes significant difference versus intact and # versus contralateral paw.

significant changes in *Cnr1* mRNA levels were observed in the lumbar spinal cord during development of neuropathic pain (Figure 3(b)). *Cnr2* (CB2) mRNA expression levels were altered in both structures (Figures 3(c) and 3(d)). In DRGs, an elevated level of *Cnr2* transcript was observed ipsilateral at day 7 after CCI procedure (1.78 ± 0.11, $^{*}P < 0.01$; fold change at day 7 in CCI rats). Expression of *Cnr2* contralateral to the injury decreased significantly 14 days after sciatic nerve injury in comparison to earlier time points ($^{\$}P < 0.05$). The strongest upregulation of *Cnr2* transcript was observed, exclusively ipsilateral to the injury, in the lumbar spinal cord at all-time points tested (6.53 ± 1.42, $^{*}P < 0.01$; 7.43 ± 1.49 $^{*}P < 0.01$ $^{\#}P < 0.05$; 6.30 ± 1.93 $^{*}P < 0.05$; fold change ipsilateral at days 3, 7, and 14 in CCI rats, resp.; Figure 3(d)). Expression of *Trpv1* mRNA was not altered in the examined structures during the development of neuropathic pain at days 3, 7, or 14 in comparison to intact animals (Figures 3(e) and 3(f)). However, an alterations in the DRGs at day 7 versus day 3 was observed ($^{\$}P < 0.01$).

2.4. Upregulation of Alternative Synthesis Enzymes of AEA in DRGs and Lumbar Spinal Cord as a Consequence of Sciatic Nerve Injury. There were no significant changes in the expression levels of *Napepld* (NAPE-PLD) mRNA, the main AEA synthesizing enzyme, in DRGs or in the lumbar spinal cord (Figures 4(a) and 4(b)). Neuropathic pain led to an upregulation of mRNA encoding enzymes of alternative synthesis pathways in L4-L6 DRGs and the lumbar spinal cord (Figure 5). *Pla2g2a* (sPLA2) transcript levels were elevated in DRGs ipsilateral to the injury 7 days after CCI compared with the intact animals (1.40 ± 0.17, $^{\#}P < 0.01$; 1.69 ± 0.07, $^{*}P < 0.01$ $^{\#}P < 0.001$; 1.40 ± 0.06, $^{\#}P < 0.01$; fold change ipsilateral at days 3, 7, and 14 in CCI rats, resp.; Figure 5(a)) and in all-time points in the lumbar spinal cord (2.15 ± 0.14, $^{*\#}P < 0.001$; 1.94 ± 0.06, $^{*\#}P < 0.001$; 1.87 ± 0.04, $^{*}P < 0.001$ $^{\#}P < 0.01$; fold change at days 3, 7 and 14 after sciatic nerve ligation, resp.; Figure 5(g)). The abundance of *Inpp5d* (INPP5D) mRNA was increased ipsilateral to the injury in all tested time points in the lumbar spinal cord exclusively (2.83 ± 0.18, $^{*\#}P < 0.001$; 2.36 ± 0.10, $^{*\#}P < 0.001$; 2.51 ± 0.05, $^{*\#}P < 0.001$; fold change ipsilateral at days 3, 7, and 14 in CCI rats, resp.; Figure 5(l)). The mRNA levels of other enzymes involved in AEA synthesis did not significantly change in the measured time points after CCI of the sciatic nerve.

2.5. Alteration in the Expression of Main and Alternative Enzymes for AEA Degradation in Tested Tissues of CCI Rats during the Development of Neuropathic Pain. Analysis of *Faah* (FAAH) transcript levels revealed that the main AEA degradation enzyme showed no significant changes in expression in the L4-L6 DRGs during the development of neuropathic pain (Figure 6(a)). Alterations of *Faah* mRNA levels were limited to the ipsilateral side of the lumbar spinal cord at days 3, 7, and 14 after CCI (1.73 ± 0.23, $^{*}P < 0.001$; 2.54 ± 0.36, $^{*}P < 0.001$; 2.57 ± 0.20, $^{*}P < 0.001$ $^{\#}P < 0.05$; fold change at respective days; Figure 6(b)). *Ptgs2* (COX2) transcript levels were altered in DRGs both at the ipsilateral and contralateral side of the injury at different time points. The highest levels of transcript were observed at day 7 after injury (3.50 ± 0.25, $^{*}P < 0.001$; 3.40 ± 0.42, $^{*}P < 0.001$; Figure 6(c)). *Ptgs2* expression declined to baseline at day 14 after CCI surgery. We observed no appreciable changes in the abundance of Ptgs2 in lumbar spinal cord, except

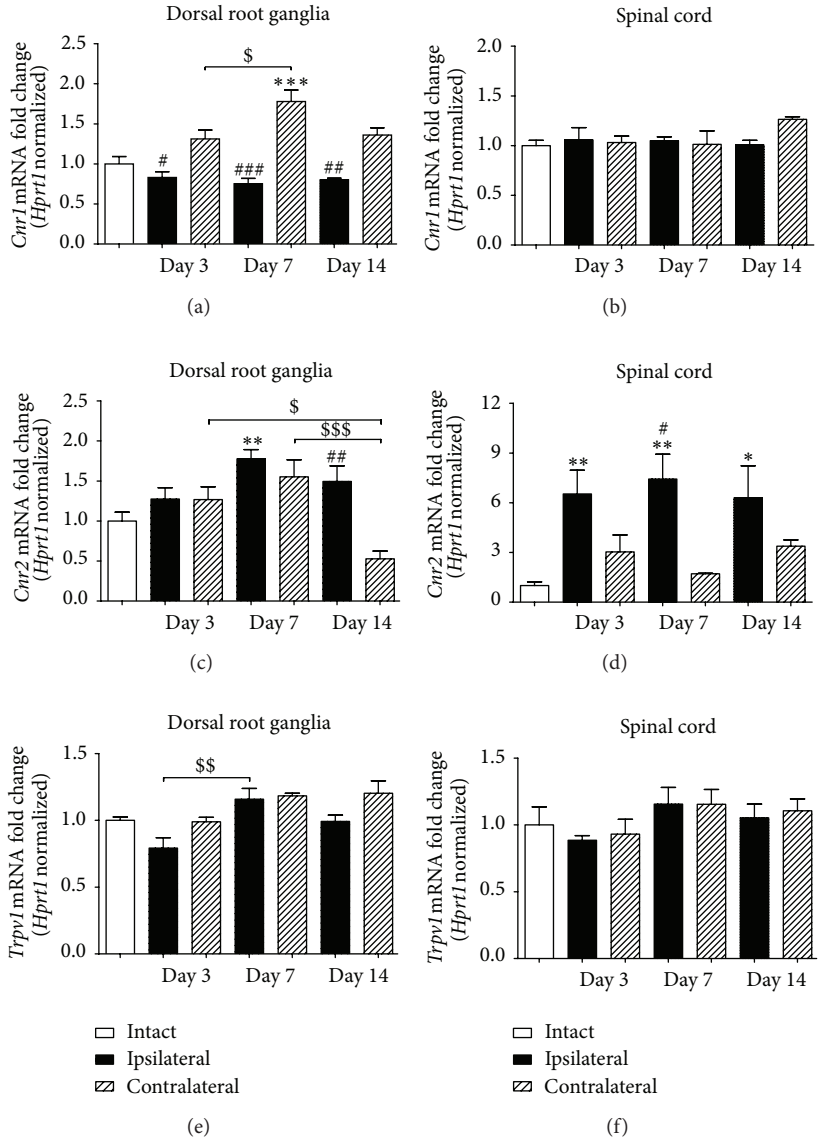

Figure 3: Results of qPCR analysis of Cnr1, Cnr2, and Trpv1 gene expression levels in the L4-L6 dorsal root ganglia and in the dorsal part of the lumbar spinal cord during the development of neuropathic pain in CCI rats. Samples were collected at 3, 7, and 14 days after CCI procedure. Data are presented as the mean ± SEM and represent normalized averages derived from 4–6 samples for each group. Results are presented as a fold change normalized to the expression of a reference gene *Hprt1*, compared to the intact animals. Statistical analysis was performed using a one-way ANOVA followed by Bonferroni post hoc tests. Values with $P < 0.05$ were considered significant. ∗ denotes significant differences versus intact, # versus contralateral side, and $ versus indicated bar.

for the *Ptgs2* ipsilateral upregulation at day 3 (1.86 ± 0.21, $^{*}P < 0.001$; fold change ipsilateral at day 3 in CCI rats; Figure 6(d)). Similar patterns of gene expression levels of the major lipoxygenases (*Alox12*, *Alox15*) in neuropathic rats were observed in the DRGs and the lumbar spinal cord (Figures 6(e)–6(h)). *Alox12* (LOX-12) mRNA levels were significantly upregulated ipsilateral to the injury in DRGs from day 7 after CCI (1.87 ± 0.17, $^{*}P < 0.001$ $^{\#}P < 0.01$ $^{\$}P < 0.001$; 1.63 ± 0.09, $^{*}P < 0.001$ $^{\$}P < 0.01$; fold change at days 7 and 14 in CCI rats, resp.; Figure 6(e)). Elevation of *Alox12* transcript levels in lumbar spinal cord was observed solely ipsilateral to the injury at all-time points measured (1.65 ± 0.06, $^{*}P < 0.001$ $^{\#}P < 0.01$; 1.52 ± 0.08, $^{*}P < 0.01$; 1.74 ± 0.18, $^{*}P < 0.001$ $^{\#}P < 0.05$; fold change ipsilateral at days 3, 7, and 14 in CCI rats, resp.; Figure 6(f)). Elevated levels of *Alox15* (LOX-15) mRNA were observed ipsilateral at days 7 and 14 after sciatic nerve injury in both of the assayed tissues (2.04 ± 0.28, $^{*}P < 0.01$ $^{\$}P < 0.05$; 2.64 ± 0.27, $^{*}P < 0.001$ $^{\#}P < 0.001$ $^{\$}P < 0.001$; fold change DRGs ipsilateral at day 7 and 14 in CCI rats, resp., and 2.26 ± 0.36, $^{*}P < 0.001$ $^{\#}P <$

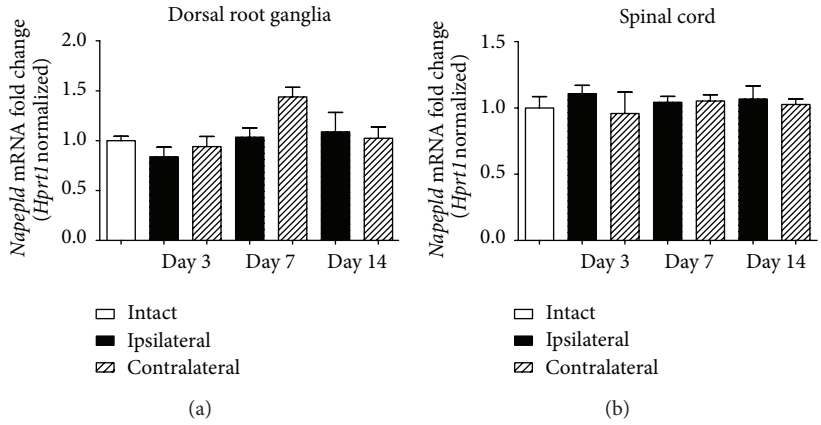

Figure 4: Expression of Napepld mRNA in L4-L6 dorsal root ganglia and in the dorsal part of the lumbar spinal cord during the development of neuropathic pain in CCI rats. Samples were collected at 3, 7, and 14 days after CCI procedure. Data are presented as the mean ± SEM and represent normalized averages derived from 4–6 samples for each group. Results are presented as a fold change normalized to the expression of a reference gene *Hprt1*, compared to the intact animals. Statistical analysis was performed using a one-way ANOVA followed by Bonferroni post hoc tests. Values with $P < 0.05$ were considered significant. ∗ denotes significant differences versus intact, # versus contralateral side, and $ versus indicated bar.

0.05 $^{\$}P < 0.001$; 2.49 ± 0.25, $^{*}P < 0.001$ $^{\$}P < 0.001$; fold change lumbar spinal cord ipsilateral at day 7 and 14 in CCI rats, resp; Figures 6(g) and 6(h)).

3. Discussion

A large number of research articles have demonstrated the efficacy of cannabinoids and modulators of the EC system in the alleviation of neuropathic pain in various animal models of surgically induced trauma, such as chronic constriction injury, partial sciatic nerve ligation, or spinal nerve ligation [14, 36]. Recent studies highlight the importance of alterations in the spinal and supraspinal EC levels in neuropathic rats [24] as well as the involvement of peripheral CB1/CB2 receptors in the antinociceptive effects of EC system modulation [37]. However, the exact mechanisms involved in the dynamic changes of EC concentrations in nervous tissues have never been investigated. Given the importance of the first-order neurons located in the DRGs and the spinal cord for pain sensation, in the present study, we investigated the putative AEA synthesizing and degradation enzymatic pathways in those structures. We reported for the first time changes in the expression of AEA metabolic enzymes at the DRG and spinal cord levels in a rat model of neuropathic pain.

In the rat CCI model of neuropathic pain, we evaluated pain behavior in three independent tests (Figure 2). We have determined that the nocifensive behavior in neuropathic animals: allodynia and hyperalgesia are accompanied by multiple changes in the expression of receptors and metabolic enzymes for AEA. ECs are produced on demand in regions of cellular stress, for example, in injured tissues during the development of neuropathic pain. Unfortunately, locally released ECs are rapidly broken down in the tissue, so their physiological effectiveness is limited. Therefore, the endogenous control of the EC system during chronic pain remains an important issue to study, and it might provide new insight into the possibilities of EC modulation. The present investigation has expanded the knowledge of endogenous control mechanisms by showing that parallel pathways of synthesis and degradation of AEA become activated in response to the development of neuropathic pain and in consequence may influence levels of AEA in effected tissues. Studies on the endogenous levels of AEA in neuronal tissues during the development of chronic pain have yielded conflicting results in this regard. It was reported that the development of chronic pain was accompanied by a significant elevation of AEA levels at the spinal cord level [6, 24, 33, 38], although other studies showed no changes or even decreases in AEA concentration in different models of chronic pain [12, 22, 23, 25, 39, 40]. Several parallel pathways are suggested to contribute to the synthesis of AEA, among which the main occurs from its membrane precursor through cleavage by NAPE-PLD. It was reported that tissues from NAPE-PLD knockout mice exhibited enzymatic activity converting NAPE to AEA in a calcium-independent manner [41], suggesting the involvement of parallel biosynthetic pathways and supporting the theory that NAPE-PLD only makes a partial contribution to the biosynthesis of AEA [42]. Although some data showed the expression of enzymes of alternative pathways in neuronal tissues [43], comparison of expression profiles between control and neuropathic pain animals has never been performed. The present investigation has supplemented these observations by showing the upregulation of AEA synthetic enzymes in parallel pathways in a rat model of neuropathic pain (Figure 5). We confirmed that NAPE-PLD shows no alteration during the induction of pain (Figure 4) (as previously reported [40]). Therefore, we hypothesized that the variations in AEA levels are derived from disparities in the activity of alternative synthesis pathways. As a matter of fact, parallel pathways for AEA synthesis involving Ca^{2+} -insensitive enzymes were elevated ipsilateral

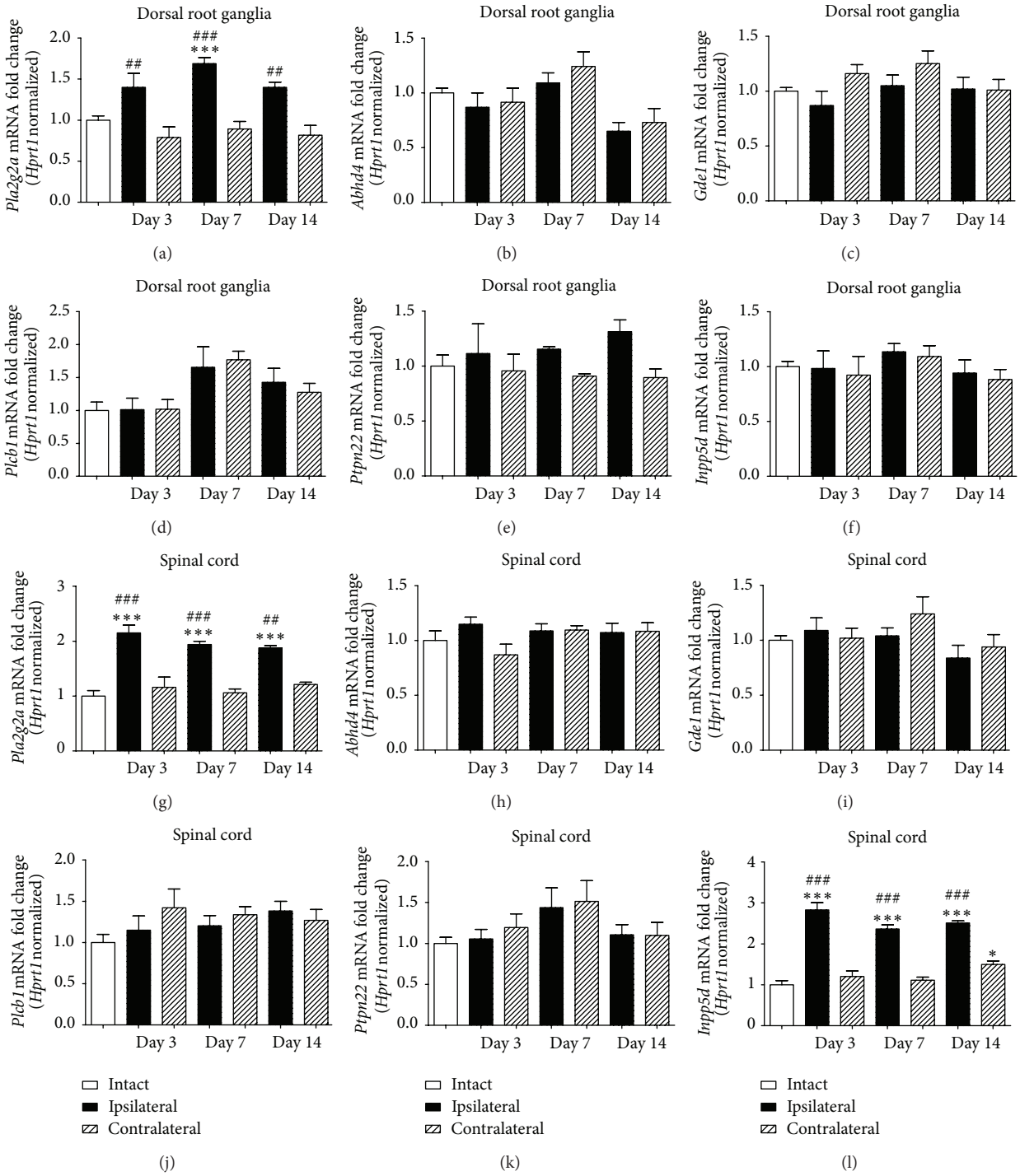

Figure 5: Gene expression analysis of enzymes involved in alternative pathways of anandamide synthesis—*Pla2g2a*, *Abdh4*, *Gde1*, *Plcb1*, *Ptpn22,* and *Inpp5d* in L4-L6 dorsal root ganglia and in the dorsal part of the lumbar spinal cord during the development of neuropathic pain in CCI rats. Samples were collected at 3, 7, and 14 days after CCI procedure. Data are presented as the mean ± SEM and represent normalized averages derived from 4–6 samples for each group. Results are presented as a fold change normalized to the expression of a reference gene *Hprt1*, compared to the intact animals. Statistical analysis was performed using a one-way ANOVA followed by Bonferroni post hoc tests. Values with $P < 0.05$ were considered significant. ∗ denotes significant differences versus intact, # versus contralateral side, and $ versus indicated bar.

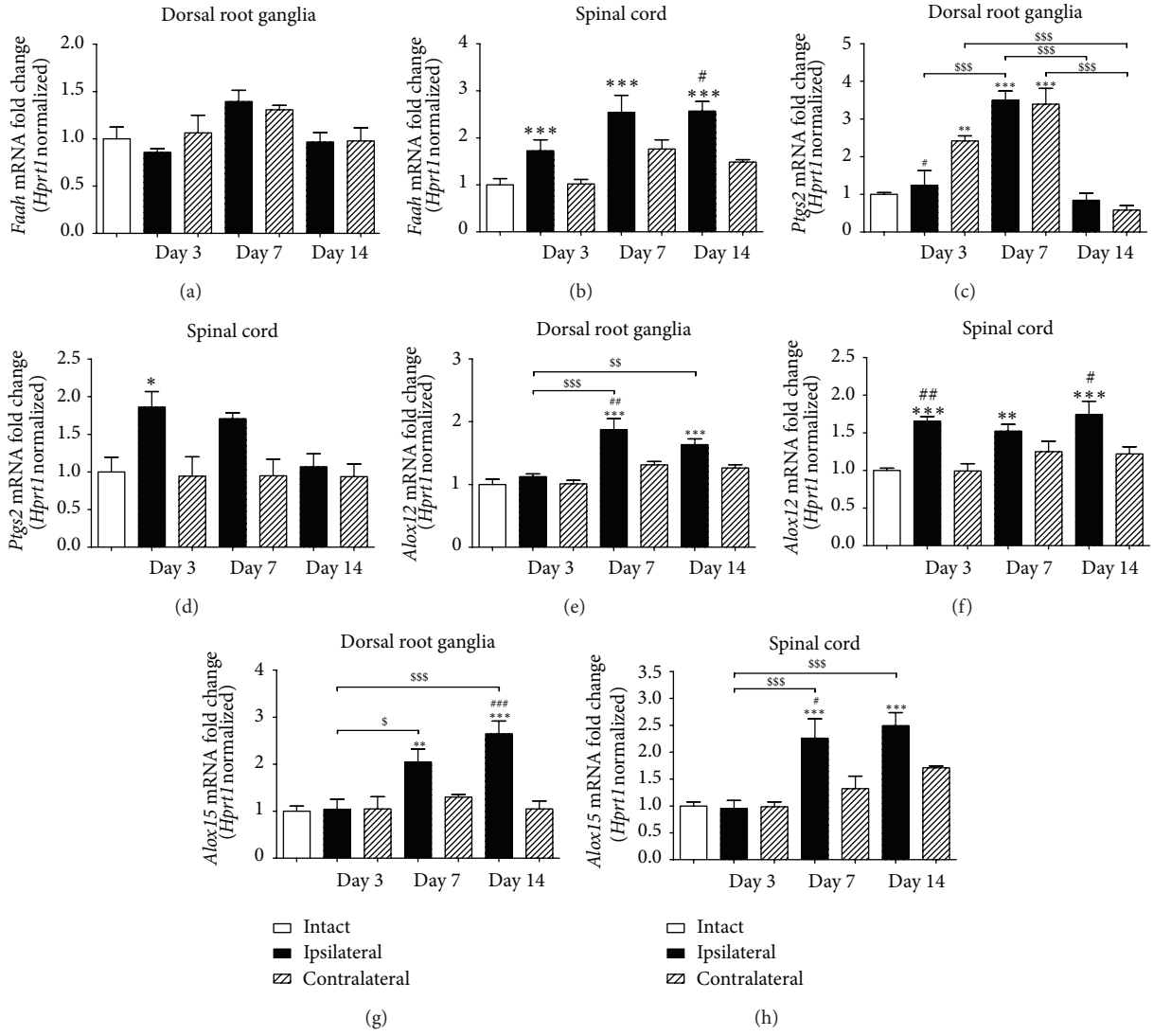

Figure 6: Expression of main anandamide degradation enzymes—*Faah*, *Ptgs2*, *Alox12,* and *Alox15* in L4-L6 dorsal root ganglia and in the dorsal part of the lumbar spinal cord during the development of neuropathic pain in CCI rats. Samples were collected at 3, 7, and 14 days after CCI procedure. Data are presented as the mean ± SEM and represent normalized averages derived from 4–6 samples for each group. Results are presented as a fold change normalized to the expression of a reference gene *Hprt1*, compared to the intact animals. Statistical analysis was performed using a one-way ANOVA followed by Bonferroni post hoc tests. Values with $P < 0.05$ were considered significant. ∗ denotes significant differences versus intact, # versus contralateral side, and $ versus indicated bar.

to the injury in both of the tissues examined in our studies (Figure 5). Additionally, PLC-dependent pathway activity was altered in the site of injury in the lumbar spinal cord exclusively (Figure 5). Our findings stress the importance of the activation of these pathways in the endogenous control of AEA levels during the development of chronic disorders.

Similar to the synthetic pathways, there is more than one degradation route of AEA. It has been assumed that AEA undergoes mainly FAAH-mediated hydrolysis. In the present study, we report strong upregulation of FAAH transcripts ipsilateral to the injury on the spinal cord level (Figure 6). This finding supports our previous studies, which were focused on investigating the role of FAAH inhibition in the alleviation of pain behavior through the endogenous elevation of AEA levels (for details see [13]). Yet, diminishing or eliminating the hydrolysis of AEA by FAAH would increase the probability that AEA might undergo alternative routes of metabolism, such as oxidation by fatty acid oxygenases that are known to act on endogenous arachidonic acid, namely, the members of the lipoxygenase (LOX) and cyclooxygenase (COX) [33, 44, 45] families. Herein, we also examined mRNA levels of LOX-12 and LOX-15 and showed an ipsilateral alteration of these enzymes in both the DRGs and lumbar spinal cord during the development of neuropathic pain (Figure 6). This result suggests that changes in LOX expression, as well metabolism of AEA via this pathway, may influence nociceptive processing. Moreover, LOX catabolism may lead to the production of active AEA metabolites, for example, 12/15-hydroxy-AEA,

which may act via TRPV1 and/or PPARalfa receptors, which contribute to the modification of pain behavior [33, 46, 47]. AEA was also shown to serve as a substrate for COX-2 [48]. As a result, it is a precursor of prostaglandins and prostamides, which can induce neuroinflammation and can result in the attenuation of therapeutic benefits of FAAH inhibitors [49, 50]. Moreover, some oxidized forms of AEA might serve as FAAH inhibitors [51]. Because they can be formed *in vivo*, they might also play an important role in controlling AEA degradation and, as a consequence, its levels in tissues. As in our studies, both LOX-12/15 and COX-2 levels were elevated, the effects of AEA metabolites should be considered based on the estimation of the benefits of pharmacological FAAH enzyme inhibition.

The analgesic effects produced by the activation of CB1 receptors have been well described and extensively reviewed [14, 52]. However, the broad distribution of CB1 receptors in the central nervous system emphasizes both their therapeutic effects, such as analgesia, as well as their side effects. Although it was reported by many authors that CB1 receptor expression is increased in the chronic pain conditions [53, 54], there is evidence showing no effect of pain development on CB1 receptor level alterations [55, 56], which is consistent with our studies. Due to the side effects mediated by CB1 receptor, it is clinically relevant to focus on the peripherally restricted CB1 agonists [57] as well as on signaling through the CB2 receptor. In our studies on neuropathic pain development, the CB2 receptor rather than the CB1 receptor showed significant upregulation, which is consistent with results obtained by other authors [58–60] and this finding might contribute to the hypothesis of the involvement of CB2 receptors in the attenuation of nociceptive response in models of neuropathic pain [61, 62]. Moreover, studies showed that the administration of CB1/CB2 agonist can attenuate pain response, although no change in expression of those receptors was observed [63]. This result might suggest more complex interactions between cannabinoid receptors during the development chronic pain dependent on the various features of the animal model used. Because AEA might act on different molecular targets, we examined the expression of the TRPV1 receptor at the transcript level as well. Although we observed no changes in the transcript levels of this receptor, its activity depends on phosphorylation and dephosphorylation processes, which are crucial for its function and act to decrease or increase channel activity, respectively [64].

4. Conclusions

The present investigation has expanded the knowledge of EC system modulation by showing that all AEA synthesis and degradation enzymes are present in DRGs and lumbar spinal cord of intact as well as neuropathic animals. Alterations in a variety of synthesis and degradation enzymes of AEA illustrate the flexibility of the EC system. This may explain why genetic ablation or pharmacological inhibition of only one of its metabolic pathways does not cause a substantial change in the cellular levels of AEA and may lead to unexpected behavioral effects. By combining behavioral tests and measuring the transcript levels of metabolic enzymes of AEA, we provide new insight into the involvement of the EC system in the development of neuropathic pain. Because therapies using ECs hold substantial promise, an understanding of the plasticity of the EC system is crucial and should be further investigated.

5. Methods

5.1. Animals. Male Wistar rats (Charles River, Hamburg, Germany), initially weighing 225–250 g, were used for all experiments. Animals were housed five per cage under a standard 12/12 h light/dark cycle (lights on at 08:00 h) with food and water available *ad libitum*. All animals were allowed to acclimatize to their holding cages for 3 to 4 days before any behavioral or surgical procedures were carried out. All experiments were conducted during the light cycle between 8:00 and 13:00. All experiments were performed according to the NIH Guide for the Care and Use of Laboratory Animals with recommendations by IASP [65] and were approved by the Local Bioethics Committee. Care was taken to implement the 3 Rs rule (replacement, reduction, and refinement) both to reduce the number of animals used and the suffering during the experiments. Different sets of animals were used for behavioral and biochemical studies to avoid changes in expression levels caused by thermal and mechanical stimulation. Results obtained in our research group [66] as well as those reported by others [67] showed no significant differences between sham operated group and intact (naive) animals in allodynia and hyperalgesia thresholds in development of neuropathic pain. Moreover Paszcuk et al. reported no significant differences in expression of EC system components in sham versus intact animals [54]. Therefore, respecting 3 R policy in laboratory animals use, we decided to compare only intact (naive) and neuropathic pain groups in our biochemical experiments.

5.2. Sciatic Nerve Surgery. Peripheral neuropathy was induced by chronic constriction injury (CCI) as described by Bennett and Xie [68]. The sciatic nerve injury was performed under sodium pentobarbital anesthesia (60 mg/kg, i.p.). The biceps femoris and the gluteus superficialis were separated, and the right sciatic nerve was exposed. Proximal to the sciatic trifurcation, approximately 7 mm of nerve was freed from the adhering tissue, and the injury was produced by tying four loose ligatures (4/0 silk, 1 mm spacing) around the sciatic nerve until they elicited a brief twitch in the respective hind limbs. This twitch prevented us from applying a ligation that was too strong. The total length of nerve affected was 5-6 mm. No procedure was conducted on the control animals.

5.3. Nociceptive Behavior. All experiments were conducted 3, 7, and 14 days after the sciatic nerve injury to determine thermal and mechanical withdrawal thresholds during the development of neuropathic pain. Thermal allodynia was assessed using the cold plate test (Cold/Hot Plate Analgesia

Meter No. 05044 Columbus Instruments, USA). The temperature of the cold plate was kept at 5°C, and the cut-off latency was 30 s. The rats were placed on the cold plate, and the time until the hind paw was lifted was recorded. The injured paw exhibited lower reaction latency. For the assessment of mechanical allodynia (von Frey's test), rats were tested for their foot withdrawal threshold in response to an automatic von Frey apparatus (Dynamic Plantar Aesthesiometer Cat. No. 37400, Ugo Basile Italy). Rats were placed in plastic cages with a wire net floor 5 min before the experiment. The von Frey's filament was applied to the midplantar surface of the ipsilateral hind paw, and the measurements of applied mechanical force were taken automatically. The strength of the von Frey's stimuli in our experiments ranged from 0.5 to 26 g. Thermal hyperalgesia (Hargreaves' test). For the assessment of paw withdrawal latency (PWD) to a noxious thermal stimulus the Analgesia Meter (mod 33, IITC INC., Landing, NJ) was used. On the day of the experiment, each animal was placed in a plastic cage with a heated glass floor. After 5 min of habituation, a noxious thermal stimulus, a light beam, was focused onto the plantar aspect of a hind paw until the animal lifted the paw away from the heat source. The paw withdrawal latency was automatically rounded to the nearest 0.1 s. A cut-off latency of 20 s was used to avoid tissue damage.

5.4. Sample Preparation & RNA Isolation. Animals were sacrificed at either the 3, 7, or 14 day after nerve ligation. A group of naive animals was used as a reference. The L4-L6 dorsal root ganglia (DRGs) and dorsal lumbar spinal cord were collected from both ipsilateral and contralateral side to the injury. Tissue samples were placed in individual tubes with the tissue storage reagent RNAlater (Qiagen Inc., Valencia, CA, USA), frozen on dry ice, and stored at −80°C until RNA isolation. Samples were homogenized in 1 mL of Trizol reagent (Invitrogen, Carlsbad, CA, USA). RNA isolation was performed according to Chomczynski's method [69]. RNA concentration was measured using a NanoDrop ND-1000 Spectrometer (Thermo Scientific, Wilmington, USA).

5.5. qPCR Analysis of Gene Expression. Reverse transcription of total RNA (1 μg per sample) was performed using Omniscript reverse transcriptase (Qiagen Inc., Valencia, CA, USA) at 37°C for 60 minutes. For quantitative PCR, 45 ng of cDNA was used as a template. Reactions were performed using Assay-On-Demand TaqMan probes and TaqMan Universal PCR Master Mix (Applied Biosystems, Foster, CA, USA) according to the manufacturer's protocol. The following assays were used: Rn02758689_s1 (*Cnr1*), Rn03993699_s1 (*Cnr2*), Rn00583117_m1 (*Trpv1*), Rn01786262_m1 (*Napepld*), Rn00668379_g1 (*Pla2g2a*), Rn01488539_m1 (*Abhd4*), Rn00583529_m1 (*Gde1*), Rn01514511_m1 (*Plcb1*), Rn01533758_m1 (*Ptpn22*), Rn01400935_m1 (*Inpp5d*), Rn00577086_m1 (*Faah*), Rn00568225_m1 (*Ptpgs2*), Rn01461082_m1 (*Alox12*), Rn00696151_m1 (*Alox15*), Rn01527840_m1 (*Hprt1*). Cycle threshold values (Ct) were calculated automatically by the iCycler IQ 3.0 software. Expression levels were normalized with the Ct for a reference gene, which was hypoxanthine phosphoribosyltransferase 1 (*Hprt1*). The abundance of RNA was calculated as $2^{-(\text{normalized threshold cycle})}$.

5.6. Statistics. All data are presented as the mean S.E.M. The results of behavioral experiments and RT-qPCR were evaluated by the analysis of variance (ANOVA) followed by Bonferroni tests. Groups included 8–10 animals for behavioral tests or 4–6 animals for RT-qPCR experiments. A value of $P < 0.05$ was considered to be statistically significant.

List of Abbreviations

AA:	Arachidonic acid
ABHD4:	α/β Hydrolase domain containing protein 4
AEA:	Anandamide
12/15-hAEA:	12/15-Hydroxyanandamide
gp-AEA:	Glycerophosphoanandamide
p-AEA:	Phosphoanandamide
LOX-12:	Arachidonate 12-lipoxygenase
LOX-15:	Arachidonate 15-lipoxygenase
CB1:	Cannabinoid receptor type 1
CB2:	Cannabinoid receptor type 2
CNS:	Central nervous system
CCI:	Chronic constriction injury to the sciatic nerve
COX-2:	Cyclooxygenase 2
DRGs:	Dorsal root ganglia
EC:	Endocannabinoid
ETA:	Ethanolamine
FAAH:	Fatty acid amide hydrolase
GDE1:	Glycerophosphodiesterphosphodiesterase 1
INPP5D:	Phosphatidylinositol-3,4,5-trisphosphate 5-phosphatase 1
NAPE:	N-Arachidonoylphosphatidylethanolamine
lysoNAPE:	Lyso-N-acylphosphatidylethanolamine
NAPE-PLD:	N-Arachidonoylphosphatidylethanolamine phospholipase D
PG:	Prostaglandins
PLC:	Phospholipase C
sPLA2:	Secreted phospholipase A2
PM:	Prostamides
PTPN22:	Protein tyrosine phosphatase nonreceptor type 22
TRPV1:	Transient receptor potential vanilloid 1.

Conflict of Interests

The authors declare that there is no conflict of interests regarding the publication of this paper.

Authors' Contribution

Natalia Malek conducted the experiments design, acquisition of data, analysis and interpretation of data, and the writing of the paper. Mateusz Kucharczyk performed the analysis and interpretation of data and the writing of paper. Katarzyna Starowicz also performed study conception, experiments

design, analysis and interpretation of data, and the writing of the paper. All authors read and approved the final paper.

Acknowledgments

This work was supported by Grant LIDER/29/60/L- 2/10/NCBiR/2011 and statutory funds. Natalia Malek is a recipient of a scholarship from the KNOW sponsored by the Ministry of Science and Higher Education, Poland. The authors acknowledge Wioletta Makuch for technical assistance.

References

[1] Z. Ali, S. N. Raja, U. Wesselmann, P. N. Fuchs, R. A. Meyer, and J. N. Campbell, "Intradermal injection of norepinephrine evokes pain in patients with sympathetically maintained pain," *Pain*, vol. 88, no. 2, pp. 161–168, 2000.

[2] M. A. Rogawski and W. Löscher, "The neurobiology of antiepileptic drugs for the treatment of nonepileptic conditions," *Nature Medicine*, vol. 10, no. 7, pp. 685–692, 2004.

[3] D. S. Goldberg and S. J. McGee, "Pain as a global public health priority," *BMC Public Health*, vol. 11, no. 1, article 770, 2011.

[4] B. Costa, M. Colleoni, S. Conti et al., "Repeated treatment with the synthetic cannabinoid WIN 55,212-2 reduces both hyperalgesia and production of pronociceptive mediators in a rat model of neuropathic pain," *British Journal of Pharmacology*, vol. 141, no. 1, pp. 4–8, 2004.

[5] B. Costa, A. E. Trovato, F. Comelli, G. Giagnoni, and M. Colleoni, "The non-psychoactive cannabis constituent cannabidiol is an orally effective therapeutic agent in rat chronic inflammatory and neuropathic pain," *European Journal of Pharmacology*, vol. 556, no. 1–3, pp. 75–83, 2007.

[6] E. Palazzo, V. de Novellis, S. Petrosino et al., "Neuropathic pain and the endocannabinoid system in the dorsal raphe: pharmacological treatment and interactions with the serotonergic system," *European Journal of Neuroscience*, vol. 24, no. 7, pp. 2011–2020, 2006.

[7] M. M. Ibrahim, H. Deng, A. Zvonok et al., "Activation of CB2 cannabinoid receptors by AM1241 inhibits experimental neuropathic pain: pain inhibition by receptors not present in the CNS," *Proceedings of the National Academy of Sciences of the United States of America*, vol. 100, no. 18, pp. 10529–10533, 2003.

[8] J. Guindon and P. Beaulieu, "Antihyperalgesic effects of local injections of anandamide, ibuprofen, rofecoxib and their combinations in a model of neuropathic pain," *Neuropharmacology*, vol. 50, no. 7, pp. 814–823, 2006.

[9] A. Jayamanne, R. Greenwood, V. A. Mitchell, S. Aslan, D. Piomelli, and C. W. Vaughan, "Actions of the FAAH inhibitor URB597 in neuropathic and inflammatory chronic pain models," *British Journal of Pharmacology*, vol. 147, no. 3, pp. 281–288, 2006.

[10] A. Fox, A. Kesingland, C. Gentry et al., "The role of central and peripheral Cannabinoid1 receptors in the antihyperalgesic activity of cannabinoids in a model of neuropathic pain," *Pain*, vol. 92, no. 1-2, pp. 91–100, 2001.

[11] S. Petrosino and V. Di Marzo, "FAAH and MAGL inhibitors: therapeutic opportunities from regulating endocannabinoid levels," *Current Opinion in Investigational Drugs*, vol. 11, no. 1, pp. 51–62, 2010.

[12] S. G. Kinsey, J. Z. Long, S. T. O'Neal et al., "Blockade of endocannabinoid-degrading enzymes attenuates neuropathic pain," *Journal of Pharmacology and Experimental Therapeutics*, vol. 330, no. 3, pp. 902–910, 2009.

[13] K. Starowicz, W. Makuch, M. Osikowicz et al., "Spinal anandamide produces analgesia in neuropathic rats: possible CB_1- and TRPV1-mediated mechanisms," *Neuropharmacology*, vol. 62, no. 4, pp. 1746–1755, 2012.

[14] K. Starowicz and B. Przewlocka, "Modulation of neuropathic-pain-related behaviour by the spinal endocannabinoid/endovanilloid system," *Philosophical Transactions of the Royal Society B: Biological Sciences*, vol. 367, no. 1607, pp. 3286–3299, 2012.

[15] V. Di Marzo and L. De Petrocellis, "Why do cannabinoid receptors have more than one endogenous ligand?" *Philosophical Transactions of the Royal Society B*, vol. 367, no. 1607, pp. 3216–3228, 2012.

[16] J. Sousa-Valente, A. Varga, K. Ananthan, A. Khajuria, and I. Nagy, "Anandamide in primary sensory neurons: too much of a good thing?" *European Journal of Neuroscience*, vol. 39, no. 3, pp. 409–418, 2014.

[17] P. M. Zygmunt, J. Petersson, D. A. Andersson et al., "Vanilloid receptors on sensory nerves mediate the vasodilator action of anandamide," *Nature*, vol. 400, no. 6743, pp. 452–457, 1999.

[18] P. Movahed, B. A. G. Jönsson, B. Birnir et al., "Endogenous unsaturated C18 *N*-acylethanolamines are vanilloid receptor ($TRPV_1$) agonists," *The Journal of Biological Chemistry*, vol. 280, no. 46, pp. 38496–38504, 2005.

[19] W. J. Martin, P. O. Coffin, E. Attias, M. Balinsky, K. Tsou, and J. M. Walker, "Anatomical basis for cannabinoid-induced antinociception as revealed by intracerebral microinjections," *Brain Research*, vol. 822, no. 1-2, pp. 237–242, 1999.

[20] J. M. Walker, S. M. Huang, N. M. Strangman, K. Tsou, and M. C. Sañudo-Peña, "Pain modulation by release of the endogenous cannabinoid anandamide," *Proceedings of the National Academy of Sciences of the United States of America*, vol. 96, no. 21, pp. 12198–12203, 1999.

[21] A. G. Hohmann, R. L. Suplita, N. M. Bolton et al., "An endocannabinoid mechanism for stress-induced analgesia," *Nature*, vol. 435, no. 7045, pp. 1108–1112, 2005.

[22] P. Bishay, H. Schmidt, C. Marian et al., "R-flurbiprofen reduces neuropathic pain in rodents by restoring endogenous cannabinoids," *PLoS ONE*, vol. 5, no. 5, Article ID e10628, 2010.

[23] P. Bishay, A. Häussler, H.-Y. Lim et al., "Anandamide deficiency and heightened neuropathic pain in aged mice," *Neuropharmacology*, vol. 71, pp. 204–215, 2013.

[24] S. Petrosino, E. Palazzo, V. de Novellis et al., "Changes in spinal and supraspinal endocannabinoid levels in neuropathic rats," *Neuropharmacology*, vol. 52, no. 2, pp. 415–422, 2007.

[25] M. D. Jhaveri, D. Richardson, D. A. Kendall, D. A. Barrett, and V. Chapman, "Analgesic effects of fatty acid amide hydrolase inhibition in a rat model of neuropathic pain," *The Journal of Neuroscience*, vol. 26, no. 51, pp. 13318–13327, 2006.

[26] M. Van Der Stelt, M. Trevisani, V. Vellani et al., "Anandamide acts as an intracellular messenger amplifying Ca2+ influx via TRPV1 channels," *The EMBO Journal*, vol. 24, no. 17, pp. 3026–3037, 2005.

[27] G. G. Muccioli, "Endocannabinoid biosynthesis and inactivation, from simple to complex," *Drug Discovery Today*, vol. 15, no. 11-12, pp. 474–483, 2010.

[28] V. Vellani, S. Petrosino, L. de Petrocellis et al., "Functional lipidomics. Calcium-independent activation of endocannabinoid/endovanilloid lipid signalling in sensory neurons by protein kinases C and A and thrombin," *Neuropharmacology*, vol. 55, no. 8, pp. 1274–1279, 2008.

[29] J. Liu, L. Wang, J. Harvey-White et al., "A biosynthetic pathway for anandamide," *Proceedings of the National Academy of Sciences of the United States of America*, vol. 103, no. 36, pp. 13345–13350, 2006.

[30] J. Liu, L. Wang, J. Harvey-White et al., "Multiple pathways involved in the biosynthesis of anandamide," *Neuropharmacology*, vol. 54, no. 1, pp. 1–7, 2008.

[31] Y. Sun, K. Tsuboi, Y. Okamoto et al., "Biosynthesis of anandamide and *N*-palmitoylethanolamine by sequential actions of phospholipase A_2 and lysophospholipase D," *Biochemical Journal*, vol. 380, part 3, pp. 749–756, 2004.

[32] M. Maccarrone, M. Attinà, M. Bari, A. Cartoni, C. Ledent, and A. Finazzi-Agrò, "Anandamide degradation and N-acylethanolamines level in wild-type and CB1 cannabinoid receptor knockout mice of different ages," *Journal of Neurochemistry*, vol. 78, no. 2, pp. 339–348, 2001.

[33] K. Starowicz, W. Makuch, M. Korostynski et al., "Full inhibition of spinal FAAH leads to TRPV1-mediated analgesic effects in neuropathic rats and possible lipoxygenase-mediated remodeling of anandamide metabolism," *PLoS ONE*, vol. 8, no. 4, Article ID e60040, 2013.

[34] C. A. Rouzer and L. J. Marnett, "Non-redundant functions of cyclooxygenases: oxygenation of endocannabinoids," *The Journal of Biological Chemistry*, vol. 283, no. 13, pp. 8065–8069, 2008.

[35] W. B. Veldhuis, M. van der Stelt, M. W. Wadman et al., "Neuroprotection by the endogenous cannabinoid anandamide and arvanil against in vivo excitotoxicity in the rat: role of vanilloid receptors and lipoxygenases," *Journal of Neuroscience*, vol. 23, no. 10, pp. 4127–4133, 2003.

[36] E. J. Rahn and A. G. Hohmann, "Cannabinoids as pharmacotherapies for neuropathic pain: from the bench to the bedside," *Neurotherapeutics*, vol. 6, no. 4, pp. 713–737, 2009.

[37] D. R. Sagar, S. Kelly, P. J. Millns, C. T. O'Shaughnessey, D. A. Kendall, and V. Chapman, "Inhibitory effects of CB1 and CB2 receptor agonists on responses of DRG neurons and dorsal horn neurons in neuropathic rats," *European Journal of Neuroscience*, vol. 22, no. 2, pp. 371–379, 2005.

[38] L. Guasti, D. Richardson, M. Jhaveri et al., "Minocycline treatment inhibits microglial activation and alters spinal levels of endocannabinoids in a rat model of neuropathic pain," *Molecular Pain*, vol. 5, article 35, 2009.

[39] I. A. Khasabova, S. G. Khasabov, C. Harding-Rose et al., "A decrease in anandamide signaling contributes to the maintenance of cutaneous mechanical hyperalgesia in a model of bone cancer pain," *The Journal of Neuroscience*, vol. 28, no. 44, pp. 11141–11152, 2008.

[40] B. N. Okine, L. M. Norris, S. Woodhams et al., "Lack of effect of chronic pre-treatment with the FAAH inhibitor URB597 on inflammatory pain behaviour: evidence for plastic changes in the endocannabinoid system," *British Journal of Pharmacology*, vol. 167, no. 3, pp. 627–640, 2012.

[41] D. Leung, A. Saghatelian, G. M. Simon, and B. F. Cravatt, "Inactivation of N-Acyl phosphatidylethanolamine phospholipase D reveals multiple mechanisms for the biosynthesis of endocannabinoids," *Biochemistry*, vol. 45, no. 15, pp. 4720–4726, 2006.

[42] G. M. Simon and B. F. Cravatt, "Characterization of mice lacking candidate *N*-acyl ethanolamine biosynthetic enzymes provides evidence for multiple pathways that contribute to endocannabinoid production *in vivo*," *Molecular BioSystems*, vol. 6, no. 8, pp. 1411–1418, 2010.

[43] A. Varga, A. Jenes, T. H. Marczylo et al., "Anandamide produced by Ca(2+)-insensitive enzymes induces excitation in primary sensory neurons," *Pflügers Archiv*, vol. 466, no. 7, pp. 1421–1435, 2013.

[44] K. R. Kozak, J. J. Prusakiewicz, and L. J. Marnett, "Oxidative metabolism of endocannabinoids by COX-2," *Current Pharmaceutical Design*, vol. 10, no. 6, pp. 659–667, 2004.

[45] M. D. Jhaveri, D. Richardson, I. Robinson et al., "Inhibition of fatty acid amide hydrolase and cyclooxygenase-2 increases levels of endocannabinoid related molecules and produces analgesia via peroxisome proliferator-activated receptor-alpha in a model of inflammatory pain," *Neuropharmacology*, vol. 55, no. 1, pp. 85–93, 2008.

[46] B. Costa, F. Comelli, I. Bettoni, M. Colleoni, and G. Giagnoni, "The endogenous fatty acid amide, palmitoylethanolamide, has anti-allodynic and anti-hyperalgesic effects in a murine model of neuropathic pain: involvement of CB1, TRPV1 and PPARγ receptors and neurotrophic factors," *Pain*, vol. 139, no. 3, pp. 541–550, 2008.

[47] S. Kelly, R. J. Chapman, S. Woodhams et al., "Increased function of pronociceptive TRPV1 at the level of the joint in a rat model of osteoarthritis pain," *Annals of the Rheumatic Diseases*, 2013.

[48] M. Yu, D. Ives, and C. S. Ramesha, "Synthesis of prostaglandin E2 ethanolamide from anandamide by cyclooxygenase-2," *The Journal of Biological Chemistry*, vol. 272, no. 34, pp. 21181–21186, 1997.

[49] D. K. Nomura, B. E. Morrison, J. L. Blankman et al., "Endocannabinoid hydrolysis generates brain prostaglandins that promote neuroinflammation," *Science*, vol. 334, no. 6057, pp. 809–813, 2011.

[50] A. Ligresti, J. Martos, J. Wang et al., "Prostamide F(2) α receptor antagonism combined with inhibition of FAAH may block the pro-inflammatory mediators formed following selective FAAH inhibition," *British Journal of Pharmacology*, vol. 171, no. 6, pp. 1408–1419, 2014.

[51] M. van der Stelt, J. A. van Kuik, M. Bari et al., "Oxygenated metabolites of anandamide and 2-arachidonoylglycerol: conformational analysis and interaction with cannabinoid receptors, membrane transporter, and fatty acid amide hydrolase," *Journal of Medicinal Chemistry*, vol. 45, no. 17, pp. 3709–3720, 2002.

[52] R. G. Pertwee, "Cannabinoid receptors and pain," *Progress in Neurobiology*, vol. 63, no. 5, pp. 569–611, 2001.

[53] D. Bridges, K. Ahmad, and A. S. C. Rice, "The synthetic cannabinoid WIN55,212-2 attenuates hyperalgesia and allodynia in a rat model of neuropathic pain," *British Journal of Pharmacology*, vol. 133, no. 4, pp. 586–594, 2001.

[54] A. F. Paszcuk, R. C. Dutra, K. A. B. S. da Silva, N. L. M. Quintão, M. M. Campos, and J. B. Calixto, "Cannabinoid agonists inhibit neuropathic pain induced by brachial plexus avulsion in mice by affecting glial cells and MAP kinases," *PLoS ONE*, vol. 6, no. 9, Article ID e24034, 2011.

[55] S. Furuse, T. Kawamata, J. Yamamoto et al., "Reduction of bone cancer pain by activation of spinal cannabinoid receptor 1 and

its expression in the superficial dorsal horn of the spinal cord in a murine model of bone cancer pain," *Anesthesiology*, vol. 111, no. 1, pp. 173–186, 2009.

[56] J. Guindon, Y. Lai, S. M. Takacs, H. B. Bradshaw, and A. G. Hohmann, "Alterations in endocannabinoid tone following chemotherapy-induced peripheral neuropathy: effects of endocannabinoid deactivation inhibitors targeting fatty-acid amide hydrolase and monoacylglycerol lipase in comparison to reference analgesics following cisplatin treatment," *Pharmacological Research*, vol. 67, no. 1, pp. 94–109, 2013.

[57] N. Agarwal, P. Pacher, I. Tegeder et al., "Cannabinoids mediate analgesia largely via peripheral type 1 cannabinoid receptors in nociceptors," *Nature Neuroscience*, vol. 10, no. 7, pp. 870–879, 2007.

[58] J. Zhang, C. Hoffert, H. K. Vu, T. Groblewski, S. Ahmad, and D. O'Donnell, "Induction of CB2 receptor expression in the rat spinal cord of neuropathic but not inflammatory chronic pain models," *European Journal of Neuroscience*, vol. 17, no. 12, pp. 2750–2754, 2003.

[59] I. Racz, X. Nadal, J. Alferink et al., "Crucial role of CB2 cannabinoid receptor in the regulation of central immune responses during neuropathic pain," *Journal of Neuroscience*, vol. 28, no. 46, pp. 12125–12135, 2008.

[60] M. Beltramo, N. Bernardini, R. Bertorelli et al., "CB2 receptor-mediated antihyperalgesia: possible direct involvement of neural mechanisms," *European Journal of Neuroscience*, vol. 23, no. 6, pp. 1530–1538, 2006.

[61] A. Romero-Sandoval, N. Nutile-Mcmenemy, and J. A. Deleo, "Spinal microglial and perivascular cell cannabinoid receptor type 2 activation reduces behavioral hypersensitivity without tolerance after peripheral nerve injury," *Anesthesiology*, vol. 108, no. 4, pp. 722–734, 2008.

[62] E. J. Rahn, A. M. Zvonok, G. A. Thakur, A. D. Khanolkar, A. Makriyannis, and A. G. Hohmann, "Selective activation of cannabinoid CB_2 receptors suppresses neuropathic nociception induced by treatment with the chemotherapeutic agent paclitaxel in rats," *The Journal of Pharmacology and Experimental Therapeutics*, vol. 327, no. 2, pp. 584–591, 2008.

[63] E. J. Rahn, A. Makriyannis, and A. G. Hohmann, "Activation of cannabinoid CB 1 and CB 2 receptors suppresses neuropathic nociception evoked by the chemotherapeutic agent vincristine in rats," *The British Journal of Pharmacology*, vol. 152, no. 5, pp. 765–777, 2007.

[64] Z. Winter, A. Buhala, F. Ötvös et al., "Functionally important amino acid residues in the transient receptor potential vanilloid 1 (TRPV1) ion channel—an overview of the current mutational data," *Molecular Pain*, vol. 9, no. 1, article 30, 2013.

[65] M. Zimmermann, "Ethical guidelines for investigations of experimental pain in conscious animals," *Pain*, vol. 16, no. 2, pp. 109–110, 1983.

[66] M. Osikowicz, J. Mika, W. Makuch, and B. Przewlocka, "Glutamate receptor ligands attenuate allodynia and hyperalgesia and potentiate morphine effects in a mouse model of neuropathic pain," *Pain*, vol. 139, no. 1, pp. 117–126, 2008.

[67] S. J. R. Elmes, M. D. Jhaveri, D. Smart, D. A. Kendall, and V. Chapman, "Cannabinoid CB2 receptor activation inhibits mechanically evoked responses of wide dynamic range dorsal horn neurons in naïve rats and in rat models of inflammatory and neuropathic pain," *European Journal of Neuroscience*, vol. 20, no. 9, pp. 2311–2320, 2004.

[68] G. J. Bennett and Y. K. Xie, "A peripheral mononeuropathy in rat that produces disorders of pain sensation like those seen in man," *Pain*, vol. 33, no. 1, pp. 87–107, 1988.

[69] P. Chomczynski and N. Sacchi, "Single-step method of RNA isolation by acid guanidinium thiocyanate-phenol-chloroform extraction," *Analytical Biochemistry*, vol. 162, no. 1, pp. 156–159, 1987.

Hindawi Publishing Corporation
BioMed Research International
Volume 2014, Article ID 871637, 7 pages
http://dx.doi.org/10.1155/2014/871637

Research Article

Lentivirus Mediated siRNA against GluN2B Subunit of NMDA Receptor Reduces Nociception in a Rat Model of Neuropathic Pain

Feixiang Wu,[1] Ruirui Pan,[1] Jiaying Chen,[1] Megumi Sugita,[2] Caiyang Chen,[1] Yong Tao,[1] Weifeng Yu,[1] and Yuming Sun[1]

[1] *Department of Anesthesiology, Eastern Hepatobiliary Hospital, Second Military Medical University, Shanghai 200438, China*
[2] *Department of Anesthesiology and Critical Care, Perelman School of Medicine at University of Pennsylvania, Philadelphia, PA 19104, USA*

Correspondence should be addressed to Weifeng Yu; ywf808@sohu.com and Yuming Sun; sunyuming2008@gmail.com

Received 28 March 2014; Revised 8 July 2014; Accepted 7 August 2014; Published 28 August 2014

Academic Editor: Katarzyna Starowicz

Although neuropathic pain (NP) is still not fully understood by scientists and clinicians alike, studies suggest that N-methyl-D-aspartate (NMDA) receptors play an important role in the induction and maintenance of NP. A promising treatment for NP is through the downregulation of NMDA subunit GluN2B by RNA interference; however, naked siRNA (small interference RNA) is not effective in long-term treatments. In order to concoct a viable prolonged treatment for NP, Lv-siGluN2B (lentivirus carrying siRNA targeting GluN2B subunit) was prepared and the antinociception effects were observed in chronic constriction injury (CCI) rats in the present study. Results showed that Lv-siGluN2B was transduced into spinal cord cells after intrathecal injections and effectively reduced the nociception induced by sciatic nerve ligation while inhibiting the mRNA and protein expression of GluN2B. This antinociception effect lasted approximately 7 weeks. These findings suggest that GluN2B subunit could be a target for NP treatment and Lv-siGluN2B represents a new potential option for long-term treatment of NP.

1. Introduction

Neuropathic pain (NP) is characterized by hyperalgesia, allodynia, and spontaneous pain. It often occurs as a result of injury to peripheral nerves, dorsal root ganglions (DRG), spinal cord, or brain. An estimated 7% to 8% of the general population suffers from mild to moderate forms of NP, and 5% may be severely affected by it [1, 2]. The N-methyl-D-aspartate (NMDA) receptor activation in animal models of chronic pain has implicated that NMDA receptors affect the polysynaptic spinal pathways and chronic nociceptive responses [3–5]. The current study focuses on the intrathecal administration of GluN2B (formally named NR2B) subunit of NMDA, which may evoke a selective, dose-dependent, and reversible hyperalgesia in mice and rats [6].

It is well documented in clinical and experimental cases that NMDA receptor agonists profoundly inhibit the long-term potentiation in the spinal cord [7]; however, their use as analgesics is limited by serious side effects [8, 9]. Currently, the available pharmacological NMDA receptor antagonists are nonspecific for NMDA receptor subtypes, but with the ever increasing knowledge of RNA interference (RNAi) and small interfering (siRNA), it is plausible to develop novel drugs that target or knock out genes for the treatment of chronic pain [10, 11]. Tan et al. [12] reported that GluN2B receptor, knocked down by intrathecal injection of siRNA, could reduce formalin-induced nociception in rats for approximately 21 days [12]. Song et al. [13] also demonstrated that mRNA levels in siRNA-treated mice were only 40% of those in control mice on day 14 and returned

to normal on day 20 after the last injection. Our prior study investigated the silencing effect of naked siRNA targeting Toll-like receptor (TLR), which lasted only 3 days after the last injection [14]. For this reason, we considered alternative mechanisms for long-term treatment of NP.

Lentiviral vector allows for sustained transgene delivery, nondividing and dividing cells infection, and broad tissue tropism, making it a more efficient and safer vehicle for spinal cord transduction [15]. Experimental transduction in neurons and glia cells of mice and rats after intraparenchymal injection displayed therapeutic effects lasting over 4 weeks [16, 17]. We hypothesize that the long-term treatment of NP can be achieved through utilizing lentivirus with siRNA targeting GluN2B receptors, and the antinociception effect can be observed in chronic constriction injury (CCI) rats.

2. Materials and Methods

2.1. Production and Identification of Recombinant Lentivirus Lv-siGluN2B. The siRNA (CCTGTGTGCCTAACAACAA) targeting GluN2B subunit of NMDA receptor gene (GenBank accession NM 000834) was screened and tested as described in our previous study [14]. Based on the sequences of lentivirus and the "Tuschl" principle, target sequences were designed and chemically synthesized in United Gene Company (Shanghai, China) and were under control of U6 promoter in lentivirus. The green fluorescent protein (GFP) was also addressed in the lentivirus to detect the transfected location of the lentivirus after intrathecal injection with *Hpa* I and *Xho* I restriction sites at the 5′ and 3′ ends, respectively. After pFU-GW-siRNA was digested by *Hpa* I and *Xho* I (TaKaRa, Japan), target gene was cloned into pFU-GW-siRNA and named pFU-GW-siGluN2B. To produce recombinant lentivirus Lv-siGluN2B (lentivirus-expressing siRNA of GluN2B), pFU-GW-si GluN2B (20 μg), pHelper 1.0 (15 μg), and pHelper 2.0 (10 μg) were cotransfected into HEK 293T cells with Lipofectamine 2000. Lentivirus was harvested at about 48 h after transfection. The final titer of recombinant virus was adjusted to 1×10^9 TU/mL.

2.2. Animals and Chronic Constriction Injury (CCI). Male Sprague-Dawley (SD) rats weighing 200–250 g were obtained from Shanghai Experimental Animal Center, the Chinese Academy of Sciences. The CCI model was established as previously described [18]. Briefly, after rats were anesthetized with sodium pentobarbital (40 mg/kg, i.p.), the right sciatic nerve was exposed at the mid-thigh level. The nerve was ligated loosely with 4-0 chromic gut threads at 4 sites with 1 mm apart, so that the nerve diameter was only slightly reduced. In the sham group, the sciatic nerve was exposed without ligation. Upon recovery from anesthesia, animals were housed individually in clear plastic cages. All animal experiments were approved by the Administrative Committee of Experimental Animal Care and Use of Second Military Medical University and conformed to the National Institute of Health guidelines on the ethical use of animals.

2.3. Lumbar Subarachnoid Catheterization. Rats were implanted with chronic indwelling catheters in the subarachnoid space on the same day after CCI procedure. Briefly, rats were anesthetized with sodium pentobarbital (40 mg/kg, i.p.). A PE-10 catheter (Becton Dickinson, Sparks, MD, USA) was inserted into the lumbar subarachnoid space between lumbar vertebrae 5 (L5) and L6 [19]. The catheter was chronically implanted and the external part of the indwelling catheter was protected according to Milligan's method [20]. A lidocaine test was given to determine the functionality and position of the catheter tip in the subarachnoid space.

2.4. Intrathecal Delivery of Lentivirus. Rats were randomly divided into 4 groups ($n = 90$ per group): sham group (sham surgery + normal saline), normal saline (NS) group (CCI + NS), Lv-GFP group (CCI + Lv-GFP), and Lv-siGluN2B group (CCI + Lv-siGluN2B). Lentivirus Lv-GFP expressing scrambled siRNA (TTCTCCGAACGTGTCACGT) was used as a control. After confirmation of the effect of CCI on the 3rd day after surgery, rats in Lv-GFP group and Lv-siGluN2B group were given Lv-GFP and Lv-siGluN2B (1×10^7 TU/10 μL), respectively. The normal saline of equal volume was administered intrathecally in rats of the remaining two groups.

2.5. Evaluation of Thermal Hyperalgesia. The paw withdrawal latency (PWL) to radiant heat was used to evaluate the thermal hyperalgesia as previously described [21]. The PWL was measured on the day and on the 1st, 3rd, 7th, 10th, 14th, 21st, 28th, and 35th days after intrathecal injection of the virus. Rats were placed under an inverted clear plexiglass cage ($23 \times 18 \times 13$ cm) on a piece of 3 mm thick glass plate and were allowed to acclimate to the surroundings for 30 min before testing. Then, the radiant heat source was positioned under the glass floor directly beneath the right hind paw. The radiant heat source consisted of a high-intensity projection lamp bulb (8 V, 50 W), locating 40 mm below the glass floor and projecting through a 5×10 mm aperture at the top of a movable case. A digital timer automatically read the time from stimuli to PWL. Detection was done twice in each rat with a 5-minute interval. The cut-off time was set at 20 sec to avoid tissue damage.

2.6. Evaluation of the Tactile Allodynia. The paw withdrawal threshold (PWT) was used to evaluate the mechanical allodynia for pain. Mechanical allodynia was assessed with von Frey filaments on the day and on the 1st, 3rd, 7th, 10th, 14th, 21st, 28th, and 35th days after intrathecal injection of the virus. Rats were placed on a wire mesh platform, covered with a transparent plastic dome, and allowed to acclimate for 30 min before testing. The filament was applied perpendicularly to the plantar surface of the right hind paw. The PWT was determined by sequentially increasing and decreasing the stimulus strength (the "up-and-down" method) (in gram, g), and data were analyzed using the nonparametric method of Dixon [22].

2.7. Spinal Cord RNA Extraction and Real-Time PCR. The real-time PCR was performed on the day and on the 1st, 3rd, 7th, 10th, 14th, 21st, 28th, and 35th days after intrathecal injection of the virus. Total RNA (6 samples of each group)

was extracted from L4-L5 spinal cord. Extracted RNA was treated with DNase I at 37°C for 30 min before reverse transcription was performed using a kit (TaKaRa, Japan). The PCR primers were as follows: 5-CGGGAG CTC TGA ATG CTC TCT TGC ATC TGG CTG GC-3 (forward) and 5-CGG GTC GAC GCC ATA CAA TTC GACCTG CTG-3 (reverse). The Real-Time PCR Detection System (Roche, Switzerland) continually monitors the increase in fluorescence, which is directly proportional to the PCR product.

2.8. Western Blot Assay. The proteins of tissues were prepared from lumbar spinal cord (L4-L5) on the 7th day after injection as previously described [23]. Proteins were separated by 8% polyacrylamide SDS-PAGE and transferred onto a nitrocellulose membrane. The nitrocellulose membrane was blotted with a primary antibody against GluN2B subunit of NMDA (1 : 100, RayBiotech, USA) and then with secondary antibody conjugated with horseradish peroxidase. Protein signals were detected with an ECL system (Amersham Pharmacia, Uppsala, Sweden). GAPDH (Sigma Chemical Co., MO, USA, 1 : 500) was used as a loading control.

2.9. Immunofluorescence Assay. Rats were anesthetized and perfused through the ascending aorta with NS and then with 4% paraformaldehyde in 0.16 M phosphate buffer (pH 7.2–7.4) containing 1.5% picric acid. After perfusion, the L5 spinal cord was collected and fixed in the same fixation solution for 3 h and then in 15% sucrose overnight. Transverse spinal sections (30 μm) were obtained on a cryostat and processed for immunofluorescence assay [24]. All the sections were blocked in 0.3% Triton X-100 containing 2% goat serum for 1 h at room temperature and incubated over two nights at 4°C with anti-GluN2B antibody (1 : 400; RayBiotech, USA). The sections were incubated for 1 h at room temperature with Cy3-conjugated secondary antibody (1 : 300; Santa Cruz, USA). These sections were examined under an Olympus (Olympus, Japan) fluorescence microscope, and representative images were captured.

2.10. Statistical Analysis. All data were expressed as mean ± standard error (SEM). Statistical analysis was carried out using two-way ANOVA followed by Turkey's multiple comparisons using GraphPad Prism software (Version 5, GraphPad Software Inc., CA, USA). The image data from western blotting was compared using one-way ANOVA. A value of $P < 0.05$ was considered statistically significant.

3. Results

3.1. Transfection of Neurocytes by Lentivirus. The location of the lentivirus could be tracked by GFP expression due to the lentiviral vector system. As shown in Figure 1, the lentivirus was efficiently transduced into cells of the spinal cord. The fluorescence of GFP was observed in the neurocytes of rats in Lv-siGluN2B group.

3.2. Lv-siGluN2B Decreased GluN2B Expression in CCI Rats. Lv-siGluN2B was intrathecally delivered into CCI rats and the expression of GluN2B was detected. As shown in Figure 2, CCI increased the mRNA expression of GluN2B. Compared

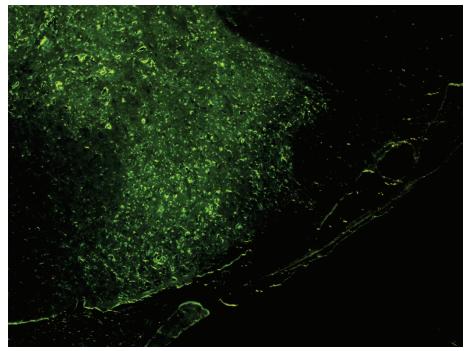

Figure 1: Detection of lentivirus Lv-siGluN2B by GFP expression (×100). As shown in Figure 1, GFP positive cells were observed in the spinal cord of the rats in Lv-siGluN2B group after intrathecal injection, which suggested that the lentivirus was efficiently transduced into cells of the spinal cord.

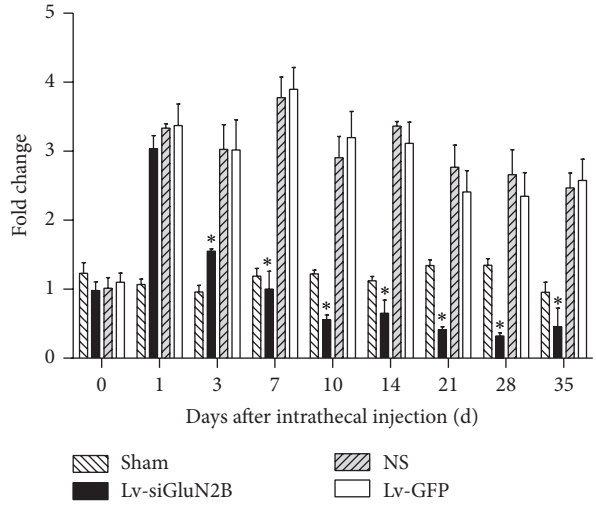

Figure 2: mRNA expression of GluN2B detected by real-time PCR. As shown in Figure 2, CCI increased the GluN2B mRNA expression in Lv-siGluN2B group, Lv-GFP group, and NS group. On the 3rd, 7th, 10th, 14th, 21st, 28th, and 35th days after delivery of Lv-siGluN2B, the GluN2B mRNA expression induced by nerve ligation decreased significantly compared to Lv-GFP group and NS group ($^*P < 0.01$ versus NS and Lv-GFP groups, two-way ANOVO analysis followed by Turkey's multiple comparisons, $N = 6$). No differences were observed on the 1st day.

to the sham group, GluN2B mRNA expression increased significantly in NS and Lv-GFP groups ($P < 0.01$, two-way ANOVO analysis followed by Turkey's multiple comparisons, $N = 6$). Three days after delivery of Lv-siGluN2B, the mRNA expression of GluN2B induced by nerve ligation decreased significantly ($P < 0.01$ versus NS and Lv-GFP groups, $N = 6$). Similarly, western blot assay (Figure 3) showed that the protein expression of GluN2B was increased in NS and Lv-GFP groups after ligation and downregulated by the Lv-siGluN2B ($^*P < 0.01$ versus NS and Lv-GFP groups, one-way ANOVO analysis, $N = 6$). These changes correspond with the results of immunohistostaining in the spinal cord, where

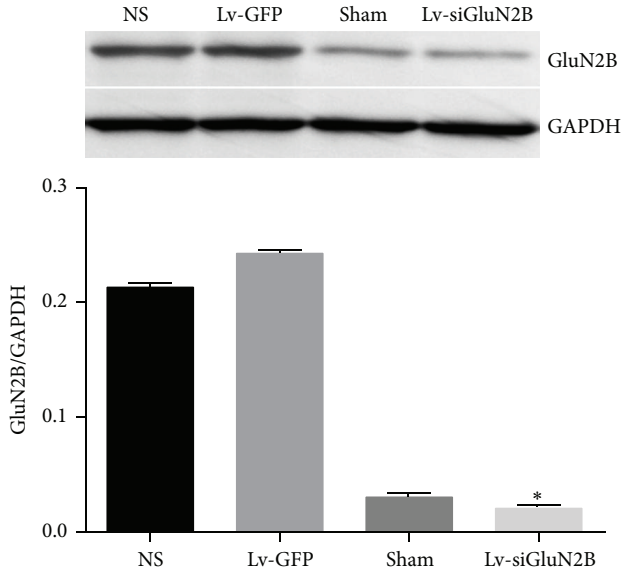

Figure 3: Western blot assay of GluN2B expression. The protein expression of GluN2B was also markedly downregulated, which was confirmed by western blot assay ($^*P < 0.01$ versus NS and Lv-GFP group, one-way ANOVO analysis, $N = 6$).

GluN2B-positive cells were detected (Figure 4). Following ligation, the GluN2B expression dramatically increased in NS group, while the GluN2B expression significantly decreased in Lv-siGluN2B group but not in LV-GFP group.

3.3. Lv-siGluN2B Attenuated NP in CCI Rats for 35 Days. To examine the impact of Lv-siGluN2B on pain response *in vivo*, modulation of pain perception in the Bennett model of NP was investigated. PWT and PWL were used to measure the mechanical allodynia and thermal hyperalgesia, respectively. After surgery, pain response such as mechanical allodynia and thermal hyperalgesia was induced, in correspondence to the reduced PWL and PWT. CCI rats receiving intrathecal Lv-siGluN2B showed significantly attenuated mechanical allodynia and thermal hyperalgesia ($P < 0.01$ versus NS and Lv-GFP groups, two-way ANOVO analysis followed by Turkey's multiple comparisons, $N = 10$), in contrast to CCI rats treated with Lv-GFP (Figure 5). The attenuation of pain response was NMDA specific since CCI rats receiving Lv-GFP intrathecally had no pain relief, as compared to NS treated CCI rats. The process lasted for about 35 days, which suggests that the anti-NP effect of Lv-siGluN2B was long lasting.

4. Discussion

In this study, the effects of NP on rat CCI models were investigated using constructed lentivirus-expressing siRNA against GluN2B subunit of NMDA receptors. Based on our results, not only could Lv-siGluN2B be successfully transfected into the spinal cord by intrathecal injection, but also its induction significantly downregulated mRNA and protein expression of GluN2B in the spinal cord. In addition, Lv-siGluN2B was effectively attenuated in the CCI-induced thermal and mechanical pain hypersensitivity for about 7 weeks. Our findings suggest that the lentivirus-mediated siRNA against GluN2B may be used for gene therapy of NP in an experimental setting. If this is successful, the downregulation of GluN2B expression by Lv-siGluN2B may be used to treat NP.

Many studies have shown that GluN2B is distributed throughout the spinal cord and plays an important role in the formation of central sensitization and persistent pain [25, 26]. GluN2B-NMDA receptor activation exacerbates a range of Ca^{2+}-sensitive signaling cascades, leading to an enhancement of responsiveness to synaptically released glutamate [27]. This increase in responsiveness leads to pain hypersensitivity. In the present study, GluN2B was found to be upregulated in RNA and protein levels after sciatic nerve ligation, consistent with the previous studies in different chronic pain models [28–30], which suggests the possibility of using this mechanism as a target for the NP treatment. Previous behavioral studies have shown that systematical application of the selective GluN2B antagonists, ifenprodil and CP-101,606, produce analgesia in animals with persistent inflammatory or neuropathic pain [29, 30]. Intrathecal (i.t.) injection of Ro 25-6981, a selective GluN2B antagonist, had a dose-dependent antiallodynic effect that leaves motor functions in tact [31]. In the present study, Lv-siGluN2B decreased the mRNA and protein expression of GluN2B along with the attenuation of hyperalgesia and mechanical allodynia. Thus, the spinal cord GluN2B is a novel target for NP treatment.

In the current study, RNAi was used as a powerful technique to "knock down" target gene of GluN2B. RNAi utilizes the ability of double-stranded RNAs (dsRNA) allowing it to form RNA duplexes of specific length and structure for the purpose of guiding the degradation of mRNA homologous sequences to siRNA and inducing sequence-specific gene silencing *in vivo* [32]. One of the potential advantages of this technology is the ability to design precisely targeted therapeutics of any specific subtype [33]. The NMDA receptor is composed of the GluN1 and GluN2 subunits (GluN2A, GluN2B, GluN2C, and GluN2D). The GluN2 subunits determine the characteristics of NMDAR channels by forming different heteromeric configurations with the GluN1 subunit [34]. In the present study, only the GluN2B subunit of NMDA was specifically targeted by the Lv-siGluN2B. The GluN2B expression was downregulated by the Lv-siGluN2B, while the Lv-GFP expressing scrambled siRNA showed no effect on GluN2B expression. The mRNA expression of Lv-siGluN2B treated group decreased up to 75%. siRNA targeting P2X3, δ-opioid receptor, and NMDA receptor have been explored as potential means to manage pain [12, 35, 36]. The motor coordination indicated by the rotarod performance test was not affected by the siRNA-GluN2B-induced analgesic effect as shown by Tan et al. [12]. All these suggest that siRNA is a feasible tool for precise, specific, and efficient "knock-down" of GluN2B, establishing a new option for NP therapy.

It has been documented that naked siRNA mediated downregulation of gene expression is transient and only lasts for 3 to 5 days [14]; hence, the lentivirus that is capable of expressing the target gene for several months and suitable for chronic pain treatment [15, 36] was introduced as a

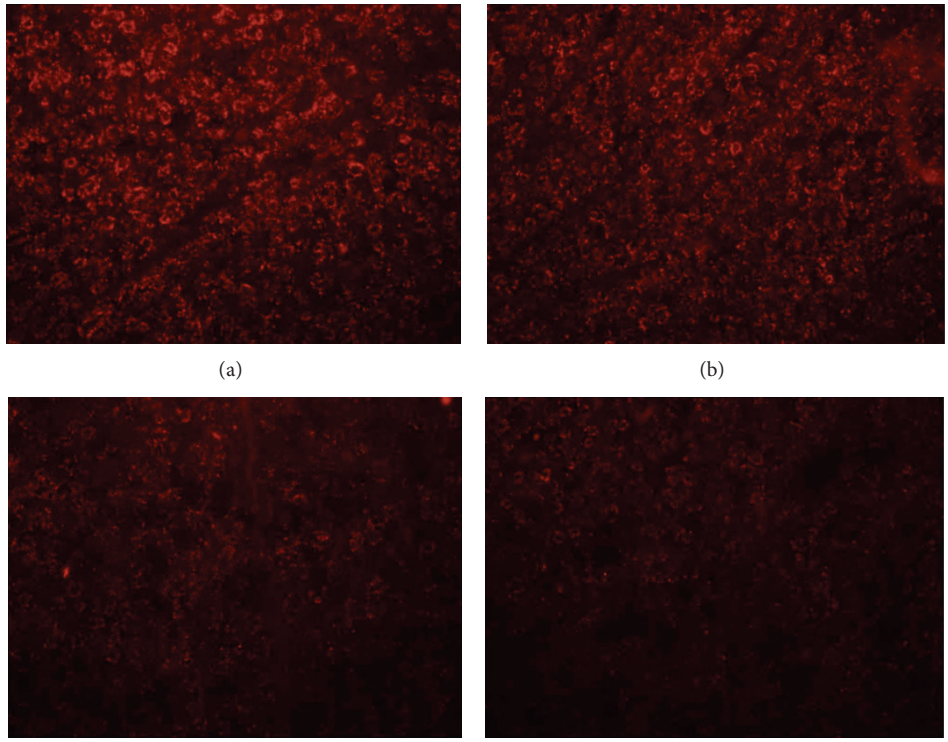

Figure 4: Immunofluorescence staining of GluN2B. Downregulation of GluN2B subunit in Lv-siGluN2B group was corroborated with findings in immunohistostaining in which the GluN2B-positive cells in the spinal cord were detected. (a) NS (×100). (b) Lv-GFP (×100). (c) Sham (×100). (d) Lv-siGluN2B (×100).

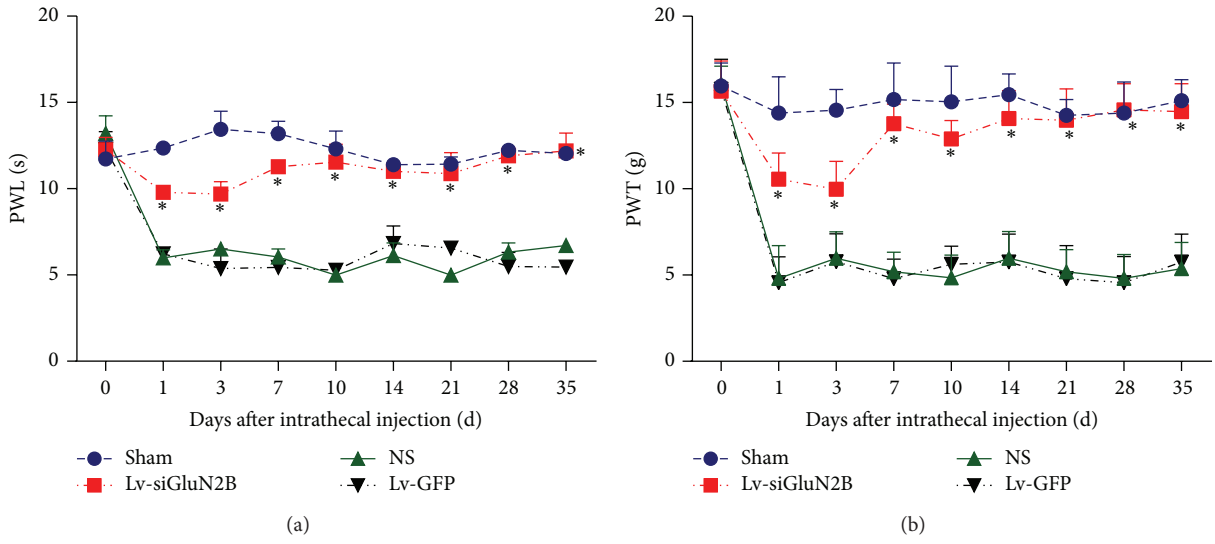

Figure 5: Impact of Lv-siGluN2B on PWL and PWT in CCI rats. On the 1st, 3rd, 7th, 10th, 14th, 21st, 28th, and 35th days after intrathecal injection, CCI rats receiving intrathecal Lv-siGluN2B showed significantly attenuated thermal hyperalgesia (a) and mechanical allodynia (b) compared to CCI rats treated with Lv-GFP and NS, as showed by PWL ($^*P < 0.01$ versus NS and Lv-GFP groups, two-way ANOVO analysis followed by Turkey's multiple comparisons, $N = 10$) and PWT ($^*P < 0.01$ versus NS and Lv-GFP groups, two-way ANOVO analysis followed by Turkey's multiple comparisons, $N = 10$).

vehicle for siRNA. As hypothesized, results showed that after intrathecal injection the antinociception effect lasted for about 35 days, which provided a suitable tool for the treatment of chronic diseases including but not limited to NP. In addition, plasmid-expressing GFP was introduced into the Lv-si GluN2B viral system for tracking. Previous studies have found that the GluN2B subunit has a relatively restricted distribution in pain regulatory pathways, such as in the superficial dorsal horn of the spinal cord [37]. Our results showed that the lentivirus was successfully transfected into dorsal horn of CCI rats, which was consistent with the location of GluN2B. Results also showed the GluN2B expression along with the pain threshold significantly decreased after the Lv-siGluN2B injection, suggesting that Lv-siGluN2B may suppress nociception in rats of the NP model through decreasing GluN2B subunit expression.

Motor behavior and other side effects caused by the decreasing GluN2B were not examined in this study. It is imperative to investigate all possible effects caused by the lentivirus before preclinical studies. Additionally, in clinical practice, the levels and timing of GluN2B expression should be controlled precisely; thus, an inducible gene expression system such as an RU486 regulating system is necessary. Further studies are warranted.

In summary, results in the present study demonstrate that an intrathecal injection of Lv-siGluN2B significantly and continuously attenuates the nociception of CCI rats. These findings suggest that Lv-siGluN2B represents a new potential option for NP management.

Conflict of Interests

The authors declare that there is no conflict of interests regarding the publication of this paper.

Authors' Contribution

Feixiang Wu and Ruirui Pan contributed equally to this work.

Acknowledgments

This work was supported by the National Natural Science Foundation of China (30901403). The authors appreciate the academic advice and review from Professor William Armstead at the Department of Anesthesiology and Critical Care at the University of Pennsylvania and the technical and statistic support from Ms. Megumi Sugita at the University of Pennsylvania.

References

[1] D. Bouhassira, M. Lantéri-Minet, N. Attal, B. Laurent, and C. Touboul, "Prevalence of chronic pain with neuropathic characteristics in the general population," *Pain*, vol. 136, no. 3, pp. 380–387, 2008.

[2] N. Torrance, B. H. Smith, M. I. Bennett, and A. J. Lee, "The epidemiology of chronic pain of predominantly neuropathic origin. Results from a general population survey," *The Journal of Pain*, vol. 7, no. 4, pp. 281–289, 2006.

[3] H. Nie and H.-R. Weng, "Glutamate transporters prevent excessive activation of NMDA receptors and extrasynaptic glutamate spillover in the spinal dorsal horn," *Journal of Neurophysiology*, vol. 101, no. 4, pp. 2041–2051, 2009.

[4] L. K. Lucas and A. G. Lipman, "Recent advances in pharmacotherapy for cancer pain management," *Cancer Practice*, vol. 10, supplement 1, pp. S14–S20, 2002.

[5] L. Radbruch and F. Elsner, "Emerging analgesics in cancer pain management," *Expert Opinion on Emerging Drugs*, vol. 10, no. 1, pp. 151–171, 2005.

[6] L. M. Pedersen and J. Gjerstad, "Spinal cord long-term potentiation is attenuated by the NMDA-2B receptor antagonist Ro 25-6981," *Acta Physiologica*, vol. 192, no. 3, pp. 421–427, 2008.

[7] T. J. Coderre and R. Melzack, "The contribution of excitatory amino acids to central sensitization and persistent nociception after formalin-induced tissue injury," *Journal of Neuroscience*, vol. 12, no. 9, pp. 3665–3670, 1992.

[8] N. Hovelsø, F. Sotty, L. P. Montezinho, P. S. Pinheiro, K. F. Herrik, and A. Mørk, "Therapeutic potential of metabotropic glutamate receptor modulators," *Current Neuropharmacology*, vol. 10, no. 1, pp. 12–48, 2012.

[9] P.-H. Tan, S.-W. Yu, V. C.-H. Lin, C.-C. Liu, and C.-F. C. Chien, "RNA interference-mediated gene silence of the NR1 subunit of the NMDA receptor by subcutaneous injection of vector-encoding short hairpin RNA reduces formalin-induced nociception in the rat," *Pain*, vol. 152, no. 3, pp. 573–581, 2011.

[10] C. Tsantoulas, L. Zhu, Y. Shaifta et al., "Sensory neuron down-regulation of the Kv9.1 potassium channel subunit mediates neuropathic pain following nerve injury," *Journal of Neuroscience*, vol. 32, no. 48, pp. 17502–17513, 2012.

[11] I. P. Kaur and G. Sharma, "siRNA: a new approach to target neuropathic pain," *BioDrugs*, vol. 26, no. 6, pp. 401–412, 2012.

[12] P.-H. Tan, L.-C. Yang, H.-C. Shih, K.-C. Lan, and J.-T. Cheng, "Gene knockdown with intrathecal siRNA of NMDA receptor NR2B subunit reduces formalin-induced nociception in the rat," *Gene Therapy*, vol. 12, no. 1, pp. 59–66, 2005.

[13] E. Song, S.-K. Lee, J. Wang et al., "RNA interference targeting Fas protects mice from fulminant hepatitis," *Nature Medicine*, vol. 9, no. 3, pp. 347–351, 2003.

[14] F.-X. Wu, J.-J. Bian, X.-R. Miao et al., "Intrathecal siRNA against toll-like receptor 4 reduces nociception in a rat model of neuropathic pain," *International Journal of Medical Sciences*, vol. 7, no. 5, pp. 251–259, 2010.

[15] A. Meunier and M. Pohl, "Lentiviral vectors for gene transfer into the spinal cord glial cells," *Gene Therapy*, vol. 16, no. 4, pp. 476–482, 2009.

[16] H. Peluffo, E. Foster, S. G. Ahmed et al., "Efficient gene expression from integration-deficient lentiviral vectors in the spinal cord," *Gene Therapy*, vol. 20, no. 6, pp. 645–657, 2013.

[17] T. Sun, J. Luo, M. Jia, H. Li, K. Li, and Z. Fu, "Small interfering RNA-mediated knockdown of NF-κBp65 attenuates neuropathic pain following peripheral nerve injury in rats," *European Journal of Pharmacology*, vol. 682, no. 1–3, pp. 79–85, 2012.

[18] G. J. Bennett and Y.-K. Xie, "A peripheral mononeuropathy in rat that produces disorders of pain sensation like those seen in man," *Pain*, vol. 33, no. 1, pp. 87–107, 1988.

[19] R. V. Størkson, A. Kjørsvik, A. Tjølsen, and K. Hole, "Lumbar catheterization of the spinal subarachnoid space in the rat," *Journal of Neuroscience Methods*, vol. 65, no. 2, pp. 167–172, 1996.

[20] E. D. Milligan, J. L. Hinde, K. K. Mehmert, S. F. Maier, and L. R. Watkins, "A method for increasing the viability of the external

portion of lumbar catheters placed in the spinal subarachnoid space of rats," *Journal of Neuroscience Methods*, vol. 90, no. 1, pp. 81–86, 1999.

[21] K. Hargreaves, R. Dubner, F. Brown, C. Flores, and J. Joris, "A new and sensitive method for measuring thermal nociception in cutaneous hyperalgesia," *Pain*, vol. 32, no. 1, pp. 77–88, 1988.

[22] S. R. Chaplan, F. W. Bach, J. W. Pogrel, J. M. Chung, and T. L. Yaksh, "Quantitative assessment of tactile allodynia in the rat paw," *Journal of Neuroscience Methods*, vol. 53, no. 1, pp. 55–63, 1994.

[23] G. An, T.-N. Lin, J.-S. Liu, J.-J. Xue, Y.-Y. He, and C. Y. Hsu, "Expression of c-fos and c-jun family genes after focal cerebral ischemia," *Annals of Neurology*, vol. 33, no. 5, pp. 457–464, 1993.

[24] R.-R. Ji, K. Befort, G. J. Brenner, and C. J. Woolf, "ERK MAP kinase activation in superficial spinal cord neurons induces prodynorphin and NK-1 upregulation and contributes to persistent inflammatory pain hypersensitivity," *The Journal of Neuroscience*, vol. 22, no. 2, pp. 478–485, 2002.

[25] M. G. Garry, S. Malik, J. Yu, M. A. Davis, and J. Yang, "Knock down of spinal NMDA receptors reduces NMDA and formalin evoked behaviors in rat," *NeuroReport*, vol. 11, no. 1, pp. 49–55, 2000.

[26] L. Quintero, R. Cardenas, and H. Suarez-Roca, "Stress-induced hyperalgesia is associated with a reduced and delayed GABA inhibitory control that enhances post-synaptic NMDA receptor activation in the spinal cord," *Pain*, vol. 152, no. 8, pp. 1909–1922, 2011.

[27] L. Chen and L.-Y. M. Huang, "Protein kinase C reduces Mg^{2+} block of NMDA-receptor channels as a mechanism of modulation," *Nature*, vol. 356, no. 6369, pp. 521–523, 1992.

[28] Q. Q. Fan, L. Li, W. T. Wang, X. Yang, Z. W. Suo, and X.D. Hu, "Activation of $\alpha 2$ adrenoceptors inhibited NMDA receptor-mediated nociceptive transmission in spinal dorsal horn of mice with inflammatory pain," *Neuropharmacology*, vol. 77, pp. 185–192, 2014.

[29] B. A. Chizh, E. Reißmüller, H. Schlütz, M. Scheede, G. Haase, and W. Englberger, "Supraspinal vs spinal sites of the antinociceptive action of the subtype-selective NMDA antagonist ifenprodil," *Neuropharmacology*, vol. 40, no. 2, pp. 212–220, 2001.

[30] E. Nakazato, A. Kato, and S. Watanabe, "Brain but not spinal NR2B receptor is responsible for the anti-allodynic effect of an NR2B subunit-selective antagonist CP-101,606 in a rat chronic constriction injury model," *Pharmacology*, vol. 73, no. 1, pp. 8–14, 2005.

[31] X. X. Qu, J. Cai, M. J. Li et al., "Role of the spinal cord NR2B-containing NMDA receptors in the development of neuropathic pain," *Experimental Neurology*, vol. 215, no. 2, pp. 298–307, 2009.

[32] L. S. Lambeth and C. A. Smith, "Short hairpin RNA-mediated gene silencing," *Methods in Molecular Biology*, vol. 942, pp. 205–232, 2013.

[33] T. E. Ichim, M. Li, H. Qian et al., "RNA interference: a potent tool for gene-specific therapeutics," *American Journal of Transplantation*, vol. 4, no. 8, pp. 1227–1236, 2004.

[34] W. Zou, Z. Song, Q. Guo, C. Liu, Z. Zhang, and Y. Zhang, "Intrathecal lentiviral-mediated rna interference targeting PKCγ attenuates chronic constriction injury-induced neuropathic pain in rats," *Human Gene Therapy*, vol. 22, no. 4, pp. 465–475, 2011.

[35] G. Dorn, S. Patel, G. Wotherspoon et al., "siRNA relieves chronic neuropathic pain," *Nucleic Acids Research*, vol. 32, no. 5, p. e49, 2004.

[36] M.-C. Luo, D.-Q. Zhang, S.-W. Ma et al., "An efficient intrathecal delivery of small interfering RNA to the spinal cord and peripheral neurons," *Molecular Pain*, vol. 1, article 29, 2005.

[37] G. G. Nagy, M. Watanabe, M. Fukaya, and A. J. Todd, "Synaptic distribution of the NR1, NR2A and NR2B subunits of the N-methyl-D-aspartate receptor in the rat lumbar spinal cord revealed with an antigen-unmasking technique," *European Journal of Neuroscience*, vol. 20, no. 12, pp. 3301–3312, 2004.

Hindawi Publishing Corporation
BioMed Research International
Volume 2014, Article ID 470983, 10 pages
http://dx.doi.org/10.1155/2014/470983

Review Article

Adult Stem Cell as New Advanced Therapy for Experimental Neuropathic Pain Treatment

Silvia Franchi,[1] Mara Castelli,[1] Giada Amodeo,[1] Stefania Niada,[2,3] Daniela Ferrari,[4] Angelo Vescovi,[4,5] Anna Teresa Brini,[2,3] Alberto Emilio Panerai,[1] and Paola Sacerdote[1]

[1] *Dipartimento di Scienze Farmacologiche e Biomolecolari, Università degli Studi Milano, 20129 Milano, Italy*
[2] *I.R.C.C.S. Istituto Ortopedico Galeazzi, 20161 Milano, Italy*
[3] *Dipartimento di Scienze Biomediche, Chirurgiche ed Odontoiatriche, Università degli Studi di Milano, 20129 Milano, Italy*
[4] *Dipartimento di Biotecnologie e Bioscienze, Università Milano Bicocca, 20126 Milano, Italy*
[5] *Istituto di Ricovero e Cura a Carattere Scientifico Opera di San Pio da Pietralcina, 71013 San Giovanni Rotondo, Italy*

Correspondence should be addressed to Silvia Franchi; silvia.franchi@unimi.it

Received 12 June 2014; Accepted 23 July 2014; Published 13 August 2014

Academic Editor: Livio Luongo

Neuropathic pain (NP) is a highly invalidating disease resulting as consequence of a lesion or disease affecting the somatosensory system. All the pharmacological treatments today in use give a long lasting pain relief only in a limited percentage of patients before pain reappears making NP an incurable disease. New approaches are therefore needed and research is testing stem cell usage. Several papers have been written on experimental neuropathic pain treatment using stem cells of different origin and species to treat experimental NP. The original idea was based on the capacity of stem cell to offer a totipotent cellular source for replacing injured neural cells and for delivering trophic factors to lesion site; soon the researchers agreed that the capacity of stem cells to contrast NP was not dependent upon their regenerative effect but was mostly linked to a bidirectional interaction between the stem cell and damaged microenvironment resident cells. In this paper we review the preclinical studies produced in the last years assessing the effects induced by several stem cells in different models of neuropathic pain. The overall positive results obtained on pain remission by using stem cells that are safe, of easy isolation, and which may allow an autologous transplant in patients may be encouraging for moving from bench to bedside, although there are several issues that still need to be solved.

1. Introduction

Neuropathic pain (NP), currently defined as "pain arising as a direct consequence of a lesion or disease affecting the somatosensory system" [1], represents the most severe form of chronic pain considering its capacity to affect both physical and mental patient's condition. The nature of NP is extremely heterogeneous and four main categories of neuropathic lesions have been recognized: focal or multifocal lesions of the *peripheral* nervous system (PNS), lesions of the central nervous system (CNS), polyneuropathies, and complex neuropathic disorders [2]. Regardless of the primary etiology, NP can present itself as spontaneous pain sensations such as paroxysmal pain (shooting pain) and superficial pain (burning sensation) or as evoked pain: mechanical/thermal allodynia (pain caused by normally nonpainful mechanical or thermal stimuli), hyperalgesia (increased sensitivity to a normally painful stimulus), or temporal summation (increasing pain sensation from repetitive application of the identical stimulus) [3]. It has recently been pointed out that neuropathic pain pathogenesis and maintenance involve interactions among neurons, inflammatory immune cells, glial cells, and a wide cascade of pro- and anti-inflammatory cytokines [4–7]. One of the main problems concerning NP regards its scarce response to the conventional analgesic therapy. Drugs, mainly represented by tricyclic antidepressant, calcium channel ligands, SSNRI, and opioids, are in fact not fully effective and their efficacy decreases over time with development of tolerance in long term use [8, 9]. It is therefore mandatory to identify and propose novel approaches to NP

treatment that could overcome many of the limitations of the available strategies.

In the last years many researchers, including us, have tried to relieve neuropathic pain by using stem cells of different origin. The first moving idea was based on the capacity of stem cell to offer a multipotent cellular source for replacing injured or lost neural cells and for delivering trophic factors to lesion site; in this way, stem cells can represent not only a pain treatment but a way for repairing the damaged nervous system at the basis of NP development. Soon we and others realized that the capacity of stem cells to contrast experimental neuropathic pain was not completely dependent upon their regenerative effect; in fact many research papers described an antinociceptive effect of the stem cell achieved before the appearance of regenerative effect [10]. In this paper we review the literature in which stem cells of different origin and species were used to treat neuropathic pain induced in experimental animal models. We divide the published papers according to the type of stem cell used, independently of the experimental NP model. We do not report the studies with embryonic stem cells considering the associated ethical problem and the major risk of tumors correlated to them. Moreover, we considered only papers in which the effect of stem cells on pain behaviour has been specifically evaluated. Today there are three main types of stem cells used for neuropathic pain: neural stem cells, mesenchymal stem cells, and bone marrow mononuclear cells.

2. Neural Stem Cells

Considering the nature of the lesion at the basis of NP development that takes place in PNS or CNS, neural stem cells (NSCs) seem to be the most appropriate type of cells to prompt a physiological repair of the lesion, due to their capacity to differentiate into neurons, astrocytes, and oligodendrocytes, even though it was suggested that also mesenchymal stem cells, under particular conditions, can originate cells of the neural lineage [11–13]. Neural stem cells were identified for the first time and isolated from the subventricular zone of adult mammalian brain in 1992 [14, 15]. They are multipotential precursors that grow and self-renew in culture for an extensive period of time as neurospheres, while retaining a stable capacity to generate mature functional brain cells. So far, NSC lines have been derived from the hippocampal dentate gyrus, the olfactory bulb, the SVZ surrounding the ventricles, the subcallosal zone underlying the corpus callosum, and the spinal cord of the embryonic, neonatal, and adult rodent CNS [15], as well as from human fetal CNS [16–18].

Our group [10] described for the first time the use of intravenous murine neural stem cells, NSCs, to treat neuropathic pain which develops as consequence of a lesion of the peripheral nervous system, that is, sciatic nerve chronic constriction injury (CCI). Cells, isolated from the subventricular zone using the neurosphere technique [19], were treated to express GFP gene thus allowing their localization after transplant. Even though efficiency of the transplant is low, we described the rapid and specific homing of NSC to the injured nerve, since these cells were present at lesion site starting from day 1 to day 7 after injection. Their short time presence at lesion site was, however, able to start a cascade of events in the main sites of pain transmission, which contributed to pain reduction.

Regarding their effects on pain relief, NSC, injected when the pathology was already established, induced a significant reduction in allodynia and hyperalgesia already 3 days after administration, demonstrating a therapeutic effect that lasted for at least 28 days. Responses changed with the number of administered NSCs and the effect on hyperalgesia could be boosted by a new NSC administration. Treatment induced changes in cytokine profile at lesion site, decreasing significantly the proinflammatory cytokine Interleukin-1 both as mRNA and protein, while cells were unable to normalize the levels of the anti-inflammatory cytokine IL-10 decreased by CCI. The effect on pain relief was also demonstrated by a reduction of spinal cord Fos expression in laminae I–VI. Moreover we observed a reparative process and an improvement of nerve morphology, due to NSC treatment, which was present at a later time, when pain was already controlled by NSC treatment. Since NSC effect on pain symptoms preceded nerve repair and was maintained after cell disappearance from the lesion site, we believe that the regenerative, behavioral, and immune NSC effects are largely due to microenvironmental changes that they might induce in the lesion. Our results support the idea of a general bystander effect exerted by transplanted NSC [20]. These positive results on neuropathic pain relief were supported by Xu and colleagues [21] by using another route for NSC administration; the authors described that an intrathecal administration of neural stem cells, 3 days after CCI injury in rat, was able to significantly attenuate mechanical and thermal hyperalgesia with a marked increase of protein and mRNA levels of glial cell line derived neurotrophic factor (GDNF) in the spinal dorsal horn and dorsal root ganglia (DRG). So far we have considered the use of NSC for treating NP which follows a peripheral lesion of the nervous system; however, neural progenitors/stem cells were also used to treat lesions at spinal cord level. One of the main problems concerning their use in these conditions is represented by their low survival in the host damaged spinal cord. For this reason combinatorial strategies were developed to try to improve their transplant efficiency but the final outcome on NP is questionable. Positive results on pain were obtained by the group of Luo [22] investigating the efficacy of a cotransplantation of NSC and OECs (olfactory ensheathing cells) in a rat spinal cord transection injury model. They found that the transplantation of NSC together with OEC could improve the sensory function to mechanical and thermal stimuli after SCI; the authors suggested that OECs can promote the NSC survival and the cotransplantation downregulates the expression of NGF. Karimi-Abdolrezaee et al. [23] instead developed a combinatorial strategy that allows the successful application of neural progenitor cells (NPC) based therapies for the treatment of chronic spinal cord injury. The authors showed that chondroitin sulfate proteoglycans (CSPGs) in the glial scar around the site of chronic SCI negatively influences the long-term survival and integration of transplanted NPC and their therapeutic potential. For this reason they

targeted CSPGs and one week later treated the same rats with transplants of NPC and transient infusion of growth factors (EGF, bFGF, and PDGF-AA). This combinatorial approach markedly increased the long-term survival of NPC and greatly optimized their migration and integration in the chronically injured spinal cord. Furthermore, this combined strategy promoted the axonal integrity and plasticity of the corticospinal tract and enhanced the plasticity of descending serotonergic pathways. These neuroanatomical changes were also associated with significantly improved neurobehavioral recovery after chronic SCI. However, cells were unable to modify the development of allodynia which follows the thoracic spinal cord injury. It is important to report that the first papers trying stem cell approaches in SCI models described negative results for pain relief. Hofstetter and colleagues [24] suggested a correlation between induction of allodynia after SCI and the transplantation of NPC. They reported that transplanted naive NPCs primarily differentiate into astrocytes and this was associated with induced aberrant sprouting of Calcitonin gene related peptide fibers rostral to the injury, leading to increased allodynia. In the same years, Macias et al. described that NSC primarily differentiated into astrocytes when transplanted into the injured spinal cord which resulted in thermal and mechanical forelimb allodynia [25].

All the papers mentioned above described the use of neural precursors/stem cells isolated from rodents; in literature, to our knowledge, there is only one paper which showed the results of using human neural stem cells in experimental animal models of NP. In this paper human neural stem cells are shown to be capable of surviving and differentiating in a traumatically injured environment improving the locomotor recovery [26]. However, in experimental paradigms of other pathologies, human neural stem cells (hNSC) have revealed anti-inflammatory and therapeutic abilities analogous to their murine counterpart [27–29]. Moreover, the possibility to isolate and expand hNSC lines of clinical grade [18] has allowed evaluating the safety of these cells in a phase I clinical trial in amyotrophic lateral sclerosis patients, which is currently underway.

3. Mesenchymal Stem Cells (MSC)

MSC are a heterogeneous subset of stromal stem cells which can be isolated from different sources: bone marrow [30], umbilical cord (UC) [31, 32], placenta [33], adipose tissue [34], dental pulp [35], and even the fetal liver [36] and lungs [37]. These cells express typical surface markers such as CD73, CD44, CD90, and CD105. Among MSC, the most representative ones are bone marrow MSC (BMSC), purified from bone marrow, and adipose tissue derived MSC (ASC), isolated from adipose tissue. ASCs are described to be BMSC migrated into the adipose tissue; hence there are no marked phenotypic differences between these two cell types [34, 38]. However, in recent years, other types of MSC, such as those derived from umbilical cord blood (UCB-MSC) and amniotic mesenchymal stem cells, have begun to attract researchers' attention for their therapeutic use.

A basic description of bone marrow may help clarify the origin of bone marrow derived mesenchymal stem cells. Bone marrow consists of a hematopoietic component (parenchyma) and a vascular component (stroma). The parenchyma includes hematopoietic stem cells and hematopoietic progenitor cells while bone marrow stroma contains multipotent nonhematopoietic progenitor cells, bone marrow stromal cells (MSC) that are known as multipotent cells capable of differentiating under specific experimental conditions into several types of cells, for example, osteoblasts, chondrocytes, adipocytes, and myocytes [30]. Moreover, some papers described the capacity of MSC to transdifferentiate also into neurons or astrocytes [11–13]. Both rodent and human MSC and bone marrow mononuclear cells were used for treating experimental neuropathic pain.

3.1. Bone Marrow MSC (BMSC)

3.1.1. Rodent BMSC. One of the first groups to assess the effect of rat bone marrow stromal cells in an experimental rat model of peripheral neuropathy was the group of Musolino [39]. They demonstrated that an ipsilateral intraganglionic injection of rat bone marrow stromal cells was able to prevent the generation of mechanical allodynia and to reduce the number of allodynic responses to cold stimuli in rats that underwent a single ligature sciatic nerve constriction [39]. One of the possible mechanisms involved in such effect was the capacity of BMSC to partially prevent the injury-induced changes in galanin, Neuropeptide Y and Neuropeptide Y receptor expression in DRG [40]. The authors compared the effect of MSC on pain relief and biochemical changes to that of bone marrow nonadherent mononuclear cells (BNMCs), but these latter stem cells were, in that case, unable to reduce pain [39].

Rat bone marrow MSC has also been used in another type of neuropathic pain treatment, not derived from a direct nerve lesion, but consequence of the metabolic dysfunction present in diabetes which is one of the main causes of painful neuropathy in human. Shibata and colleagues tried in fact to improve diabetic polyneuropathy induced in rat by using Streptozotocin (STZ) [41]. MSC (1×10^6) were therapeutically injected into the hind limb muscle 8 weeks after diabetes induction. The authors described an increase in VEGF and bFGF mRNA expression in MSC-injected diabetic rats and colocalized VEGF and bFGF in MSC in the transplanted site thus suggesting that MSC are responsible for growth factors secretion at the injected site. MSC were able to ameliorate all the alterations induced by diabetes such as hypoalgesia, delayed nerve conduction velocity, and decreased sciatic nerve blood flow. Moreover, MSC transplantation was able to normalize sural nerve morphometry restoring the axonal circularity, decreased in diabetic rats. The same positive effect on nerve conduction velocity amelioration was also reported by Kim and Jin [42], using the same model of diabetic neuropathy in mice, by injecting murine MSC into the hind limb muscle percutaneously along the course of the sciatic nerve at 4 sites. The improvement in nerve conduction velocity was attributed to the ability of MSC to increase trophic factors specific for neuronal populations in the PNS such as nerve growth factor (NGF) and neurotrophin-3 (NT-3). The authors did not directly assess pain.

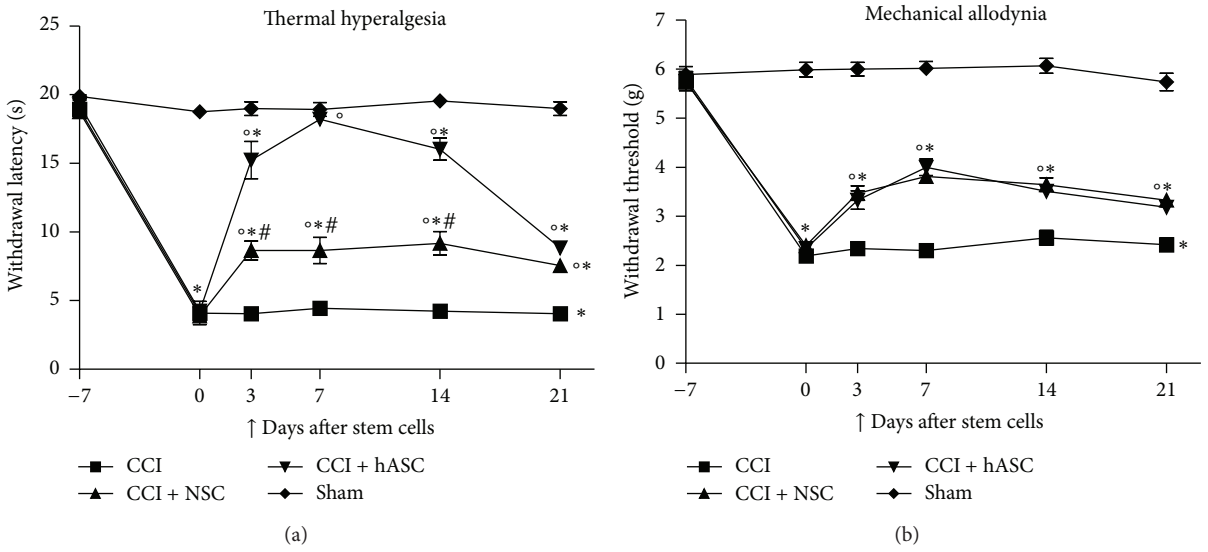

Figure 1: Time course of the effect of murine neural stem cells (NSCs) and human adipose derived stem cells (hASC) on thermal hyperalgesia (a), measured by Plantar test, and mechanical allodynia, measured by Dynamic Plantar Aesthesiometer (b), in neuropathic mice. 1×10^6 NSCs/ASCs were injected intravenously 7 days after mice chronic constriction injury; their effect on pain was measured 3, 7, 14, and 21 days after the administration. Data represent mean +/− SEM of 7 mice. The statistical analysis was performed by using the two-way ANOVA analysis of variance followed by Bonferroni test. $^{*}P < 0.001$ versus Sham, $^{\circ}P < 0.001$ versus CCI, and $^{\#}P < 0.001$ versus hASC.

3.1.2. h(Human)BMSC. The Maione's group is the main user of human BMSC for treating experimental neuropathic pain. The authors use, as model of NP, the spared nerve injury (SNI) model in mice and administer hBMSC therapeutically, that is, 4 days after the surgery, injecting them either in the mouse lateral cerebral ventricle [43] or systemically into the caudal vein [44]. When intravenously injected, cells were able to home into the spinal cord and prefrontal cortex of SNI neuropathic mice. In both papers, hBMSC reduced pain-like behaviors, such as mechanical allodynia and thermal hyperalgesia, with an effect which was evident one week after cell transplantation and was long lasting. Indeed, when cells were injected into the caudal vein, their effect on pain relief was still present three months after transplant. The authors described the capacity of these cells to reduce glial [43] and macrophage activation [44] switching to an anti-inflammatory phenotype by decreasing the proinflammatory cytokines (IL-1 beta and IL-17) and increasing the anti-inflammatory cytokine IL-10 [43, 44].

The group of Waterman [45] developed a method to optimize the anti-inflammatory effects of human bone marrow MSC, skewing them in vitro, before their injections, towards a protective MSC2 phenotype. These MSC demonstrated a higher capacity to counteract mechanical allodynia and heat hypoalgesia induced in mice by STZ treatment. These cells were also able to decrease the serum level of proinflammatory cytokines and were described to be safe.

3.2. Adipose Tissue Derived MSC (ASC). The great advantage of these cells, over the other kinds of MSC, is given by the possibility of isolating them by using low invasive procedures. These cells are in fact located in mature subcutaneous adipose tissue and can be obtained as litter of the fatty tissue after liposuction; the use of this tissue allows to obtain a large amount of MSC thus reducing, in some cases, the need of ex vivo culturing, leading eventually to lower the risk of developing chromosomal abnormalities due to the culture itself. Moreover, these cells are characterized by low immunogenicity and by high immunomodulatory properties which make them suitable for treating diseases in which the neuroinflammatory component plays a crucial role, such as NP. Not least these cells might be easily used for autologous transplant. Despite the high potential of these cells, their use for experimental neuropathic pain treatment is still limited. Our paper, recently published [46], was the first to assess the antinociceptive effect of hASC isolated from human adipose tissue of female donors undergoing plastic surgery. This paper is a complete work in which safety, antinociceptive effects, and biochemical changes induced by these cells were assessed. hASC were in vitro expanded [47, 48] and, after karyotype assessment, were injected into the caudal vein of neuropathic mice (CCI mice). Cells were injected, with a therapeutic intent, seven days after the surgery, in presence of a fully developed thermal hyperalgesia and mechanical allodynia. We clearly demonstrated a rapid, long lasting, and dose dependent antihyperalgesic and antiallodynic effect which could be reestablished with a second dose of cells when it began to vanish. The intravenous injection of 1×10^6 hASCs was able to completely abolish thermal hyperalgesia starting one day after the injection [46]. The effects of hASCs on thermal hyperalgesia seem to be more potent than those of NSC [10]. In fact, as shown in Figure 1(a), the withdrawal thresholds of hASC treated mice were overall higher than those of NSC treated mice, and 7 days after hASC injection thermal hyperalgesia was completely abolished,

while, for allodynia, a comparable effect of the two cells is evident (Figure 1(b)). The effect on pain relief well correlates with a general systemic and injured nerve localized anti-inflammatory effect of hASC. In fact, a significant increase of IL-10 serum concentration is already evident 1 day after hASC treatment; moreover at nerve site, the protein levels of IL-1, increased by the pathology, appeared normalized 1 day after the hASC injection, while the anti-inflammatory cytokine IL-10, decreased by CCI, gradually increased until reaching levels 3 times higher over control group [46]. The dose response effect, described for pain, was also evident for cytokines, indicating a clear correlation between pain relief and anti-inflammatory effect of hASCs. If we compare the effect on cytokines of hASC versus NSC, it is clear that the big difference between these two cell types regard their effect on IL-10. No changes at nerve site on IL-10 protein is evident seven days after NSC injection while, at the same time, IL-10 is strongly increased by hASC [46]. We assume that this effect, together with the general systemic anti-inflammatory one, could be responsible of the stronger antihyperalgesic effect of hASC. Besides the effects induced by hASC at nerve site we described also a normalization of the spinal cord iNOS protein level which is evident with a full neuropathic pain recovery. This paper clearly suggests a possible therapeutic use of hASC for neuropathic pain treatment.

These same cells and hATSCs, human adipose tissue-derived stem cells treated in vitro with ZnO shell nanoparticles in order to improve stem cell function, were recently used by In Choi et al. [49]; these cells, intrathecally injected, were able to reduce the pain consequent to a spinal cord injury by increasing the paw withdrawal thresholds to mechanical and thermal stimuli.

3.3. Umbilical Cord-Derived Mesenchymal Stem Cells (UC-MSC). Human umbilical cord (UC) is a promising source of mesenchymal stem cells (MSC) and is nowadays under researchers' investigation. UC contains two umbilical arteries (UCAs) and one umbilical vein (UCV), both embedded within a specific mucous connective tissue, known as Wharton's jelly (WJ), which is covered by amniotic epithelium. MSC can be isolated from all these compartments by using different techniques; today it is still unclear which one is the best compartment in UC for clinical use. UC-MSC possess a gene expression profile similar to that of embryonic stem cells, but their collection procedure is considered ethically correct, and they are characterized by a faster self-renewal rate than MSC isolated, for example, from bone marrow. Moreover they have other attractive advantages which are summarized here: (1) a noninvasive collection procedure for autologous or allogeneic use; (2) a lower risk of infection; (3) a low risk of developing teratoma; (4) multipotency, and (5) low immunogenicity with a good immunosuppressive ability [50]. Roh and colleagues [51] recently investigated the therapeutic effect of transplanting human umbilical cord blood-derived mesenchymal stem cells (hUCB-MSC) or amniotic epithelial stem cells (hAESCs) on SCI-induced mechanical allodynia and thermal hyperalgesia in T13 spinal cord hemisected rats. Two weeks after SCI, hUCB-MSC or hAESC were transplanted around the spinal cord lesion site, and behavioral tests were performed; moreover, immunohistochemical and Western blot analyses were performed to evaluate possible therapeutic effects on SCI-induced inflammation and the nociceptive-related phosphorylation of the NMDA NR1 receptor subunit. The authors described only a weak antiallodynic effect of hUCB-MSC if compared to that of hAESCs and no effect on thermal hyperalgesia of either cell type. The antiallodynic effect of hAESCs is associated with a decrease in spinal cord microglia activity and NMDA receptor NR1 phosphorylation. In contrast to the weak efficacy of hUCB-MSC on pain symptoms, the group of Yang [52] using HUMSCs from Wharton's jelly of the umbilical cord transplanted into the spinal cord described a beneficial effect for wound healing and locomotor recovery after spinal cord injury in rats suggesting a potential use of these cells if not for pain at least for motor recovery.

4. Bone Marrow Derived Mononuclear Cells

An improvement in experimental neuropathic pain treatment was also obtained using other types of cells isolated from bone marrow and in particular by using bone marrow derived mononuclear cells. A paper of Klass et al. [53] described that the infusion (1×10^7, i.v.) of rat marrow mononuclear cells, containing mixed stem cell populations, 10 days after rat CCI, was able to induce neuropathic pain recovery (both hyperalgesia and allodynia). The authors did not investigate into the mechanisms involved in such modulations. Freshly isolated rat bone marrow-derived mononuclear cells (BM-MNCs) were also used for contrasting diabetes neuropathy induced in rats by STZ [54]. Cells injected into the hind limb skeletal muscles two weeks after STZ were able to ameliorate mechanical hyperalgesia and cold allodynia in the BM-MNC-injected side. Furthermore, the slowed sciatic nerve conduction velocities (MNCV/SNCV) and decreased sciatic nerve blood flow in diabetic rats were improved in the BM-MNC-injected side. BM-MNC transplantation further decreased mRNA expression of NT-3 and number of microvessels in the hind limb.

5. Conclusions

In recent years, the possibility to apply stem cells for the treatment of neuropathic pain has attracted much attention, as demonstrated by the increasing number of preclinical studies in the literature (Table 1).

In whole the preclinical data here reported suggest positive effects of stem cells for relieving experimental neuropathic pain. An interesting point that emerges from the detailed analysis of the preclinical data is that peripheral neuropathic pain seems to be more responsive to stem cell treatment than pain arising from central lesion such as spinal cord injury. Moreover in SCI, stem cell treatment is not always able to positively and contemporarily affect both pain symptoms and motor recovery, indicating that different mechanisms can underlie the different effects.

It is important to underline that one of the main aspects concerning stem cells usage is both their fast onset and long lasting effect on pain relief; a single administration of cells is

Table 1: Stem cells used for experimental neuropathic pain treatment.

Cell source	Delivery site	Number of cells	Model of NP and species	Effect on pain	Author and year
Neural stem cells					
NSC (mouse)	Intravenous	$1, 2, 3 \times 10^6$	CCI (mouse)	Improvement of thermal hyperalgesia and mechanical allodynia	Franchi et al., 2012 [10]
NSC (rat)	Intrathecal	1×10^6	CCI (rat)	Improvement of thermal and mechanical hyperalgesia	Xu et al., 2013 [21]
NSC + OEC (rat)	Injury site	3×10^5	SCI (rat)	Cotransplantation improves sensory function	Luo et al., 2013 [22]
NPC (mouse)	Injury site	4×10^5	SCI (rat)	No effect on pain (allodynia)	Karimi-Abdolrezaee et al., 2010 [23]
NPC (rat)	Injury site	1×10^5	SCI (rat)	Induction of allodynia	Hofstetter et al., 2005 [24]
NSC (mouse)	Injury site	1×10^5	SCI (rat)	Induction of thermal and mechanical forelimb allodynia	Macias et al., 2006 [25]
Bone marrow mesenchymal stem cells					
MSC (rat)	Intraganglionic (DRG)	2×10^5	SLNC (rat)	Prevention of mechanical and thermal allodynia	Musolino et al., 2007 [39]
MSC (rat)	Injection in the hind limb skeletal muscle	1×10^6	STZ-induced diabetes (rat)	Improvement of hypoalgesia	Shibata et al., 2008 [41]
MSC (human)	Lateral cerebral ventricle	5×10^4	SNI (mouse)	Improvement of mechanical allodynia and thermal hyperalgesia	Siniscalco et al., 2010 [43]
MSC (human)	Intravenous	2×10^6	SNI (mouse)	Improvement of thermal hyperalgesia and mechanical allodynia	Siniscalco et al., 2011 [44]
MSC2 (human)	Intraperitoneal	$5 \times 10^5, 1 \times 10^6$	STZ-induced diabetes (mouse)	Improvement of mechanical allodynia and heat hypoalgesia	Waterman et al., 2012 [45]
Adipose tissue derived-mesenchymal stem cells					
ASC (human)	Intravenous	$5 \times 10^5, 1 \times 10^6$	CCI (mouse)	Improvement of thermal hyperalgesia and mechanical allodynia	Sacerdote et al., 2013 [46]
ATSC/core shell particle-treated ATSC (human)	Intrathecal	Not indicated	SCI (mouse)	Improvement of mechanical allodynia and thermal hyperalgesia	In Choi et al., 2013 [49]
Umbilical cord mesenchymal stem cells					
UCB-MSC (human)	Injury site	1×10^6	SCI (rat)	Tendency to reduce mechanical allodynia	Roh et al., 2013 [51]
(HUMSCs) isolated from Wharton's jelly (human)	Injury site	5×10^5	SCI (rat)	Locomotor recovery	Yang et al., 2008 [52]

Table 1: Continued.

Cell source	Delivery site	Number of cells	Model of NP and species	Effect on pain	Author and year
Bone marrow derived mononuclear cells					
Marrow mononuclear cells (rat)	Intravenous	1×10^7	CCI (rat)	Improvement of thermal and mechanical allodynia	Klass et al., 2007 [53]
BM-MNC (rat)	Injected into 10 points in the unilateral femoral quadriceps, femoral biceps, and soleus muscles	1×10^6	STZ-induced diabetes (rat)	Improvement of mechanical and thermal allodynia	Naruse et al., 2011 [54]

in fact able to induce an antiallodynic and antihyperalgesic effect which persists for long time, as it is still present up to 90 days after injection [44]. Generally, the conventional [8] and the newer pharmacological strategies [55, 56] for neuropathic pain treatment need a chronic treatment to be effective. The analgesic success of the commonly available drugs is often limited by side effects that appear increasing the administration dose or by the development of tolerance [8]. Moreover, in order to successfully approach this type of pain, patients often are treated with a combination of drugs with different mechanisms of action, increasing the risk of drug interaction and often reducing patient's compliance [9]. A more long lasting effect for some type of neuropathic pain such as low back pain or disk herniation can eventually be achieved by surgical approaches or epidural treatment, obviously exposing the patients to all the risks of the surgery. The clamorous effect of stem cells on pain relief in the preclinical tests may be related to their capacity to not only control pain as a symptom, but to act as disease modifier on the mechanisms at the basis of the development and maintenance of pain condition, for example, modulating the neuroimmune component which plays a relevant role in neuropathic pain. Despite these positive and encouraging considerations, there are many issues that need to be addressed and solved for a successful clinical translation. These points are well summarized in the review by Bonfield and Caplan [57] and include the classification of the cells, their efficacy and potency, their mode of administration, their dosage and their source, together with the final goal of the analysis, and the tracking of the stem cell. Among these, as emerged in this review, the route of administration of stem cells represents an important variable which may also influence the choice of the final number of cells to be injected. Strategies for local stem cell delivery can be applied to the treatment of well localized lesions but are, however, described to increase risks and side effects such as bleeding and tissue injury [58]; certainly, from a clinical point of view, a systemic delivery is attractive, given the broad biodistribution and easy access. On the other hand, we have to point out that this route is, in some cases, associated with a passive cell entrapment within tissues that do not represent the main target of treatment, which may potentially lead to unwanted effects and may be eventually associated to a reduced effect of the cells. The homing of stem cells after a systemic injection represents in fact a much debated topic. In our first paper we described the capacity of stem cells to specifically reach the damaged nerve [10]. Although we observed a low transplant efficiency, we did not find the cells into other critical tissues such as lungs. Also Maione's group [44] reported the ability of MSC to home central nervous system areas critically involved in NP signaling describing only a scarce presence of stem cell in the lungs. In general, however, other papers report a marked lung first passage effect of the cells which limits the number of cells which can reach the area of injury [59–61]. Overall the literature agrees with the general idea that stem cells, even in a limited number, can interact with the host cells and orchestrate a long lasting modulation resulting, most of the times, in a final beneficial therapeutic effect [10, 44, 58]. Another strictly related question is the toxicity and the possible malignant transformation and cytogenetic aberrations of stem cells. The literature quite agrees on the safety of stem cells [62, 63] but by a careful analysis of the preclinical papers reported here, it emerges that this aspect has not been specifically or adequately considered. In our work [46] we injected different doses of hASC reaching the highest dose of 6×10^6 cells/mice and we did not register any macroscopic adverse effect: no animal died or changed its habits/behaviour and no side effects have been observed. The safety of a similar dose of hASC intravenously infused in animals and humans was also described by Ra and colleagues [64]; the authors did not register any side effect or tumor mass formation in the three months after cell infusion. Also the paper by Waterman et al. [45] described no premature mortality or morbidity due to MSC treatment and the necropsy of the cell treated animals revealed no macroscopic pathology of any of the major organs. In contrast, Djouad and colleagues [65] described an increase of tumor formation in animals likely due to the immunosuppressive effects of MSC, rather than to a direct transformation of stem cells in tumor cells. Even though, as discussed, there are still many open points that need better understanding, a clear trend to clinical use of stem cells also in treating pain is apparent, as demonstrated by a very recent and scientifically sound paper [66] that reported a preliminary human study in which the

autologous administration of adipose derived stem cells in the facial tissue was able to attenuate orofacial neuropathic pain symptoms. The cells were injected perineurally directly into the center of origin of pain and in the adjacent pain field of the affected branches of the trigeminal nerve. The effect of the treatment was evident 6 months after cell injection and cells were described to be safe, well tolerated by the patients, and accompanied by a significant reduction of analgesic drug doses. What is clear is that the research on stem cells is evolving; newly discovered populations of stem cells begin to be characterized and used in the regenerative medicine. The bioactive molecules that can be released by these same stem cells are starting to be identified and are likely effectors/candidates for the therapeutic effect. As an example the beneficial role of the medium conditioned by MSC for improving motor recovery was recently described [67]. Finally several reports indicate that the regenerative [68] and immunomodulatory [69] effects of MSC can be partially reproduced by the microvesicles (MVs) that are shed by activated MSC and that can be isolated from their culture medium [69]. On the basis of these considerations it is to be expected that the panorama of neuropathic pain treatment will change again shortly.

Conflict of Interests

The authors declare that there is no conflict of interests regarding the publication of this paper.

References

[1] R.-D. Treede, T. S. Jensen, J. N. Campbell et al., "Neuropathic pain: redefinition and a grading system for clinical and research purposes," *Neurology*, vol. 70, no. 18, pp. 1630–1635, 2008.

[2] R. Baron, "Mechanisms of disease: Neuropathic pain—a clinical perspective," *Nature Clinical Practice Neurology*, vol. 2, no. 2, pp. 95–106, 2006.

[3] R. Baron, A. Binder, and G. Wasner, "Neuropathic pain: diagnosis, pathophysiological mechanisms, and treatment," *The Lancet Neurology*, vol. 9, no. 8, pp. 807–819, 2010.

[4] C. Sommer and M. Kress, "Recent findings on how proinflammatory cytokines cause pain: peripheral mechanisms in inflammatory and neuropathic hyperalgesia," *Neuroscience Letters*, vol. 361, no. 1–3, pp. 184–187, 2004.

[5] P. J. Austin and G. Moalem-Taylor, "The neuro-immune balance in neuropathic pain: involvement of inflammatory immune cells, immune-like glial cells and cytokines," *Journal of Neuroimmunology*, vol. 229, no. 1-2, pp. 26–50, 2010.

[6] M. Calvo, J. M. Dawes, and D. L. Bennett, "The role of the immune system in the generation of neuropathic pain," *The Lancet Neurology*, vol. 11, no. 7, pp. 629–642, 2012.

[7] P. Sacerdote, S. Franchi, S. Moretti et al., "Cytokine modulation is necessary for efficacious treatment of experimental neuropathic pain," *Journal of Neuroimmune Pharmacology*, vol. 8, no. 1, pp. 202–211, 2013.

[8] A. B. O'Connor and R. H. Dworkin, "Treatment of neuropathic pain: an overview of recent guidelines," *The American Journal of Medicine*, vol. 122, no. 10, pp. S22–S32, 2009.

[9] I. Gilron, T. S. Jensen, and A. H. Dickenson, "Combination pharmacotherapy for management of chronic pain: from bench to bedside," *Lancet Neurology*, vol. 12, pp. 1084–1095, 2013.

[10] S. Franchi, A. E. Valsecchi, E. Borsani et al., "Intravenous neural stem cells abolish nociceptive hypersensitivity and trigger nerve regeneration in experimental neuropathy," *Pain*, vol. 153, no. 4, pp. 850–861, 2012.

[11] S. Wislet-Gendebien, F. Wautier, P. Leprince, and B. Rogister, "Astrocytic and neuronal fate of mesenchymal stem cells expressing nestin," *Brain Research Bulletin*, vol. 68, no. 1-2, pp. 95–102, 2005.

[12] C. Bossio, R. Mastrangelo, R. Morini et al., "A simple method to generate adipose stem cell-derived neurons for screening purposes," *Journal of Molecular Neuroscience*, vol. 51, no. 2, pp. 274–281, 2013.

[13] P. J. Kingham, D. F. Kalbermatten, D. Mahay, S. J. Armstrong, M. Wiberg, and G. Terenghi, "Adipose-derived stem cells differentiate into a Schwann cell phenotype and promote neurite outgrowth in vitro," *Experimental Neurology*, vol. 207, no. 2, pp. 267–274, 2007.

[14] B. A. Reynolds and S. Weiss, "Generation of neurons and astrocytes from isolated cells of the adult mammalian central nervous system," *Science*, vol. 255, no. 5052, pp. 1707–1710, 1992.

[15] A. Gritti, E. A. Parati, L. Cova et al., "Multipotential stem cells from the adult mouse brain proliferate and self-renew in response to basic fibroblast growth factor," *Journal of Neuroscience*, vol. 16, no. 3, pp. 1091–1100, 1996.

[16] A. L. Vescovi, A. Gritti, R. Galli, and E. A. Parati, "Isolation and intracerebral grafting of nontransformed multipotential embryonic human CNS stem cells," *Journal of Neurotrauma*, vol. 16, no. 8, pp. 689–693, 1999.

[17] A. L. Vescovi, E. A. Parati, A. Gritti et al., "Isolation and cloning of multipotential stem cells from the embryonic human CNS and establishment of transplantable human neural stem cell lines by epigenetic stimulation," *Experimental Neurology*, vol. 156, no. 1, pp. 71–83, 1999.

[18] M. Gelati, D. Profico, M. Projetti-Pensi, G. Muzi, G. Sgaravizzi, and A. L. Vescovi, "Culturing and expansion of "clinical grade" precursors cells from the fetal human central nervous system," *Methods in Molecular Biology*, vol. 1059, pp. 65–77, 2013.

[19] D. Ferrari, E. Binda, L. De Filippis, and A. L. Vescovi, "Isolation of neural stem cells from neural tissues using the neurosphere technique," *Current Protocols in Stem Cell Biology*, no. 15, article no. 2D.6, 2010.

[20] E. Butti, M. Cusimano, M. Bacigaluppi, and G. Martino, "Neurogenic and non-neurogenic functions of endogenous neural stem cells," *Frontiers in Neuroscience*, vol. 8, article 92, 2014.

[21] Q. Xu, M. Zhang, J. Liu, and W. Li, "Intrathecal transplantation of neural stem cells appears to alleviate neuropathic pain in rats through release of GDNF," *Annals of Clinical and Laboratory Science*, vol. 43, no. 2, pp. 154–162, 2013.

[22] Y. Luo, Y. Zou, L. Yang et al., "Transplantation of NSCs with OECs alleviates neuropathic pain associated with NGF down-regulation in rats following spinal cord injury," *Neuroscience Letters*, vol. 549, pp. 103–108, 2013.

[23] S. Karimi-Abdolrezaee, E. Eftekharpour, J. Wang, D. Schut, and M. G. Fehlings, "Synergistic effects of transplanted adult neural stem/progenitor cells, chondroitinase, and growth factors promote functional repair and plasticity of the chronically injured spinal cord," *Journal of Neuroscience*, vol. 30, no. 5, pp. 1657–1676, 2010.

[24] C. P. Hofstetter, N. A. V. Holmström, J. A. Lilja et al., "Allodynia limits the usefulness of intraspinal neural stem cell grafts; directed differentiation improves outcome," *Nature Neuroscience*, vol. 8, no. 3, pp. 346–353, 2005.

[25] M. Y. Macias, M. B. Syring, M. A. Pizzi, M. J. Crowe, A. R. Alexanian, and S. N. Kurpad, "Pain with no gain: allodynia following neural stem cell transplantation in spinal cord injury," *Experimental Neurology*, vol. 201, no. 2, pp. 335–348, 2006.

[26] B. J. Cummings, N. Uchida, S. J. Tamaki et al., "Human neural stem cells differentiate and promote locomotor recovery in spinal cord-injured mice," *Proceedings of the National Academy of Sciences of the United States of America*, vol. 102, no. 39, pp. 14069–14074, 2005.

[27] S. Pluchino, A. Gritti, E. Blezer et al., "Human neural stem cells ameliorate autoimmune encephalomyelitis in non-human primates," *Annals of Neurology*, vol. 66, no. 3, pp. 343–354, 2009.

[28] D. Ferrari, C. Zalfa, L. R. Nodari et al., "Differential pathotropism of non-immortalized and immortalized human neural stem cell lines in a focal demyelination model," *Cellular and Molecular Life Sciences*, vol. 69, no. 7, pp. 1193–1210, 2012.

[29] L. Rota Nodari, D. Ferrari, F. Giani et al., "Long-term survival of human neural stem cells in the ischemic rat brain upon transient immunosuppression," *PLoS ONE*, vol. 5, no. 11, Article ID e14035, 2010.

[30] M. F. Pittenger, A. M. Mackay, S. C. Beck et al., "Multilineage potential of adult human mesenchymal stem cells," *Science*, vol. 284, no. 5411, pp. 143–147, 1999.

[31] G. Kögler, S. Sensken, J. A. Airey et al., "A new human somatic stem cell from placental cord blood with intrinsic pluripotent differentiation potential," *Journal of Experimental Medicine*, vol. 200, no. 2, pp. 123–135, 2004.

[32] M. Aktas, A. Buchheiser, A. Houben et al., "Good manufacturing practice-grade production of unrestricted somatic stem cell from fresh cord blood," *Cytotherapy*, vol. 12, no. 3, pp. 338–348, 2010.

[33] I. Nazarov, J. W. Lee, E. Soupene et al., "Multipotent stromal stem cells from human placenta demonstrate high therapeutic potential," *Stem Cells Translational Medicine*, vol. 1, no. 5, pp. 359–372, 2012.

[34] P. A. Zuk, M. Zhu, P. Ashjian et al., "Human adipose tissue is a source of multipotent stem cells," *Molecular Biology of the Cell*, vol. 13, no. 12, pp. 4279–4295, 2002.

[35] S. Gronthos, M. Mankani, J. Brahim, P. G. Robey, and S. Shi, "Postnatal human dental pulp stem cells (DPSCs) in vitro and in vivo," *Proceedings of the National Academy of Sciences of the United States of America*, vol. 97, no. 25, pp. 13625–13630, 2000.

[36] T. Lu, P. Hu, X. Su, C. Li, Y. Ma, and W. Guan, "Isolation and characterization of mesenchymal stem cells derived from fetal bovine liver," *Cell Tissue Bank*, 2013.

[37] X. Gong, Z. Sun, D. Cui et al., "Isolation and characterization of lung resident mesenchymal stem cells capable of differentiating into alveolar epithelial type II cells," *Cell Biology International*, vol. 38, no. 4, pp. 405–411, 2014.

[38] A. C. W. Zannettino, S. Paton, A. Arthur et al., "Multipotential human adipose-derived stromal stem cells exhibit a perivascular phenotype in vitro and in vivo," *Journal of Cellular Physiology*, vol. 214, no. 2, pp. 413–421, 2008.

[39] P. L. Musolino, M. F. Coronel, T. Hökfelt, and M. J. Villar, "Bone marrow stromal cells induce changes in pain behavior after sciatic nerve constriction," *Neuroscience Letters*, vol. 418, no. 1, pp. 97–101, 2007.

[40] M. F. Coronel, P. L. Musolino, P. R. Brumovsky, T. Hökfelt, and M. J. Villar, "Bone marrow stromal cells attenuate injury-induced changes in galanin, NPY and NPY Y1-receptor expression after a sciatic nerve constriction," *Neuropeptides*, vol. 43, no. 2, pp. 125–132, 2009.

[41] T. Shibata, K. Naruse, H. Kamiya et al., "Transplantation of bone marrow-derived mesenchymal stem cells improves diabetic polyneuropathy in rats," *Diabetes*, vol. 57, no. 11, pp. 3099–3107, 2008.

[42] B. J. Kim and H. K. Jin, "Bone marrow-derived mesenchymal stem cells improve the functioning of neurotrophic factors in a mouse model of diabetic neuropathy," *Laboratory Animal Research*, vol. 27, no. 2, pp. 171–176, 2011.

[43] D. Siniscalco, C. Giordano, U. Galderisi et al., "Intra-brain microinjection of human mesenchymal stem cells decreases allodynia in neuropathic mice," *Cellular and Molecular Life Sciences*, vol. 67, no. 4, pp. 655–669, 2010.

[44] D. Siniscalco, C. Giordano, U. Galderisi et al., "Long-lasting effects of human mesenchymal stem cell systemic administration on pain-like behaviors, cellular, and biomolecular modifications in neuropathic mice," *Frontiers in Integrative Neuroscience*, vol. 5, article 79, 2011.

[45] R. S. Waterman, J. Morgenweck, B. D. Nossaman, A. E. Scandurro, S. A. Scandurro, and A. M. Betancourt, "Anti-inflammatory mesenchymal stem cells (MSC2) attenuate symptoms of painful diabetic peripheral neuropathy," *Stem Cells Translational Medicine*, vol. 1, no. 7, pp. 557–565, 2012.

[46] P. Sacerdote, S. Niada, S. Franchi et al., "Systemic administration of human adipose-derived stem cells reverts nociceptive hypersensitivity in an experimental model of neuropathy," *Stem Cells and Development*, vol. 22, no. 8, pp. 1252–1263, 2013.

[47] L. De Girolamo, M. F. Sartori, E. Arrigoni et al., "Human adipose-derived stem cells as future tools in tissue regeneration: osteogenic differentiation and cell-scaffold interaction," *International Journal of Artificial Organs*, vol. 31, no. 6, pp. 467–479, 2008.

[48] L. D. Girolamo, S. Lopa, E. Arrigoni, M. F. Sartori, F. W. Baruffaldi Preis, and A. T. Brini, "Human adipose-derived stem cells isolated from young and elderly women: their differentiation potential and scaffold interaction during in vitro osteoblastic differentiation," *Cytotherapy*, vol. 11, no. 6, pp. 793–803, 2009.

[49] J. In Choi, H. Tae Cho, M. Ki Jee, and S. Kyung Kang, "Core-shell nanoparticle controlled hATSCs neurogenesis for neuropathic pain therapy," *Biomaterials*, vol. 34, no. 21, pp. 4956–4970, 2013.

[50] T. Nagamura-Inoue and H. He, "Umbilical cord-derived mesenchymal stem cells: their advantages and potential clinical utility," *World Journal of Stem Cells*, vol. 6, pp. 195–202, 2014.

[51] D. H. Roh, M. S. Seo, H. S. Choi et al., "Transplantation of human umbilical cord blood or amniotic epithelial stem cells alleviates mechanical allodynia after spinal cord injury in rats," *Cell Transplantation*, vol. 22, pp. 1577–1590, 2013.

[52] C. C. Yang, Y. H. Shih, M. H. Ko, S. Y. Hsu, H. Cheng, and Y. S. Fu, "Transplantation of human umbilical mesenchymal stem cells from Wharton's jelly after complete transection of the rat spinal cord," *PLoS ONE*, vol. 3, no. 10, Article ID e3336, 2008.

[53] M. Klass, V. Gavrikov, D. Drury et al., "Intravenous mononuclear marrow cells reverse neuropathic pain from experimental mononeuropathy," *Anesthesia and Analgesia*, vol. 104, no. 4, pp. 944–948, 2007.

[54] K. Naruse, J. Sato, M. Funakubo et al., "Transplantation of bone marrow-derived mononuclear cells improves mechanical

hyperalgesia, cold allodynia and nerve function in diabetic neuropathy," *PLoS ONE*, vol. 6, no. 11, Article ID e27458, 2011.

[55] C. Martucci, A. E. Trovato, B. Costa et al., "The purinergic antagonist PPADS reduces pain related behaviours and interleukin-1β, interleukin-6, iNOS and nNOS overproduction in central and peripheral nervous system after peripheral neuropathy in mice," *Pain*, vol. 137, no. 1, pp. 81–95, 2008.

[56] A. E. Valsecchi, S. Franchi, A. E. Panerai, P. Sacerdote, A. E. Trovato, and M. Colleoni, "Genistein, a natural phytoestrogen from soy, relieves neuropathic pain following chronic constriction sciatic nerve injury in mice: Anti-inflammatory and antioxidant activity," *Journal of Neurochemistry*, vol. 107, no. 1, pp. 230–240, 2008.

[57] T. L. Bonfield and A. I. Caplan, "Adult mesenchymal stem cells: an innovative therapeutic for lung diseases," *Discovery Medicine*, vol. 9, no. 47, pp. 337–345, 2010.

[58] U. M. Fischer, M. T. Harting, F. Jimenez et al., "Pulmonary passage is a major obstacle for intravenous stem cell delivery: the pulmonary first-pass effect," *Stem Cells and Development*, vol. 18, no. 5, pp. 683–691, 2009.

[59] J. Gao, J. E. Dennis, R. F. Muzic, M. Lundberg, and A. I. Caplan, "The dynamic in vivo distribution of bone marrow-derived mesenchymal stem cells after infusion," *Cells Tissues Organs*, vol. 169, no. 1, pp. 12–20, 2001.

[60] S. Schrepfer, T. Deuse, H. Reichenspurner, M. P. Fischbein, R. C. Robbins, and M. P. Pelletier, "Stem cell transplantation: the lung barrier," *Transplantation Proceedings*, vol. 39, no. 2, pp. 573–576, 2007.

[61] H. E. Daldrup-Link, M. Rudelius, S. Metz et al., "Cell tracking with gadophrin-2: a bifunctional contrast agent for MR imaging, optical imaging, and flourescence microscopy," *European Journal of Nuclear Medicine and Molecular Imaging*, vol. 31, no. 9, pp. 1312–1321, 2004.

[62] L. Mazzini, A. Vercelli, I. Ferrero, M. Boido, R. Cantello, and F. Fagioli, "Transplantation of mesenchymal stem cells in ALS," *Progress in Brain Research*, vol. 201, pp. 333–359, 2012.

[63] J. M. Hare, J. H. Traverse, T. D. Henry et al., "A randomized, double-blind, placebo-controlled, dose-escalation study of intravenous adult human mesenchymal stem cells (prochymal) after acute myocardial infarction," *Journal of the American College of Cardiology*, vol. 54, no. 24, pp. 2277–2286, 2009.

[64] J. C. Ra, I. S. Shin, S. H. Kim et al., "Safety of intravenous infusion of human adipose tissue-derived mesenchymal stem cells in animals and humans," *Stem Cells and Development*, vol. 20, no. 8, pp. 1297–1308, 2011.

[65] F. Djouad, P. Plence, C. Bony et al., "Immunosuppressive effect of mesenchymal stem cells favors tumor growth in allogeneic animals," *Blood*, vol. 102, no. 10, pp. 3837–3844, 2003.

[66] E. R. Vickers, E. Karsten, J. Flood, and R. Lilischkis, "A preliminary report on stem cell therapy for neuropathic pain in humans," *Journal of Pain Research*, vol. 7, pp. 255–263, 2014.

[67] D. Cantinieaux, R. Quertainmont, S. Blacher et al., "C onditioned medium from bone marrow-derived mesenchymal stem cells improves recovery after spinal cord injury in rats: an original strategy to avoid cell transplantation," *PLoS ONE*, vol. 8, no. 8, Article ID e69515, 2013.

[68] L. Biancone, S. Bruno, M. C. Deregibus, C. Tetta, and G. Camussi, "Therapeutic potential of mesenchymal stem cell-derived microvesicles," *Nephrology Dialysis Transplantation*, vol. 27, no. 8, pp. 3037–3042, 2012.

[69] A. Fierabracci, A. Del Fattore, R. Luciano, M. Muraca, A. Teti, and M. Muraca, "Recent advances in mesenchymal stem cell immunomodulation. The role of microvesicles," *Cell Transplantation*, 2013.

Hindawi Publishing Corporation
BioMed Research International
Volume 2014, Article ID 937568, 9 pages
http://dx.doi.org/10.1155/2014/937568

Research Article

Ceftriaxone, a Beta-Lactam Antibiotic, Modulates Apoptosis Pathways and Oxidative Stress in a Rat Model of Neuropathic Pain

Bahareh Amin,[1] Valiollah Hajhashemi,[2] Khalil Abnous,[3] and Hossein Hosseinzadeh[4]

[1] *Department of Pharmacology and Physiology, Faculty of Medicine, Sabzevar University of Medical Sciences, Sabzevar, Iran*
[2] *Department of Pharmacology, Pharmaceutical Sciences Research Center, School of Pharmacy, Isfahan University of Medical Sciences, Isfahan, Iran*
[3] *Department of Biotechnology, Pharmaceutical Research Center, School of Pharmacy, Mashhad University of Medical Sciences, Mashhad, Iran*
[4] *Pharmaceutical Research Center, Pharmacodynamy and Toxicology Department, School of Pharmacy, Mashhad University of Medical Sciences, P.O. Box 1365-91775, Vakilabad Boulevard, Mashhad, Iran*

Correspondence should be addressed to Hossein Hosseinzadeh; hosseinzadehh@mums.ac.ir

Received 23 February 2014; Revised 13 May 2014; Accepted 13 May 2014; Published 16 June 2014

Academic Editor: Livio Luongo

Purpose. In our previous study, ceftriaxone, a beta-lactam antibiotic, elicited antinociceptive effects in the chronic constriction injury (CCI) of neuropathic pain. In this study, we assessed apoptosis and oxidative stress in the spinal cord of neuropathic rats treated with ceftriaxone. *Methods*. 45 male Wistar rats were divided as naïve, sham, normal saline-treated CCI rats, and CCI animals treated with the effective dose of ceftriaxone. Involvement of Bax, Bcl2, and caspases 3 and 9, important contributors of programmed cell death (apoptosis), was determined using western blotting at days 3 and 7. The markers of oxidative stress including malondialdehyde (MDA) and reduced glutathione (GSH) were measured on days 3 and 7. *Results*. Increased Bax/Bcl2 ratio and cleaved active forms of caspases 3 and 9 were observed in the spinal cord of CCI rats on day 3. Ceftriaxone attenuated the increased levels of Bax and cleaved forms of caspases 3 and 9, while it increased Bcl2 levels. Bax and active forms of caspases declined by day 7. Consequently, comparison among groups showed no difference at this time. CCI enhanced MDA and decreased GSH on days 3 and 7, while ceftriaxone protected against the CCI-induced oxidative stress. *Conclusion*. Our results suggest that ceftriaxone, an upregulator/activator of GLT1, could concomitantly reduce oxidative stress and apoptosis and producing its new analogs lacking antimicrobial activity may represent a novel approach for neuropathic pain treatment.

1. Introduction

Nerve injury induced chronic pain, often referred as neuropathic pain, is caused by a primary lesion in both central and more frequently peripheral nervous systems and is a challenging condition to treat [1]. Molecular mechanisms involved in this pathological chronic pain syndrome have currently been an area of much interest.

Excitotoxicity via elevated excitatory neurotransmitters (glutamate and aspartate) has been associated in different kinds of pain such as neuropathic pain [2]. In recent years, different studies have pointed out the role of apoptosis in neuropathic pain. In a study by de Novellis et al., apoptotic pathways were activated in rat spinal cord of sciatic nerve chronic constriction injury (CCI), and the early overexpression of proapoptotic genes and morphological changes in dorsal horn were prevented by blockade of glutamate mGlu5 receptors [3]. Afrazi et al. reported that diabetes-induced hyperalgesia in rats was attenuated by neurosteroid, allopregnanolone through inhibiting caspase-3 and decreased ratio of Bax to Bcl2 [4]. Moreover, numerous studies revealed that oxidative stress plays an important role in neuropathic pain [5, 6]. Considering that extra levels of glutamate lead to a

number of deleterious effects, including excessive activation of central glutamate receptors, impairment in buffering of calcium, production of free radicals by lipid peroxidation, secondary excitotoxicity, and cell death following neuropathic pain maintaining low extracellular glutamate, is very important [7, 8]. Glutamate hemostasis is performed via high affinity transporters in which GLT 1 is the predominant subtype and accounts for clearance of the bulk of released glutamate. Downregulation of glutamate transporters is thought to be very important in various experimental neuropathic pain models [9]. Recently, ceftriaxone a third generation beta-lactam antibiotic has been discovered to have neuroprotective effects in various *in vitro* and *in vivo* studies [10, 11]. The precise primary molecular mechanism of ceftriaxone is thought to be mediated by the increased expression and activation of GLT1 in the CNS [11–13]. We and others have previously reported that ceftriaxone could attenuate pain behaviors of rats subjected to the CCI model of neuropathic pain [14, 15]. If apoptosis process and oxidative stress were linked to excitotoxicity, then treatment with ceftriaxone would be predicted to reverse spinal cord protein changes involved in the apoptosis and oxidative stress following CCI.

Therefore, the aim of the present study was to determine time course of changes in the spinal cord levels of apoptosis-related proteins. Bax, a promoting factor, Bcl2, which can prevent apoptosis, caspase-9, the initiator caspase for the activation of downstream caspases, and caspase-3, a factor in downstream of several apoptotic pathways [16], were analyzed with western blotting on days 3 and 7 after CCI. To study whether treatment with ceftriaxone was able to show antioxidant activity, we assessed spinal cord levels of MDA, the last product of lipid peroxidation [17] and glutathione, the major sulfhydryl (-SH) antioxidant, and enzyme cofactor [18], in 3 and 7 days in CCI rats.

2. Materials and Methods

2.1. Animals. Adult male Wistar strain rats weighing 220–270 g at the time of surgery were used in this experiment and randomly gathered from the animal room of the School of Pharmacy, Mashhad University of Medical Sciences, Iran. The animals were housed under standard environmental conditions (12-12 h light/dark cycle at 22°C). Rat chow and tap water were available *ad libitum*. The experimental protocol was approved by Mashhad University of Medical Sciences and performed in accordance with the Internationally Accepted Principles for Laboratory Animal Use and Care [19].

2.2. Drugs and Solutions. Ceftriaxone (Jaber Ebne Hayyan Pharmaceutical Co., Tehran, Iran) was dissolved in normal saline solution (0.9% NaCl) and intraperitoneally injected at the dose of 200 mg/kg. Ceftriaxone administration started when CCI was induced and continued for 7 consecutive days. Ketamine and xylazine (Alfasan Pharmaceutical Co., Woerden, Holland) were intraperitoneally injected at doses of 64 and 1.6 mg/kg, respectively.

2.3. CCI Surgery of Sciatic Nerve. At first, rats were anaesthetized with a cocktail of ketamine and xylazine. Mononeuropathy was induced by performing chronic constriction injury model on the left sciatic nerve of animals in accordance with the method of Bennet and Xie [20]. After the incision of the skin, the sciatic nerve was exposed and four ligatures of 4-0 gauge chromic catgut were tied loosely with an interval of 1 mm, until a slight twitching was observed in the expected hind paw. Finally, muscle and skin were separately sutured with 4-0 silk catgut and animals were placed in a warm condition until recovery. Rats in the sham group had their sciatic nerve exposed but not ligated.

2.4. Study Protocol. Based on our previous study, CCI led to a significant development of mechanical allodynia (4.3 ± 0.6 g versus 53 ± 6.7 g) and cold allodynia (73.3 ± 8.4% versus 8 ± 4.9%) on day 3 in comparison to sham group, as revealed by von Frey hairs and acetone drop, respectively. Pain behaviors progressively increased during the study on days 5 and 7. In that study, mechanical and cold allodynia were significantly attenuated by the dose of 200 mg/kg of ceftriaxone on days 3 and 7 [14]. Accordingly the effective antinociceptive dose of ceftriaxone (200 mg/kg) was chosen in this study.

In the present study, to examine the time course of changes in apoptosis-related proteins and oxidative stress markers (MDA and GSH) in the spinal cord of CCI rats, three animals from each group were harvested on postoperative day 3 or day 7 after the behavioral tests. Hence, 54 rats were randomly assigned into the following groups. (1, 2) The animals were subjected to CCI surgery, treated with normal saline (NS) at a dose of 1 mL/kg, and killed on day 3 or day 7 for evaluation of apoptotic factors ($n = 3$). (3, 4) In sham group, the animals underwent a similar surgery except that sciatic nerves were not ligated and treated with the normal saline and killed on day 3 or day 7 for evaluation of apoptotic factors ($n = 3$). (5, 6) CCI animals were treated with ceftriaxone (200 mg/kg, administered at a dose of 1 mL/kg) for seven days and killed on day 3 or day 7 for evaluation of apoptotic factors ($n = 3$). (7, 8) The CCI animals were treated with NS and killed on day 3 or day 7 for evaluation of MDA ($n = 3$) and GSH ($n = 3$). (9, 10) Sham-operated animals were killed on day 3 or day 7 for evaluation of MDA ($n = 3$) and GSH ($n = 3$). (11, 12) CCI animals were treated with ceftriaxone (200 mg/kg) for seven days and killed on day 3 or day 7 for evaluation of MDA ($n = 3$) and GSH ($n = 3$). (13) Naïve animals were killed for evaluation of apoptotic factors ($n = 3$), MDA ($n = 3$), and GSH ($n = 3$) contents.

For the protein extraction, the lumbar spinal cord was rapidly ejected from the vertebral column using a saline-filled syringe and then separated on dry ice. Lumbar (L4 and L5) segments were excised to measure apoptotic and oxidative stress markers considering that these segments are the major contributor to the sciatic nerve [19].

2.5. Western Blotting. At the time of experiment, samples were homogenized in the lysis buffer containing 50 mM Tris-HCl (pH: 7.4), 2 mM EDTA, 2 mM EGTA, 10 mM

NaF, 1 mM sodium orthovanadate (Na3VO4), 10 mM β-glycerophosphate, 0.2% W/V sodium deoxycholate, 1 mM phenylmethylsulfonyl fluoride (PMSF), and complete protease inhibitor cocktail (Roche, Mannheim, Germany). The homogenate was sonicated on ice with three 10 sec bursts at high intensity with a 10 sec cooling period between each burst. The samples were centrifuged at 10,000 g for 10 min at 4°C. After determining protein content by Bradford assay kit and adjusting the protein content [20], each adjusted sample was mixed 1 : 1 v : v with 2x SDS blue buffer, boiled, aliquoted, and kept in the −80°C freezer.

100 micrograms of each protein extracts was separated on a 12% sodium dodecyl sulfate-polyacrylamide gel (SDS-PAGE) by electrophoresis and transferred onto polyvinylidene fluoride (PVDF) membranes. Then, blots were blocked with 5% skim milk in TBST (20 mM Tris-HCl pH 7.6, 137 mM NaCl, and 0.05% Tween-20) at 4°C overnight. Mouse monoclonal anticaspase-9 (cell signaling number 9508, 1 : 1000), rabbit polyclonal anticaspase-3 (cell signaling number 9665, 1 : 1000), rabbit polyclonal anti-Bax (cell signaling number 2772, 1 : 1000), rabbit polyclonal anti-Bcl2 (cell signaling number 2870, 1 : 1000), and rabbit polyclonal anti-β-actin antibodies (cell signaling number 4967, 1 : 1000) were used as a primary antibody with incubation time of about 1-2 hours at room temperature, washing three times with TBST and 1-hour incubation by rabbit horseradish peroxidase-conjugate anti-rabbit IgG (cell signaling number 7074, 1 : 2000) or anti-mouse IgG (cell signaling number 7076, 1 : 2000). Enhanced chemiluminescence (Pierce) was used to visualize the peroxidase-coated bands and Alliance 4.7 Gel Doc (UK). Densitometric analysis for protein bands was performed using UVtec software (UK). The protein levels were normalized against β-actin intensity.

2.6. Measurement of MDA Levels in the Spinal Cord of Animals. Estimation of lipid peroxidation was performed by measuring the thiobarbituric acid reactive substances as described previously [21]. At the time of experiment, each sample was weighed and homogenized in 1.15% potassium chloride solution. Then, 3 mL phosphoric acid (1%) and 1 mL TBA (0.6%) were added to 0.5 mL of homogenate in a centrifuge tube and the mixture was heated for 45 min in a boiling water bath. After cooling, 4 mL n-butanol was added to the mixture and vortex mixed for 1 min followed by centrifugation at 3000 rpm for 15 minutes. The organic layer was transferred to a fresh tube and the absorbance of pink colored product was read at 532 nm. A set of MDA standards was freshly prepared and the standard curve was constructed. The results were expressed as the nmol of malondialdehyde formed per mg of protein.

2.7. Measurement of GSH Levels in the Spinal Cord of Animals. Total SH groups belonging to GSH were measured using DTNB (2,2′-dinitro-5,5′-dithiodibenzoic acid) as the reagent. This reagent reacts with the SH groups to produce a yellow colored complex with a peak absorbance at 412 nm. Briefly, a 10% tissue homogenate in buffer phosphate 7.4 was mixed with an equal volume of 10% trichloroacetic acid (TCA) and vortexed. The contents were then centrifuged at 5000 rpm for 10 min. Subsequently 500 μL of supernatant was mixed with a reaction mixture containing 2.5 mL 0.1 M phosphate buffer (pH 8.4) and 0.5 mL DTNB. Within 10 min, the absorbance was measured at 412 nm using a spectrophotometer. A set of GSH standards was freshly prepared using commercially available standard GSH (Sigma Chemicals, USA) and the standard curve was constructed. Levels of GSH were expressed as nmol/mg protein [22].

2.8. Statistics. Data were expressed as means ± SEM and statistically analyzed by one-way ANOVA followed by Tukey's *post hoc* tests, using SPSS version 13. A P value of < 0.05 was considered to be significant.

3. Results

3.1. Bax and Bcl2 Protein Levels. To analyze the amount of the apoptotic proteins, a relative protein ratio to naïve animals was used. The results of western blotting analysis indicated that lumbar spinal cord levels of the proapoptotic protein, Bax increased within 3 days following sciatic nerve CCI (control group), as compared to naïve and sham groups, while a slight but not significant decrease in the level of antiapoptotic protein, Bcl2 was observed (Figure 1(a)). Therefore, a significantly higher level of Bax/Bcl2 ratio was obtained in the spinal cord of CCI animals in comparison to naïve and sham groups ($P < 0.05$) on day 3 after surgery (Figure 1(b)). Whereas, there was no significant difference in the levels of proteins between sham and naïve animals treated with ceftriaxone. In NS-CCI animals, protein levels of Bax decreased and Bcl2 increased on day 7 after CCI. Accordingly, there was no significant difference between Bax/Bcl2 ratio of control group and that of sham and naïve groups (Figures 1(c) and 1(d)). CCI animals treated with 200 mg/kg of ceftriaxone (once daily, for 7 days) showed a significant increase in the levels of antiapoptotic protein, Bcl2, and decreased contents of Bax protein on day 3 after CCI, resulting in a significant reduction in the Bax/Bcl2 ratio as compared to control group ($P < 0.05$). No significant difference was observed in the Bax/Bcl2 ratio between ceftriaxone treated animals and that of control group on day 7 (Figure 1).

3.2. Caspase-9 Protein Levels. Our data showed that there was no significant difference in the levels of procaspase-9 protein between sham and naïve animals treated with ceftriaxone. The expression of procaspase-9 increased on day 3 after CCI when compared to that of the sham and naïve groups ($P < 0.01$). A significant increase in the activated cleaved forms of 37 kDa and specially 35 kDa species was observed 3 days after the CCI as compared to that detected in the sham and naïve groups ($P < 0.01$) (Figures 2(a) and 2(b)). In CCI rats who received 200 mg/kg ceftriaxone (once daily, for 7 days) contents of procaspase-9 ($P < 0.05$) as well as activated forms ($P < 0.01$) decreased after 3 days of sciatic nerve injury (Figures 2(a) and 2(b)).

Levels of procaspase-9 decreased from day 3 to day 7 after surgery in normal saline CCI animals and activate cleaved

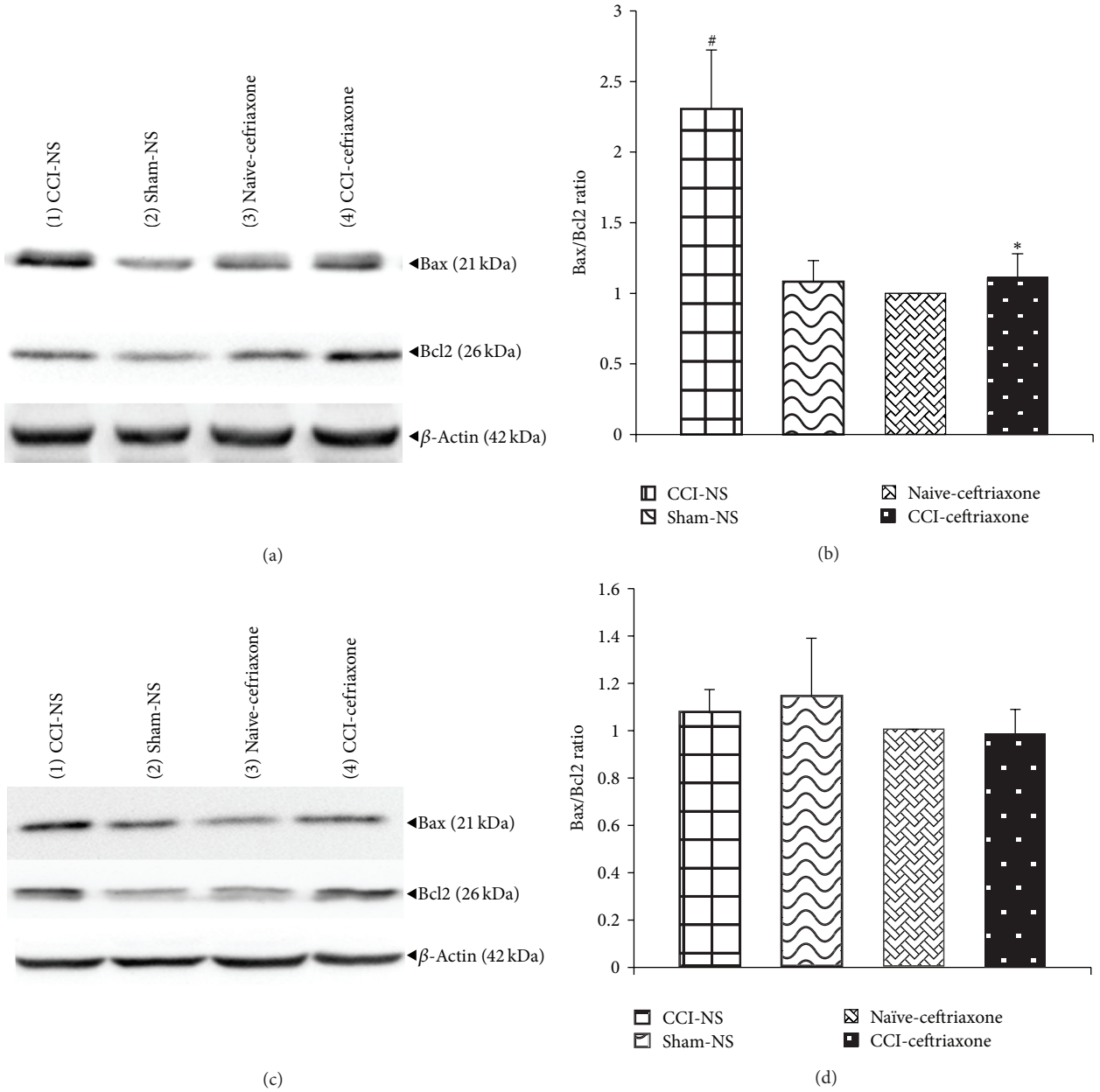

Figure 1: Effect of ceftriaxone on the spinal cord protein levels of Bax (21 kDa) and Bcl2 (26 kDa) and relative density of Bax/Bcl2, following western immunoblotting on days 3 (a and b, resp.) and 7 (c and d, resp.) after CCI. Administration of ceftriaxone (Cef 200 mg/kg, i.p.) started when CCI was induced and continued for 7 successive days. The semiquantitative analysis of protein levels was carried out by the "Gel Doc 2000 UV System" (Alliance 4.7). Each lane was loaded with 100 μg of proteins. β-actin is the loading protein control. Data are mean ± SEM (n = 3/group). One-way ANOVA followed by Tukey's *post hoc* test was used for multiple comparisons. $^{\#}P < 0.05$ difference between CCI-NS and sham/naive groups. $^{*}P < 0.05$ CCI-Cef versus NS-CCI group (control).

forms of caspase-9 were no longer detected by day 7. As a result, no significant difference was observed among groups at this time (Figures 2(c) and 2(d)).

3.3. Caspase-3 Protein Levels. On day 3 after surgery, procaspase-3 protein levels increased in the spinal cord of normal saline-treated CCI animals (control group), although not to a significant extent. Cleaved form of the protein (17 kD) was significantly increased in control group as compared to naïve and sham groups ($P < 0.05$) (Figures 3(a) and 3(b)). Despite the fact that there is no significant difference between the relative density of procaspase-3 in CCI rats and ceftriaxone treated animals, activated forms of caspase-3 were significantly attenuated by ceftriaxone (200 mg/kg), as compared to CCI NS-treated rats ($P < 0.05$) (Figures 3(a) and 3(b)). Activated cleaved forms of caspase-3 were no longer detected by day 7. Accordingly, no significant difference was observed among groups at this time (Figures 3(c) and 3(d)).

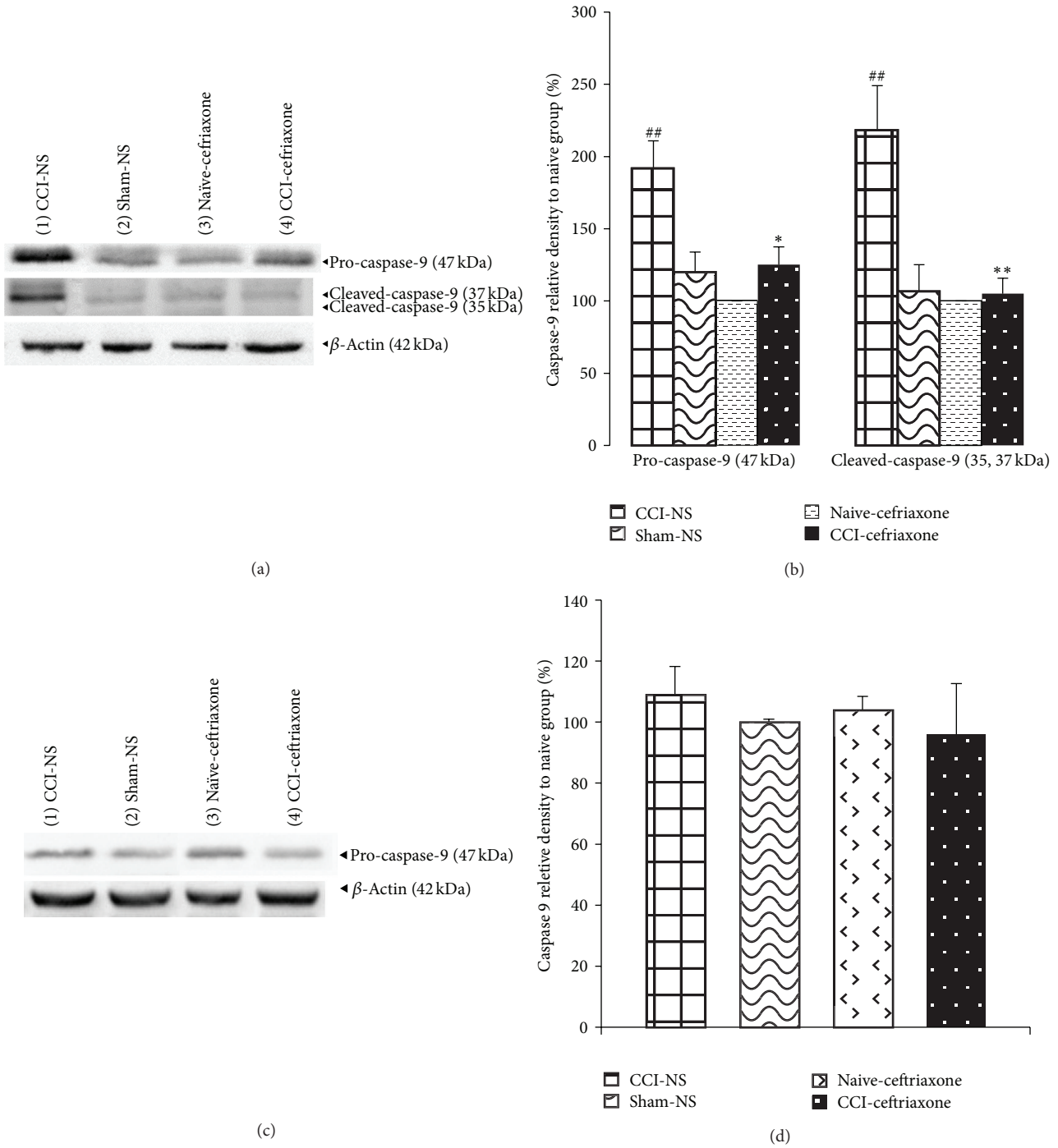

Figure 2: Effect of ceftriaxone on the spinal cord protein levels of procaspase-9 (47 kDa) and cleavage products (37 and 35 kDa) and relative density following western immunoblotting on days 3 (a and b, resp.) and 7 (c and d, resp.) after CCI. Administration of ceftriaxone (Cef 200 mg/kg, i.p.) started when CCI was induced and continued for 7 successive days. The semiquantitative analysis of protein levels was carried out by the "Gel Doc 2000 UV System" (Alliance 4.7). Each lane was loaded with 100 μg of proteins. β-Actin is the loading protein control. Data were mean ± SEM (n = 3/group). One-way ANOVA followed by Tukey's *post hoc* test was used for multiple comparisons. $^{\#\#}P < 0.01$ difference between CCI-NS and sham/naive animals. $^{*}P < 0.05$, $^{**}P < 0.05$ CCI-Cef versus NS-CCI group (control).

3.4. Malondialdehyde Levels. As indicated in Table 1, at day 3 after operation, there was a significant increase in the spinal cord MDA levels following CCI in animals that received normal saline as compared with naïve ($P < 0.05$) and sham-operated groups ($P < 0.01$). Levels of MDA remained high on day 7 after CCI. Seven days of treatment with ceftriaxone resulted in a significant reduction in the free radical-mediated lipid peroxidation on days 3 and 7 as indicated by the decreased levels of MDA compared to CCI saline-treated group ($P < 0.05$).

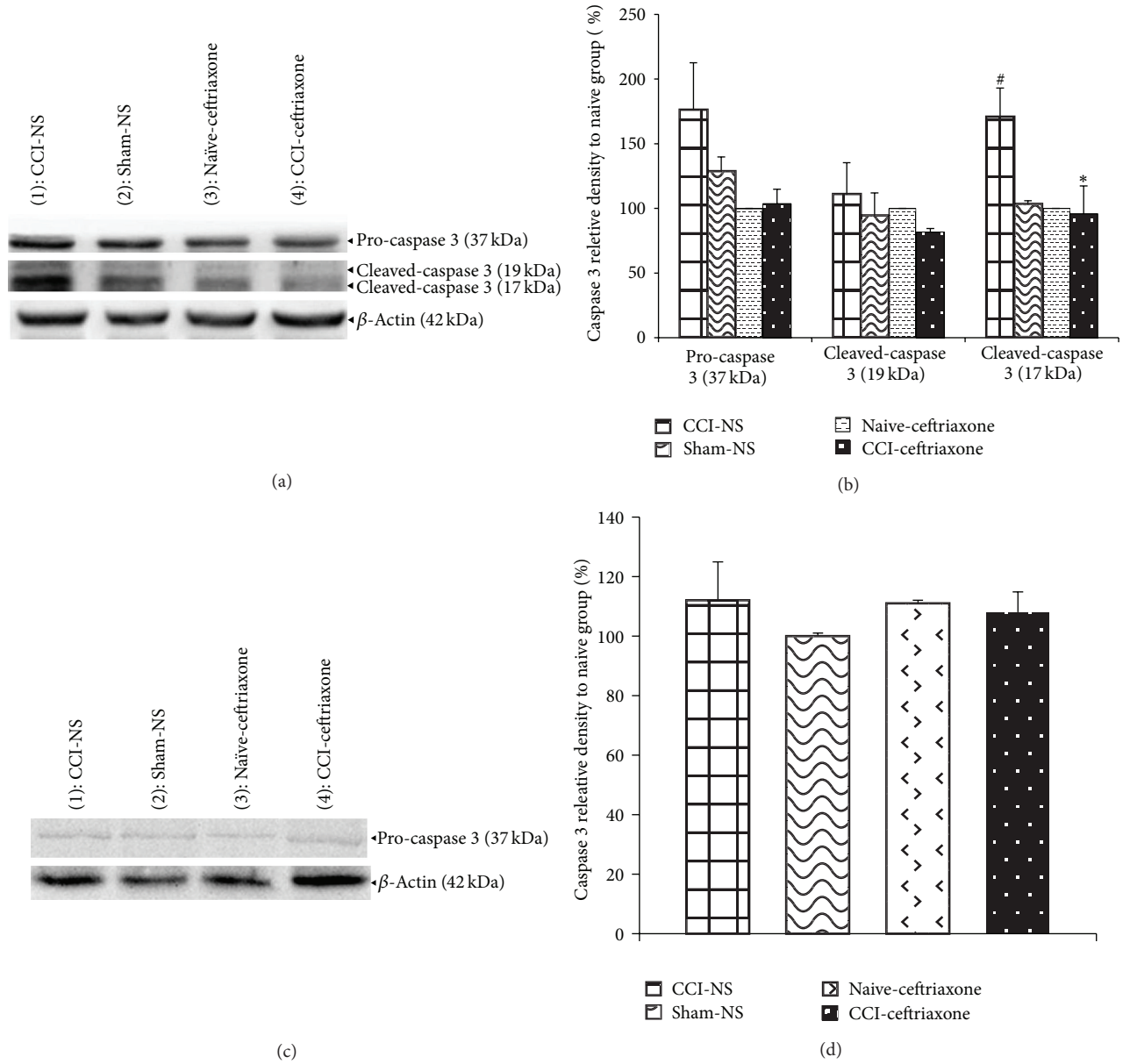

Figure 3: Effect of ceftriaxone on the spinal cord protein levels of procaspase-3 (37 kDa) and cleavage product (17 kDa) and relative density following western immunoblotting on days 3 (a and b, resp.) and 7 (c and d, resp.) after CCI. Administration of ceftriaxone (Cef 200 mg/kg, i.p.) started when CCI was induced and continued for 7 successive days. The semiquantitative analysis of protein levels was carried out by the "Gel Doc 2000 UV System" (Alliance 4.7). Each lane was loaded with 100 μg of proteins. β-Actin is the loading protein control. Data were mean ± SEM (n = 3/group). One-way ANOVA followed by Tukey's *post hoc* test was used for multiple comparisons. $^{\#}P < 0.05$ difference between CCI-NS and sham/naive animals. $^{*}P < 0.05$ CCI-Cef versus NS-CCI group (control).

3.5. Glutathione Levels. After 7 days of CCI, GSH levels were significantly decreased in the spinal cord of animals receiving normal saline, in relation to that of the sham and naïve groups ($P < 0.01$). Ceftriaxone significantly increased antioxidant power by a significant increase in the levels of GSH on day 7 in the spinal cord of CCI animals ($P < 0.05$) (Table 1).

4. Discussion

Antinociceptive effects of ceftriaxone have been shown in our previous study [14]. GLT1 upregulation and activation are assumed to be the main mechanisms of neuroprotective effects of ceftriaxone in various experimental models including neuropathic pain [7, 11, 12, 15]. In the present study, the time course alterations in apoptosis markers (Bax : Bcl2), as well as caspases 3 and 9, were evaluated on days 3 and 7 after CCI. We also measured oxidative markers, MDA and GSH, in the lumbar spinal cord of animals on the 3rd and 7th days after CCI. On day 3, after operation, CCI induced elevated level of Bax protein, while a slight decrease was observed in the Bcl2 protein level. Therefore, a significant

Table 1: The effect of intraperitoneal ceftriaxone (200 mg/kg) on the levels of malondialdehyde (MDA) and glutathione (GSH) in the lumbar spinal cord of 3- and 7-day CCI rats. Animals were treated with ceftriaxone for 7 days and administration started when CCI was induced. Data are presented as mean ± SEM ($n = 3$). One-way ANOVA followed by Tukey's *post hoc* test was used for multiple comparisons. $^{\#\#}P < 0.01$, $^{\#}P < 0.05$ difference between CCI-NS and sham/naive animals. $^{*}P < 0.05$ CCI-Cef group versus NS-CCI group (control).

	Control group (normal saline CCI rats)	Sham group	Naive group (intact rats with daily 200 mg/kg ceftriaxone)	Treated group (CCI rats with daily 200 mg/kg ceftriaxone)
MDA (nmol/mg protein)				
Day 3	$12.9 \pm 2.5^{\#\#}$	4.3 ± 0.23	4.7 ± 0.23	$5.9 \pm 1.2^{*}$
Day 7	$10.7 \pm 2.1^{\#}$	3 ± 0.16	3.1 ± 0.17	$4.5 \pm 1.2^{*}$
GSH (nmol/mg protein)				
Day 3	37.7 ± 10.4	49 ± 11	41 ± 3.4	42.5 ± 3.8
Day 7	$33.5 \pm 4.6^{\#\#}$	55.2 ± 2.5	48.9 ± 2.3	$40.6 \pm 2.4^{*}$

elevation was detected in the Bax/Bcl2 ratio in animals subjected to CCI at this time. Bax is representative apoptotic protein in the Bcl2 family and responsible for the subsequent activation of caspases and cell apoptosis. Indeed, the ratio of Bax to Bcl2 can determine the susceptibility of cells to cell death. A functional imbalance between proapoptotic Bax and antiapoptotic Bcl2 has been implicated following chronic constriction of sciatic nerve in rats [23]. As there was not a significant difference between apoptotic protein levels of naïve animals treated with ceftriaxone relative to those of sham-operated animals, it could be suggested that ceftriaxone has no direct effect on apoptotic proteins. However, ceftriaxone reduced Bax and increased Bcl2 levels in CCI animals and as a result a significant decrease was detected in the Bax/Bcl2 ratio of spinal cord in the sciatic nerve CCI rats on postoperative day 3. In this study, we found a significant induction of cleaved forms of caspases 3 and 9 on day 3 after CCI followed by a decrease at day 7. In agreement with this, a recent study by Wu et al. showed that treatment of CCI animals with inhibitor of caspase-3 and siRNA targeting caspase-3 significantly inhibited the apoptosis of neurons and the thermal hyperalgesia following sciatic nerve ligation [24]. Joseph and Levine showed that caspase signaling pathway contributed to the pain induced in two models of painful peripheral neuropathy [16]. In CCI animals treated with normal saline, Bax/Bcl2 ratio of spinal cord declined thereafter on day 7. There were also no detectable cleaved forms of caspases 3 and 9 in the spinal cord of NS-CCI animals. Thereafter, there was no difference among CCI-vehicle, sham, naïve, and CCI-ceftriaxone treated groups by day 7. Our data in the present study supports the evidence that, in the CCI of sciatic nerve, the development of neuropathic pain may be associated with the activation of apoptosis process [16, 24]. However, depending on the time point of study, there are differences in pattern of apoptosis occurrence. As the antiapoptotic protein, Bcl2, increased in the control group, it seems that as a modulatory mechanism apoptotic process via mitochondria is limited to the first few days after nerve injury which is consistent with some studies. An early apoptosis (2-3 days after CCI) occurred transiently by the increased ratio of Bax/Bcl2 genes in a study by de Novellis and collogues. An inversed pattern of Bcl2 family genes expression was detected at later stages [3]. Thus, there was a significant lowering in Bax/Bcl2 and Bcl-Xs/Bcl-xL ratios over time as a consequence of increased expression of antiapoptotic Bcl2 and Bcl-xL. In a study by Costa et al., increase in the ratio between pro- and antiapoptotic gene Bax/Bcl2 expression in the spinal cord of neuropathic rats was also limited to the first few days following nerve injury [25]. Siniscalco and coworkers revealed that the levels of Bax, apoptotic protease-activating factor-1 (apaf-1), nestin, GFAP, and caspase-7 mRNA increased in the dorsal horn spinal cord by 3 days after CCI. At 7 days after CCI, only overexpression of Bcl2, nestin, and GFAP mRNA was observed [26]. In a study by Rezende et al., expression of Bax gene and Bax protein increased, while the expression of Bcl2 RNA was decreased in 5 days sciatic nerve transection rats [27].

Despite the decreased levels of proapoptotic proteins after 7 days of CCI, elevated levels of MDA and decreased levels of GSH remained in the spinal cord of 7-day CCI rats, which was consistent with the development of behavioral data in our previous study. Consequently, it seems that other mechanisms other than apoptosis through mitochondrial pathways at this time contribute to the behavioral parameters of neuropathic pain. Moreover, the important contributory role of oxidative stress is supported in the pathogenesis of neuropathic pain [6, 28]. However, it might be possible that apoptosis process again is activated after the time course of our study. Hence, taking more stage samples such as days 10 or 14 may help to better characterize time course of apoptotic factors activation. Treatment with ceftriaxone in CCI rats decreased spinal cord levels of MDA and increased contents of GSH, on days 3 and 7 after CCI, as compared with the vehicle treated control group. It has been shown that increased levels of glutamate with the prevention of cysteine uptake into the cells lead to cysteine and glutathione depletion from cells which is subsequently accompanied by an increase in reactive oxygen species (ROS). On the other hand, depletion of GSH is correlated with glutamate excitotoxicity [29]. Glutamate transporters contribute not only to the prevention of toxicity caused by glutamate but also to the stimulation of cysteine uptake through the cysteine/glutamate antiporter and also generation of GSH by providing intracellular glutamate [30].

Although the exact mechanism of antioxidant and antiapoptotic effects of ceftriaxone was not evaluated in our study, it seems that ceftriaxone through different mechanisms and

pathways shows neuroprotective effects. For example, in a study by Sari et al., ceftriaxone reduced ethanol consumption in an animal model of alcohol abuse; however, only the highest doses increased the GLT1 expression. They suggested that ceftriaxone may have additional pharmacological effects independent of the activation and/or upregulation of GLT1 [31]. An *in vitro* study showed that ceftriaxone treatment increased GSH and glutamate/cystine-antiporter levels and suggested that neuroprotective effects of ceftriaxone might relate more strongly to activation of the antioxidant defense system [32]. Chu et al. revealed that ceftriaxone protected against focal cerebral ischemia by increasing the levels of GLT1 as well as reducing the levels of proinflammatory cytokines (tumor necrosis factor), matrix metalloproteinase 9 (MMP-9), and activated caspase-9 [33]. In a study by Ramos and coworkers, ceftriaxone inhibited astrocyte activation by downregulation of GFAP as well as upregulation of GLT1 expression, in CCI animals [34]. MacAluso et al. reported that a single dose of ceftriaxone but not cefazolin, a structurally similar cephalosporin antibiotic to ceftriaxone, produced analgesia in patients with painful neuropathies and mouse models of inflammatory or postsurgical pain [35]. It has previously been demonstrated that increased expression of GLT1 by ceftriaxone occurs after a few days [8, 11].

5. Conclusion

Taken together, ceftriaxone as a GLT1 upregulator/activator could concomitantly prevent lipid peroxidation and oxidative stress-mediated apoptosis and activate the antioxidant defense system with restoring the levels of GSH. Ceftriaxone and new drugs that act in a similar manner but without antibiotic properties could be a suitable approach for ameliorating and potentially preventing a wide range of neurodegenerative diseases caused by glutamate excitotoxicity.

Conflict of Interests

The authors declare that there is no conflict of interests regarding the publication of this paper.

Acknowledgment

The authors are thankful to the Vice Chancellor of Research, Mashhad University of Medical Sciences, Iran, for the financial support. The results described in this paper are part of a Ph.D. thesis.

References

[1] M. Zimmermann, "Pathobiology of neuropathic pain," *European Journal of Pharmacology*, vol. 429, no. 1–3, pp. 23–37, 2001.

[2] M. Osikowicz, J. Mika, and B. Przewlocka, "The glutamatergic system as a target for neuropathic pain relief," *Experimental Physiology*, vol. 98, no. 2, pp. 372–384, 2013.

[3] V. de Novellis, D. Siniscalco, U. Galderisi et al., "Blockade of glutamate mGlu5 receptors in a rat model of neuropathic pain prevents early over-expression of pro-apoptotic genes and morphological changes in dorsal horn lamina II," *Neuropharmacology*, vol. 46, no. 4, pp. 468–479, 2004.

[4] S. Afrazi, S. Esmaeili-Mahani, V. Sheibani, and M. Abbasnejad, "Neurosteroid allopregnanolone attenuates high glucose-induced apoptosis and prevents experimental diabetic neuropathic pain: *in vitro* and *in vivo* studies," *The Journal of Steroid Biochemistry and Molecular Biology*, vol. 139, pp. 98–103, 2014.

[5] D. Varija, K. P. Kumar, K. P. Reddy, and V. K. Reddy, "Prolonged constriction of sciatic nerve affecting oxidative stressors & antioxidant enzymes in rat," *Indian Journal of Medical Research*, vol. 129, no. 5, pp. 587–592, 2009.

[6] N. N. Pathak, V. Balaganur, M. C. Lingaraju et al., "Atorvastatin attenuates neuropathic pain in rat neuropathy model by down-regulating oxidative damage at peripheral, spinal and supraspinal levels," *Neurochemistry International*, vol. 68, pp. 1–9, 2014.

[7] K. Chu, S.-T. Lee, D.-I. Sinn et al., "Pharmacological induction of ischemic tolerance by glutamate transporter-1 (EAAT2) upregulation," *Stroke*, vol. 38, no. 1, pp. 177–182, 2007.

[8] P. Yogeeswari, A. Semwal, R. Mishra, and D. Sriram, "Current approaches with the glutamatergic system as targets in the treatment of neuropathic pain," *Expert Opinion on Therapeutic Targets*, vol. 13, no. 8, pp. 925–943, 2009.

[9] B. Sung, G. Lim, and J. Mao, "Altered expression and uptake activity of spinal glutamate transporters after nerve injury contribute to the pathogenesis of neuropathic pain in rats," *Journal of Neuroscience*, vol. 23, no. 7, pp. 2899–2910, 2003.

[10] P. H. Chandrasekar, K. V. I. Rolston, B. R. Smith, and J. L. LeFrock, "Diffusion of ceftriaxone into the cerebrospinal fluid of adults," *Journal of Antimicrobial Chemotherapy*, vol. 14, no. 4, pp. 427–430, 1984.

[11] J. D. Rothstein, S. Patel, M. R. Regan et al., "β-Lactam antibiotics offer neuroprotection by increasing glutamate transporter expression," *Nature*, vol. 433, no. 7021, pp. 73–77, 2005.

[12] C. Thöne-Reineke, C. Neumann, P. Namsolleck et al., "The β-lactam antibiotic, ceftriaxone, dramatically improves survival, increases glutamate uptake and induces neurotrophins in stroke," *Journal of Hypertension*, vol. 26, no. 12, pp. 2426–2435, 2008.

[13] A. V. Jelenkovic, M. D. Jovanovic, D. D. Stanimirovic, D. D. Bokonjic, G. G. Ocic, and B. S. Boskovic, "Beneficial effects of ceftriaxone against pentylenetetrazole-evoked convulsions," *Experimental Biology and Medicine*, vol. 233, no. 11, pp. 1389–1394, 2008.

[14] V. Hajhashemi, H. Hosseinzadeh, and B. Amin, "Antiallodynia and antihyperalgesia effects of ceftriaxone in treatment of chronic neuropathic pain in rats," *Acta Neuropsychiatrica*, vol. 25, no. 1, pp. 27–32, 2013.

[15] Y. Hu, W. Li, L. Lu et al., "An anti-nociceptive role for ceftriaxone in chronic neuropathic pain in rats," *Pain*, vol. 148, no. 2, pp. 284–301, 2010.

[16] E. K. Joseph and J. D. Levine, "Caspase signalling in neuropathic and inflammatory pain in the rat," *European Journal of Neuroscience*, vol. 20, no. 11, pp. 2896–2902, 2004.

[17] M. Uchiyama and M. Mihara, "Determination of malonaldehyde precursor in tissues by thiobarbituric acid test," *Analytical Biochemistry*, vol. 86, no. 1, pp. 271–278, 1978.

[18] R. Dringen, "Metabolism and functions of glutathione in brain," *Progress in Neurobiology*, vol. 62, no. 6, pp. 649–671, 2000.

[19] J. Tannenbaum, "Ethics and pain research in animals," *ILAR Journal*, vol. 40, no. 3, pp. 97–110, 1999.

[20] G. J. Bennett and Y.-K. Xie, "A peripheral mononeuropathy in rat that produces disorders of pain sensation like those seen in man," *Pain*, vol. 33, no. 1, pp. 87–107, 1988.

[21] M. M. Bradford, "A rapid and sensitive method for the quantitation of microgram quantities of protein utilizing the principle of protein dye binding," *Analytical Biochemistry*, vol. 72, no. 1-2, pp. 248–254, 1976.

[22] M. Uchiyama and M. Mihara, "Determination of malonaldehyde precursor in tissues by thiobarbituric acid test," *Analytical Biochemistry*, vol. 86, no. 1, pp. 271–278, 1978.

[23] S. Maione, D. Siniscalco, U. Galderisi et al., "Apoptotic genes expression in the lumbar dorsal horn in a model neuropathic pain in rat," *NeuroReport*, vol. 13, no. 1, pp. 101–106, 2002.

[24] F. Wu, X. Miao, J. Chen et al., "Down-regulation of GAP-43 by inhibition of caspases-3 in a rat model of neuropathic pain," *International Journal of Clinical and Experimental Pathology*, vol. 5, no. 9, pp. 948–955, 2012.

[25] B. Costa, D. Siniscalco, A. E. Trovato et al., "AM404, an inhibitor of anandamide uptake, prevents pain behaviour and modulates cytokine and apoptotic pathways in a rat model of neuropathic pain," *British Journal of Pharmacology*, vol. 148, no. 7, pp. 1022–1032, 2006.

[26] D. Siniscalco, C. Giordano, C. Fuccio et al., "Involvement of subtype 1 metabotropic glutamate receptors in apoptosis and caspase-7 over-expression in spinal cord of neuropathic rats," *Pharmacological Research*, vol. 57, no. 3, pp. 223–233, 2008.

[27] A. C. S. Rezende, A. S. Vieira, F. Rogério et al., "Effects of systemic administration of ciliary neurotrophic factor on Bax and Bcl-2 proteins in the lumbar spinal cord of neonatal rats after sciatic nerve transection," *Brazilian Journal of Medical and Biological Research*, vol. 41, no. 11, pp. 1024–1028, 2008.

[28] D. Siniscalco, C. Fuccio, C. Giordano et al., "Role of reactive oxygen species and spinal cord apoptotic genes in the development of neuropathic pain," *Pharmacological Research*, vol. 55, no. 2, pp. 158–166, 2007.

[29] C. F. Pereira and C. R. D. Oliveira, "Oxidative glutamate toxicity involves mitochondrial dysfunction and perturbation of intracellular Ca^{2+} homeostasis," *Neuroscience Research*, vol. 37, no. 3, pp. 227–236, 2000.

[30] A.-C. Rimaniol, P. Mialocq, P. Clayette, D. Dormont, and G. Gras, "Role of glutamate transporters in the regulation of glutathione levels in human macrophages," *American Journal of Physiology: Cell Physiology*, vol. 281, no. 6, pp. C1964–C1970, 2001.

[31] Y. Sari, M. Sakai, J. M. Weedman, G. V. Rebec, and R. L. Bell, "Ceftriaxone, a beta-lactam antibiotic, reduces ethanol consumption in alcohol-preferring rats," *Alcohol and Alcoholism*, vol. 46, no. 3, pp. 239–246, 2011.

[32] J. Lewerenz, P. Albrecht, M.-L. T. Tien et al., "Induction of Nrf2 and xCT are involved in the action of the neuroprotective antibiotic ceftriaxone *in vitro*," *Journal of Neurochemistry*, vol. 111, no. 2, pp. 332–343, 2009.

[33] K. Chu, S.-T. Lee, D.-I. Sinn et al., "Pharmacological induction of ischemic tolerance by glutamate transporter-1 (EAAT2) upregulation," *Stroke*, vol. 38, no. 1, pp. 177–182, 2007.

[34] K. M. Ramos, M. T. Lewis, K. N. Morgan et al., "Spinal upregulation of glutamate transporter GLT-1 by ceftriaxone: therapeutic efficacy in a range of experimental nervous system disorders," *Neuroscience*, vol. 169, no. 4, pp. 1888–1900, 2010.

[35] A. MacAluso, M. Bernabucci, A. Trabucco et al., "Analgesic effect of a single preoperative dose of the antibiotic ceftriaxone in humans," *Journal of Pain*, vol. 14, no. 6, pp. 604–612, 2013.

Hindawi Publishing Corporation
BioMed Research International
Volume 2014, Article ID 251785, 11 pages
http://dx.doi.org/10.1155/2014/251785

Research Article

The Inhibitory Effect of Somatostatin Receptor Activation on Bee Venom-Evoked Nociceptive Behavior and pCREB Expression in Rats

Li Li,[1] Rong Luo,[2] Yuan Guo,[1] Fanrong Yao,[1] Dongyuan Cao,[3] Shaojie Ma,[1] Jun Wang,[1] Huisheng Wang,[1] and Yan Zhao[1]

[1] *Department of Physiology and Pathophysiology, Xi'an Jiaotong University School of Medicine, Xi'an, Shaanxi 710061, China*
[2] *Medical Scientific Research Centre, Guangxi Medical University, Nanning, Guangxi 530021, China*
[3] *Department of Neural and Pain Sciences, University of Maryland Dental School, 650 West Baltimore Street, Baltimore, MD 21201, USA*

Correspondence should be addressed to Rong Luo; luorong77@126.com

Received 8 January 2014; Revised 31 March 2014; Accepted 14 April 2014; Published 7 May 2014

Academic Editor: Livio Luongo

The present study examined nociceptive behaviors and the expression of phosphorylated cAMP response element-binding protein (pCREB) in the dorsal horn of the lumbar spinal cord and the dorsal root ganglion (DRG) evoked by bee venom (BV). The effect of intraplantar preapplication of the somatostatin analog octreotide on nociceptive behaviors and pCREB expression was also examined. Subcutaneous injection of BV into the rat unilateral hindpaw pad induced significant spontaneous nociceptive behaviors, primary mechanical allodynia, primary thermal hyperalgesia, and mirror-thermal hyperalgesia, as well as an increase in pCREB expression in the lumbar spinal dorsal horn and DRG. Octreotide pretreatment significantly attenuated the BV-induced lifting/licking response and mechanical allodynia. Local injection of octreotide also significantly reduced pCREB expression in the lumbar spinal dorsal horn and DRG. Furthermore, pretreatment with cyclosomatostatin, a somatostatin receptor antagonist, reversed the octreotide-induced inhibition of the lifting/licking response, mechanical allodynia, and the expression of pCREB. These results suggest that BV can induce nociceptive responses and somatostatin receptors are involved in mediating the antinociception, which provides new evidence for peripheral analgesic action of somatostatin in an inflammatory pain state.

1. Introduction

Somatostatin (SST) is a small neuropeptide with wide distribution in the central and peripheral tissues [1–3]. Local administration of somatostatin or its analog octreotide (OCT) reduces lifting/licking behaviors induced by formalin and capsaicin [1, 4] and mechanical hyperalgesia in carrageenan-induced inflammation [5]. In addition, octreotide reduces responses to thermal stimulation in C-mechanoheat sensitive fibers in Sprague-Dawley (SD) rats [1]. However, our previous study indicated that local administration of octreotide did not alter paw withdrawal thermal latency (PWTL) in arthritic Dark-Agouti rats [6]. These inconsistent data led us to further determine the local antinociceptive effects of octreotide.

The bee venom test is a well-established inflammatory pain model. Subcutaneous (s.c.) injection of bee venom solution into a hindpaw of rats and cats has been reported to induce unique expressions of a prolonged, persistent, and spontaneous flinching reflex (lifting and licking behaviors indicative of pain) in a monophasic manner for 1-2 hours followed by a profound, persistent, mechanical, and thermal hyperalgesia in the injured site for 72–96 hours [7–9]. The bee venom (BV) test can closely mimic the complicated state of clinical inflammatory pain caused by tissue injury, which includes both spontaneous nociception and subsequent mechanical and thermal hyperalgesia [7]. The previous studies on the antinociceptive effect of somatostatin or octreotide considered only spontaneous nociception or hypersensitivity [1, 4–6]. Therefore, the inflammatory pain

induced by BV and the local antinociceptive effects of octreotide were observed in the present study.

The cAMP response element-binding protein (CREB) is a transcription factor that has been implicated in the transcriptional regulation of many genes [10]. Several studies have shown that the activation of CREB in spinal cord dorsal horn neurons plays a central role in the transmission of nociceptive stimuli [11–13]. CREB phosphorylation at Ser133 has been identified as an essential trigger for CREB activation, which leads to the transcription of a number of immediate early genes, including those coding for the important pain-related proteins c-Fos and cyclooxygenase-2 [10]. An increase of phosphorylated CREB (pCREB) in the dorsal horn of the spinal cord occurs in inflammation pain [14] and neuropathic pain models [15, 16]. After a unilateral injection of formalin into the hindpaw, a strong and bilateral increase of pCREB in the spinal cord was induced [17]. In addition, intrathecal injection of CREB antisense oligonucleotide attenuates tactile allodynia caused by partial sciatic nerve ligation [18]. Thus, pCREB is considered a good marker for neuronal activity after noxious stimulation. Some dorsal root ganglion (DRG) neurons are also pCREB-positive [17]. Accordingly, another aim of the present study was to observe the expression of pCREB induced by BV in the spinal cord and DRG.

2. Materials and Methods

2.1. Animals. A total of 91 male SD rats weighing 250–300 g were used in the present study (66 for the nociception behavior test and 25 for the immunochemistry experiment). SD rats were provided by the Laboratory Animal Center of Xi'an Jiaotong University School of Medicine. All procedures were approved by the Institutional Animal Ethics Committee of the Xi'an Jiaotong University and were in accordance with the ethical guidelines of the International Association for the Study of Pain. In addition, every attempt was made to minimize the number of animals used. Rats were housed under a 12 h light-dark cycle with food and water available *ad libitum*.

2.2. Groups and Pharmacological Intervention. A volume of 50 μL BV (0.1 mg lyophilized whole venom of *Apis mellifera* (Sigma Co., St. Louis, USA) dissolved in 0.9% sterile normal saline (NS)) was intraplantarly injected into right hindpaw to produce nociception [19]. A concentration of 20 μM octreotide diluted in 0.9% NS (Sandostatin, Novartis Pharma Schweiz AG, Bern, Switzerland) was utilized in the present study based on the literature [6].

SD rats were divided into five groups: (1) NS + NS group: 60 μL NS intraplantar injection followed by 50 μL NS injection as the control group; (2) NS + BV group: 60 μL NS intraplantar injection followed by 50 μL BV injection as the pain model group; (3) ipsilateral OCT + BV group: 60 μL octreotide (20 μM) injection prior to the BV injection; (4) contralateral OCT + ipsilateral BV group: 50 μL BV injection into the right hindpaw after injection of 60 μL octreotide into the contralateral hindpaw to determine whether the local injection of octreotide can bring about systemic effects; (5) c-SOM + OCT + BV group: local injection of 60 μL, 128 μM cyclosomatostatin (c-SOM, Sigma Co., St. Louis, USA), a somatostatin receptor (SSTR) antagonist, before the intraplantar injection of 60 μL octreotide to determine whether the effect of octreotide was somatostatin receptor specific. A ten-minute interval was allowed between the applications of each drug in all groups.

2.3. Spontaneous Nociceptive Behavioral Observation. Behavioral observations were carried out by the same investigator from 9 to 11 am. All rats were habituated for 3 days before the start of experiment. The rats were placed in a $30 \times 30 \times 30$ cm^3 transparent glass test box for at least 30 min until their cage exploration and grooming activities ceased. The spontaneous nociceptive behavioral responses were quantified by counting the number of flinches and the cumulative time (in seconds) spent lifting and/or licking the injected hindpaw during each 5 min period for 1 hour after an intraplantar injection of BV [19, 20]. A flinch was defined as a spontaneous, rapid jerk of the foot. Lifting indicated that the injected paw was elevated without touching the floor. Licking meant that the injected paw was licked or bitten.

2.4. Measurement of Persistent Mechanical and Thermal Sensitivity. Mechanical sensitivity was calculated by measuring the 50% paw withdrawal mechanical threshold (PWMT) in response to mechanical stimuli [21] as assessed by a set of calibrated von Frey filaments with bending force ranging from 0.4 to 15 g (Stoelting Company, Wood Dale, USA). Beginning with the 2.0 g filament, each filament was applied underneath both hindpaws perpendicular to them with enough force to cause slight buckling for 6–8 s. The pattern of positive and negative responses was converted into a 50% threshold using the formula given by Dixon [22].

Thermal sensitivity was measured as previously described [23]. The animals were placed in a transparent plastic box ($28 \times 25 \times 21$ cm^3) on a 3 mm thick elevated horizontal glass plate. A radiant heat stimulator (BME-410A, Beijing Sunny Instruments Co. Ltd, Beijing, China) was placed under one hindpaw, and the PWTL was determined to an accuracy of 0.01 s. Both hindpaws were tested. A 20 s cut-off was imposed on the stimulus duration to prevent tissue damage. Five stimuli were repeatedly applied to each hindpaw in turn, with a 10 min interval between applications in the same region and 5 min interval between applications in different hindpaws. The PWTL for each hindpaw was defined as the mean value of the latter four stimuli. Based on a previous report [20], the PWMT and PWTL on the injected side and the contralateral hindpaw were investigated 30 min prior to the injection of BV and 2 hours after the injection.

2.5. Immunohistochemistry. SD rats were deeply anesthetized with pentobarbital (80 mg/kg, i.p.) and perfused through the left ventricle with 200 mL 37°C warm saline followed by 400 mL of 4% paraformaldehyde in 0.1 M phosphate buffer (PB, pH 7.4, 4°C) 30 min after injection of BV into one hindpaw. The L4-L5 spinal cord segments and L5 DRG were removed, postfixed for 24 hours in the same fixative, and then cryoprotected overnight in 30% sucrose in PB.

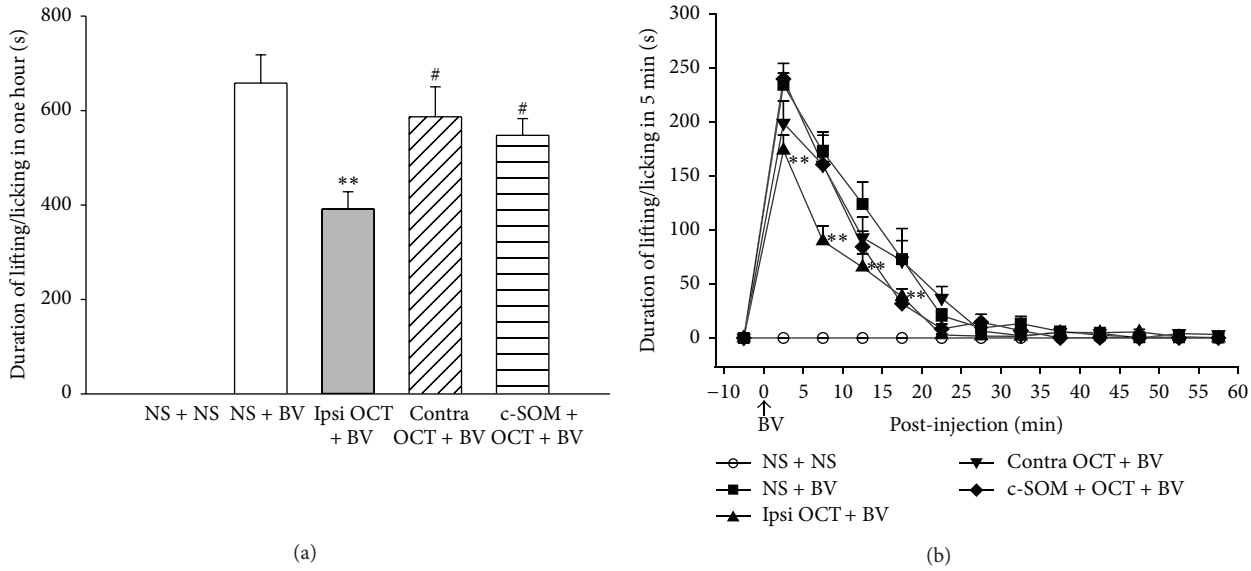

Figure 1: Effects of octreotide on lifting/licking (a) and time course (b). $n = 18$ for the NS + BV and ipsilateral OCT + BV groups, and $n = 10$ for other groups. $^{**}P < 0.01$, compared with those in the NS + BV group. $^{\#}P < 0.05$, compared with those in the OCT + BV group. One-way ANOVA tests followed by the Student-Newman-Keuls method were used to compare different treatments. NS, normal saline; BV, bee venom; OCT, octreotide; c-SOM, cyclosomatostatin; contra, contralateral; ipsi, ipsilateral.

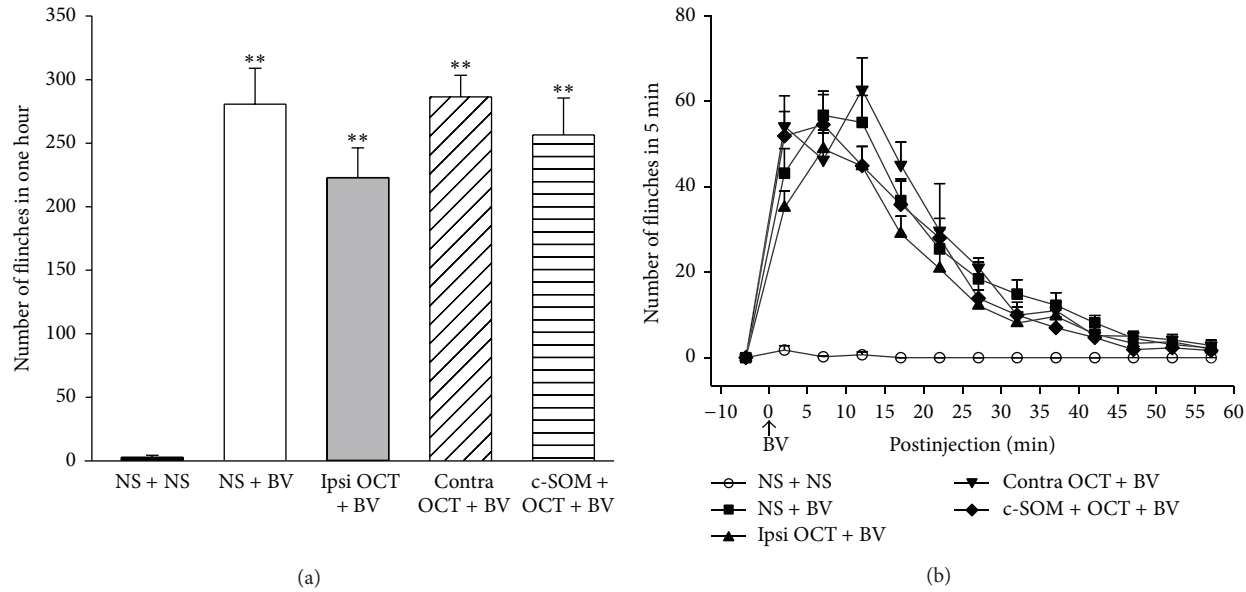

Figure 2: Effects of octreotide on flinch (a) and time course (b). $n = 18$ for the NS + BV and ipsilateral OCT + BV groups, and $n = 10$ for other groups. $^{*}P < 0.05$, $^{**}P < 0.01$, compared with the NS + NS group. One-way ANOVA tests followed by the Student-Newman-Keuls method were used to compare different treatments. NS, normal saline; BV, bee venom; OCT, octreotide; c-SOM, cyclo-somatostatin; contra, contralateral; ipsi, ipsilateral.

Tissues were cut coronally in a cryostat (Leica CM1900, Germany) at 35 μm thickness for the spinal cord and 14 μm for the DRG. One of every three sections through the L4-L5 spinal cord segments and all the L5 DRG sections were collected and rinsed twice in 0.01 M phosphate buffer saline (PBS). The sections were immunostained for pCREB with the avidin-biotin-peroxidase (ABC) method [24]. After being pretreated with 0.3% H_2O_2 for 10 min and 5% normal goat serum (NGS) for 1 hour at room temperature, sections were incubated with the primary antibody, anti-pCREB (1 : 100, Cell Signaling Technology, Inc., Beverly, MA, USA), in 5% NGS for 48 hours at 4°C. Subsequently, the sections were incubated overnight with biotinylated goat anti-rabbit IgG at 4°C and further processed using avidin biotin peroxidase complex (ABC, Zhongshan Biotechnology CO., LTD, Beijing, China) according to the instructions of the manufacturer.

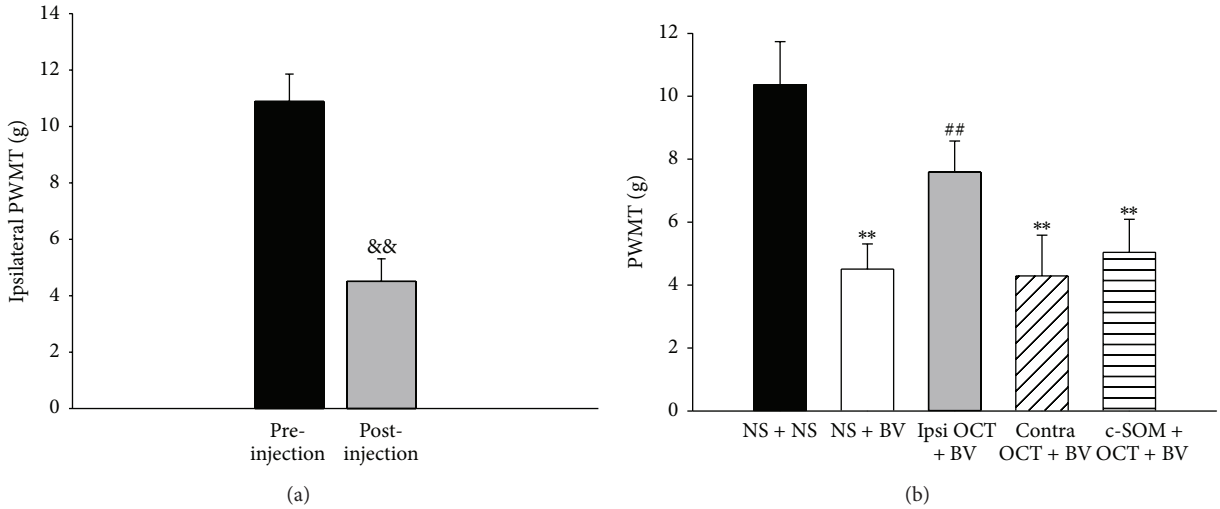

Figure 3: The PWMTs. (a) The ipsilateral pre- and postinjection PWMTs in the NS + BV group. A paired t-test was used to compare the PWMTs between pre- and postinjection. (b) The PWMT of the ipsilateral hindpaw after injection of different drugs. One-way ANOVA tests followed by the Student-Newman-Keuls method were used to compare different treatments. $n = 18$ for the NS + BV and ipsilateral OCT + BV groups, and $n = 10$ for the other groups. $^{\&\&}P < 0.01$, compared with preinjection in the same hindpaw; $^{**}P < 0.01$, compared with the NS + NS group; $^{\#\#}P < 0.01$, compared with the NS + BV group. PWMT, paw withdrawal mechanical threshold; BV, bee venom; OCT, octreotide; ipsi, ipsilateral hindpaw; contra, contralateral hindpaw.

Between each step, the tissue was rinsed at least 3 times in 0.01 M PBS containing 0.3% Triton X-100 for at least 10 min each. Then, the sections were incubated with 0.02% 3,3′-diaminobenzidine (DAB, Zhongshan Biotechnology CO., LTD, Beijing, China) for 5–10 min. Finally, the sections were mounted onto gelatin-coated glass slides and allowed to air dry. To observe whether pCREB was located in neurons of the DRG, the sections were restained by Nissl's staining method. All sections were then dehydrated through a graded alcohol series, cleaned with dimethylbenzene, and cover-slipped with neutral balsam.

All sections were observed under a light microscope (BX-60; Olympus, Tokyo, Japan). Images were captured using a SensiCam digital camera and imported into SigmaScan Pro Image Analysis Software (SPOT-Insight QE, Diagnostic Instruments Inc., Sterling Heights, MI, USA). To discriminate positive immunostaining from the background, the cells showing a staining twice as intense as the average background were considered positive for pCREB immunoreactivity. In the control experiments, the primary antibodies were replaced with 5% NGS; no positive staining for the replaced antibodies was detected. Four to five random sections from the L4-L5 spinal cord and the L5 DRG were counted and averaged for each animal, and five animals were included in each group [25–27]. Every positive cell was counted in lamina I–VI in the spinal cord. The percentage of neurons stained with pCREB in the DRG was determined by counting the total number of positive neuronal profiles and the total number of neuronal profiles in each section.

2.6. Statistical Analysis. All data are presented as the means ± SEM. One-way ANOVA tests followed by the Student-Newman-Keuls method were used to compare differences between the five treatment groups. Paired t-tests were used to compare the differences in PWMT and PWTL between pre- and postinjection of BV in the same hindpaw. All analyses were performed with SigmaStat 2.0 software. $P < 0.05$ was considered to be statistically significant.

3. Results

3.1. Effects of Octreotide on Spontaneous Nociceptive Behaviors Induced by BV. Intraplantar injection of BV produced a prompt, tonic nociceptive response characterized by flinches and continuously lifting/licking of the injected hindpaw for approximately 1 hour. In the control group, there were few flinches observed in the first 5 min, and no lifting/licking occurred.

Compared with the NS + BV group, the cumulative time spent lifting/licking over 1 hour in the ipsilateral OCT + BV group was significantly shorter (391.4 ± 36.9 s versus 658.2 ± 60.0 s, $n = 18$, $P < 0.05$, Figure 1(a)). In addition, there are significant differences between the NS + BV and ipsilateral OCT + BV groups at the 5-, 10-, 15-, and 20-minute time points after injection of BV (Figure 1(b)). To exclude the systemic effect of OCT, the same dose of the drug was subcutaneously preadministered in the contralateral hindpaw of the BV-treated side. Contralateral pretreatment with OCT did not affect BV-evoked nociceptive lifting/licking duration (586.9 ± 63.4 s $n = 10$, Figure 1(a)). To illustrate the effect of OCT by activation of the somatostatin receptor, the specific antagonist cyclosomatostatin (c-SOM) was applied 10 min before OCT and it reversed the antinociceptive effects of OCT on lifting/licking responses (547.6 ± 35.5 s $n = 10$, Figure 1(a)).

Similar to other studies [20, 23, 28], intraplantar injection of BV evoked tonic nociceptive flinching behavior with an

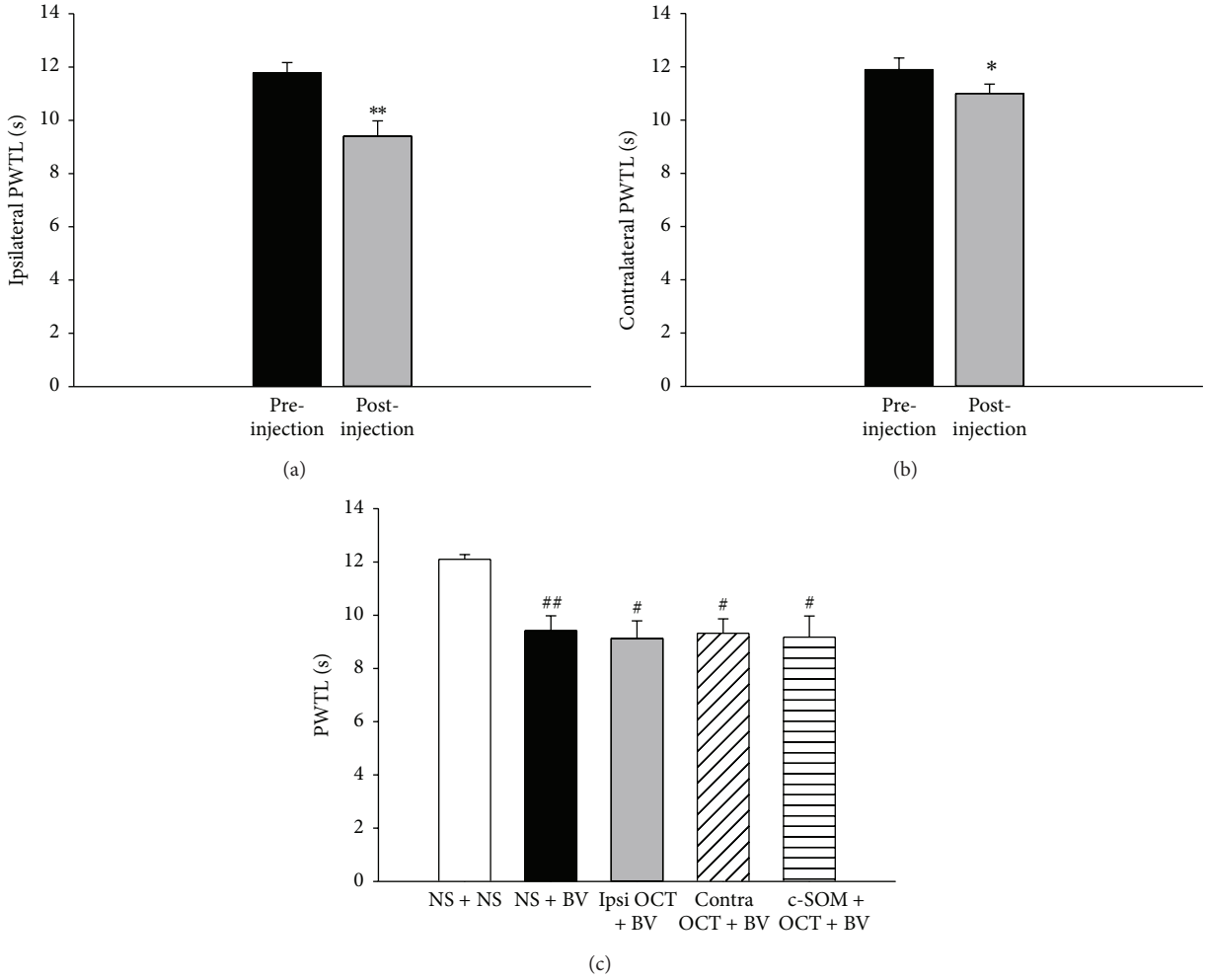

Figure 4: The PWTL. (a) The ipsilateral pre- and postinjection PWTLs in the NS + BV group. A paired t-test was used to compare the PWTLs between pre- and postinjection. (b) The PWTL of the contralateral hindpaw in the NS + BV group. A paired t-test was used to compare the PWTLs between pre- and postinjection. (c) The ipsilateral postinjection PWTLs of the five different treatment groups. One-way ANOVA tests followed by the Student-Newman-Keuls method were used to compare different treatments. $n = 18$ for NS + BV and ipsilateral OCT + BV groups, $n = 10$ for the other groups. $^{*}P < 0.05$; $^{**}P < 0.01$, compared with the preinjection in the same hindpaw; $^{\#}P < 0.05$; $^{\#\#}P < 0.01$, compared with the ipsilateral postinjection in the NS + NS group. PWTL, paw withdrawal thermal latency; BV, bee venom; OCT, octreotide; ipsi, ipsilateral hindpaw; contra, contralateral hindpaw.

average of 280.7 ± 28.3 times in 1 hour. Both total flinches in 1 hour and number of flinches at every time point after injection are visually smaller in the ipsilateral OCT + BV group than in the NS + BV group. However, neither cumulative flinches in 1 hour (222.9 ± 23.4 versus 286.4 ± 17.0, $P > 0.05$, Figure 2(a)) nor the number of flinches in each 5 min period was significantly different in the ipsilateral OCT + BV group compared with the NS + BV group (Figures 2(a) and 2(b)).

3.2. Effects of Octreotide on BV-Induced Mechanical Allodynia. At 2 hours after intraplantar injection of BV, the PWMTs dramatically decreased in the injected hindpaw from 10.89 ± 0.97 g to 4.51 ± 0.80 g, suggesting the occurrence of primary mechanical hyperalgesia ($n = 18$, $P < 0.01$, Figure 3(a)). There was no significant difference between the preinjection and postinjection PWMTs in the contralateral side (11.52 ± 0.87 g versus 11.32 ± 0.94 g). In the NS + NS group, the PWMT did not change significantly after NS injection (ipsilateral: 10.66 ± 1.21 g versus 10.37 ± 1.37 g; contralateral: 10.48 ± 1.12 g versus 10.83 ± 1.40 g; $n = 10$, $P > 0.05$).

The PWMTs in the ipsilateral hindpaw in the NS + BV group were significantly lower after injection than in the NS + NS group (Figure 3(b), $P < 0.05$). However, ipsilateral preapplication of OCT attenuated the PWMTs and there was no significant difference compared with the NS + NS group ($P > 0.05$, Figure 3(b)). This antinociceptive effect on mechanical hyperalgesia did not occur when OCT was injected contralaterally (Figure 3(b)), and intraplantar pretreatment with the somatostatin receptor antagonist c-SOM reversed octreotide's antinociceptive effects (Figure 3(b)).

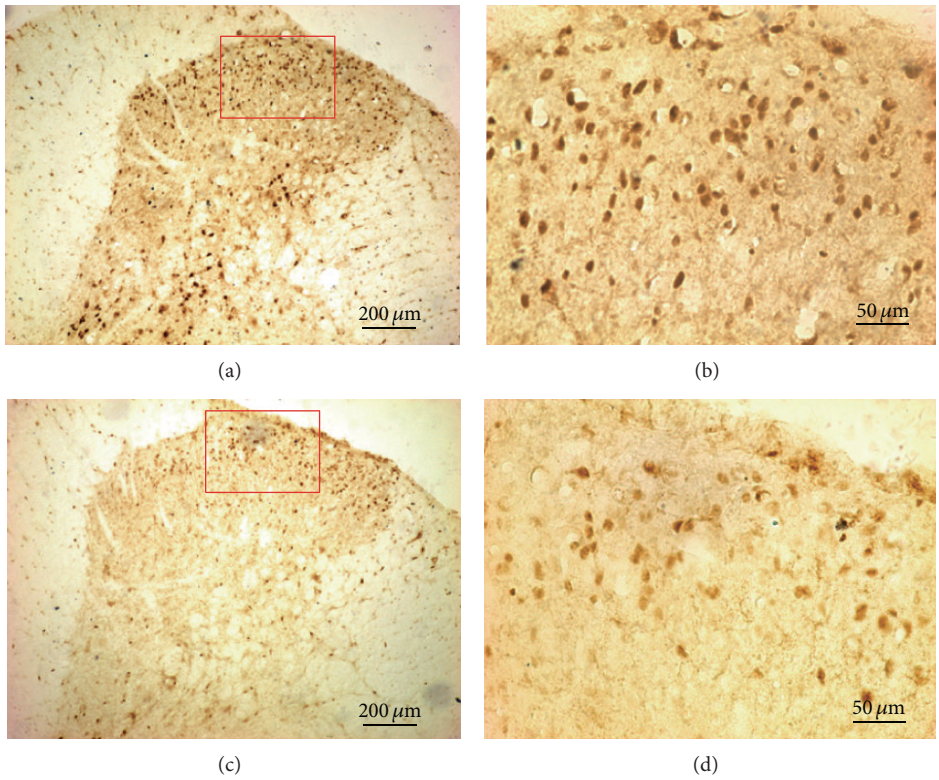

Figure 5: Photomicrograph showing the example of pCREB expression in the L4 spinal cord induced by BV injection following NS or octreotide administration. (a) NS + BV group, (c) OCT + BV group, and (b) and (d) are amplifications of the framed areas in (a) and (c), respectively.

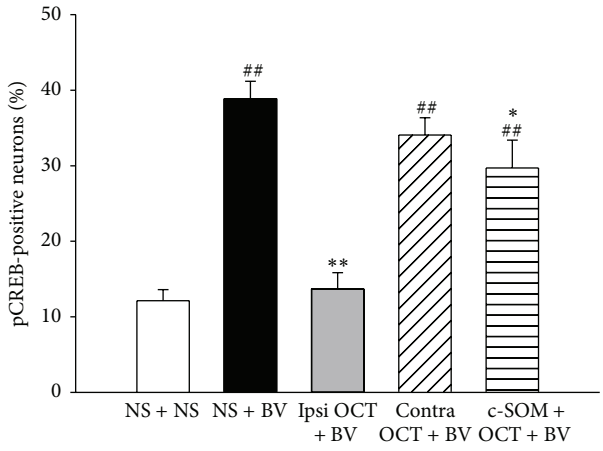

Figure 6: The percentage of pCREB-positive neurons in the ipsilateral DRG in the five groups. One-way ANOVA tests followed by the Student-Newman-Keuls method were used to compare different treatments. $^{\#\#}P < 0.01$, compared with those in the NS + NS group; $^{*}P < 0.05$, $^{**}P < 0.01$, compared with those in the NS + BV group.

3.3. Effects of Octreotide on Thermal Hyperalgesia Induced by BV. Compared with PWTLs prior to BV injection, the PWTLs in the ipsilateral hindpaw decreased significantly after intraplantar injection of BV in the NS + BV group from 11.78 ± 0.39 s to 9.41 ± 0.57 s ($P < 0.01$, Figure 4(a)), demonstrating primary thermal hyperalgesia. In addition, the PWTLs in the contralateral hindpaw also decreased significantly after injection of BV (11.89±0.44 s versus 11.00± 0.35 s; $P < 0.05$, Figure 4(b)), indicating a mirror-thermal hyperalgesia. In the NS + NS group, the PWTL did not change significantly after NS injection.

However, in the ipsilateral OCT + BV group, primary thermal hyperalgesia was still observed ($P < 0.05$). When comparing PWTLs among different groups, PWTLs in the ipsilateral hindpaw after injection of BV in the other four groups were significantly lower than in the NS + NS group ($P < 0.05$, Figure 4(c)). Meanwhile, mirror-thermal hyperalgesia in the ipsilateral OCT + BV group was still observed.

3.4. The Expression of pCREB in the Spinal Cord and DRG. After the injection of BV, the pCREB-positive staining was localized to cell nuclei throughout the bilateral spinal cord and dramatically increased as shown in Table 1 Column 1 and Column 2 ($P < 0.05$). No significant difference was found between the ipsilateral and contralateral sides ($P > 0.05$). In addition, the majority of the pCREB-positive cells were observed in laminae I-II and V-VI in the spinal cord, which is the major terminal of nociceptive afferent fibers and the mediator of nociceptive input. It also showed that preapplication of OCT significantly decreased pCREB expression compared with the NS + BV group ($P < 0.05$), while contralateral pretreatment with OCT and ipsilateral

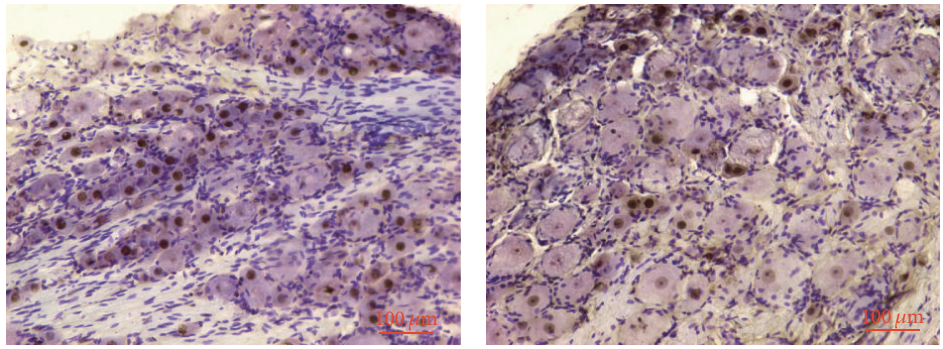

(a) (b)

Figure 7: Photomicrograph showing the example of pCREB expression in the L5 DRG induced by BV injection following NS or octreotide administration. (a) and (c) present the example of pCREB expression in the NS + BV group and the ipsilateral OCT + BV group, respectively.

Table 1: Number of pCREB-positive cells in the ipsilateral and contralateral dorsal horn of the lumbar spinal cord in SD rats.

Subregion	NS + NS	NS + BV	Ipsilateral OCT + BV	Contralateral OCT + ipsilateral BV	c-SOM + OCT + BV
Ipsi I-II	41.06 ± 2.52	127.20 ± 2.96$^{\#\#}$	64.93 ± 4.39$^{\#\#**}$	109.80 ± 6.48$^{\#\#\$\$}$	110.80 ± 6.65$^{\#\#\$\$}$
Contra I-II	34.47 ± 3.99	121.40 ± 5.03$^{\#\#}$	63.87 ± 4.09$^{\#\#**}$	112.20 ± 6.09$^{\#\#\$\$}$	111.20 ± 7.13$^{\#\#\$\$}$
Ipsi III-IV	5.00 ± 1.41	17.60 ± 1.86$^{\#\#}$	12.20 ± 2.22$^{\#\#}$	15.40 ± 1.53$^{\#\#}$	13.20 ± 2.25$^{\#\#}$
Contra III-IV	4.60 ± 1.06	17.20 ± 1.52$^{\#\#}$	12.40 ± 2.27$^{\#\#}$	15.00 ± 2.28$^{\#\#}$	13.80 ± 1.74$^{\#\#}$
Ipsi V-VI	33.60 ± 5.99	64.80 ± 3.87$^{\#}$	38.87 ± 5.95*	54.60 ± 3.12	45.20 ± 8.94
Contra V-VI	25.20 ± 4.11*	61.60 ± 3.19$^{\#\#}$	38.20 ± 8.79*	50.00 ± 3.03$^{\#}$	51.00 ± 9.53$^{\#}$

Data are presented as the means ± SEM from 5 rats. For each rat, counts from 5 sections were averaged. $^{*}P < 0.05$; $^{**}P < 0.01$, compared with the NS + BV group; $^{\#}P < 0.05$; $^{\#\#}P < 0.01$, compared with the NS + NS group. $^{\$\$}P < 0.01$, compared with the OCT + BV group. Ipsi: ipsilateral spinal cord; Contra: contralateral spinal cord.

pretreatment with c-SOM + OCT did not reduce the expression of pCREB throughout the spinal cord evoked by BV as shown in Columns 4 and 5. Figure 5 shows the examples of pCREB expression in the right dorsal horn of the L4 spinal cord.

After Nissl restaining of the neuron bodies in the DRG, the expression of pCREB was mostly located in small neurons (Figure 7). Compared with the NS + NS group, the expression of pCREB was significantly increased in the NS + BV group in the ipsilateral DRG ($P < 0.05$, Figure 6). Local injection of octreotide also reduced the BV-induced expression of pCREB in the DRG, and intraplantar pretreatment of the somatostatin receptor antagonist c-SOM reversed the octreotide effects ($P < 0.05$, Figure 6). Figure 7 shows the examples of pCREB expression in L5 DRG neurons.

4. Discussion

The most important finding of the present study is that local application of octreotide suppresses the BV-induced nociceptive lifting/licking behavior and pCREB expression in the superficial spinal cord and ipsilateral DRG, and this effect is reversed by pretreatment with cyclosomatostatin, an antagonist of the SSTR.

In the present study, intraplantar injection of BV elicited persistent nociceptive responses such as lifting, licking, and flinches, as well as mechanical allodynia and thermal hyperalgesia, which is consistent with a previous study [20]. BV is a mixed toxin containing melittin, phospholipase A2, apamin, histamine, and mast cell-degranulating peptide [19, 29]. Among these components, melittin is likely to play the most important role in the production of pain, hyperalgesia, allodynia, and inflammatory process [29]. Melittin has been reported to selectively activate capsaicin-sensitive primary afferent fibers [30] and small- to medium-sized DRG cells by opening the nonselective transient receptor potential vanilloid 1 (TRPV1) cation ion channel [31]. Either pre- or post-treatment with capsazepine, a selective blocker of thermal nociceptor TRPV1, significantly prevents or suppresses the persistent, spontaneous nociception induced by intraplantar injection of melittin [29]. These results suggest that the nociceptive and hyperalgesic effects of BV might be mediated by activation of the peripheral capsaicin receptor TRPV1. TRPV1 activation plays a key role in inflammatory pain [4] and TRPV1 knockout mice do not develop inflammatory pain behaviors [32, 33]. TRPV1 is a nonselective cation channel with a preference for calcium [4, 34]. Agonist binding to the TRPV1 operated nonspecific cation channel is likely to induce a conformational change in receptor protein, leading to cation (predominantly calcium) influx [35]. This cation influx may cause membrane depolarization [36]. When membrane depolarization reaches the threshold level, an action potential is generated. The action potential is propagated along the entire length of the neuron and may be perceived as pain by the CNS [34, 37].

The present study showed that intraplantar pretreatment with octreotide attenuated the increase in the duration of lifting/licking induced by BV. However, contralateral octreotide treatment did not demonstrate any antinociceptive effect. Ipsilateral pretreatment with cyclosomatostatin, an antagonist of somatostatin receptors, reversed the effect of octreotide. Thus, the present study indicates that local antinociceptive effects of octreotide occur through the activation of peripheral somatostatin receptors. Five receptor subtypes have been found: SSTR1–5. SSTR1–4 had been identified on afferent terminals and in the DRG [1, 38–40]. In addition, OCT has high affinity to three receptor subtypes (SSTR2, 3, 5) that would be blocked by c-SOM [41]. Moreover, it has been reported that SSTR2 was located in the axon terminal of peripheral unmyelinated nerve fibers [1]. Furthermore, by using SSTR2-deficient mice and immunohistochemistry, the antinociceptive effects of OCT were completely abolished and only SSTR1 and SSTR2A were detected in a subset of small- and medium-diameter neurons in the dorsal root ganglia of naive wild-type mice [42]. Thus, the present study indicates that local antinociceptive effects of octreotide occurred through the activation of peripheral somatostatin receptors, most likely by SSTR2. The results are also consistent with previous studies demonstrating that somatostatin has analgesic effects in rodents and humans by acting on peripheral somatostatin receptors [5, 43, 44]. It is reported that SSTR2 inhibits activity through the presynaptic release of glutamate evoked by TRPV1 in the spinal cord [3]. SST is also synthesized and stored in capsaicin-sensitive transient receptor potential vanilloid 1 (TRPV1) expressing nociceptive afferents, and it has been identified in spinal dorsal horn neurons [45, 46]. Modulation of pain transmission has a complex circuitry that includes SSTR [46, 47]. During the sensitization of nociceptors, it has been demonstrated that SST interacts with the vanilloid receptor TRPV1 [4, 47].

The present study showed that intraplantar pretreatment with OCT depressed BV-induced increases in the duration of L/L but not the numbers of flinches. The mechanism by which flinches and L/L behavior were differentially affected in this study is not clear. The lack of an effect of OCT on flinch behavior suggests that the neural circuit underlying this reflexive behavior presumed to be segmentally organized may be distinct from that underlying L/L behavior, which is more likely to involve supraspinal mechanisms [1, 48].

Another finding in the present study is that intraplantar pretreatment with octreotide inhibits BV-induced mechanical, but not thermal, hyperalgesia. These results are consistent with the previous studies showing that octreotide relieves mechanical hyperalgesia in arthritic DA rats [6] and somatostatin reduces mechanical hyperalgesia in carrageenan-induced inflammation [5]. The inconsistent effect of octreotide on thermal and mechanical hyperalgesia may be due to thermal and mechanical hyperalgesia relying on the activation of two different intracellular cascades of events in the spinal cord. Neural substrates underlying mechanical hypersensitivity and thermal hypersensitivity have been dissociated in a number of ways [49, 50].

Mirror-thermal hyperalgesia was a typical characteristic of the BV test in SD rats that had not been reported in other inflammatory pain models such as nociception induced by formalin [1, 20] and capsaicin [4]. Both NMDA and non-NMDA receptors involved in central sensitization contribute to the development of BV-induced mirror-thermal hyperalgesia [51]. A temporal spinal summation of the ongoing primary afferent input from the BV injection site directly contributed to the development or establishment of the mirror-thermal hyperalgesia. The BV-induced paw flinches may reflect an increase in spontaneous activity of peripheral primary afferents and spinal neurons involved in the BV test [28]. Thus, both peripheral and central mechanisms may be involved in the spontaneous nociceptive behaviors and the thermal hyperalgesia.

The present study demonstrates that BV injection into the rat hindpaw induces, within minutes, the phosphorylation of CREB at the transcriptional regulatory site serine-133 in the spinal cord and ipsilateral DRG neurons. Interestingly, unilateral peripheral inflammation induces this phosphorylation event bilaterally in the spinal cord. These results are similar to the previous reports that pCREB increased after paw inflammation induced by carrageenan and formalin [14, 17], nerve injury [15], and neuropathic pain [16, 17], indicating that pCREB is involved in hyperalgesia and spontaneous nociception. A majority of the cells containing pCREB-positive nuclei in the spinal cord after BV stimulation were observed in laminae I-II and V-VI, which are the regions where a majority of the noxious primary afferents terminate and the cell bodies of nociceptive neurons are localized [52]. Furthermore, pCREB was also observed in a few small DRG neurons, which are involved in mediating pain transmission. pCREB is a component of the intracellular mechanisms active during persistent pain [15, 53]. Taken together, these results indicate that BV-induced expression of pCREB is predominantly confined to the neurons involved in the pain response. CREB binds specifically to the CRE present in the promoters of many genes, including the gene encoding somatostatin, for which transcription rates are strongly regulated by cAMP [54, 55]. Increases in pCREB may be associated with pain-related behaviors. The present study demonstrates that the expression of pCREB in the spinal cord can be suppressed by local application of octreotide, and cyclosomatostatin pretreatment antagonizes this effect. Through activating local SSTR, octreotide decreased the peripheral nociceptive messages transmitted to the spinal cord. Therefore, the nociceptive marker pCREB was reduced in ipsilateral DRG and spinal cord neurons.

In conclusion, the present study showed that octreotide relieved the BV-induced lifting/licking, mechanical allodynia, and spinal pCREB expression, which confirmed that somatostatin exerted peripheral analgesic effects through its receptors. In addition, pCREB may contribute to these nociceptive responses.

Abbreviations

DRG: Dorsal root ganglion
BV: Bee venom
OCT: Octreotide
SD: Sprague-Dawley

PWMT: Paw withdrawal mechanical threshold
PWTL: Paw withdrawal thermal latency
CREB: cAMP response element-binding protein
pCREB: Phosphorylated cAMP response element-binding protein
NS: Normal saline
c-SOM: Cyclosomatostatin
PBS: Phosphate buffer saline
NGS: Normal goat serum
ABC: Avidin-biotin-peroxidase
SST: Somatostatin
SSTR: Somatostatin receptor.

Conflict of Interests

The authors declare that there is no conflict of interests regarding the publication of this paper.

Acknowledgments

The authors are grateful to Dr. Mao Jiang and Professor Stephen M. Sims for their expert help in preparing the paper. The work was supported by Grants from the National Natural Science Foundation of China (nos. 81160141 and 81200604), Guangxi Natural Science foundation in China (no. 2012GXNSFBA053116), and the Postdoctoral Science Foundation of China (no. 2013M542120).

References

[1] S. M. Carlton, J. Du, E. Davidson, S. Zhou, and R. E. Coggeshall, "Somatostatin receptors on peripheral primary afferent terminals: inhibition of sensitized nociceptors," *Pain*, vol. 90, no. 3, pp. 233–244, 2001.

[2] D. Ferone, M. Boschetti, E. Resmini et al., "Neuroendocrine-immune interactions: the role of Cortistatin/somatostatin system," *Annals of the New York Academy of Sciences*, vol. 1069, pp. 129–144, 2006.

[3] I. Bencivinni, F. Ferrini, C. Salio, M. Beltramo, and A. Merighi, "The somatostatin analogue octreotide inhibits capsaicin-mediated activation of nociceptive primary afferent fibres in spinal cord lamina II (substantia gelatinosa)," *European Journal of Pain*, vol. 15, no. 6, pp. 591–599, 2011.

[4] S. M. Carlton, S. Zhou, J. Du, G. L. Hargett, G. Ji, and R. E. Coggeshall, "Somatostatin modulates the transient receptor potential vanilloid 1 (TRPV1) ion channel," *Pain*, vol. 110, no. 3, pp. 616–627, 2004.

[5] M. M. Corsi, C. Ticozzi, C. Netti et al., "The effect of somatostatin on experimental inflammation in rats," *Anesthesia and Analgesia*, vol. 85, no. 5, pp. 1112–1115, 1997.

[6] F. Yao, Y. Guo, S. Lu et al., "Mechanical hyperalgesia is attenuated by local administration of octreotide in pristane-induced arthritis in Dark-Agouti rats," *Life Sciences*, vol. 83, no. 21-22, pp. 732–738, 2008.

[7] K.-C. Li and J. Chen, "Altered pain-related behaviors and spinal neuronal responses produced by s.c. injection of melittin in rats," *Neuroscience*, vol. 126, no. 3, pp. 753–762, 2004.

[8] Y.-Y. Sun, K.-C. Li, and J. Chen, "Evidence for peripherally antinociceptive action of propofol in rats: behavioral and spinal neuronal responses to subcutaneous bee venom," *Brain Research*, vol. 1043, no. 1-2, pp. 231–235, 2005.

[9] J. Chen, H.-L. Li, C. Luo, Z. Li, and J.-H. Zheng, "Involvement of peripheral NMDA and non-NMDA receptors in development of persistent firing of spinal wide-dynamic-range neurons induced by subcutaneous bee venom injection in the cat," *Brain Research*, vol. 844, no. 1-2, pp. 98–105, 1999.

[10] M. Sheng, M. A. Thompson, and M. E. Greenberg, "CREB: a Ca^{2+}-regulated transcription factor phosphorylated by calmodulin-dependent kinases," *Science*, vol. 252, no. 5011, pp. 1427–1430, 1991.

[11] E. D. Crown, Z. Ye, K. M. Johnson, G.-Y. Xu, D. J. McAdoo, and C. E. Hulsebosch, "Increases in the activated forms of ERK 1/2, p38 MAPK, and CREB are correlated with the expression of at-level mechanical allodynia following spinal cord injury," *Experimental Neurology*, vol. 199, no. 2, pp. 397–407, 2006.

[12] J. Wu, G. Su, L. Ma et al., "Protein kinases mediate increment of the phosphorylation of cyclic AMP-responsive element binding protein in spinal cord of rats following capsaicin injection," *Molecular Pain*, vol. 1, article 26, 2005.

[13] E. Niederberger, C. Ehnert, W. Gao et al., "The impact of CREB and its phosphorylation at Ser142 on inflammatory nociception," *Biochemical and Biophysical Research Communications*, vol. 362, no. 1, pp. 75–80, 2007.

[14] D. J. Messersmith, D. J. Kim, and M. J. Iadarola, "Transcription factor regulation of prodynorphin gene expression following rat hindpaw inflammation," *Molecular Brain Research*, vol. 53, no. 1-2, pp. 259–269, 1998.

[15] W. Ma and R. Quirion, "Increased phosphorylation of cyclic AMP response element-binding protein (CREB) in the superficial dorsal horn neurons following partial sciatic nerve ligation," *Pain*, vol. 93, no. 3, pp. 295–301, 2001.

[16] G. Miletic, M. T. Pankratz, and V. Miletic, "Increases in the phosphorylation of cyclic AMP response element binding protein (CREB) and decreases in the content of calcineurin accompany thermal hyperalgesia following chronic constriction injury in rats," *Pain*, vol. 99, no. 3, pp. 493–500, 2002.

[17] R.-R. Ji and F. Rupp, "Phosphorylation of transcription factor CREB in rat spinal cord after formalin-induced hyperalgesia: relationship to c-fos induction," *The Journal of Neuroscience*, vol. 17, no. 5, pp. 1776–1785, 1997.

[18] W. Ma, C. Hatzis, and J. C. Eisenach, "Intrathecal injection of cAMP response element binding protein (CREB) antisense oligonucleotide attenuates tactile allodynia caused by partial sciatic nerve ligation," *Brain Research*, vol. 988, no. 1-2, pp. 97–104, 2003.

[19] W. R. Lariviere and R. Melzack, "The bee venom test: a new tonic-pain test," *Pain*, vol. 66, no. 2-3, pp. 271–277, 1996.

[20] J. Chen, C. Luo, H.-L. Li, and H.-S. Chen, "Primary hyperalgesia to mechanical and heat stimuli following subcutaneous been venom injection into the plantar surface of hindpaw in the conscious rat: a comparative study with the formalin test," *Pain*, vol. 83, no. 1, pp. 67–76, 1999.

[21] S. R. Chaplan, F. W. Bach, J. W. Pogrel, J. M. Chung, and T. L. Yaksh, "Quantitative assessment of tactile allodynia in the rat paw," *Journal of Neuroscience Methods*, vol. 53, no. 1, pp. 55–63, 1994.

[22] W. J. Dixon, "Efficient analysis of experimental observations," *Annual Review of Pharmacology and Toxicology*, vol. 20, pp. 441–462, 1980.

[23] H.-S. Chen, X. He, Y. Wang, W.-W. Wen, H.-J. You, and L. Arendt-Nielsen, "Roles of capsaicin-sensitive primary afferents

in differential rat models of inflammatory pain: a systematic comparative study in conscious rats," *Experimental Neurology*, vol. 204, no. 1, pp. 244–251, 2007.

[24] S. M. Hsu, L. Raine, and H. Fanger, "Use of Avidin-Biotin-Peroxidase Complex (ABC) in immunoperoxidase techniques: a comparison between ABC and unlabeled antibody (PAP) procedures," *Journal of Histochemistry and Cytochemistry*, vol. 29, no. 4, pp. 577–580, 1981.

[25] C. Luo, J. Chen, H.-L. Li, and J.-S. Li, "Spatial and temporal expression of c-Fos protein in the spinal cord of anesthetized rat induced by subcutaneous bee venom injection," *Brain Research*, vol. 806, no. 2, pp. 175–185, 1998.

[26] V. Kayser, F. Viguier, M. Ioannidi et al., "Differential anti-neuropathic pain effects of tetrodotoxin in sciatic nerve- versus infraorbital nerve-ligated rats—behavioral, pharmacological and immunohistochemical investigations," *Neuropharmacology*, vol. 58, no. 2, pp. 474–487, 2010.

[27] L. Zhao, S. Chen, J. Ming Wang, and R. D. Brinton, "17β-estradiol induces Ca^{2+} influx, dendritic and nuclear Ca^{2+} rise and subsequent cyclic AMP response element-binding protein activation in hippocampal neurons: a potential initiation mechanism for estrogen neurotrophism," *Neuroscience*, vol. 132, no. 2, pp. 299–311, 2005.

[28] H.-S. Chen, J. Chen, J. Chen, W.-G. Guo, and M.-H. Zheng, "Establishment of bee venom-induced contralateral heat hyperalgesia in the rat is dependent upon central temporal summation of afferent input from the site of injury," *Neuroscience Letters*, vol. 298, no. 1, pp. 57–60, 2001.

[29] Y.-N. Chen, K.-C. Li, Z. Li et al., "Effects of bee venom peptidergic components on rat pain-related behaviors and inflammation," *Neuroscience*, vol. 138, no. 2, pp. 631–640, 2006.

[30] K. S. Hong and H. K. Jin, "Melittin selectively activates capsaicin-sensitive primary afferent fibers," *NeuroReport*, vol. 15, no. 11, pp. 1745–1749, 2004.

[31] J. Chen, K. Li, C. Luo, Z. Li, Y. Chen, and Y. Yu, "Activation of thermal nociceptor TRPV1 by a honeybee toxic peptide via a phospholipase 2-lipoxygenase pathway," in *Proceedings of the 11th World Congress on Pain*, pp. 403–409, Sydney, Australia, 2005.

[32] M. J. Caterina, A. Leffler, A. B. Malmberg et al., "Impaired nociception and pain sensation in mice lacking the capsaicin receptor," *Science*, vol. 288, no. 5464, pp. 306–313, 2000.

[33] J. B. Davis, J. Gray, M. J. Gunthorpe et al., "Vanilloid receptor-1 is essential for inflammatory thermal hyperalgesia," *Nature*, vol. 405, no. 6783, pp. 183–187, 2000.

[34] A. Szallasi and P. M. Blumberg, "Vanilloid (Capsaicin) receptors and mechanisms," *Pharmacological Reviews*, vol. 51, no. 2, pp. 159–212, 1999.

[35] S. J. Marsh, C. E. Stansfeld, D. A. Brown, R. Davey, and D. McCarthy, "The mechanism of action of capsaicin on sensory C-type neurons and their axons in vitro," *Neuroscience*, vol. 23, no. 1, pp. 275–289, 1987.

[36] S. Bevan and J. Szolcsanyi, "Sensory neuron-specific actions of capsaicin: mechanisms and applications," *Trends in Pharmacological Sciences*, vol. 11, no. 8, pp. 330–333, 1990.

[37] P. Holzer, "Capsaicin: cellular targets, mechanisms of action, and selectivity for thin sensory neurons," *Pharmacological Reviews*, vol. 43, no. 2, pp. 143–201, 1991.

[38] S. M. Carlton, S. Zhou, B. Kraemer, and R. E. Coggeshall, "A role for peripheral somatostatin receptors in counter-irritation-induced analgesia," *Neuroscience*, vol. 120, no. 2, pp. 499–508, 2003.

[39] A. M. Elhassan, A. Adem, K. Hultenby, and J. U. Lindgren, "Somatostatin immunoreactivity in bone and joint tissues," *NeuroReport*, vol. 9, no. 11, pp. 2573–2575, 1998.

[40] Y. C. Patel, "Somatostatin and its receptor family," *Frontiers in Neuroendocrinology*, vol. 20, no. 3, pp. 157–198, 1999.

[41] J. P. Hannon, C. Petrucci, D. Fehlmann, C. Viollet, J. Epelbaum, and D. Hoyer, "Somatostatin sst2 receptor knock-out mice: localisation of sst1-5 receptor mRNA and binding in mouse brain by semi-quantitative RT-PCR, in situ hybridisation histochemistry and receptor autoradiography," *Neuropharmacology*, vol. 42, no. 3, pp. 396–413, 2002.

[42] A.-K. Imhof, L. Glück, M. Gajda et al., "Differential antiinflammatory and antinociceptive effects of the somatostatin analogs octreotide and pasireotide in a mouse model of immune-mediated arthritis," *Arthritis and Rheumatism*, vol. 63, no. 8, pp. 2352–2362, 2011.

[43] G. C. Ji, S. T. Zhou, G. Shapiro, J. C. Reubi, S. M. Carlton, and S. Jurczyk, "Analgesic activity of a non-peptide imidazolidinedione somatostatin agonist: in vitro and in vivo studies in rat," *Pain*, vol. 124, no. 1-2, pp. 34–49, 2006.

[44] D. Paran, D. Kidron, A. Mayo et al., "Somatostatin analogue treatment attenuates histological findings of inflammation and increases mRNA expression of interleukin-1 beta in the articular tissues of rats with ongoing adjuvant-induced arthritis," *Rheumatology International*, vol. 25, no. 5, pp. 350–356, 2005.

[45] G. Horváth and L. Mécs, "Antinociception by endogenous ligands at peripheral level," *Ideggyógyászati Szemle*, vol. 64, no. 5-6, pp. 193–207, 2011.

[46] H. L. Pan, Z. Z. Wu, H. Y. Zhou, S. R. Chen, H. M. Zhang, and D. P. Li, "Modulation of pain transmission by G-protein-coupled receptors," *Pharmacology & Therapeutics*, vol. 117, no. 1, pp. 141–161, 2008.

[47] R. Moncayo, "Reflections on the theory of, "silver bullet" octreotide tracers: implications for ligand-receptor interactions in the age of peptides, heterodimers, receptor mosaics, truncated receptors, and multifractal analysis," *EJNMMI Research*, vol. 1, article 9, 2011.

[48] H. Wheeler-Aceto and A. Cowan, "Standardization of the rat paw formalin test for the evaluation of analgesics," *Psychopharmacology*, vol. 104, no. 1, pp. 35–44, 1991.

[49] S. T. Meller, "Thermal and mechanical hyperalgesia: a distinct role for different excitatory amino acid receptors and signal transduction pathways?" *APS Journal*, vol. 3, no. 4, pp. 215–231, 1994.

[50] J. S. Mogil, S. G. Wilson, K. Bon et al., "Heritability of nociception II. "Types" of nociception revealed by genetic correlation analysis," *Pain*, vol. 80, no. 1-2, pp. 83–93, 1999.

[51] H.-S. Chen, J. Chen, and Y.-Y. Sun, "Contralateral heat hyperalgesia induced by unilaterally intraplantar bee venom injection is produced by central changes: a behavioral study in the conscious rat," *Neuroscience Letters*, vol. 284, no. 1-2, pp. 45–48, 2000.

[52] Y. Sugiura, C. L. Lee, and E. R. Perl, "Central projections of identified, unmyelinated (C) afferent fibers innervating mammalian skin," *Science*, vol. 234, no. 4774, pp. 358–361, 1986.

[53] E. D. Crown, Z. Ye, K. M. Johnson et al., "Upregulation of the phosphorylated form of CREB in spinothalamic tract cells following spinal cord injury: relation to central neuropathic pain," *Neuroscience Letters*, vol. 384, no. 1-2, pp. 139–144, 2005.

[54] M. R. Montminy, M. J. Low, and L. Tapia-Arancibia, "Cyclic AMP regulates somatostatin mRNA accumulation in primary

diencephalic cultures and in transfected fibroblast cells," *The Journal of Neuroscience*, vol. 6, no. 4, pp. 1171–1176, 1986.

[55] M. R. Montminy, K. A. Sevarino, J. A. Wagner, G. Mandel, and R. H. Goodman, "Identification of a cyclic-AMP-responsive element within the rat somatostatin gene," *Proceedings of the National Academy of Sciences of the United States of America*, vol. 83, no. 18, pp. 6682–6686, 1986.